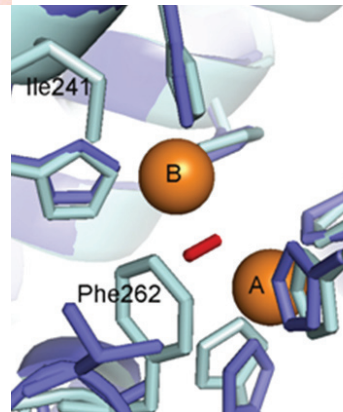


Biochemical and structural characterisation of the copper containing oxidoreductases catechol oxidase, tyrosinase, and laccase from ascomycete fungi

Chiara Gasparetti



Biochemical and structural characterisation of the copper containing oxidoreductases catechol oxidase, tyrosinase, and laccase from ascomycete fungi

Chiara Gasparetti

Doctoral dissertation for the degree of Doctor of Philosophy to be presented with due permission of the School of Chemical Technology for public examination and debate in Auditorium KE2 (Komppa Auditorium) at the Aalto University School of Chemical Technology (Espoo, Finland) on the 26th of October, 2012, at 12 noon.

ISBN 978-951-38-7934-1 (soft back ed.)

ISSN 2242-119X (soft back ed.)

ISBN 978-951-38-7935-8 (URL: <http://www.vtt.fi/publications/index.jsp>)

ISSN 2242-1203 (URL: <http://www.vtt.fi/publications/index.jsp>)

Copyright © VTT 2012

JULKAISIJA – UTGIVARE – PUBLISHER

VTT

PL 1000 (Tekniikantie 4 A, Espoo)

02044 VTT

Puh. 020 722 111, faksi 020 722 7001

VTT

PB 1000 (Teknikvägen 4 A, Esbo)

FI-2044 VTT

Tfn. +358 20 722 111, telefax +358 20 722 7001

VTT Technical Research Centre of Finland

P.O. Box 1000 (Tekniikantie 4 A, Espoo)

FI-02044 VTT, Finland

Tel. +358 20 722 111, fax +358 20 722 7001

Technical editing Anni Repo

Kopijyvä Oy, Kuopio 2012

Biochemical and structural characterisation of the copper containing oxidoreductases catechol oxidase, tyrosinase, and laccase from ascomycete fungi

Chiara Gasparetti. Espoo 2012. VTT Science 16. 124 p. + app. 55 p.

Abstract

Catechol oxidase (EC 1.10.3.1), tyrosinase (EC 1.14.18.1), and laccase (EC 1.10.3.2) are copper-containing metalloenzymes. They oxidise substituted phenols and use molecular oxygen as a terminal electron acceptor. Catechol oxidases and tyrosinases catalyse the oxidation of *p*-substituted *o*-diphenols to the corresponding *o*-quinones. Tyrosinases also catalyse the introduction of a hydroxyl group in the *ortho* position of *p*-substituted monophenols and the subsequent oxidation to the corresponding *o*-quinones. Laccases can oxidise a wide range of compounds by removing single electrons from the reducing group of the substrate and generate free radicals. The reaction products of these oxidases can react further non-enzymatically and lead to formation of polymers and cross-linking of proteins and carbohydrates, in certain conditions.

The work focused on examination of the properties of catechol oxidases, tyrosinases and laccases. A novel catechol oxidase from the ascomycete fungus *Aspergillus oryzae* was characterised from biochemical and structural point of view. Tyrosinases from *Trichoderma reesei* and *Agaricus bisporus* were examined in terms of substrate specificity and inhibition. The oxidation capacity of laccases was elucidated by using a set of laccases with different redox potential and a set of substituted phenolic substrates with different redox potential. Finally, an evaluation of the protein cross-linking ability of catechol oxidase from *A. oryzae*, tyrosinases from *T. reesei* and *A. bisporus* and laccases from *Trametes hirsuta*, *Thielavia arenaria*, and *Melanocarpus albomyces* was performed.

A novel extracellular catechol oxidase from *A. oryzae* (AoCO4; UniProtKB: Q2UNF9; Entrez gene ID: 5990879) was chosen for cloning and expression as representative of the newly discovered family of short tyrosinases sequences. AoCO4 gene was heterologously expressed in *T. reesei*. The protein produced did not show activity on L-tyrosine and 3,4-dihydroxy-L-phenylalanine (L-DOPA), which are typical substrates for tyrosinases. Consequently, the protein was classified as a catechol oxidase. AoCO4 was produced in a bioreactor and the expression resulted in high yields. The purified AoCO4 was partially processed at a Kex2/furin-type protease site and showed a molecular weight of 39.3 kDa. AoCO4 was able to oxidise a limited range of diphenolic compounds, e.g., catechol, caffeic acid, hydrocaffeic acid, and 4-*tert*-butylcatechol. AoCO4 oxidised also the monophenolic compounds aminophenol and guaiacol. AoCO4 showed a pH optimum in the acidic range and was observed to be a relatively thermostable enzyme. A crystal structure of AoCO4 was solved at 2.5 Å

resolution. AoCO4 was a monomer and the overall structure of AoCO4 was found to be similar to the known structures of catechol oxidases and tyrosinases.

A detailed characterisation of the substrate-specificity of the extracellular tyrosinase from *T. reesei* (TrT) was accomplished and compared to the commercial tyrosinase from *A. bisporus* (AbT). TrT generally showed lower affinity than AbT on substrates that had a free amino group, such as L-tyrosine, L-DOPA, and YGG tripeptide. The reaction end product of TrT and AbT was studied via mass spectrometry and dopachrome was found to be the only reaction end product of L-DOPA oxidation catalysed by both tyrosinases. Dopachrome produced by AbT-catalysed oxidation of L-DOPA was also shown to inhibit the TrT tyrosinase by an end product inhibition mechanism. Further, when the type of inhibition of potential inhibitors for TrT was analysed with *p*-coumaric acid and caffeic acid as substrates, potassium cyanide and kojic acid were the strongest inhibitors of TrT.

The kinetics of three laccases, with different redox potential (E°), for three *p*-substituted dimethoxy phenolic substrates (2,6-dimethoxyphenol, syringic acid, and methyl syringate) with different E° were determined at two pHs. The laccases studied were from *M. albomyces*, *T. arenaria*, and *T. hirsuta*. The enzyme from the ascomycete fungus *T. arenaria* was a novel laccase produced in *T. reesei*. *T. arenaria* laccase was purified, and biochemically and structurally characterised. By comparison of the three laccases it could be shown that both the difference in redox potential (ΔE°) and the pH had an effect on the kinetics. However, the effect of ΔE° was found to prevail over that of the pH for substrates with a high E° , such as methyl syringate.

All oxidative enzymes studied in this work were also tested for their cross-linking ability, with α -caseins utilised as a model substrate with and without a cross-linking agent. TrT was found to be the best enzyme for cross-linking of α -caseins, whereas AbT was found to be the best enzyme for cross-linking α -caseins in the presence of catechol as a cross-linking agent. Interestingly, AoCO4 was also found to cross-link α -caseins in the presence of catechol as a cross-linking agent.

Keywords

Trichoderma reesei, *Agaricus bisporus*, *Aspergillus oryzae*, *Thielavia arenaria*, tyrosinase, catechol oxidase, laccase, purification, characterisation, oxidation capacity, inhibition, three-dimensional structure, cross-linking

Preface

This work was carried out at VTT Technical Research Centre of Finland in the Development of Industrial Enzymes team. Former Vice President R&D Biotechnology, Prof. Juha Ahvenainen, Vice President R&D Bio- and process technology, Prof. Anu Kaukovirta-Norja and Technology Managers Niklas von Weymann and Raija Lantto are thanked for providing excellent working facilities and supporting the finalisation of this thesis. The study was lead for the first three years with financial support of the Marie Curie mobility actions as part of the EU project “Enzymatic tailoring of polymer interactions in food matrix” (MEST-CT-2005-020924) and subsequently with the financial support of Raisio Oy. In addition, the study presented in Publication III was partially supported by Roal Oy, the Academy of Finland, and Tekes – the Finnish Funding Agency for Technology and Innovation. Professor Matti Leisola at Aalto University is warmly acknowledged for the encouragement during the course of the work and for wearing the hat once more during my PhD defence.

I would like to thank Prof. Johanna Buchert for challenging me in this EU project. I am grateful to my supervisor Prof. Kristiina Kruus for excellent guidance and the lively discussions on the specific activity of catechol oxidases. Special thanks go to Dr. Emilia Nordlund for keeping fingers crossed anytime it was needed and for the crazy discussions on the reaction mechanism of tyrosinases. I warmly acknowledge all my colleagues and co-authors for being supportive and encouraging all over these years at VTT. Dr. Martina Andberg, Dr. Anu Koivula, and Dr. Harry Boer are specially thanked for the stimulating discussions on the laccases. I express my gratitude to Dr. Juha Kallio, Dr. Nina Hakulinen, Prof. Janne Jänis, Prof Juha Rouvinen, and MSc Heidi Kaljunen at University of Eastern Finland for the fruitful collaboration. In particular, Prof. Janne Jänis is thanked for catching dopachrome by ESI-MS. Docent Maija-Liisa Mattinen is acknowledged for the enlightening discussions about spectroscopy and mass spectrometry. Dr. Greta Faccio, Dr. Mikko Arvas, and Dr. Markku Saloheimo are warmly thanked for their appreciated contribution to Publication II. The valuable input of Dr. Charlotte L. Steffensen to Publication I is acknowledged. Dr. Raija Lantto, Dr. Riitta Partanen, Dr. Pirkko Forsell are kindly thanked for their participation in the ProEnz meetings. I am grateful to the ProEnz Kids, Dilek Ercili Cura, Hairan Ma, Evi Monogioudi, and Greta Faccio for the scientific discussions during the ProEnz

meetings, as well for the comic non-work related activities all over these years in Finland. My deepest gratitude goes to the technicians Brigit Hillebrandt-Chellaoui, Outi Liehunen, and Riitta Isoniemi for being in the lab with me and transmitting to me their many years of experience, without you three all this work would not be achieved.

The precious pre-examination work on the thesis by Adjunct Prof. Taina Lundell and Prof. Giovanni Sannia is acknowledged. I am grateful to all the participants of the OxiZymes meetings for the valuable discussions on the oxidative enzymes. Riku Haulisto at Semantix is thanked for revising the language of this thesis. The assistance of Päivi Vahala, Annemari Kuokka-Ihalainen, Olli Lappalainen, Eva Fredriksson, Timo Almgren, Christer Holm, and Sirje Liukko is sincerely recognised.

The members of the Development of Industrial Enzymes team, as well as Dr. Hanna Kontkanen and MSc Saara Mikander are frankly thanked for supporting me in any situation and for their friendship. The players in the VTT volleyball, rowing, floorball, and basketball teams are also sincerely thanked for the enjoyable games.

The friendship with all those that crossed my way for a little while or for many years is highly recognised. Zsuzsa, Eva L., Orquidea, Lise, Catarina, Dagmar, Nadia, Elena, Rossana, and Isabel you all have been important to me in different times of these years at VTT. The companionship of those living faraway has been really supportive to me. Benedetta, Aurelie, Eva B., Elisabetta, Anna, Matteo, Valentina, and Paola your friendship is treasured. The more recent friendship with Bartosz, Timo, Roberto, Michal, Andrea M., Amir, Erkin, Julio, and Oleg has been an anchor in the last two years. I am grateful to Yanli, Sari and Mili for their sincere friendship and for never pretending to understand what I do as a profession. Mei Yen is acknowledged for the nerdy discussions on everyday life subjects. I am really grateful to Dilek for our introspective walks around VTT building and to Hairan for his friendship. I thank Evi for our early morning talks in the office.

I am indebted to my mother and father for supporting me all this time and never making me feel that I am too far from home. I thank my brother and his new family. In particular, I am thankful my nephew Diego that being born when I started the PhD has shown me how quickly time passes. The dog in Italy is also acknowledged for making me feel really welcome whenever I go home. Finally, I sincerely thank Andrea V. for sharing his life with me.

Academic dissertation

Supervisors	Research Professor Kristiina Kruus Bio and Process Technology VTT Technical Research Centre of Finland Espoo, Finland
	Research Professor Johanna Buchert Bio and Process Technology VTT Technical Research Centre of Finland Espoo, Finland
Pre-examiners	Adjunct Professor Taina Lundell Department of Food and Environmental Sciences University of Helsinki Helsinki, Finland
	Full Professor Giovanni Sanna Department of Organic Chemistry and Biochemistry University of Naples Federico II Napoli, Italy
Opponent	Professor Lúgia O. Martins Instituto de Tecnologia Química e Biológica Univesidade Nova de Lisboa Oeiras, Portugal
Custos	Professor Matti Leisola Department of Biotechnology and Chemical Technology Aalto University Espoo, Finland

List of publications

This thesis is based on the following original publications which are referred to in the text as I–IV. The publications are reproduced with kind permission from the publishers.

- I Selinheimo, E., Gasparetti, C., Mattinen, M.-L., Steffensen, C.L., Buchert, J., Kruus, K. Comparison of substrate specificity of tyrosinases from *Trichoderma reesei* and *Agaricus bisporus*. *Enzyme and Microbial Technology* (2009) 44:1–10.
- II Gasparetti, C., Faccio, G., Arvas, M., Buchert, J., Saloheimo, M., Kruus, K. Discovery of a new tyrosinase-like enzyme family lacking a C-terminally processed domain: production and characterization of an *Aspergillus oryzae* catechol oxidase. *Applied Microbiology and Biotechnology* (2010) 86:213–226.
- III Kallio, J.P., Gasparetti, C., Andberg, M., Boer, H., Koivula, A., Kruus, K., Rouvinen, J., Hakulinen, N. Crystal structure of an ascomycete fungal laccase from *Thielavia arenaria* – common structural features of asco-laccases. *FEBS Journal* (2011) 278:2283–2295.
- IV Gasparetti, C., Nordlund, E., Jänis, J., Buchert, J., Kruus, K. Extracellular tyrosinase from the fungus *Trichoderma reesei* shows product inhibition and different inhibition mechanism from the intracellular tyrosinase from *Agaricus bisporus*. *BBA – Proteins and Proteomics* (2012) 1824:598–607.

Author's contributions

- I The author planned the work in collaboration with the co-authors. The author purified the tyrosinases from *Trichoderma reesei* and *Agaricus bisporus* and determined the kinetic parameters, i.e., K_M and V_{max} for the two tyrosinases. The author interpreted the results and contributed to writing of the publication with Emilia Nordlund (*née* Selinheimo), Sc.D.; Kristiina Kruus, Research Professor; and the other authors.
- II The author planned and conducted the laboratory work related to the purification and the biochemical characterisation of the *Aspergillus oryzae* catechol oxidase. The author interpreted the data and significantly contributed to writing of the publication. The author and the co-author, Greta Faccio, Ph.D., contributed equally to this work.
- III The author planned and conducted the work related to the purification and the determination of the kinetic parameters and pH optima of the laccase from *Thielavia arenaria*. The author interpreted the results and compared the kinetic data of the three laccases, i.e., from *T. arenaria*, *Melanocarpus albomyces* and *Trametes hirsuta*. The author contributed significantly to the writing process.
- IV The author had the main responsibility for designing and carrying out the experiments, for the interpretation of the results, and in writing of the publication. The author conducted the spectroscopy and polarography experiments. The author conducted the experiments using mass spectrometry jointly with Professor Janne Jänis in the Chemistry Department of University of Eastern Finland. The author developed a method to produce dopachrome by utilising the tyrosinase from *A. bisporus* and conducted the dopachrome inhibition experiments of the *T. reesei* tyrosinase. The author determined the K_i parameters of *T. reesei* tyrosinase for several inhibitors.

Contents

Abstract	3
Preface.....	5
Academic dissertation.....	7
List of publications.....	8
Author's contributions	9
List of abbreviations.....	13
1. Introduction.....	15
1.1 Distribution of tyrosinases, catechol oxidases and laccases	16
1.2 Physiological role of tyrosinases, catechol oxidases and laccases.....	17
1.3 Biochemical properties.....	20
1.3.1 Tyrosinases and catechol oxidases	20
1.3.2 Laccases.....	21
1.4 Active sites of copper-containing enzymes	24
1.5 Reaction mechanisms.....	26
1.5.1 Tyrosinases and catechol oxidases	26
1.5.2 Laccases.....	31
1.6 Structures.....	33
1.6.1 Tyrosinases and catechol oxidases	33
1.6.2 Laccases.....	37
1.7 Applications of tyrosinases and laccases.....	43
1.7.1 Food-related applications.....	43
1.7.1.1 Development in the organoleptic properties of food products	43
1.7.1.2 Cross-linking reactions related to food applications	43
1.7.2 Non-food-related applications.....	46
1.7.2.1 Large-scale applications of laccases.....	46
1.7.2.2 Other potential non-food applications of tyrosinases and laccases	46

2. Aims of the work	51
3. Material and methods	52
3.1 Substrates and inhibitors.....	52
3.2 Enzymes.....	52
3.3 Enzyme activity assays.....	54
3.4 Production and purification of enzymes	55
3.4.1 Production and purification of catechol oxidase from <i>Aspergillus oryzae</i> (Publication II).....	55
3.4.2 Production and purification of laccase from <i>Thielavia arenaria</i> (Publication III)	55
3.5 Biochemical characterisation of enzymes	56
3.5.1 Biochemical and structural characterisation of catechol oxidase from <i>Aspergillus oryzae</i> (Publication II and unpublished results).....	56
3.5.2 Biochemical characterisation of tyrosinase from <i>Trichoderma reesei</i> (Publications I and IV).....	57
3.5.3 Determination of kinetic parameters of laccases from <i>Thielavia arenaria</i> , <i>Melanocarpus albomyces</i> , and <i>Trametes</i> <i>hirsuta</i> (Publication III)	58
3.5.4 Enzymatic cross-linking of α -caseins by catechol oxidase, tyrosinases, and laccases (Unpublished results)	58
4. Results and discussion	60
4.1 Biochemical and structural characterisation of a catechol oxidase from <i>Aspergillus oryzae</i> (Publication II and unpublished results).....	60
4.1.1 Discovery and production of <i>Aspergillus oryzae</i> catechol oxidase.....	60
4.1.2 Purification and characterisation of <i>Aspergillus oryzae</i> catechol oxidase.....	61
4.1.3 Crystal structure and spectroscopic features of <i>Aspergillus</i> <i>oryzae</i> catechol oxidase.....	64
4.2 Detailed characterisation of the tyrosinase from <i>Trichoderma</i> <i>reesei</i> and comparison with the tyrosinase from <i>Agaricus bisporus</i> (Publications I and IV).....	70
4.2.1 Characterisation of the substrate-specificity of tyrosinases from <i>Trichoderma reesei</i> and <i>Agaricus bisporus</i>	70
4.2.2 <i>Trichoderma reesei</i> tyrosinase end product inhibition by dopachrome	75
4.2.3 Effect of inhibitors on the monophenolase and diphenolase activities of <i>Trichoderma reesei</i> tyrosinase.....	77
4.3 Three-dimensional structure of a laccase from <i>Thielavia arenaria</i> and elucidation of the oxidation capacity of fungal laccases with different redox potential (Publication III).....	78

4.3.1	Purification and three-dimensional structure of <i>Thielavia arenaria</i> laccase	78
4.3.2	Elucidation of the oxidation capacity of fungal laccases with different redox potential as related to their available crystal structures	82
4.4	Enzymatic cross-linking of α -casein proteins by means of catechol oxidase, tyrosinases, and laccases (Unpublished results)	86
5.	Conclusions and future prospects	89
	References.....	91

Appendices

Publications I–IV

*Publications II is not included in the PDF version.
Please order the printed version to get the complete publication
(<http://www.vtt.fi/publications/index.jsp>).*

List of abbreviations

2,6-DMP	2,6-dimethoxyphenol
AbT	tyrosinase from <i>Agaricus bisporus</i>
ABTS	2,2'-azino-bis(3-ethylbenzthiazoline-6-sulphonic acid)
AoCO4	catechol oxidase from <i>Aspergillus oryzae</i>
BmT	tyrosinase from <i>Bacillus megaterium</i>
CD	circular dichroism
DHI	5,6-dihydroxyindole
DHICA	5,6-dihydroxyindole-2-carboxylic acid
D-DOPA	3,4-dihydroxy-D-phenylalanine
E^0	redox potential
EPR	electron paramagnetic resonance
GGY	glycine-glycine-tyrosine peptide
GYG	glycine-tyrosine-glycine peptide
IbCO	catechol oxidase from <i>Ipomea batatas</i>
L-DOPA	3,4-dihydroxy-L-phenylalanine
LMS	laccase mediator system
MBTH	3-methyl-2-benzothiazolinone hydrazone
MW	molecular weight

PDB	Protein Data Bank
Phe-OH	phenolic substrate
PPO	polyphenol oxidase
rMaL	laccase from <i>Melanocarpus albomyces</i> (recombinant)
ScT	tyrosinase from <i>Streptomyces castaneoglobisporus</i>
T1	type-1 copper site
T2	type-2 copper site
T3	type-3 copper site
TaLcc1	laccase 1 from <i>Thielavia arenaria</i>
TBC	4- <i>tert</i> -butylcatechol
ThL	laccase from <i>Trametes hirsuta</i>
TrT	tyrosinase from <i>Trichoderma reesei</i>
VvCO	catechol oxidase from <i>Vitis vinifera</i>
Y	L-tyrosine
YGG	tyrosine-glycine-glycine peptide

1. Introduction

Tyrosinase (EC 1.14.18.1; monophenol monooxygenase), catechol oxidase (EC 1.10.3.1; 1,2-benzenediol:oxygen oxidoreductase) and laccase (EC 1.10.3.2; benzenediol:oxygen oxidoreductase) are copper-containing metalloenzymes that catalyse the oxidation of substituted phenols and use molecular oxygen as a terminal electron acceptor. Molecular oxygen is reduced to water. Tyrosinases oxidise *p*-substituted monophenols and *p*-substituted *o*-diphenols to the corresponding *o*-quinones. Catechol oxidases catalyse the oxidation of *p*-substituted *o*-diphenols to the corresponding *o*-quinones, but do not oxidise *p*-substituted monophenols. Laccases have a wide range of substrate-specificity, e.g., monophenols, diphenols, aryl amines, aminophenols, and inorganic compounds can be oxidised by laccases. While tyrosinases and catechol oxidases remove an electron pair from the hydroxyl groups of a diphenolic substrate and generate quinones, laccases remove single electrons from the reducing group of the substrate and the products generated are usually free radicals (Sanchez-Amat & Solano 1997) (**Figure 1**).

Tyrosinases, catechol oxidases and laccases are essential oxidoreductases in nature, where they are involved, e.g., in defence mechanisms. Tyrosinases, catechol oxidases and laccases, especially those of plant origin, are sometimes also called polyphenol oxidases (PPOs) (Mayer 1987). This classification is misleading for the reason that it does not differentiate these enzymes on the basis of their distinct enzymatic activities (Flurkey & Inlow 2008). Tyrosinase- and catechol oxidase-formed quinones are the building blocks of melanins, which play a physiological role in defence mechanisms, such as sclerotisation, primary immune response, and host defence. The principal role of fungal laccases is degradation of lignin in synergy with other lignin-modifying enzymes, such as lignin peroxidases and manganese peroxidases (for a review, see Lundell et al. 2010). Laccases are also involved in melanogenesis and are important virulence factors (Nagai et al. 2003).

Laccases are used in industrial applications for bleaching of denim in the textile industry (for a review, see Galante & Formantici 2003). Laccases and tyrosinases of fungal origin have been shown to be potent cross-linking agents, i.e., they can be used to introduce specific covalent bonds between proteins, as well as between proteins and carbohydrates (Selinheimo et al. 2007b). Thus far, catechol oxidases have been less studied also in terms of applications.

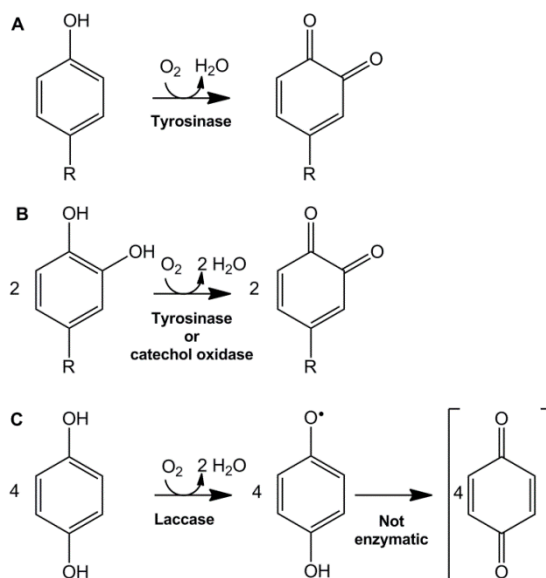


Figure 1. Oxidation of phenolic compounds catalysed by tyrosinase (A and B), catechol oxidase (B), and laccase (C).

1.1 Distribution of tyrosinases, catechol oxidases and laccases

Tyrosinases are scattered among animals, plants, fungi and invertebrates, as well as in prokaryotic and eukaryotic microbes (for a review, see Lerch 1983, Seo et al. 2003, Claus & Decker 2006, Halaoui et al. 2006a, Wang & Hebert 2006). Tyrosinases exist in mammals, including humans (Kwon et al. 1987). While human tyrosinase is a trans-membrane enzyme, tyrosinases of other origins are mainly intracellular enzymes. The first fungal tyrosinase was isolated from the edible mushroom *Agaricus bisporus* (AbT) (Nakamura et al. 1966) and the first bacterial tyrosinase from *Streptomyces glaucescens* (Lerch & Ettinger 1972). Well-characterised intracellular fungal tyrosinases have been reported from the species *Neurospora crassa* (Fling et al. 1963, Lerch 1983, Kupper et al. 1989), *Lentinula edodes* (Kanda et al. 1996), *Aspergillus oryzae* (Nakamura et al. 2000), *Pycnoporus sanguineus* (Halaoui et al. 2005, Halaoui et al. 2006b), and *Thermomicrobium roseum* (Kong et al. 2000). The known extracellular tyrosinases are from the bacteria *Streptomyces michiganensis* (Philipp et al. 1991) and *Streptomyces antibioticus* (Bernan et al. 1985), and from the fungi *Amylomyces rousii* (Montiel et al. 2004) and *Trichoderma reesei* (TrT) (Selinheimo et al. 2006b). Thus far, the tyrosinase from *T. reesei* is the best-characterised extracellular tyrosinase.

The few characterised catechol oxidases are originated from plant and fungi. There are no reports on catechol oxidases of bacterial or mammal origins. All known catechol oxidases are intracellular enzymes. The best-characterised plant catechol oxidases are from *Ipomea batatas* (Eicken et al. 1998), *Populus nigra*, *Lycopus europaeus* (Rompel et al. 1999a), and *Melissa officinalis* (Rompel et al. 2012). Among fungi, one polyphenol

oxidase from the ascomycete fungus *Alternaria tenuis* has been classified as a catechol oxidase (Motoda 1979a, Motoda 1979b).

Laccases are widely distributed in plants and fungi, and they are also present in some bacteria and insects (for a review, see Hoegger et al. 2006). Unlike tyrosinases, laccases are not found in animals (for a review, see Mayer & Staples 2002). Most of the characterised laccases are of fungal origin; however, the first laccase was found from the tree *Rhus vernicifera* (Yoshida 1883). The majority of the characterised laccases are extracellular enzymes, although intracellular laccases have also been characterised (Froehner & Eriksson 1974, Palmieri et al. 2000, Langfelder et al. 2003, Nagai et al. 2003, McMahon et al. 2007).

1.2 Physiological role of tyrosinases, catechol oxidases and laccases

Tyrosinases and catechol oxidases are the key enzymes in the first reactions of melanogenesis, the formation of melanins. Melanins are involved in many biologically essential functions such as pigmentation, sclerotisation, primary immune response, and host defence. In mammals, melanogenesis is related to the pigmentation of the hair, skin, and eyes. Malfunctions in tyrosinase activity result in hyperpigmentation and albinism in mammals (for a review, see Ito & Wakamatsu 2008). It has been suggested that a tyrosinase activity in bacteria participate in the detoxification of phenolic compounds (Borthakur et al. 1987), and that the formed melanins prevent the dehydration of the cells (Coyne & Al-Harhi 1992).

In plants, the melanins may contribute to the formation of barriers, or be involved in alkylation reactions reducing the bioavailability of proteins, or even in the creation of a toxic environment for the attacker (for a review, see Mayer 1987, Walker & Ferrar 1998). Both tyrosinases and catechol oxidases may contribute to the formation of catechol melanins. Catechol melanins are specific melanins produced in plants, and they are formed by derivatives of catechol quinones. Catechol melanins protect the damaged plant from pathogens and insects (Dervall 1961, Felton et al. 1989, Bi & Felton 1995, Melo et al. 2006). In insects, melanins are involved in the sclerotisation of cuticle, in defence mechanism, and in wound-healing processes (Sugumaran 2002).

In fungi, melanins serve as a mechanism of resistance to stress factors, e.g., UV radiations (Bell & Wheeler 1986), as well as defence against virulence mechanisms (Soler-Rivas et al. 1997, Jacobson 2000). Fungal melanins contribute to cell walls' resistance against hydrolytic enzymes in avoiding cell lysis (Bell & Wheeler 1986). Furthermore, fungal melanins are produced during sexual differentiation (Lerch 1983) and spore formation (Mayer & Harel 1979). It has also been suggested that extracellular tyrosinases play a role in the polymerization and detoxification of plant phenolic compounds in soil environments (Sjoblad & Bollag 1981).

Laccases from plant origin are located in the xylem and play an important role in the early stages of lignin biosynthesis, presumably oxidising monolignols (Bao et al. 1993, O'Malley et al. 1993, Gavnholt & Larsen 2002, Mayer & Staples 2002). Plant laccases have also been shown to be involved in the first steps of healing in wounded leaves (de Marco & Roubelakis-Angelakis 1997). Fungal laccases, in particular from white-rot fungi,

are involved mainly in the degradation of lignin in synergy with other lignin-modifying enzymes, such as lignin peroxidases and manganese peroxidases (for a review, see Hoegger et al. 2006).

More than the two thirds of the known laccase sequences are of fungal origin (for a review, see Valderrama et al. 2003, Hoegger et al. 2006). The characterised laccases from basidiomycete fungi are from *Trametes* species (Coll et al. 1993, Yaver et al. 1996, Yaver et al. 1999, Dedeyan et al. 2000, Bertrand et al. 2002, Galhaup et al. 2002, Klonowska et al. 2002, Xiao et al. 2004), *Pycnoporus cinnabarinus* (Eggert et al. 1996, Sigoillot et al. 1999), *Ceriporiopsis subvermispota* (Karahanian et al. 1998), *Lentinula edodes* (Nagai et al. 2002, Nagai et al. 2003) *Pleurotus ostreatus* (Sannia et al. 1986, Giardina et al. 1999, Garzillo et al. 2001, Palmieri et al. 2003), *Volvariella volvacea* (Chen et al. 2004) *Coprinopsis cinerea* (*Coprinus cinereus*) (Schneider et al. 1999, Yaver et al. 1999), *Thanatephorus cucumeris* (Wahleithner et al. 1996). The characterised laccases from ascomycete fungi are from *Aspergillus* species (Wood 1980a, Huang et al. 1995), *Botrytis cinerea* (Marbach et al. 1984, Schouten et al. 2002), *Cryphonectria parasitica* (Rigling & Van Alfen 1993) *Gaeumanomyces graminis* (Litvintseva & Henson 2002) *Melanocarpus albomyces* (Kiiskinen et al. 2002, Kiiskinen et al. 2004), *Chaetomium thermophilum* (Chefetz et al. 1998), *Neurospora crassa* (Froehner & Eriksson 1974, Germann & Lerch 1986) and *Podospora anserina* (Fernandez-Larrea & Stahl 1996). Laccases are produced also in plant-pathogenic fungi, where they play an important role as virulence factors, e.g., the laccase from the grape-vine grey mould *Botrytis cinerea* participates in the infection of a variety of hosts (Bar Nun et al. 1988). Furthermore, a cell wall-localised laccase of *Cryptococcus neoformans* plays a relevant role in the infection of humans (Williamson 1994).

Among bacteria, the laccases from the genus *Streptomyces* are well known. The laccases from *Streptomyces lavendulae* (Suzuki et al. 2003), *Streptomyces cyaneus* (Arias et al. 2003), *Streptomyces coelicolor* (Dubé et al. 2008), and *Streptomyces psammoticus* (Niladevi et al. 2008) have been characterised. Other known bacterial laccases are from *Azospirillum lipoferum* (Faure et al. 1994) and *Bacillus subtilis* (Martins et al. 2002), both involved in pigments production. The role of laccases in insects is related to cuticle sclerotisation (Sugumaran et al. 1992, Dittmer et al. 2004). The distribution and physiological role of tyrosinases, catechol oxidases, and laccases are summarised in **Table 1**.

Table 1. Biochemical and structural properties of tyrosinase, catechol oxidase and laccase.

	Tyrosinase	Catechol oxidase	Laccase	Refer to paragraph
Enzyme classification	EC 1.14.18.1	EC 1.10.3.1	EC 1.10.3.2	
Distribution	Mammals, plants, insects, fungi, bacteria	Plants, insects, fungi, bacteria	Plants, insects, fungi, bacteria	1.1
Physiological role	Pigment formation, wound healing, sclerotisation	Pigment formation, wound healing, sclerotisation	Lignin degradation, pigment and fruiting body formation, detoxification, plant pathogenesis	1.2
Location in the cell	Mainly intracellular	Mainly intracellular	Mainly extracellular	1.1
Molecular weight	30–50 kDa	30–60 kDa	60–80 kDa (three domain laccases) 30–40 kDa (monomer of two domain laccases)	1.6
Substrates	<i>p</i> -Monophenols, <i>o</i> -diphenols	<i>o</i> -Diphenols	Monophenols, diphenols, aryl amines, amino phenols	1.3 and 1.5
Primary oxidation product	<i>o</i> -Quinone	<i>o</i> -Quinone	Phenoxy radical	1.5
O ₂ stoichiometry	1 Monophenol : 1 O ₂	2 Diphenol : 1 O ₂	4 Phe-OH : 1 O ₂ ^a	1.5
Specific inhibitors	Tropolone, salicyl hydroxamic acid, 4-hexyl resorcinol, phenyl hydrazine	Phenylthiourea, N,N-diethylthiocarbamate	Small anions, N-hydroxyl glycine, cetyltrimethylammonium bromide, azide	1.3
Protein family	PF00264	PF00264	PF00394	1.4
Copper centre	T3 ^b	T3 ^b	T1 and trinuclear T2/T3 ^b	1.4
EPR signal	No	No	Yes	1.4
UV/VIS absorption maximum	345 nm (strong); 600 nm (weak) ^c	330 nm (weak)	330 nm (T3 centre); 600 nm (T1 centre)	1.4
Tertiary structure	Monomer, dimer, tetramer	Monomer	Monomer	1.6

^a Phe-OH is a generic phenolic substrate of laccase.

^b T1 is a type 1 copper centre; T2 is a type 2 copper centre; T3 is a type 3 copper centre.

^c UV/VIS absorption maxima of the oxy-form of tyrosinase.

1.3 Biochemical properties

1.3.1 Tyrosinases and catechol oxidases

Many tyrosinases have their pH optima in a neutral or acidic range. Only a few tyrosinases have been reported with an optimum in an alkaline pH range: the tyrosinase from *Thermomicrobium roseum* (pH 9.5 on L-DOPA) (Kong et al. 2000), the tyrosinase from *Pinus densiflora* (pH 9–9.5 on L-DOPA) (Kong et al. 1998), and the extracellular tyrosinase from *T. reesei* (pH 9 on L-tyrosine) (Selinheimo et al. 2006b). The known tyrosinases are not very thermostable enzymes and the most commonly known thermostable ones are from *T. roseum* and *P. sanguineus*. *T. roseum* tyrosinase has been shown to retain 100% of its activity on L-DOPA after ten minutes of incubation at 70 °C, but it was rapidly inactivated at temperatures higher than 75 °C (Kong et al. 2000). *P. sanguineus* tyrosinase activity on L-tyrosine was completely inactivated after 20 minutes of incubation at 60 °C (Halaoui et al. 2005). Low temperatures also inactivate tyrosinases, as reported for tyrosinases from *Aspergillus flavipes* (Gukasyan 1999) and *N. crassa* (Fling et al. 1963).

Most of the characterised catechol oxidases are of plant origin and have pH optima in the neutral-basic range. These include catechol oxidases from *I. batatas* (optimum pH 7.8 on catechol) (Eicken et al. 1998), from *P. nigra* (optimum pH 8.0 on catechol) (Rompel et al. 1999a), and from *L. europaeus* (optimum pH 6.5–7.5 on catechol) (Rompel et al. 1999a). In contrast, the characterised catechol oxidase from the ascomycete fungus *A. tenuis* is active in an acidic pH range (4.0–5.8) and has an optimum at pH 4.7 (Motoda 1979a, Motoda 1979b). *A. tenuis* catechol oxidase is not thermostable; it has a half-life of 30 minutes at 44 °C on substrate D-catechin and is inactivated after 30 minutes of incubation at 60 °C (Motoda 1979a, Motoda 1979b).

Tyrosinases and catechol oxidases are not distinguishable from a comparison of their primary sequences, both belong to the same family (PF00264). Substrate-specificity determines the classification of tyrosinase and catechol oxidase activities. While tyrosinases can oxidise a wide range of *p*-substituted mono- and diphenolic compounds, catechol oxidases oxidise various *p*-substituted diphenolic compounds but lack activity on *o*-substituted monophenols (Klabunde et al. 1998, Marusek et al. 2006). L-Tyrosine and L-DOPA, respectively, are the typical monophenolic and diphenolic substrates of tyrosinases and are commonly used to measure tyrosinase activity. In turn, L-DOPA and caffeic acid are the diphenolic substrates mainly used for analysis of the activity of catechol oxidases. It has been reported that *p*-coumaric acid, i.e., the corresponding monophenolic compound of caffeic acid can be oxidised by the tyrosinases from the fungi *P. sanguineus* and *T. reesei*, whereas it cannot be oxidised by the tyrosinase from fungus *A. bisporus* or in general by tyrosinases of plant origin (Halaoui et al. 2005, Selinheimo et al. 2006b, Selinheimo et al. 2007b). Tyrosinases are also capable of oxidising a variety of aromatic amines and *o*-aminophenols (Toussaint & Lerch 1987, Rescigno et al. 1998, Sanjust et al. 2003, Gasowska et al. 2004, Selinheimo et al. 2007b, Muñoz-Muñoz et al. 2011). Tyrosinases can also oxidise larger compounds containing a tyrosyl residue, such as catechins, peptides, and proteins (Selinheimo et al. 2007b, Mattinen et al. 2008a, Mattinen et al. 2008b). Furthermore, some plant catechol oxidases (known also as

polyphenol oxidases) have weak monophenolase activity but cannot oxidise L-tyrosine. It has been suggested that L-tyrosine is a specific substrate for tyrosinase and can be used to distinguish tyrosinases and catechol oxidases (Mayer & Harel 1979, Walker & Ferrar 1998, Gerdemann et al. 2002). The known substrates for tyrosinases and catechol oxidases are summarised in **Table 2**.

Inhibitors of tyrosinases have been extensively studied, because these enzymes are also responsible for undesired reactions, such as browning reactions in fruits and vegetables (for a review, see Seo et al. 2003). The enzymatic browning reactions are started by endogenous tyrosinases, which oxidise the phenolic compounds present in the tissues of fruits, vegetables, and mushrooms. The non-enzymatic reactions consist of Maillard reactions, which are reactions between a nucleophilic amino group of a protein and the carbonyl group of a carbohydrate. Browning reactions cause changes in food products' organoleptic properties and appearance, leading to a short shelf life and a lower market value, so the prevention of browning reactions is highly important (Lertsiri et al. 2003). Antibrowning agents are chemical compounds that decrease the browning reactions. They can be divided into reducing agents and enzyme inhibitors. Reducing agents react with the enzymatic end product, preventing the non-enzymatic reactions that lead to the formation of colourful products. Enzyme inhibitors prevent the primary enzymatic oxidation of a phenolic substrate (for a review, see Seo et al. 2003, Kim & Uyama 2005, Chang 2009). 4-Hexylresorcinol, salicylhydroxamic acid and tropolone are specific inhibitors of tyrosinases, whereas phenylthiourea and *N,N*-diethyldithiocarbamate are specific inhibitors of catechol oxidases (Dawley & Flurkey 1993). Substrate analogues, e.g., cinnamic acids have also been described as having an inhibitory effect on tyrosinases (Lim et al. 1999). Inhibition of tyrosinases has also been reported by small anions, such as azide, cyanide, mercaptoethanol, and carbon dioxide. Small anions bind to the copper ions in the active site (Himmelwright et al. 1980, Beltrami & Lerch 1982).

In humans, the production of anti-tyrosinase antibodies causes vitiligo, an autoimmune disorder that produces a white colour in patches of the skin. Overproduction of tyrosinase in humans, on the other hand, causes melasma and solar lentigines, which represent an aesthetic problem. Skin-whitening agents are chemical substances that reduce the formation of melanins in skin (for a review, see Parvez et al. 2006, Draelos 2007, Chang 2009). Skin-whitening agents react with the tyrosinase-formed quinones reducing them to colourless compounds. Thus far, the skin-whitening agents most often used in cosmetic preparations have been aloesin and arbutin, which are extracted from the plant *Aloe vera* (Yagi et al. 1987). Also, kojic acid, derived from various fungal species, such as those in the *Aspergillus* and *Penicillium* spp. (Parrish et al. 1966), is used in cosmetic and medical preparations as a skin-whitening agent (Masse et al. 2001). Hydroquinone is a strong skin-whitening agent with high melanocyte-specific cytotoxicity. While it is used in depigmenting medication, the use of hydroquinone in cosmetic preparations has been discouraged because of its side effects, including skin irritation (Breathnach 1996).

1.3.2 Laccases

Thermotolerant and thermostable laccases have been recently reviewed by Hildén et al. (2009). The most thermostable laccases are of bacterial origin, e.g., the half-life of laccase from *Streptomyces lavendulae* is 100 minutes at 70 °C (activity on catechol)

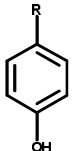
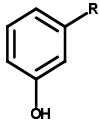
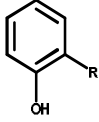
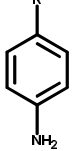
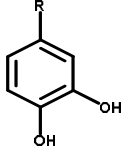
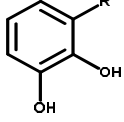
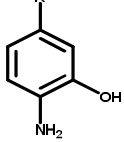
(Suzuki et al. 2003) and that of *Bacillus subtilis* CoTA is 112 minutes at 80 °C (activity on 2,2'-azino-bis(3-ethylbenzthiazoline-6-sulphonic acid) (ABTS)) (Martins et al. 2002). Fungal laccases are generally stable enzymes in the temperature range 30–50 °C, whereas plant laccases are less thermostable. Among laccases of fungal origin, a laccase from *Agaricus bisporus* has a half-life of ten minutes at 70 °C on *p*-phenylenediamine (Wood 1980a), a laccase from *Trametes sanguinea* is stable for only ten minutes at 70 °C on substrate N,N-dimethyl-*p*-phenylenediamine (Nishizawa et al. 1995), and a laccase from *Coprinopsis cinerea* has a half-life of 4.6 minutes at 70 °C on substrate syringaldazine (Schneider et al. 1999).

Laccases with temperature optima below 35 °C have also been reported: for example, a laccase from *Ganoderma lucidum* has the highest short-time activity at 25 °C on *o*-tolidine (Ko et al. 2001). In general, fungal laccases are more stable at acidic than at alkaline pH (Bollag & Leonowicz 1984), although exceptions exist (Mayer 1987, Baldrian 2006). Laccases generally have a bell-shaped pH activity profiles for phenolic substrates, and optima in the pH range 4–6 (Hoffmann & Esser 1977, Palmieri et al. 1993, Eggert et al. 1996, Xu 1997, Chefetz et al. 1998, Schneider et al. 1999, Garzillo et al. 2001). At alkaline pH values the activity of laccase is negatively affected by the hydroxide ion inhibition, but positively affected by the lower redox potential of the substrates at higher pH values (Xu 1997).

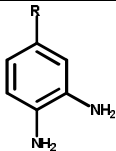
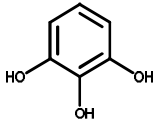
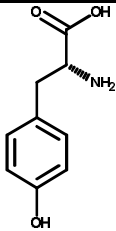
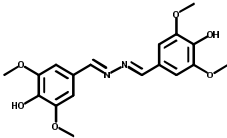
ABTS, guaiacol and 2,6-dimethoxyphenol (2,6-DMP) are substrates generally used to assay a laccase activities. Syringaldazine, tolidine, and *p*-phenylene diamine are considered specific substrates for laccases (Flurkey et al. 1995, Ramirez et al. 2004, Baldrian 2006), whereas L-tyrosine and *p*-cresol are typical substrates of tyrosinases (Käärik 1965). It has, however, been shown also that fungal laccases can oxidise L-tyrosine with a radical mechanism, nevertheless, the affinity and the activity of laccases on L-tyrosine is very low (Selinheimo et al. 2007a). The known substrates for fungal laccases are summarised in **Table 2**.

Small anions, such as azide, cyanide and fluoride ions are the most effective inhibitors of laccases: they bind to the trinuclear copper centre, preventing the binding of molecular oxygen (Solomon et al. 1996, Xu 1996a, Battistuzzi et al. 2003, Johnson et al. 2003). N-hydroxyglycine and cetyltrimethylammonium bromide are more specific inhibitors of laccases (Dawley & Flurkey 1993). EDTA, fatty acids, kojic acid, and coumaric acid are also laccase inhibitors, but they are less effective than small anions (Wood 1980b, Bollag & Leonowicz 1984, Faure et al. 1995, Eggert et al. 1996, Chefetz et al. 1998, Sethuraman et al. 1999, Xu et al. 1999, Jung et al. 2002).

Table 2. Summary of the known substrates of tyrosinase, catechol oxidase and laccase oxidative enzymes. The activity is reported with a plus sign (+) when an activity for the substrate has been reported, with a minus sign (-) when the enzyme is not active on the substrate, or with n.r. for “not reported” when there is no information available from literature. Relevant references are listed in the footnotes ^{a-c}.

Substrate	Structure	Activity		
		Tyrosinase ^a	Catechol oxidase ^b	Laccase ^c
Monophenols				
<i>p</i> -Substituted phenols		+	-	+ (Not tyrosine) ^d
<i>m</i> -Substituted phenols		-	-	+
<i>o</i> -Substituted phenols		-	+	+
Aromatic monoamines		+	-	+
Diphenols				
<i>p</i> -Substituted <i>o</i> -diphenols		+	+	+
<i>m</i> -Substituted <i>o</i> -diphenols		-	-	+
<i>p</i> -Substituted <i>o</i> -aminophenols		+	n.r.	+

1. Introduction

Substrate	Structure	Activity		
		Tyrosinase ^a	Catechol oxidase ^b	Laccase ^c
<i>p</i> -Substituted <i>o</i> -diamines		+	n.r.	+
Polyphenols				
Pyrogallol		+	+	+
Other polyphenols		+	+	+
Selective substrates				
L-tyrosine		+	-	- ^d
Syringaldazine		-	-	+
<i>p</i> -Phenylene diamine		-	-	+

^a Espín et al. 1998, Espín et al. 2000, Rodríguez-López et al. 2000, Fenoll et al. 2002, Selinheimo et al. 2006b, Xie et al. 2007.

^b Mayer & Harel 1979, Motoda 1979a, Motoda 1979b, Eicken et al. 1998, Walker & Ferrar 1998, Rompel et al. 1999b.

^c Flurkey et al. 1995, Xu 1996a, Xu et al. 1996, Ramirez et al. 2004, Baldrian 2006.

^d Oxidation of L-tyrosine by *Trametes hirsuta* laccase has been reported by Selinheimo et al. (2007a).

1.4 Active sites of copper-containing enzymes

The copper ions at the active sites of tyrosinases, catechol oxidases, and laccases are co-ordinated by His residues. Definition of the active sites is based on the co-ordination of

the copper ions (for a review, see Solomon et al. 1996, Solomon et al. 2001). Tyrosinase and catechol oxidase belong to the same family (PF00264) and contain a pair of copper ions, i.e., a type 3 (T3) copper site. A T3 copper site contains a pair of two antiferromagnetically coupled copper ions named CuA and CuB, and therefore the site is EPR-silent. Each copper ion is co-ordinated by three His residues. The T3 copper site shows an absorption maximum at a wavelength of 330–345 nm (Jolley et al. 1974). A T3 copper site is also found in haemocyanins, which are oxygen carrier proteins found in molluscs and arthropods (Cuff et al. 1998). Laccases (family PF00394) are multicopper oxidases and they contain four copper ions arranged as a type 1 (T1) copper site and a trinuclear centre formed by one T3 copper site and one type 2 (T2) copper site. The T1 copper site of laccases contains one copper ion co-ordinated by two His residues and one Cys residue. The T1 copper site has a strong absorption at 600 nm due to the $S(\text{Cys})\pi \rightarrow \text{Cu}_{dx^2-y^2}$ transition, which also creates the blue colour observed in the oxidised state. The T1 copper site also shows a weak absorption at the wavelengths of 400–485 nm caused by the $S(\text{Cys})\sigma \rightarrow \text{Cu}_{dx^2-y^2}$ transition. The T1 copper site in laccases is 13 Å from the trinuclear copper centre. The copper ions in the trinuclear copper centre are co-ordinated by eight His residues, of which six co-ordinate the T3 copper ions and two co-ordinate the copper ion of the T2 copper site in connection with one solvent molecule (e.g., water in *Trametes versicolor* laccase) (Bertrand et al. 2002). Both T1 and T2 copper sites are EPR-detectable.

Proteins containing only a T1 copper site are also known. These proteins, called cupredoxins, are electron transfer proteins. The copper ion in the T1 centre of cupredoxins is co-ordinated by two His residues and one Cys residues and by a weaker axial ligand, usually a Met residue (for a review, see Choi & Davidson 2011). Similarly, also enzymes containing only one T2 copper site are known, i.e., galactose oxidase (EC 1.1.3.9), primary-amine oxidase (EC 1.4.3.21) and diamine oxidase (EC 1.4.3.22). Galactose oxidase catalyses the two-electron oxidation of D-galactose to D-galactohexodialose with the concomitant two-electron reduction of oxygen to hydrogen peroxide. In galactose oxidase, the copper ion is co-ordinated by four equatorial ligands (two His residues, one Tyr residue, and one water) and one axial ligand (one Tyr residue). The axial Tyr residue is covalently linked to a Cys residue (Lee et al. 2008, Rokhsana et al. 2012). This Tyr-Cys cross-link participates in the reaction functioning as a second redox centre in the active state of the enzyme (for a review, see Rogers & Dooley 2003). Primary-amine oxidases and diamine oxidases catalyse the deamination of various amines to aldehydes with the concomitant two-electron reduction of oxygen to hydrogen peroxide. The copper ion is co-ordinated by three equatorial His ligands and one modified Tyr residue, i.e., 2,4,5-trihydroxyphenylalanine quinone (TOPA-quinone) (Parsons et al. 1995). Structures of the enzyme copper sites are shown in **Figure 2**.

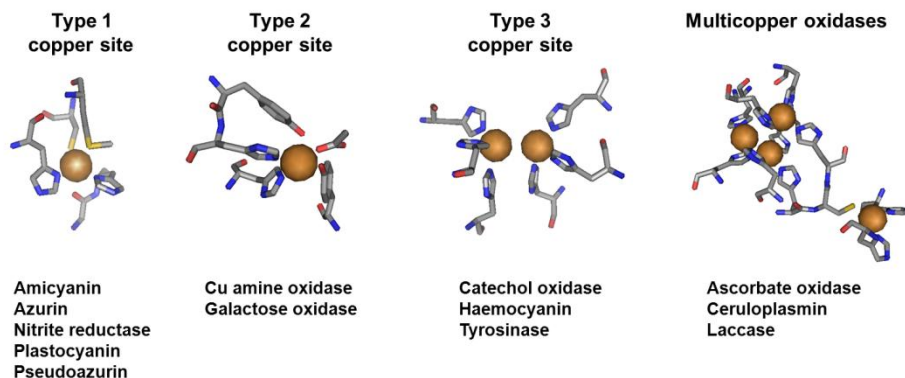


Figure 2. The structure of copper sites and examples of proteins containing these copper sites. Copper ions are illustrated in brown spheres. The figure was made using PyMOL (The PyMOL Molecular Graphics System, Educational Version Schrödinger, LLC) with PDB IDs 1PLC (plastocyanin), 1GOF (galactose oxidase), 1WX2 (tyrosinase), and 1GW0 (laccase).

1.5 Reaction mechanisms

1.5.1 Tyrosinases and catechol oxidases

The active sites of tyrosinases and catechol oxidase exist in different forms during the catalytic cycle: two oxidised forms *oxy*-form ($[\text{Cu}(\text{II})-\text{O}_2^2-\text{Cu}(\text{II})]$) and *met*-form ($[\text{Cu}(\text{II})-\text{OH}^--\text{Cu}(\text{II})]$), and a reduced unstable *deoxy*-form ($[\text{Cu}(\text{I})\text{Cu}(\text{I})]$) (Klabunde et al. 1998, Matoba et al. 2006).

The *met*- and *oxy*-form of tyrosinase and catechol oxidase have different spectroscopic features. While the *met*-form shows a weak absorption maximum at around 330–350 nm, the *oxy*-form shows a strong absorption at 345–350 nm and weaker absorption at 600 nm (Jolley et al. 1974, Himmelwright et al. 1980, Rompel et al. 1999a). The *deoxy*-form is not characterised as well as the *met*- and *oxy*-form, because it is unstable and rapidly binds molecular oxygen to generate the *oxy*-form. The *oxy*-form also shows two signals in Raman resonance spectroscopy, but the two signals are not detectable in the *met*-form of the enzyme. Early studies on the tyrosinase from *Agaricus bisporus* showed different circular dichroism (CD) spectra for the *oxy*- and *met*-form (Duckworth & Coleman 1970, Schoot Uiterkamp et al. 1976). All three forms are EPR-silent (Himmelwright et al. 1980, Wilcox et al. 1985). The *met*-form of tyrosinase or catechol oxidase can be transformed into the corresponding *oxy*-form of the enzyme by addition of hydrogen peroxide (Jolley et al. 1974, Rompel et al. 1999a, Rompel et al. 2012). Furthermore, the *met*-form can be partially reduced to *half-met*-tyrosinase $[\text{Cu}(\text{II})\text{Cu}(\text{I})]$, which is EPR-detectable (Himmelwright et al. 1980, van Gastel et al. 2000, Bubacco et al. 2003). The spectroscopic characteristics of T3 copper enzymes are summarised in **Table 3**.

Table 3. Spectroscopic features of the oxidised and reduced forms of type-3 (T3) copper enzymes.

Property of the active site	oxy-form	met-form	deoxy-form	References
Oxidation state of the copper ions	[Cu(II)-O ₂ ²⁻ Cu(II)]	[Cu(II)-OH ⁻ -Cu(II)]	[Cu(I) Cu(I)]	Himmelwright et al. 1980
Bridging molecule between the copper ions	H ₂ O ₂	H ₂ O	H ₂ O (unstable)	Tepper 2005
Signal in EPR spectroscopy	No	No	No	Himmelwright et al. 1980, Wilcox et al. 1985
Signal in UV/VIS absorption spectroscopy	345 nm (strong) 600 nm (weak)	330–340 nm (weak)	n.d.	Jolley et al. 1974, Hepp et al. 1979
Signal in circular dichroism spectroscopy	260 nm 350 nm	270 nm 290 nm	n.d.	Duckworth & Coleman 1970, Schoot Uiterkamp et al. 1976
Signal in emission fluorescence spectroscopy	330 nm	330 nm	330 nm	Beltramini & Lerch 1982
Signal in Raman spectroscopy	274 cm ⁻¹ 755 cm ⁻¹	n.d.	n.d.	Eickman et al. 1978, Rompel et al. 1999a

n.d. = not detected

Both the *oxy*- and the *met*- form of the tyrosinase oxidise diphenols (diphenolase catalytic cycle). In contrast, the oxidation of monophenols requires the presence of the *oxy*-form of the enzyme (monophenolase or cresolase cycle). One of the atoms of a molecular oxygen molecule that is bound to the *oxy*-form is incorporated in the *o*-position of the monophenolic substrate during the monophenolase cycle (Itoh et al. 2001). The product of tyrosinase-catalysed oxidation of monophenolic or diphenolic substrate is an *o*-quinone. After the *o*-quinone is released, the enzyme is left in the reduced *deoxy*-form. Molecular oxygen has high affinity to the *deoxy*-form and it rapidly binds to the active site, generating the *oxy*-form of tyrosinase (**Figure 3**).

The native form of a tyrosinase typically consists of about 85–90% *met*-form, with the rest being in the *oxy*-form (for a review, see Solomon et al. 1996). When monophenolic substrates are oxidised by tyrosinase, a lag period is usually detected. The lag is related to the state of the active site of the tyrosinase. During the lag period, the enzyme is transformed from the *met*-form to the *oxy*-form, which can oxidise the monophenolic substrate. The *met*-form oxidises the diphenolic substrate (e.g., L-DOPA) which is formed because of the non-enzymatic reactions.

Tyrosinases can oxidise a variety of *p*-substituted monophenols and diphenols other than L-tyrosine and L-DOPA. The affinity of a substrate to a tyrosinase strongly depends on the hydrophobic, steric, and electrostatic properties of the group in the *p*-position of the *o*-diphenol. It has been shown that when the diphenolic substrate has an electron-donating group in the *p*-position of the *o*-diphenol, the reaction mechanism will follow the diphenolase pathway. In contrast, when the substrate has a withdrawing-group in the *p*-position of the *o*-diphenol, the reaction mechanism leads the enzyme to a suicide inactivation pathway. In the suicide inactivation pathway, the tyrosinase is irreversibly inactivated by reduction and loss of one of the copper ion from the T3 copper site. Furthermore, certain monophenols can bind to the *met*-form of the enzyme but cannot be oxidised; this leads the enzyme into a dead-end pathway (for a recent review, see Muñoz-Muñoz et al. 2010b) (**Figure 3**).

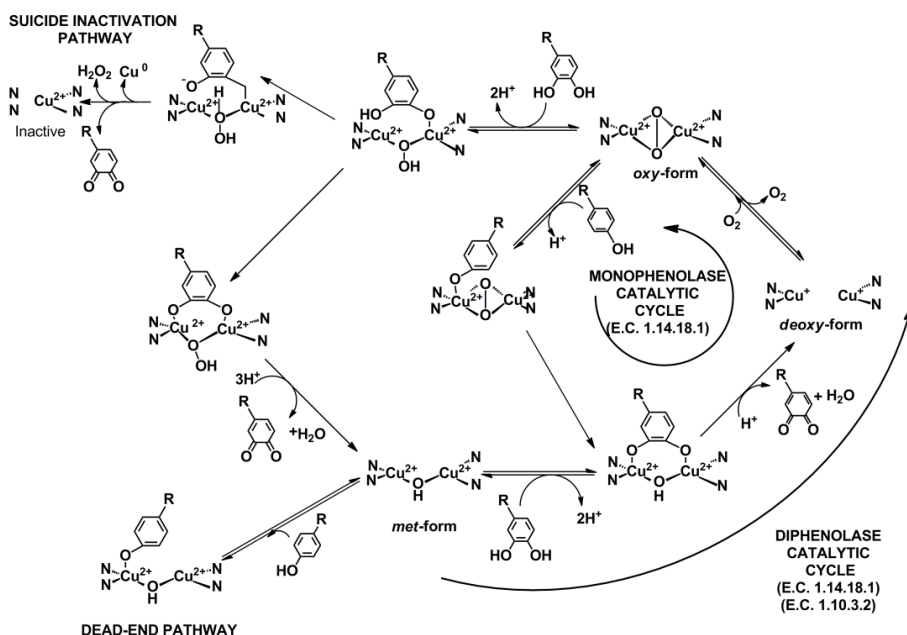


Figure 3. Molecular mechanism for the catalytic cycles of tyrosinase (EC 1.14.18.1) and catechol oxidase (EC 1.10.3.1). The monophenolase catalytic cycle occurs only for tyrosinase. The dead-end and suicide inactivation pathways are also represented (Figure modified from the review articles Kim & Uyama 2005, Muñoz-Muñoz et al. 2010a).

Catechol oxidases catalyse only the oxidation of *p*-substituted diphenols to quinones; but they do not catalyse the hydroxylation of *p*-substituted monophenols, so catechol oxidases cannot complete the monophenolase catalytic cycle (**Figure 3**) (Mayer & Harel 1979, Walker & Ferrar 1998, Gerdemann et al. 2002). Why a catechol oxidase does not show a monophenolase activity is not clearly understood. From the comparison of the three-dimensional structures of tyrosinase and catechol oxidase (see Subsection 1.6.1), it has been shown that the access to the active site of catechol oxidase is partly blocked by a Phe residue (i.e., Phe261 in *I. batatas* catechol oxidase). Furthermore, the corresponding Glu182 residue in *Streptomyces castaneoglobisporus* tyrosinase is smaller; therefore, the active site is more exposed in tyrosinase than in catechol oxidase. The Glu182 residue has been proposed as a putative residue in the orientation of the monophenolic substrate to the active site of tyrosinase (Decker et al. 2006). Thus far, the information on catechol oxidases has been limited, because most of the research has focused on tyrosinases, which appear more attractive also on account of the monophenolase activity.

In view of the three-dimensional structures of tyrosinases (see Subsection 1.6.1), different binding mechanisms of the *oxy-form* of tyrosinase have been proposed for monophenols (Decker et al. 2006, Matoba et al. 2006, Land et al. 2007, Ismaya et al. 2011, Sendovski et al. 2011). Based on the three-dimensional structure of *Streptomyces castaneoglobisporus* tyrosinase in complex with the caddie protein ORF378, Matoba et

al. (2006) proposed that the monophenolic substrate is oriented towards the second copper ion at the active site (CuB), in a similar way to the Tyr98 of the caddie protein. Divergently, Decker et al. (2006) suggested that one His co-ordinating the CuB orients the monophenolic substrate towards the first copper at the active site (CuA) via a hydrophobic interaction and that the hydroxyl group of the substrate binds to the CuA. The binding mechanism proposed by Decker et al. (2006) is supported by Olivares and Solano (2009) and Sendovski et al. (2011). On the basis of a directed-evolution study, Sendovski et al. (2011) suggested that monophenolic substrates bind to the CuA, in agreement with Decker et al. (2006), whereas diphenolic substrates bind to the CuB. In the mutant R209H of the tyrosinase from *Bacillus megaterium* (BmT), the newly introduced His residue blocks the entrance to the active site, interfering with the binding of L-DOPA to CuB. The activity of the mutant R209H of BmT is lower than the activity of the wild-type BmT on L-DOPA 1 mM, by a factor of 1.6 (Shuster Ben-Yosef et al. 2010, Sendovski et al. 2011).

L-tyrosine is the natural substrate of tyrosinase. The *o*-quinones generated by the tyrosinase-catalysed oxidation of L-tyrosine undergo a series of non-enzymatic oxidative and coupling reactions to form hetero-polymers. These reactions are called melanogenesis. Melanogenesis occurs in mammals, fungi and bacteria. In all cases tyrosinase catalyses the first step of this pathway, i.e., the formation of dopaquinone (*o*-quinone of L-DOPA) (Prota 1988). Dopaquinone is the product of a tyrosinase-catalysed oxidation of L-tyrosine and L-DOPA (Cooksey et al. 1997). The tyrosinase-catalysed step is the rate-limiting step in melanogenesis. The reactions following dopaquinone formation can proceed spontaneously at physiological pH (Halaban et al. 2002). The amount of melanins formed is proportional to the production of dopaquinone, and, thereby, to the tyrosinase activity. Melanins can be grouped into eumelanins and pheomelanins. Eumelanins are insoluble brown to black pigments and work as photoprotective antioxidants. Pheomelanins are alkali-soluble yellow to reddish-brown pigments and work as phototoxic pro-oxidants (Chedekel et al. 1980, De Leeuw et al. 2001, Takeuchi et al. 2004, Samokhvalov et al. 2005). Both eumelanins and pheomelanins are produced in melanogenesis and together they form the mixed melanins (**Figure 4**).

The eumelanin pathway occurs in the absence of sulphhydryl compounds and can be divided into two phases. The first is a proximal phase in which dopachrome is the end product. The second one is a distal phase, that represents the enzymatic and non-enzymatic reactions occurring from dopachrome to eumelanins (for a review, see Cooksey et al. 1997, Kim & Uyama 2005, Ito & Wakamatsu 2008). In the proximal phase dopaquinone undergoes the intramolecular addition of the amino group to produce leukodopachrome (known also as cyclodopa). A fast redox reaction between leukodopachrome and dopaquinone forms L-DOPA and dopachrome, which is an orange-red unstable compound (Raper 1927, Mason 1948, Canovas et al. 1982, Rodríguez-López et al. 1991). At neutral pH, dopachrome is gradually decarboxylated to 5,6-dihydroxyindole (DHI) (Raper 1927, Palumbo et al. 1987). In mammals, the dopachrome tautomerase activity converts dopachrome to 5,6-dihydroxyindole-2-carboxylic acid (DHICA) (Raper 1927, Palumbo et al. 1987, Aroca et al. 1990, Tsukamoto et al. 1992). DHI and DHICA are the main components of eumelanins (Swan & Waggott 1970, Swan 1974). The pheomelanin pathway occurs in the presence of sulphhydryl compounds (e.g., Cys), where a nucleophilic attack of the sulphhydroxyl group of a Cys on

the benzene ring of dopaquinone occurs and cysteinyl-dopa isomers are generated. The main isomer formed is 5-S-cysteinyl-dopa (5-S-CD), which is considered to be the precursor of the pheomelanins (Prota 1980).

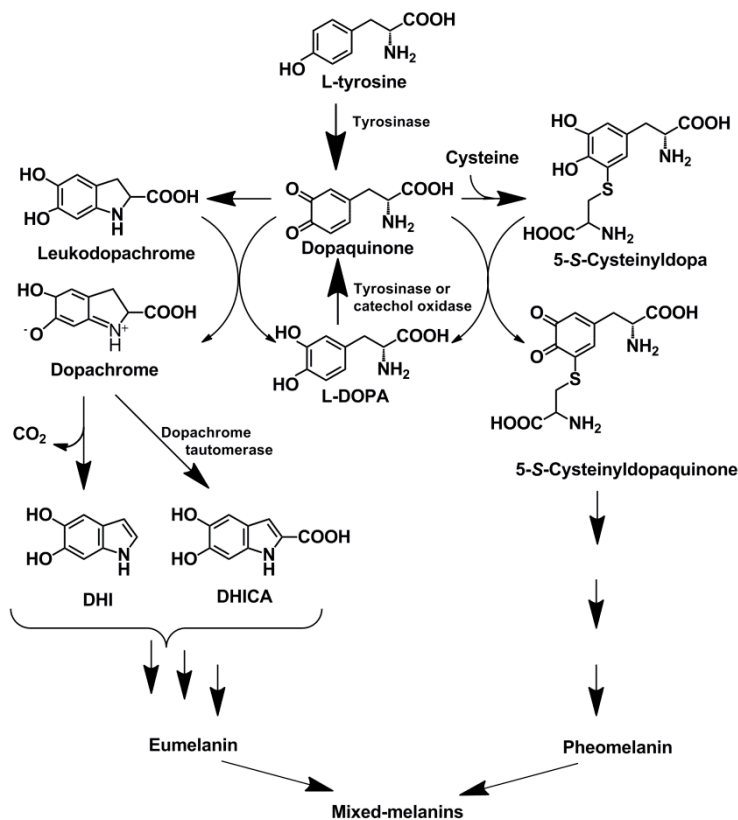


Figure 4. Early stages of the biosynthetic pathways leading to melanin production. 5,6-Dihydroxyindole (DHI) is formed by a spontaneous decarboxylation of dopachrome and 5,6-dihydroxyindole-2-carboxylic acid (DHICA) by a dopachrome tautomerase activity (Figure modified from the review article Ito & Wakamatsu 2008).

1.5.2 Laccases

Substrates for laccases include various compounds, such as diphenols, substituted phenols, diamines, aromatic amines, benzenethiols, and even inorganic compounds (Xu 1996a). Laccase catalyses the oxidation of these compounds with a radical mechanism. In one catalytic cycle, four electrons in all are removed from the substrate(s) and molecular oxygen is reduced to two molecules of water. In the resting form of laccase, the four copper ions are in an oxidised state. The substrate binds in a pocket close to the T1 copper site of laccase. A single electron is removed from the reducing group of the substrate molecule(s), e.g., the hydroxyl group of a phenolic substrate at the T1 copper

site. The electron is transferred to the trinuclear copper centre through a conserved His-Cys-His tripeptide (Messerschmidt et al. 1992, Bertrand et al. 2002, Piontek et al. 2002). The four-electron reduction of molecular oxygen to water takes place in the trinuclear copper centre (for a review, see Solomon et al. 1996, Solomon et al. 2001, Rodgers et al. 2009, Lundell et al. 2010). A peroxy intermediate is involved in the reduction of molecular oxygen to water. In the absence of reducing substrates (e.g., Phe-OH), the native intermediate slowly transforms into the resting oxidised form of laccase. On the contrary, in the case reducing substrates are available, the native intermediate can be fully reduced in concomitance with the oxidation of the substrates. Radiolabeling studies have shown that at the end of the catalytic cycle one of the oxygen atoms of molecular oxygen is bound as hydroxyl to the T2 copper site (Brändén & Deinum 1977, Brändén et al. 1978, Shin et al. 1996). A schematic representation of the catalytic cycle of laccases is shown in **Figure 5**.

From the three-dimensional structure of the multicopper oxidase ascorbate oxidase, it has been shown that access of the solvents to the trinuclear copper site is provided by a broad and a narrow channel (Messerschmidt et al. 1992). The same channels were found in the laccase from the basidiomycete fungus *Trametes versicolor* (Piontek et al. 2002). Differently, in the laccase from the ascomycete fungus *Melanocarpus albomyces*, only the narrow channel is found and the broad channel is occluded by the four conserved residues of the C-terminus (Asp-Ser-Gly-Leu/Val/Ile known as the C-terminal plug). Accordingly, the entrance of molecular oxygen and the exit of water may not occur via this tunnel in *M. albomyces* laccase. Furthermore, in the laccase from *M. albomyces*, the protons are also transferred from the T1 copper site to the trinuclear copper site via a triangle of amino acids (Ser, Ser and Asp), called a SDS-gate. The SDS-gate is conserved among the sequences of laccases from ascomycete fungi, but is not found in laccases of other origin, such as the laccase from *T. versicolor*, *Rigidoporus lignosus*, and *Bacillus subtilis* (Hakulinen et al. 2008).

Besides the affinity of the substrate to the active site of laccase, the laccase-catalysed reactions also depend on the redox potential of the substrate. The redox potential (E^0) of the substrate must be low enough, since the reaction depends on the difference between the redox potentials of the enzyme and the substrate (ΔE^0). The rate of laccase-catalysed oxidation of a phenolic substrate is expected to increase as the ΔE^0 increases. Furthermore, the E^0 of a phenolic substrate decreases with an increase of a pH value, thus the ΔE^0 increases. Hydroxyl ions inhibit laccases, and at high pH values the dissociation of the hydroxyl group of the phenolic substrate is more favourable; therefore inhibition of the laccase may occur (Xu 1996a, Xu 1997, Xu et al. 2000, Xu et al. 2001). The E^0 of laccases refers to T1 copper. Differently from the phenolic substrate, the E^0 of the T1 copper is not pH-dependent. The redox potential of fungal laccases is in the range of 0.4–0.8 V (Morpurgo et al. 1980, Xu 1996a, Palmer et al. 1999, Xu et al. 1999).

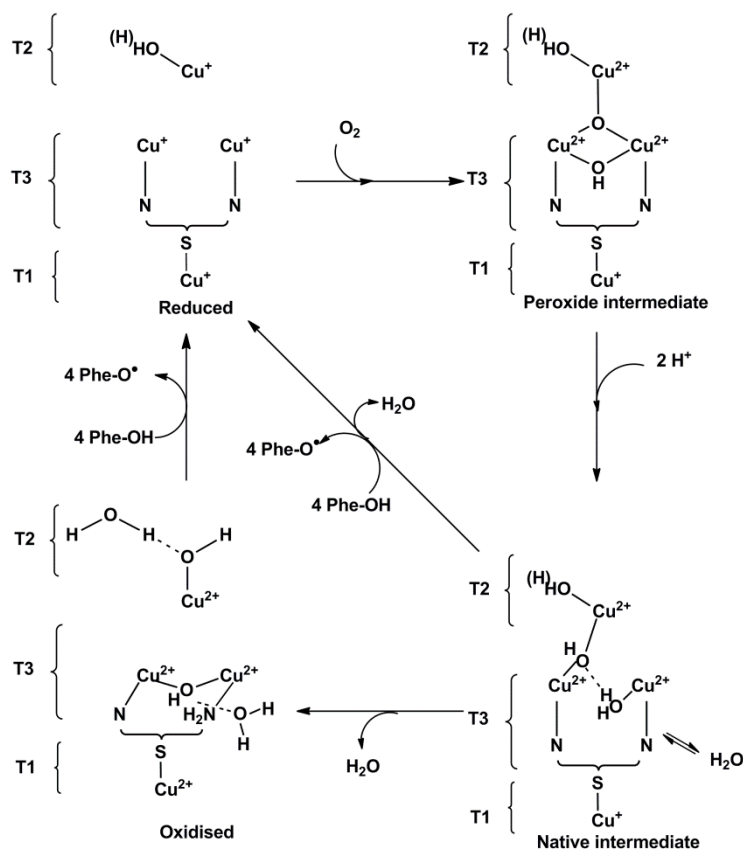


Figure 5. Catalytic cycle of laccase. Phe-OH is the phenolic substrate compound. Phe-O \cdot is the reactive phenoxyl radical. T1 is the type-1 copper centre, T2 is the type-2 copper centre, and T3 is the type-3 copper centre of laccase. (Figure modified from the review articles Solomon et al. 2001, Lee et al. 2002, Yoon et al. 2007)

1.6 Structures

1.6.1 Tyrosinases and catechol oxidases

The primary structures of tyrosinase and catechol oxidase are typically formed by three domains: an N-terminal domain, a central catalytic domain, and a C-terminal domain. The central catalytic domain contains the conserved His residues, which co-ordinate the two copper ions of the T3 copper site. Tyrosinases of animal and plant origins have all three domains, whereas tyrosinases of fungal origin lack the N-terminal domain. Tyrosinases of bacterial origin only have the central catalytic domain, but they are produced in association with a caddie protein that acts as a C-terminal domain. The N-terminal domain directs the protein to the chloroplast thylakoid lumen in plants and is involved in the maturation process of the tyrosinase. The role of the C-terminal domain is to cover

the active site of tyrosinase, keeping the enzyme inactive in the secretory pathway. Tyrosinases are usually activated by cleavage of the N- and C-terminal domains, or in the case of bacterial tyrosinases, by removal of the caddie protein (Marusek et al. 2006, Flurkey & Inlow 2008).

Until now, there have been three crystal structures of tyrosinases available, from *Streptomyces castaneoglobisporus* (ScT) (Matoba et al. 2006), from *Bacillus megaterium* (BmT) (Sendovski et al. 2011), and from *A. bisporus* (AbT) (Ismaya et al. 2011) (**Figure 6**), and two crystal structures of plant catechol oxidases, from *I. batatas* (IbCO) (Klabunde et al. 1998), and from *Vitis vinifera* (VvCO) (Virador et al. 2009) (**Figure 7**). The PDB IDs of the structures of tyrosinases and catechol oxidases are shown in **Table 4**.

The three-dimensional structure of tyrosinase is mainly α -helical. Two β -strands located in the N- and C-terminus of the central catalytic domain form a short parallel-sheet structure. The residues forming this short parallel-sheet structure are highly conserved and mark the beginning and the end of the central catalytic domain. The core of the enzyme is formed by a four-helix bundle where the catalytic dinuclear copper centre is located. The active site is lodged in the bottom of a large concavity, where the substrate is bound (Matoba et al. 2006, Ismaya et al. 2011, Sendovski et al. 2011).

The first three-dimensional structure presented for a tyrosinase is from *S. castaneoglobisporus* (ScT) (Matoba et al. 2006). The ScT three-dimensional structure was solved as a complex with a caddie protein, the dimensions of the heterodimer are 40 x 55 x 60 Å. The caddie protein is involved in the copper assembly, and in the secretion and activation of the enzyme. A Tyr residue (i.e., Tyr98) from the caddie protein occupies the putative substrate-binding site of ScT, but it is at a 3.0 Å distance from the active site, so too far away to be oxidised. The structure of the bacterial tyrosinase from BmT was solved with a resolution of 2.0–2.3 Å (Sendovski et al. 2011). BmT is a homodimer, the dimensions of each unit are 45 x 25 x 80 Å. Each unit contains an active site, with the two substrate-binding sites facing alternate directions. The structure of AbT was also very recently solved (Ismaya et al. 2011). This is the first structure revealed for a full-length tyrosinase of fungal origin. The enzyme is a tetramer composed of two heavy (H) chains and two light (L) chains, the dimensions of the tetramer are 139 x 97 x 59 Å. The active site is located in the H subunit, where it is lodged in the four-helix bundle as in ScT and BmT. The substrate-binding site is found at the bottom of a spacious cavity in the surface of the H subunit. The L chain has a β -trefoil fold, consisting of 12 antiparallel β -strands. The L chain is about 25 Å away from the active site and it does not hinder access to the active site. The L chain does not show any sequence or structure similarity to the caddie protein of ScT. The functional role of the L chain is not yet clear; it is possible that it plays a role in the folding, copper-binding, and stability of AbT *in vivo* (**Figure 6**) (Ismaya et al. 2011).

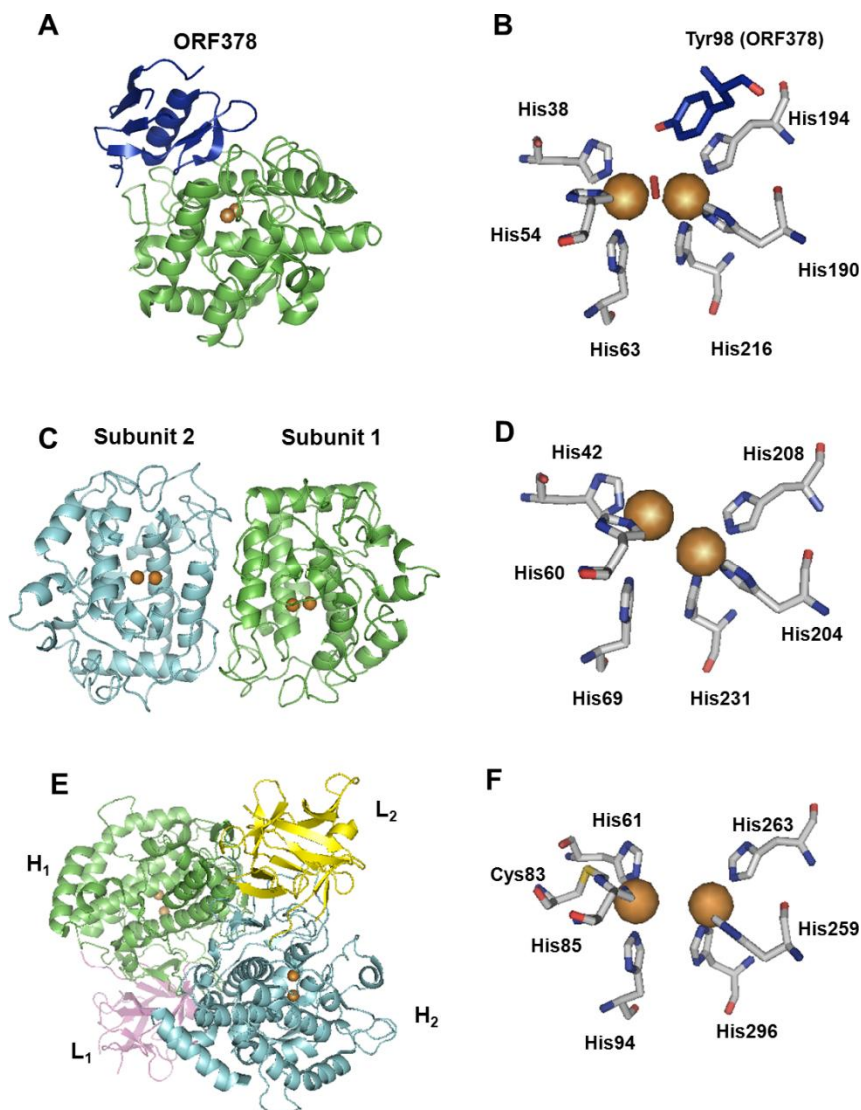


Figure 6. (A) Three-dimensional structure of *Streptomyces castaneoglobisporus* tyrosinase (PDB ID 1WX2) in complex with the caddie protein ORF378. The tyrosinase is in green and the caddie protein ORF378 in blue. (B) The active centre of *S. castaneoglobisporus* tyrosinase. (C) Homodimeric structure of *Bacillus megaterium* tyrosinase (PDB ID 3NM8). Subunit 1 and subunit 2 are shown in green and light blue, respectively. (D) Active centre of *B. megaterium* tyrosinase. (E) Tetrameric structure of *Agaricus bisporus* tyrosinase (PDB ID 2Y9W). Chains are shown as H (heavy chain) and L (light chain). (F) Active centre of *A. bisporus* tyrosinase. The copper ions in the active centre are shown with brown spheres, the bridging molecule in red and the thioether bond in yellow. The figure was created with PyMOL (The PyMOL Molecular Graphics System, Educational Version Schrödinger, LLC).

The first solving of a three-dimensional structure of a catechol oxidase from *I. batatas* (IbCO) was in 1998 (Klabunde et al. 1998) (**Figure 7**). IbCO is a monomer with dimensions 55 x 45 x 45 Å. The overall structure of IbCO is similar to that of tyrosinase, i.e., IbCO is mainly α -helical, and the short-parallel sheet structure formed by two β -strands located in the N-terminus and C-terminus of the central catalytic domain is also present. The active site of IbCO is found in the four-helix bundle as in ScT, but, differently from ScT, it is partially covered by a gatekeeper residue (i.e., Phe261 in IbCO), which shields the CuA and prevents the docking of a monophenolic substrate to the active site of catechol oxidase. IbCO contains a thioether bond between the C ϵ carbon of His109 (i.e., one copper ligand) and the sulphur of a Cys92 (Klabunde et al. 1998). The thioether bond was not found in ScT, and it has been suggested that the His54 of ScT co-ordinating CuB was flexible during catalysis, whereas in IbCO the flexibility of the corresponding residue His109 is restricted by the thioether bond. More recently, the thioether bond was also found in the structures of AbT (Ismaya et al. 2011) and VvCO (Virador et al. 2009). The Cys residue forming the thioether bond is also found in the sequence of the fungal tyrosinase from *N. crassa* (Lerch 1982). Hence, the presence or absence of the thioether bond and the flexibility of the His co-ordinating the CuB are not enough for elucidation of the different substrate-specificity of tyrosinases and catechol oxidases.

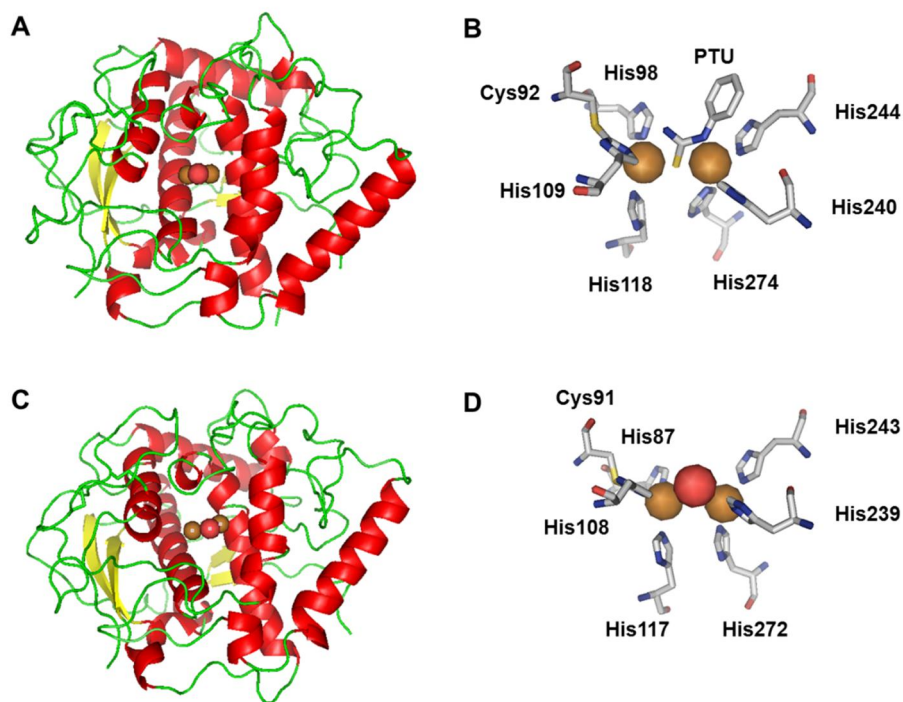


Figure 7. (A) Three-dimensional structure of *Ipomea batatas* catechol oxidase (PDB ID 1BT1). (B) Active centre of the phenylthiourea (PTU) inhibitor-bound *I. batatas* catechol oxidase. (C) Three-dimensional structure of *Vitis vinifera* catechol oxidase (PDB ID 2P3X). (D) Active centre of the *Vitis vinifera* catechol oxidase. The secondary structures are shown in red (α helix), yellow (β sheet), and green (loop). The copper ions are shown with brown spheres, the bridging molecule in red and the thioether bond in yellow. The figure was created with PyMOL (The PyMOL Molecular Graphics System, Educational Version Schrödinger, LLC).

1.6.2 Laccases

The three-dimensional structures of laccases published so far are of laccases of fungal and bacterial origins (**Table 4**). The three-dimensional structure of a plant laccase has not been solved yet. The first three-dimensional structure published was of the laccase from the basidiomycete fungus *Coprinopsis cinerea*, but it was T2 copper depleted (Ducros et al. 1998). The first complete three-dimensional structures of laccases became available in 2002, when the structures of the laccase both from the basidiomycete fungus *Trametes versicolor* (Bertrand et al. 2002, Piontek et al. 2002) and from the ascomycete fungus *M. albomyces* (Hakulinen et al. 2002) were published. Thus far, most of the three-dimensional structures of fungal laccases reported have been from basidiomycete fungi, such as *T. versicolor* (Bertrand et al. 2002, Piontek et al. 2002), *Rigidoporus lignosus* (Garavaglia et al. 2004), *Coriolus zonatus* (Zhukova et al. 2006, Lyashenko et al. 2007),

Lentinus tigrinus (Ferraroni et al. 2007), *Trametes trogii* (Matera et al. 2008), *Coriolopsis gallica* (De La Mora et al. 2008), *Cerrena maxima* (Lyashenko et al. 2007), and *Trametes hirsuta* (Polyakov et al. 2009). The only three-dimensional structure of an ascomycete fungus laccase published so far is from *M. albomyces* (Hakulinen et al. 2002, Hakulinen et al. 2006, Hakulinen et al. 2008). Among bacterial laccases, the structures published are from *Bacillus subtilis* (Enguita et al. 2003), *Escherichia coli* (Li et al. 2007), *Nitrosomonas europaea* (Lawton et al. 2009), and *Streptomyces coelicolor* (Skálová et al. 2011). Furthermore, a model of the plant laccase from *Populus trichocarpa* has been predicted through homology modelling approach using the ascorbate oxidase from zucchini (PDB ID 1AOZ) as a template, and it was compared to the bacterial laccase from *B. subtilis* and the fungal laccase from *T. versicolor* (for a review, see Dwivedi et al. 2011). Two examples of three-dimensional structures of laccases, from the ascomycete fungus *M. albomyces* and from the basidiomycete fungus *T. versicolor*, are presented in **Figure 8**.

Laccases of different origin share similar structural features. The overall structure of laccases consists of three cupredoxin-like domains (A, B, and C), with each domain having a “Greek key motif” β -barrel structure. The mononuclear T1 copper site is located in domain C. The putative substrate-binding site is in a cleft between domains B and C. The trinuclear T2/T3 copper cluster is located at the interface between domains A and C, with both domains providing residues for the co-ordination of the copper ions. The electrons are donated from the substrate to the copper ion of the T1 copper site, and subsequently they are transferred to the trinuclear site where the reduction of molecular oxygen to water occurs. Electron transfer from the T1 copper site to the T2/T3 copper cluster occurs via a His-Cys-His pathway. The substrate-binding sites of laccases are rather dissimilar, i.e., the bacterial laccase from *B. subtilis* has a larger putative substrate-binding site cavity as compared to the fungal laccases from *T. versicolor* (Dwivedi et al. 2011) and *M. albomyces* (Hakulinen et al. 2008). Messerschmidt et al. (1992) reported the presence of two solvent channels in the ascorbate oxidase from zucchini. A broad channel leads to the pair of copper ions at the T3 site, and a narrow channel leads to the T2 copper. Similar channels are found in laccases of fungal origin; however, in the laccase from *M. albomyces*, the broad channel is plugged by the C-terminal residues Asp-Ser-Gly-Leu (Hakulinen et al. 2002, Hakulinen et al. 2008). The four residues of the C-terminus are conserved also in other ascomycete laccases, so it is possible that the C-terminal plug is present also in these ascomycete laccases. The C-terminal plug is not found in the basidiomycete laccases. One characteristic feature of fungal laccases is that they are glycosylated proteins, typically with 3–10 glycosylation sites per monomer (Solomon et al. 1996, Rodgers et al. 2009). The functional role of the glycans in laccases is not yet clear.

Recently, the three-dimensional structures of two-domain laccases have been established. Two-domain laccases are smaller than the three-domain laccases, but they are surprisingly temperature stable and have high activity on typical substrates of laccases, such as 2,6-dimethoxy phenol (2,6-DMP). The two-domain laccase from *Nitrosomonas europaea* was characterised already in 1985 (DiSpirito et al. 1985), but the three-dimensional structure was published only recently (Lawton et al. 2009). The three-dimensional structure of a two-domain laccase from *Streptomyces coelicolor* (Skálová et al. 2009) is also known. The three-dimensional structure of two-domain laccases is a

homotrimer, with each monomer is comprised of two cupredoxin-like domains (domain 1 and domain 2). The T1 copper site is in domain 1, and the trinuclear site is embedded in the inter-molecular interface between the subunits (Komori et al. 2009, Lawton et al. 2009, Skálová et al. 2011).

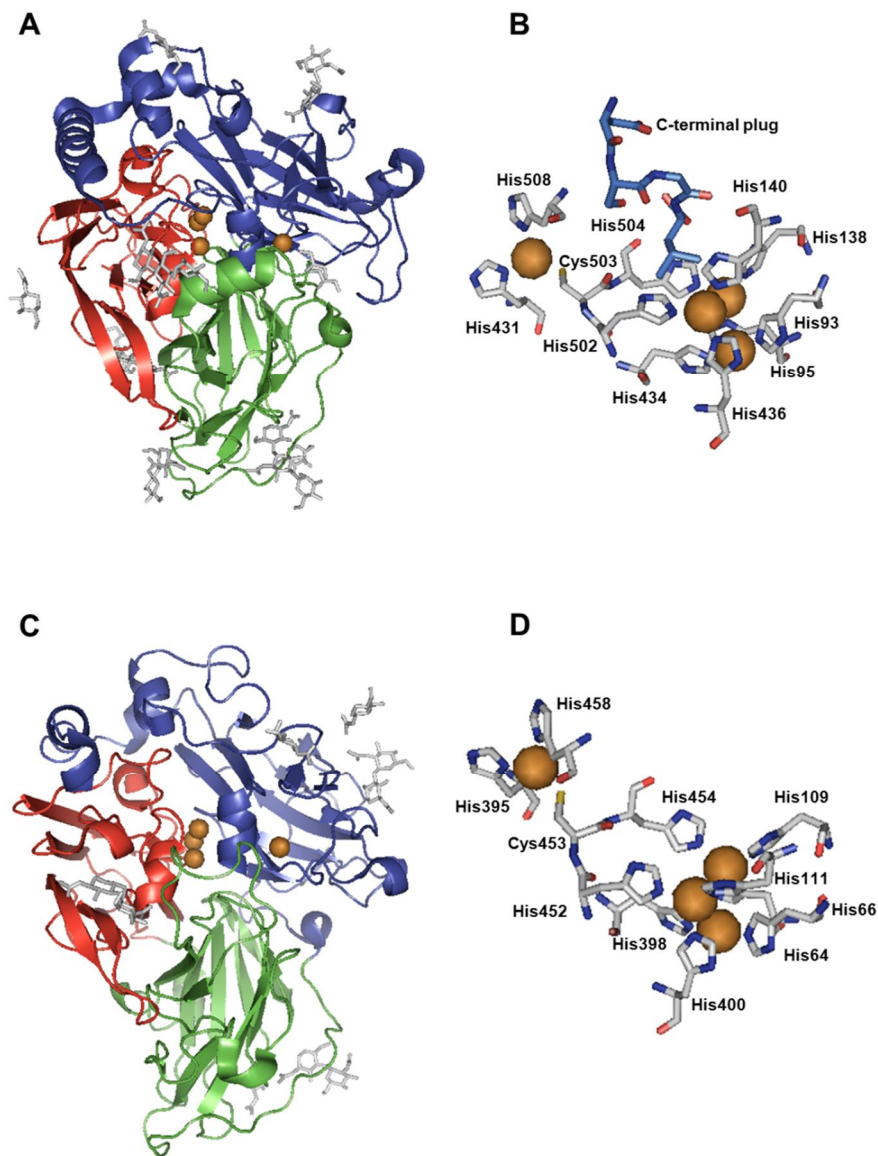


Figure 8. (A) Three-dimensional structure of the laccase from ascomycete fungus *Melanocarpus albomyces* (PDB ID 1GWO). (B) Active centre of *M. albomyces* laccase. The C-terminal plug (Asp556-Ser557-Gly558-Leu559) is also shown. (C) Three-dimensional structure of the laccase from basidiomycete fungus *Trametes versicolor* (PDB ID 1GYC). (D) Active centre of *T. versicolor* laccase. Domain A is represented in red, domain B in green, and domain C in blue. The copper ions are represented with brown spheres. The figure was created with PyMOL (The PyMOL Molecular Graphics System, Educational Version Schrödinger, LLC).

Table 4. Summary of the crystal structures of tyrosinase, catechol oxidase and laccase available from RCSB PDB (www.pdb.org).

Enzyme	Kingdom	Species	PDB ID	Best resolution (Å)	References
Tyrosinase	Bacteria	<i>Bacillus megaterium</i>	3NM8, 3NPY, 3NQ0, 3NQ1, 3NQ5, 3NTM	2.00 Å	Sendovski et al. 2011
Tyrosinase	Bacteria	<i>Streptomyces castaneoglobbisorus</i>	1WXC, 1WX2, 1WX4, 1WX5, 2AHK, 2AHL, 2ZMX, 2ZMY, 2ZMZ, 2ZWD, 2ZWE, 2ZWF, 2ZWG, 3AWS, 3AWT, 3AWU, 3AWV, 3AWW, 3AWX, 3AWY, 3AWZ, 3AX0	1.16 Å	Matoba et al. 2006, Matoba et al. 2011
Tyrosinase	Fungi	<i>Agaricus bisporus</i>	2Y9W, 2Y9X	2.30 Å	Ismaya et al. 2011
Catechol oxidase	Plantae	<i>Ipomea batatas</i>	1BT1, 1BT2, 1BT3, 1BUG	2.50 Å	Klabunde et al. 1998
Catechol oxidase	Plantae	<i>Vitis vinifera</i>	2P3X	2.20 Å	Virador et al. 2009
Laccase	Bacteria	<i>Bacillus subtilis</i>	1GSK, 1OF0, 1UVW, 1W6L, 1W6W, 1W8E, 2BHF, 2WSD, 2X87, 2X88	1.60 Å	Enguita et al. 2003
Laccase	Bacteria	<i>Escherichia coli</i>	2FQD, 2FQE, 2FQF, 2FQG, 2ZWN, 1Z9T	1.54 Å	Li et al. 2007
Laccase ^a	Bacteria	<i>Nitrosomonas europaea</i>	3G5W	1.90 Å	Lawton et al. 2009
Laccase ^a	Bacteria	<i>Streptomyces coelicolor</i>	3CG8, 3KW8	2.29 Å	Skálová et al. 2009, Skálová et al. 2011

Enzyme	Kingdom	Species	PDB ID	Best resolution (Å)	References
Laccase	Fungi	<i>Cerrrena maxima</i>	2H5U, 3DIU	1.76 Å	Lyashenko et al. 2007
Laccase	Fungi	<i>Coprinopsis cinerea</i> (<i>Coprinus cinereus</i>)	1A65, 1HFU	1.68 Å	Ducros et al. 1998
Laccase	Fungi	<i>Coriolus zonatus</i>	2HZH	2.60 Å	Lyashenko et al. 2007
Laccase	Fungi	<i>Corioloopsis gallica</i>	4A2H, 2VDZ, 2VE0	1.70 Å	De La Mora et al. 2008
Laccase	Fungi	<i>Melanocarpus albomyces</i>	1GW0, 2IH8, 2IH9, 2Q90, 3DKH, 3FU7, 3FU8, 3FU9, 3QPK	1.30 Å	Hakulinen et al. 2002, Hakulinen et al. 2006, Hakulinen et al. 2008, Andberg et al. 2009, Kallio et al. 2009
Laccase	Fungi	<i>Lentinus tigrinus</i>	2QT6	1.50 Å	Ferraroni et al. 2007
Laccase	Fungi	<i>Trametes hirsuta</i>	3FPX, 3PXL	1.20 Å	Polyakov et al. 2009
Laccase	Fungi	<i>Trametes</i> sp. AH28-2	3KW7	3.44 Å	Ge et al. 2010
Laccase	Fungi	<i>Trametes trogii</i>	2HRG, 2HRH	1.58 Å	Matera et al. 2008
Laccase	Fungi	<i>Trametes versicolor</i>	1GYC, 1KYA	1.90 Å	Bertrand et al. 2002, Piontek et al. 2002
Laccase	Fungi	<i>Rigidoporus lignosus</i>	1V10	1.70 Å	Garavaglia et al. 2004

^a Two-domain laccase

1.7 Applications of tyrosinases and laccases

Among tyrosinases, catechol oxidases, and laccases, laccases are the only commercially available enzymes for industrial purposes and they are already used on a large scale in the textile industry. The tyrosinase from the edible mushroom *Agaricus bisporus* is commercially available for research purposes, whereas catechol oxidase preparations are not available. Several potential applications of tyrosinases and laccases in food and non-food processes have been reported, whilst only a few promising applications for catechol oxidases have been described. Moreover, several potential applications that use catechol oxidase, and monophenolase activity have been reported without a clear indication of whether the enzyme applied is a tyrosinase or a catechol oxidase. Indeed, catechol oxidases could be utilised as an alternative to tyrosinases in the oxidation of diphenolic substrates. It is worth noticing that most of the research on tyrosinases and catechol oxidases focuses on their inhibition mechanism, because of the interest in the related reactions of browning and hyperpigmentation (see Subsection 1.5.1). However, more recently interest in the utilisation of tyrosinases has rapidly increased. Food- and non-food-related applications of tyrosinases, catechol oxidases, and laccases are discussed below and summarised in **Table 5** and **Table 6**.

1.7.1 Food-related applications

1.7.1.1 Development in the organoleptic properties of food products

The enzymatic activity of tyrosinases, catechol oxidases and laccases present in fruits and seeds and in the microbes associated with fruits and seeds are exploited in the fermentation processes of black tea, coffee, cocoa, and black raisins. They confer organoleptic properties and colour on the final food products (for a review, see Yoruk & Marshall 2003). In the fermentation process of tea leaves, tyrosinase can oxidise the catechins to theaflavins. Theaflavins, antioxidant compounds with an orangish colour, impart colour and brightness to the black tea and reduce the astringency, i.e., the dry feeling in the mouth of black tea liquors (Subramanian et al. 1999).

Tyrosinases and laccases have been shown to have a positive effect in the fermentation of cocoa beans. Tyrosinase from *A. bisporus* can oxidise the polyphenols that contribute to astringency, thus improving the taste of cocoa (Selamat et al. 2002). Also laccase from *Pleurotus osteratus* has been shown to reduce the tannin content of cocoa. Tannins have astringency properties and negatively affect the digestion process by binding to various digestive enzymes (Mensah et al. 2012).

1.7.1.2 Cross-linking reactions related to food applications

A cross-linking reaction introduces a covalent bond between proteins (homo-cross-link) or between a protein and a carbohydrate (hetero-cross-link). Cross-linking reactions can be used for food structure modification and can affect the sensory properties of the final product. Laccases and tyrosinases can be used to cross-link proteins. The reactive residues in proteins are Gln, Lys, Tyr, and Cys.

Tyrosinase can oxidise protein-bound Tyr residues to the corresponding quinone, which can further react with protein-bound Lys, Tyr, and Cys residues (Ito et al. 1984, Bittner 2006, Mattinen et al. 2008a, Mattinen et al. 2008b, Selinheimo et al. 2008). As compared to other fungal and plant tyrosinases, the extracellular tyrosinase from the fungus *T. reesei* has shown extremely good cross-linking abilities for random coil proteins such as α -caseins (Selinheimo et al. 2007a, Selinheimo et al. 2007b, Selinheimo et al. 2008, Monogioudi et al. 2009, Ercili Cura et al. 2010) as well as short tyrosine-containing peptides (Mattinen et al. 2008b). However, application of *T. reesei* tyrosinase in the food industry is so far limited by the formation of undesired colour (Monogioudi et al. 2009).

Differently from that with tyrosinases, laccase-catalysed cross-linking is based on the formation of free radicals, which, in turn, can further react with other phenolic radicals or free aromatic and amino groups present in proteins. Laccases act on the protein-bound Tyr, Trp, and Cys residues. Laccases can act also on ferulic acid and *p*-coumaric acid residues, which are present in arabinoxylans and pectins (for a review, see Harjinder 1991). Among laccases, the effects of the fungal laccase from *T. hirsuta* have been extensively investigated in the baking applications (Selinheimo et al. 2006a, Selinheimo et al. 2007a, Selinheimo et al. 2008).

Other than laccases and tyrosinases several enzymes are known to be able to cross-link proteins. For example, peroxidase (EC 1.11.1.7), and sulphhydryl oxidase (EC 1.8.3.3) have also been extensively studied (for a review see Buchert et al. 2007, Buchert et al. 2010). Transglutaminase (EC 2.3.2.13) reacts with protein-bound Gln and Lys residues, resulting in the formation of an isopeptide linkage. During the reaction, one molecule of ammonia is generated per a cross-link (Folk & Finlayson 1977, Griffin et al. 2002). A transglutaminase from *Streptovercillium mobaraense* was the first cross-linking enzyme to see a market launch (Ando et al. 1989). At present, microbial transglutaminases are the only commercially available food-grade proteins directly cross-linking enzymes.

Table 5. Food related applications of tyrosinases and laccases. Industrial applications are indicated with *** when the enzyme is commercially available, the commercial name and the distributor are also indicated in brackets. Pilot-scale developed applications are indicated with **, and applications tested at research-level are indicated with *.

Food related applications	Tyrosinase	Laccase	References
Development of organoleptic properties ^a	Removal of polyphenols during fermentation of cocoa beans* Oxidation of catechins to theaflavins during fermentation of black tea leaves* Better flavour in coffee*	Removal of tannins during fermentation of cocoa beans*	Subramanian et al. 1999, Selamat et al. 2002, Mensah et al. 2012
Baking	Increased softness of bread crumbs and added volume for bread*	Improved loaf volume, dough-handling, and crumb structure of bread*	Si 1994, Labat et al. 2000, Labat et al. 2001, Selinheimo et al. 2007a
Beverages		Cork stopper treatment (Suberase [®] , Novozymes)*** Wine and beer stabilisation* Clarification of juices*	Conrad et al. 2000, Minussi et al. 2002, Minussi et al. 2007
Dairy	Cross-linking of dairy proteins*	Cross-linking of dairy proteins*	Færgemand et al. 1998, Thalmann & Lötzbeyer 2002, Halaoui et al. 2005, Selinheimo et al. 2006a, Selinheimo et al. 2007a, Selinheimo et al. 2008
Emulsions	Improved emulsifying properties via conjugation of different types of proteins and polysaccharides*	Stabilisation of beet pectin emulsions*	Kato et al. 1991, Kato et al. 1993, Littoz & McClements 2008
Meat	Increased firmness of myofibrillar gels*	Improved forming of myofibrillar gels at high salt concentrations* Decreased formation of myofibrillar gels with high laccase dosage*	Lantto et al. 2005b, Lantto et al. 2007

^a Endogenous enzymes are utilised in these applications.

1.7.2 Non-food-related applications

1.7.2.1 Large-scale applications of laccases

A laccase from ascomycete fungus *Myceliophthora thermophila* distributed by Novozymes with the commercial name of Suberase[®] is used in the preparation of cork stoppers for wine bottles. Cork is a desirable stopper material; however, frequently a cork taint (i.e., an off-flavour) is conveyed to the wine in contact with the cork. The enzymatic treatment polymerises phenolic compounds in the cork and thus reduces the astringency, bitterness, and tannic flavour imparted to the wine by the cork (Conrad et al. 2000).

In some applications, laccases are used in combination with mediators in so-called laccase mediator systems (LMS). Mediators are small molecules with a redox potential (E°) between the E° of the laccase and the E° of the substrate. Mediators are used to oxidise bulky substrates that could not be oxidised by laccase alone. Thus the use of a mediator enlarges the substrate-specificity of the laccase. In LMS, the laccase first oxidises the mediator, and subsequently a redox reaction occurs between the oxidised mediator and the substrate. The reaction products are the oxidised substrate and the reduced mediator, which can often be recycled. The first LMS to bleach denim garments (i.e., to decolourise indigo) was developed with a laccase from *M. thermophila* and the mediator methyl ester of syringic acid (Berka et al. 1997). This LMS oxidises indigo, and the reaction products are two molecules of isatin, which is a colourless chemical more biodegradable than indigo. Currently there are various commercial laccase preparations available for bleaching of denim (for a review, see Galante & Formantici 2003, Rodriguez Couto & Toca Herrera 2006). For instance DeniLite (Novozymes) utilises a laccase from *Aspergillus niger* (Niladevi 2009).

Laccases have also been used in the enzymatic removal of lignin. The LignoZym[®] system (GmbH) utilises a laccase from *T. versicolor* and a group of mediators containing N-OH-, N-oxide-, oxime- or hydroxamic acid-functional groups to remove lignin from pulp. The LignoZym[®] system has been tested on pilot-scale, and it has been shown that 50–70% of lignin can be removed within 1–4 hours (for a review, see Call & Mücke 1997). Moreover, the combination of a laccase from *T. hirsuta* with cellulases has been shown to increase the sugar yield in the enzymatic hydrolysis of steam-pre-treated softwood by 13% (Palonen & Viikari 2004). Generally, the industrial applicability of the LMS has suffered on account of high costs, recycling, and toxicity of the mediators used (Bourbonnais & Paice 1992).

1.7.2.2 Other potential non-food applications of tyrosinases and laccases

Tyrosinases and laccases may be used in non-food applications, but these enzymes are not yet utilised in large-scale applications. Tyrosinase- and laccase-catalysed cross-linking may be used in tailoring biopolymers: e.g., the softness of wool fibres can be increased via tyrosinase or laccase-cross-linking of the fibres (Lantto et al. 2005a, Freddi et al. 2006, Jus et al. 2008, Mattinen et al. 2008b). Tyrosinase-catalysed cross-linking may be utilised in grafting of carboxyl groups to chitosan with potential application in cosmetics (Chao et al. 2004), as well as to immobilise antibodies on membranes with potential for applications in microarray technology (Ahmed et al. 2006).

The oxidation of phenols catalysed by tyrosinases, catechol oxidases and laccases has a potential application in biosensors (e.g., quantification of phenols) and in bioremediation (i.e., removal of phenols). Phenols are commonly found in industrial waste waters and can have toxic effects. Some phenols are endocrine disruptors: i.e., they are able to mimic or antagonise the effects of endogenous hormones. Therefore, the detection of low concentrations of phenols is of fundamental importance (Mita et al. 2007). Several tyrosinase-based biosensors have been proposed (for a review, see Dong & Chen 2002). A biosensor based on *A. bisporus* tyrosinase was tested for the determination of bisphenol A, which can be found in food and drink packaging (Mita et al. 2007). A catechol oxidase electrode made with a catechol oxidase from *Solanum melangena* L. (eggplant) immobilised in gelatine was found to be a specific biosensor for catechol and to be stable for 70 days (Dinckaya et al. 1998).

Laccases have potential in decolourisation of brewers and olive-mill waste waters. One laccase from *Corioloopsis gallica* has been suggested as an efficient tool to remove the colourful tannins seen in brewery waste waters (Yagüe et al. 2000). The efficacy of an immobilised laccase from *Lentinula edodes* has been tested for removal of toxic phenols from oil-mill effluents. This system was most effective on *o*-diphenols (D'Annibale et al. 2000).

Biofuel cells are devices that convert chemical energy into electrical energy via electrochemical reactions catalysed by oxidoreductases. The electrons for production of electricity are produced via the enzymatic oxidation of a fuel (sugar or alcohol) at the bioanode of the fuel cell. The electrons are transferred to the biocathode and gained by the electron acceptor, typically molecular oxygen or peroxide, through an enzymatic reaction. Laccases have been investigated in biofuel applications (Palmore & Kim 1999, Lim & Palmore 2007, Smolander et al. 2008).

Tyrosinases, catechol oxidases, and laccases may be used in medical applications, such as drug development and diagnostics. Thus far, of the three enzymes, tyrosinases have been the most studied in this field. Human tyrosinase is overexpressed in melanosome malignant cells. A vaccine against melanosome that uses specific antibodies for tyrosinase has been developed and successfully passed phase I clinical trials (Chen et al. 1995, Bergman et al. 2003, Liao et al. 2006). Also, a melanocyte-directed enzyme prodrug therapy (MDEPT) has been developed. The prodrug is a tyrosinase substrate (dopamine) linked to a drug (phenyl mustard) by a carbamate linkage. The tyrosinase-catalysed oxidation of dopamine releases the drug *in situ* (Morrison et al. 1985, Jordan et al. 1999, Jordan et al. 2001). L-DOPA, used as a drug for treatment of Parkinson's disease, is currently chemically produced (Knowles 2003). A cost-effective means of enzymatic production of L-DOPA has been proposed, with immobilised tyrosinase used to oxidise L-tyrosine to dopaquinone and ascorbic acid used to reduce dopaquinone to L-DOPA (Carvalho et al. 2000).

The catechol oxidase from *I. batatas* has potential application in the medical field in the quantitative determination of L-DOPA and carbidopa in pharmaceutical preparations. L-DOPA is used as a neurotransmitter against Parkinson's disease, and carbidopa is often present in the same preparation with L-DOPA as an inhibitor of decarboxylase activity. The catechol oxidase oxidation products of L-DOPA and carbidopa absorb at different wavelengths so can be detected and quantified (Fatibello-Filho & da Cruz Vieira 1997).

A laccase system has been proposed as an alternative to a peroxidase system to convert iodide to iodine, which is used as a disinfectant. This laccase system allows *in situ* production of iodine and, differently from the peroxidase system, does not require the presence of hydrogen peroxide, which is a harmful chemical. The laccase used in this system is from *Myceliophthora thermophila* (Xu 1996b). Laccases from *Trametes* sp. have potential application in the synthesis of novel antibiotics: i.e., laccases catalyse the amination of catechols with amino- β -lactams to produce antibiotics, such as cephalosporins, penicillins, and carbacephems (Mikolasch et al. 2006, Mikolasch et al. 2008).

Table 6. Non-food related applications of tyrosinases and laccases. Industrial applications are indicated with *** when the enzyme is commercially available, the commercial name and the distributing company are also indicated in brackets. Pilot-scale level applications are indicated with **, and applications tested at research-level are indicated with *.

	Tyrosinase	Laccase	References
Non-food-related applications			
Biosensors and biofuel cells	Electrodes in pure organic phase* Quantification of polar organic solvents* Biosensor of phenol* Phenols and amines degradation* Catechol oxidation* Phenolic compound polymerisation* Pesticides detection (based on inhibition)*	Detection of phenolic compounds* Detection of oxygen* Detection of azides* Immobilised in the biocathode of biofuel cells*	Yaropolov et al. 1995, Dinckaya et al. 1998, Palmore & Kim 1999, Streffer et al. 2001, Minussi et al. 2002, Chao et al. 2004, Busch et al. 2006, Gill et al. 2006, Lim & Palmore 2007, Liu & Dong 2007, Mita et al. 2007, Smolander et al. 2008, Akyilmaz et al. 2010
Medical field	Melanosome vaccine (clinical trials)** Treatment of malignant melanoma in the form of a melanocyte-directed enzyme prodrug therapy (MDEPT)* Production of L-DOPA as a drug for Parkinson's treatment* Grafting of phenolic moieties or proteins onto chitosan to create hydrogels for skin substitutes* Immobilisation of antibody via tyrosinase-catalysed reaction*	Skin lightening* <i>In-situ</i> generation of iodine (disinfectant)* Production of antibiotics* Glucose determination* Detection of morphine* Hair dyes*	Morrison et al. 1985, Roure et al. 1992, Chen et al. 1995, Aaslyng et al. 1996, Fatibello-Filho & da Cruz Vieira 1997, Lang & Cotteret 1998, Jordan et al. 1999, Carvalho et al. 2000, Jordan et al. 2001, Takada et al. 2003, Ahmed et al. 2006, Liao et al. 2006, Littoz & McClements 2008
Textile industry		Denim finishing (DeniLite® and DeniLite IIs®, Novozymes; Zylite®, ZylTex)*** Synthesis of dyes* Decolourisation of dyes-house	Reyes et al. 1999, Setti et al. 1999, Wong & Yu 1999, Abadulla et al. 2000, Galante & Formantici 2003, Peralta-Zamora et al. 2003, Ossola & Galante 2004, Pazarlioglu et al. 2005, Zille et al.

Non-food-related applications	Tyrosinase	Laccase	References
Lignocellulose processing	<ul style="list-style-type: none"> effluents* Bleaching of cotton* Rove scouring* Dyeing of wool* Anti-shrinkage treatment for wool* 	<ul style="list-style-type: none"> Lignin modification (Lignozym[®], GmbH and Novozym[®] 51003, Novozymes)** Pulp-bleaching* 	<ul style="list-style-type: none"> 2005, Rodriguez Couto & Toca Herrera 2006 Bourbonnais & Paice 1992, Bourbonnais et al. 1997, Poppius-Levlin et al. 1999, Palonen & Viikari 2004, Camarero et al. 2007, Gutiérrez et al. 2007
Tailoring of biopolymers by means of cross-linking reactions	<ul style="list-style-type: none"> Grafting of chitosan to silk proteins* Grafting of peptides or fluorescent proteins to chitosan* Modification of wool fibres* Protein cross-linked chitosans with adhesive properties* Protein cross-linked chitosans for use as matrices for drug delivery* 	<ul style="list-style-type: none"> Modification of wool fibres* 	<ul style="list-style-type: none"> Lantto et al. 2005a, Freddi et al. 2006, Anghileri et al. 2007
Nanotechnology	<ul style="list-style-type: none"> Modification of surfaces of nano-scale structures* 		<ul style="list-style-type: none"> Basnar et al. 2007
Bioremediation and decontamination of feed	<ul style="list-style-type: none"> Xenobiotic compounds' removal* 	<ul style="list-style-type: none"> Oxidation of polycyclic aromatic hydrocarbons and chlorophenols* Removal of dioxins and polychlorinated biphenyls from fishmeal* 	<ul style="list-style-type: none"> Torres et al. 2003, Zille et al. 2005, Baron et al. 2007, Martin et al. 2007, Canfora et al. 2008

2. Aims of the work

The overall aim of the work was to characterise oxidative cross-linking enzymes that can be used for cross-linking of proteins, as well as proteins with carbohydrates in industrial food production. The work focused on the characterisation of three oxidoreductases: catechol oxidase, tyrosinase, and laccase.

The aims of the work at more detailed level were:

1. Biochemical and structural characterisation of a novel catechol oxidase from the fungus *Aspergillus oryzae*. The gene encoding for the *A. oryzae* catechol oxidase belongs to the newly discovered short-tyrosinases sequence group (Publication II and unpublished).
2. Detailed characterisation of the extracellular tyrosinase from the fungus *Trichoderma reesei* in terms of substrate-specificity and inhibition, and comparison with the commercially available tyrosinase from *Agaricus bisporus* (Publications I and IV).
3. Elucidation of the oxidation capacity of fungal laccases using a set of laccases with different redox potential and a set of substituted phenolic substrates with different redox potential. The laccases used in this work were the basidiomycete laccase from *Trametes hirsuta* and the ascomycete laccases from *Thielavia arenaria* and *Melanocarpus albomyces* (Publication III).
4. Evaluation of the cross-linking ability of catechol oxidase from *A. oryzae*, tyrosinases from *T. reesei* and *A. bisporus* and laccases from *T. hirsuta*, *T. arenaria*, and *M. albomyces* through the use of α -casein proteins as a model substrate (unpublished).

3. Material and methods

A summary of the materials and methods used in the work is presented in this Chapter, detailed descriptions can be found in the original articles (I–IV).

3.1 Substrates and inhibitors

The substrates and inhibitors used in this work are listed in **Table 7**. Various low-molecular-weight monophenolic and diphenolic compounds were used for determination of the substrate-specificity of tyrosinases and catechol oxidase. Tripeptides were used as a simplified model of protein bound tyrosine for tyrosinases. A range of small chemical compounds were tested for analysis of the inhibition of *Trichoderma reesei* tyrosinase (TrT). 2,2'-Azino-bis(3-ethylbenzthiazoline-6-sulphonic acid) (ABTS), 2,6-dimethoxy phenol (2,6-DMP), syringic acid, and methyl syringate were used specifically for the laccase work (Publication III), and α -casein proteins were used as model proteins for assaying of the cross-linking ability of the enzymes.

3.2 Enzymes

The enzymes studied in this work are listed in **Table 8**. TrT was produced and purified as described by Selinheimo et al. (2006b). The intracellular tyrosinase from *Agaricus bisporus* (AbT) was purchased from Sigma-Aldrich and purified as described in Publication I. The extracellular catechol oxidase from *Aspergillus oryzae* (AoCO₄) was produced in *T. reesei* under the *cbhI* promoter and purified as described in Publication II. Laccase 1 from *Thielavia arenaria* (TaLcc1) was produced and purified as described in Publication III. Laccase from *Trametes hirsuta* (ThL) was produced and purified as described by Rittstiegl et al. (2002), and laccase from *Melanocarpus albomyces* (rMaL) was produced and purified as described in Kiiskinen et al. (2004).

Table 7. Substrates and inhibitors used in this work.

Common name	IUPAC name	Supplier	Studied in publication
2,6-DMP	2,6-Dimethoxy phenol	Aldrich	III
4-Aminophenol	4-Aminophenol	Aldrich	II
4- <i>tert</i> -Butylcatechol	4- <i>tert</i> -Butylbenzene-1,2-diol	Fluka	I–II, Unpublished
ABTS	2,2'-Azino-bis(3-ethylbenzthiazoline-6-sulphonic acid)	Roche	III
Aniline	Phenylamine	Sigma	I
Benzaldehyde	Benzaldehyde	Fluka	IV
Benzoic acid	Benzoic acid	Merck	I, IV
Caffeic acid	3,4-Dihydroxycinnamic acid	Fluka	I–II, IV
α -Caseins		Calbiochem	Unpublished
(+)-Catechin hydrate	<i>trans</i> -3,3',4',5,7-Pentahydroxyflavane	Sigma	II
Catechol	1,2-Dihydroxybenzene	Fluka	I–II, Unpublished
<i>p</i> -Coumaric acid	<i>trans</i> -4-Hydroxycinnamic acid	Sigma	I, IV
L-DOPA	3,4-Dihydroxy-L-phenylalanine	Fluka	I–II, IV
L-Dopamine	4-(2-Aminoethyl)benzene-1,2-diol	Sigma	I
(-)-Epicatechin	(-)- <i>cis</i> -3,3',4',5,7-Pentahydroxyflavane	Sigma	II
GGY	Glycine-glycine-tyrosine	Bachem	I
Guaiacol	2-Methoxyphenol	Sigma	II
GYG	Glycine-tyrosine-glycine	Bachem	I
Hydrogen peroxide	Dihydrogen dioxide	Merck	Unpublished
Hydroxycaffeic acid	3-(3,4-Dihydroxyphenyl) propanoic acid	Aldrich	I–II
Kojic acid	5-Hydroxy-2-(hydroxymethyl)-4H-pyran-4-one	Merck	IV
MBTH	3-Methyl-2-benzothiazolinone hydrazone	Sigma	I
Methyl syringate	Methyl 3,5-dimethoxy-4-hydroxybenzoate	Aldrich	III
Phenol	Hydroxybenzene	Merck	I–II
Phloretic acid	3-(4-Hydroxyphenyl) propanoic acid	Aldrich	I
Potassium cyanide	Potassium cyanide	Merck	IV
L-Tyramine	2-(4-Hydroxyphenyl) ethylamine	Sigma	I
L-Tyrosine	3-(4-Hydroxyphenyl)-L-alanine	Sigma	I–II, IV
<i>p</i> -Tyrosol	2-(4-Hydroxyphenyl) ethanol	Aldrich	I–II
Sodium azide	Sodium azide	Merck	IV
Syringic acid	4-Hydroxy-3,5-dimethoxybenzoic acid	Fluka	III
YGG	Tyrosine-glycine-glycine	Bachem	I

Table 8. Enzymes studied in this work.

Enzyme	Origin	Abbreviation	Reference	Studied in publication
Tyrosinase (EC 1.14.18.1)	<i>Trichoderma reesei</i>	TrT	Selinheimo et al. 2006b	I, IV
	<i>Agaricus bisporus</i>	AbT	Purchased from Sigma-Aldrich	I, IV
Catechol oxidase (EC 1.10.3.1)	<i>Aspergillus oryzae</i>	AoCO4	Produced and purified as described in Publication II	II, Unpublished
Laccase (EC 1.10.3.2)	<i>Thielavia arenaria</i>	TaLcc1	Produced and purified as described in Publication III	III
	<i>Trametes hirsuta</i>	ThL	Rittstieg et al. 2002	III
	<i>Melanocarpus albomyces</i> (recombinant)	rMaL	Kiiskinen et al. 2004	III

3.3 Enzyme activity assays

Tyrosinase activity was measured with 15 mM L-DOPA or 2 mM L-tyrosine as the substrate. Activity assays were performed in 0.1 M phosphate buffer pH 7.0 at 25 °C, either by monitoring of dopachrome formation at 475 nm ($\epsilon_{\text{dopachrome}}=3400 \text{ M}^{-1} \text{ cm}^{-1}$) as described by Robb (1984) or by monitoring of the consumption of the co-substrate molecular oxygen, with a single-channel fibre-optic oxygen meter for mini-sensors (Precision sensing GmbH, Regensburg, Germany) as described by Selinheimo et al. (2006b).

Catechol oxidase activity was measured with 15 mM catechol and 15 mM 4-*tert*-butylcatechol (TBC) as substrates. Activity assays were performed at 25 °C in 0.1 M phosphate buffer pH 7.0, with monitoring of the quinone formation at 400 nm ($\epsilon_{\text{quinone}}=1450 \text{ M}^{-1} \text{ cm}^{-1}$; $\epsilon_{\text{o-tert-butylquinone}}=1200 \text{ M}^{-1} \text{ cm}^{-1}$) as described by Robb (1984).

Laccase activity was measured with ABTS as a substrate. Activity assays were performed at 25 °C in 25 mM succinate buffer pH 4.5, with the product formation monitored at 436 nm ($\epsilon_{\text{product}}=29300 \text{ M}^{-1} \text{ cm}^{-1}$) as described by Niku-Paavola et al. (1988).

3.4 Production and purification of enzymes

3.4.1 Production and purification of catechol oxidase from *Aspergillus oryzae* (Publication II)

The putative tyrosinase protein sequences were retrieved via the VTT in-house database (Arvas et al. 2007). The putative tyrosinase AoCO4 gene (Entrez gene ID 5990879) was amplified by PCR from the genomic DNA of the *A. oryzae* strain VTT-D-88348. The AoCO4 gene was ligated into the *T. reesei* expression construct pMS186 to create the plasmid pGF007. The construct pGF007 was transformed into *T. reesei* strain VTT-D-00775 (Penttilä et al. 1987). Transformants were selected as described by Selinheimo et al. (2006b). Based on shake flask cultures, the best overexpressing transformant of AoCO4 was grown in a bioreactor of a volume of 10 L.

For purification of AoCO4, a concentrated culture supernatant was first desalted on a PD-10 desalting column (Sephadex G-25 medium, GE Healthcare) in 20 mM sodium acetate buffer, pH 4.8. The desalted sample was applied to a HiPrep™ 16/10 CM Sepharose Fast Flow column (20 mL volume, Amersham Biosciences, Uppsala, Sweden), in 20 mM sodium acetate buffer, pH 4.8. Bound proteins were eluted with a linear NaCl gradient (0–150 mM in 20 column volumes) in the equilibration buffer. Catechol-positive fractions were pooled, concentrated with a Vivaspin concentrator (20 mL, 5000-Da MWCO; Vivascience, Hannover, Germany), and subjected to anion-exchange chromatography in a ResourceQ column (6 mL volume, Amersham Biosciences, Uppsala, Sweden) in 10 mM Tris-HCl buffer, pH 7.2. Bound proteins were eluted with a linear NaCl gradient (0–150 mM in 20 column volumes) in the equilibration buffer. Active fractions were pooled, concentrated, and stored at –20 °C in aliquots. SDS-PAGE (12% Tris-HCl Ready Gel, Bio-Rad) was performed according to Laemmli (1970). Coomassie Brilliant Blue (R350; Pharmacia Biotech, St Albans, UK) was used for staining the proteins, and prestained SDS-PAGE standards (Broad Range, Cat no. 161-0318) were used for the determination of molecular weight.

3.4.2 Production and purification of laccase from *Thielavia arenaria* (Publication III)

Thielavia arenaria laccase 1 (TaLcc1) was produced at Roal Oy (Rajamäki, Finland) with *T. reesei* used as a host organism, as described by Paloheimo et al. (2006).

For purification of TaLcc1, a concentrated culture supernatant was first desalted on a Sephadex G-25 M column (70 mL volume, Pharmacia Biotech, Uppsala, Sweden) in 5 mM Tris-HCl buffer pH 8.5. The desalted sample was applied to a DEAE Sepharose Fast Flow column (70 mL volume, Amersham Biosciences, Uppsala, Sweden), in 5 mM Tris-HCl buffer, pH 8.5. Bound proteins were eluted with a linear sodium sulphate gradient (0–100 mM in 6 column volumes) in the equilibration buffer. ABTS-active fractions were pooled, concentrated with a Vivaspin concentrator (20 mL, 10000-Da MWCO; Vivascience, Hannover, Germany), and subjected to anion-exchange chromatography in a ResourceQ column (6 column volume, Amersham Biosciences, Uppsala, Sweden) pre-equilibrated in 5 mM Tris-HCl buffer pH 8.5. Bound proteins were eluted with a linear sodium sulphate gradient (0–100 mM in 20 column volumes) in the equilibration buffer.

ABTS-active fractions were pooled, concentrated with a Vivaspin concentrator (20 mL, 10000-Da MWCO; Vivascience, Hannover, Germany). Subsequently, the buffer was changed to 20 mM Tris-HCl pH 7.2 on a PD-10 desalting column (Sephadex G-25 medium, GE Healthcare).

3.5 Biochemical characterisation of enzymes

3.5.1 Biochemical and structural characterisation of catechol oxidase from *Aspergillus oryzae* (Publication II and unpublished results)

The isoelectric point of AoCO4 was determined by isoelectric focusing on an LKB 2117 Multiphor II Electrophoresis System. Catecholase activity was visualised by staining of the gel with 15 mM 4-*tert*-butylcatechol (TBC) in 0.1 M phosphate buffer, pH 7.0, and proteins were visualised via Coomassie Blue staining. The molecular weight of AoCO4 was determined by MALDI-TOF MS with an Ultraflex TOF/TOF instrument (Bruker Daltonik, Bremen, Germany). Tryptic peptides were analysed by MALDI-TOF MS. The N-terminus of AoCO4 was sequenced with a PE Biosystems Procise Sequencer (PE Biosystems, Foster City, CA, USA) on the basis of Edman degradation as described by Kiiskinen et al. (2002).

Determination of the pH optimum of AoCO4 was carried out at 25 °C with 15 mM TBC as a substrate in 50 mM sodium acetate buffer in the pH range 4.0–5.6, in 50 mM phosphate buffer in the pH range 5.8–8.0, and in 50 mM Tris-HCl buffer in the pH range 7.5–8.6. The stability of AoCO4 at different pH-values was determined through incubation of the enzyme at different pHs at 25 °C for one, two, and three days in 50 mM Mcllvaine universal buffer, and with measurement of the residual activity on TBC as described in Section 3.3. Temperature stability of AoCO4 was determined with the enzyme placed at 30 °C, 40 °C, 50 °C, and 60 °C in Tris-HCl buffer, pH 7.2, with measurement of the residual activity on TBC as described in Section 3.3.

The substrate-specificity of AoCO4 was qualitatively evaluated on the basis of following the colour change of the substrate visually after 30 minutes of incubation of the enzyme with different substrates: L-tyrosine, *p*-coumaric acid, tyramine, phloretic acid, phenol, 4-aminophenol, tyrosol, 4-mercaptoethanol, guaiacol, creasol, aniline, caffeic acid, hydrocaffeic acid, dopamine, L-DOPA, 3,4-dihydroxy-D-phenylalanine (D-DOPA), catechol, TBC, ABTS, (-)-epicatechin, and (+)-catechin at 25 °C. All the substrates tested were dissolved in 0.1 M phosphate buffer, pH 7.0, to a final concentration of 15 mM, except L-tyrosine, which was used in 2 mM final concentration. Kinetic constants K_M , V_{max} , and k_{cat} of AoCO4 on catechol, caffeic acid and hydrocaffeic acid were determined by means of spectrophotometric measurements at 25 °C in 0.1 M phosphate buffer, pH 7.0, monitoring the quinone formation at 400 nm for catechol and TBC ($\epsilon_{\text{quinone}}=1450 \text{ M}^{-1} \text{ cm}^{-1}$; $\epsilon_{\text{0-tert-butylquinone}}=1200 \text{ M}^{-1} \text{ cm}^{-1}$), and at 460 nm for hydrocaffeic acid ($\epsilon_{\text{quinone}}=1120 \text{ M}^{-1} \text{ cm}^{-1}$) (Waite 1976). The enzyme concentration was 6.4 mM (0.25 mg mL⁻¹) with all the three substrates. The Michaelis–Menten curves for determination of K_M , V_{max} , and k_{cat} were obtained by curve-fitting analysis with the GRAPHPAD PRISM 4.01 program (GraphPad Software Inc., San Diego, CA, USA).

For the characterisation of the secondary structure of AoCO4, intrinsic fluorescence intensity measurements were carried out by means of a Varian Cary Eclipse Fluorescence Spectrophotometer according to Gheibi et al. (2005), and far UV (250–190 nm) circular dichroism (CD) spectra were recorded on a Jasco model J-720 CD spectrophotometer as described by Boer and Koivula (2003). The UV/VIS absorption spectra were obtained with a Varian Cary 100 Bio spectrophotometer at 25 °C using a quartz cuvette (1 cm path length). Titration of AoCO4 with hydrogen peroxide (H₂O₂) was performed in 10 mM Tris-HCl buffer, pH 7.2. The spectrum was recorded immediately after an addition of equivalents (0–10 equivalents) of hydrogen peroxide to a solution containing AoCO4 (0.1 mM). Difference spectra of AoCO4 were obtained by subtracting a spectrum of the native AoCO4 from that of H₂O₂ treated AoCO4. The percentage of oxy-form present in the native form of AoCO4 was calculated as relative to the 100% oxy-form of AoCO4 generated after addition of 10 equivalents of H₂O₂ using the following equation:

$$\text{oxy – form in native AoCO4 (\%)} = \frac{\left(\frac{A_{350}}{A_{280}}\right) \text{ of native AoCO4}}{\left(\frac{A_{350}}{A_{280}}\right) \text{ of 10 eq. H}_2\text{O}_2 \text{ treated AoCO4}} * 100$$

Crystallisation experiments were performed via the hanging-drop vapour-diffusion method in Linbro 24-well plates and the commercial screens Crystal Screen (Hampton Research) and Clear Strategy Screen (Molecular Dimensions) as described by Kaljunen et al. (2011). Several optimisation screens were done and the best measurable crystals grew in a solution containing 12% PEG 8000, 10% ethanol, 0.2 M magnesium chloride, and 0.1 M acetate buffer, pH 4.5. The X-ray data from crystals of a preparation containing both processed and non-processed forms of AoCO4 were collected at DESY beam line X12, whereas the X-ray data from crystals of a preparation containing only the processed form of AoCO4 were collected at ESRF beam line ID14-1. X-ray data analysis of these crystals is still in progress.

3.5.2 Biochemical characterisation of tyrosinase from *Trichoderma reesei* (Publications I and IV)

The substrate specificity of TrT and AbT was analysed on small mono- and diphenolic compounds and tyrosine-containing tripeptides. Kinetic constants K_M and V_{max} of TrT and AbT with the small mono- and diphenolic compounds were determined in line with the enzymatic reaction by spectrophotometer as described in Section 3.3. The enzyme concentrations of TrT and AbT were 3.8 $\mu\text{g mL}^{-1}$ and 3.1 $\mu\text{g mL}^{-1}$, respectively for the monophenols and 0.9 $\mu\text{g mL}^{-1}$ and 0.8 $\mu\text{g mL}^{-1}$, respectively for the diphenols. Kinetic constants K_M , V_{max} and k_{cat} for TrT and AbT with the tyrosine-containing peptides were determined on the basis of the consumption of the co-substrate oxygen during the enzymatic reaction. The enzyme concentrations of TrT and AbT were 22 $\mu\text{g mL}^{-1}$ and 17 $\mu\text{g mL}^{-1}$, respectively.

The oxidation of L-DOPA by TrT and AbT was also followed by mass spectrophotometry, using a 4.7-T Bruker APEX-Qe Fourier-transform ion cyclotron resonance (FT-ICR) mass spectrometer (Bruker Daltonics, Billerica, MA, USA) in the negative mode. Ions of interest were further isolated by mass-selective quadrupole, and

subsequently irradiated with IR-photons for infrared multiphoton dissociation (IRMPD). Enzymatic oxidation of L-DOPA to dopachrome by tyrosinases was carried out at 25 °C in 0.1 M ammonium acetate solution pH 7.0. The reaction was started by an addition of the tyrosinase (15 µg mL⁻¹) to L-DOPA (1 mM) solution, and the formation of dopachrome was followed by mass spectrophotometry at predetermined time intervals.

To evaluate the product inhibition of TrT, dopachrome was prepared via 30 minutes' enzymatic oxidation of 5 mM L-DOPA with AbT (0.7 mg mL⁻¹) at 25 °C in 0.1 M sodium acetate buffer, pH 5.6. The enzyme was removed by means of ultracentrifugation in a Vivaspin concentrator (20 mL, 5000-Da MWCO; Vivascience, Hannover, Germany). The concentration of the dopachrome formed in the solution was calculated from the intensity of absorbance at 475 nm, with the extinction coefficient $\epsilon_{\text{dopachrome}}=3400 \text{ M}^{-1} \text{ cm}^{-1}$. Dopachrome product inhibition of TrT was analysed by oxygen consumption measurements at 25 °C in 0.1 M sodium acetate buffer, pH 5.6. The reaction mixture typically contained 8 mM L-DOPA and had a varying concentration of dopachrome (from 0 to 1.5 mM). The enzyme concentration of TrT was 7 µg mL⁻¹.

The inhibition of TrT by potassium cyanide, sodium azide, arbutin, kojic acid, benzaldehyde, and benzoic acid was analysed with caffeic acid and *p*-coumaric acid used as substrates. The reactions were carried out in 0.1–15 mM substrate and 0–60 mM inhibitor concentrations at 25 °C in 0.1 M phosphate buffer, pH 7.0. The enzyme concentrations were 3 µg mL⁻¹ for caffeic acid and 6 µg mL⁻¹ for *p*-coumaric acid oxidation. The initial rate of product formation was determined as the increase of absorbance at wavelength 480 nm per minute for caffeic acid and at 360 nm per minute for *p*-coumaric acid. The type of inhibition and the K_i constant for each inhibitor were determined, with the data plotted as Lineweaver-Burk and Dixon plots. The Cornish plot was used for determination of the K_i' constant.

3.5.3 Determination of kinetic parameters of laccases from *Thielavia arenaria*, *Melanocarpus albomyces*, and *Trametes hirsuta* (Publication III)

Kinetic parameters K_M and V_{max} , for the laccases *rMaL*, *TaLcc1*, and *ThL* were determined at 25°C with 2,6-DMP, syringic acid, and methyl syringate both in 25 mM succinate buffer, pH 4.5 and in 40 mM MES buffer, pH 6.0. Kinetic measurements were performed by spectrophotometric assay, following the product formation at specific wavelengths as described in Section 3.3. The kinetic parameters were calculated via curve-fitting analysis by means of the GRAPHPAD PRISM 4.01 program (GraphPad Software Inc., San Diego, CA, USA). The pH optima of the three laccases were measured at 25 °C with a substrate concentration of 1.7 mM in McIlvaine's universal buffer at pHs from 2 to 8.

3.5.4 Enzymatic cross-linking of α -caseins by catechol oxidase, tyrosinases, and laccases (Unpublished results)

The ability of catechol oxidase (AoCO4), tyrosinases (TrT and AbT), and laccases (*TaLcc1*, *rMaL*, and *ThL*) to cross-link model protein α -caseins was studied as described by Selinheimo et al. (2007b), with few modifications. α -Casein proteins were dissolved in

0.1 M phosphate buffer, pH 7.0, at a concentration of 3 g L⁻¹. Also studied was the potential of a cross-linking agent, i.e., a small phenolic molecule to induce cross-linking reactions. Catechol (2 mM) was used a cross-linking agent in the cross-linking experiments with catechol oxidase- or tyrosinase, whereas *p*-coumaric acid (2 mM) was the cross-linking agent in the experiments with laccase. The enzyme dosages were 10, 100 and 1000 nkat g⁻¹ of α -caseins. The activity of AoCO₄, TrT, and AbT was measured on catechol, while that of TaLcc1, rMaL, and ThL on ABTS. The corresponding amounts of protein used were 1, 10, and 100 mg of AoCO₄ g⁻¹ of α -caseins, 0.016, 0.16, and 1.6 mg of TrT g⁻¹ of α -caseins, 0.011, 0.11, and 1.1 mg of AbT g⁻¹ of α -caseins. The enzymatic incubations with α -caseins were performed at 25 °C for two and 24 hours, after which the samples were transferred to 95 °C for ten minutes for inactivation of the enzymes. The enzymes' efficiency in cross-linking the α -caseins was monitored through SDS-PAGE analysis with Criterion strain-free 4–20% gradient gels (BioRad).

4. Results and discussion

4.1 Biochemical and structural characterisation of a catechol oxidase from *Aspergillus oryzae* (Publication II and unpublished results)

4.1.1 Discovery and production of *Aspergillus oryzae* catechol oxidase

A bioinformatics approach was used to discover novel fungal extracellular tyrosinases. The VTT in-house data base of public genomes of fungi (Arvas et al. 2007) was searched for sequences containing the tyrosinase Interpro entry (IPR002227) and an N-terminal signal sequence. In total, 134 sequences were retrieved, of which 114 sequences had the HA1-X(n)-HA2-X(8)-HA3 and HB1-X(3)-HB2-X(n)-HB3 pattern for the CuA and CuB site of tyrosinases and catechol oxidases. The 114 sequences clearly fell into two groups on the basis of their length. Proteins with a length of 500–800 amino acids were named “long tyrosinases” while proteins with a length 300–500 amino acids as “short tyrosinases”. Both long and short tyrosinases contained the conserved residues for tyrosinases, the conserved N-terminal Arg residue, the C-terminal “tyrosine motif” (Y-X-Y/F or Y/F-X-Y), and the two conserved His patterns, that co-ordinate the two copper ions at the active site of tyrosinases and catechol oxidases (Flurkey & Inlow 2008).

Three main differences between the long and short tyrosinases were found: a) the histidine pattern of CuA was HA1-X(7)-HA2-X(8)-HA3 in the short tyrosinases, whereas it was HA1-X(n)-HA2-X(8)-HA3, with n=20–23 amino acids in the long tyrosinases; b) the short tyrosinases presented a stop codon a few residues after the conserved C-terminal “tyrosine motif” and, accordingly, the linker region and the C-terminal domain were absent in these sequences; and c) a novel conserved pattern of six Cys was found in the short tyrosinases, but not in the long tyrosinases (**Figure 9**). The short tyrosinase sequence from *Aspergillus oryzae* (AoCO4; UniProtKB: Q2UNF9; Entrez gene ID: 5990879) had 14.7% overall amino acid sequence homology with the sequence of *Trichoderma reesei* tyrosinase (TrT), which has been shown to have excellent cross-linking properties (Selinheimo et al. 2007b). The *A. oryzae* short tyrosinase gene was chosen for cloning and expression as a representative of short putative tyrosinase proteins.

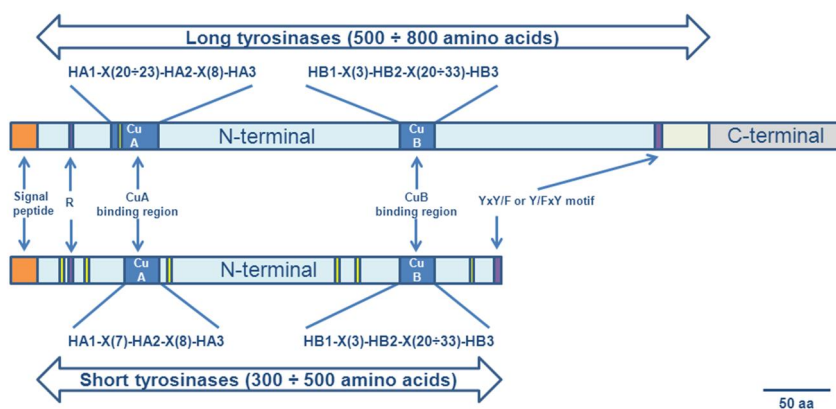


Figure 9. Schematic representation of the domains and the conserved residues of long and short tyrosinase sequences. Colour legend: signal peptide in orange, N-terminal domain in light blue, linker region in light green, C-terminal domain in light grey, copper-binding regions in blue, conserved Arg (R), conserved “tyrosine motif” (Y-X-Y/F or Y/F-X-Y) in purple, conserved Cys in yellow. HA1, HA2, and HA3 are the His residues coordinating the first copper ion (CuA), HB1, HB2, and HB3 are the His residues coordinating the second copper ion (CuB), and X is a generic amino acid residue.

The *A. oryzae* short tyrosinase gene was heterologously expressed in *T. reesei*. Transformants were first selected on plates containing L-tyrosine (55 mM) and copper (0.1 mM) and subsequently grown in shake flasks in medium supplemented with copper. Positive transformants grown on plates showed a black colour around the colonies, which indicates an oxidation of L-tyrosine. Differently, the transformants grown in liquid cultures did not show a significant activity on L-tyrosine and a high background was found in measurement of the activity of the parental strain on L-DOPA. Liquid cultures were thus selected on the basis of their activity on catechol. Despite the indications of tyrosine oxidation on the plate cultivation, the protein produced did not in the end show activity on L-tyrosine and L-DOPA, which are typical substrates for tyrosinases. Instead, it showed activity on catechol, which is a typical substrate of catechol oxidases. Therefore, the protein was classified as a catechol oxidase and named AoCO4. Production of AoCO4 was first optimised in shake flasks in different copper concentrations (0–6 mM), and subsequently AoCO4 was produced in a 10 L bioreactor in inducing medium at pH 5.5 with 0.5 mM copper. Expression of AoCO4 resulted in high yields, approximately 1.5 g L⁻¹ protein.

4.1.2 Purification and characterisation of *Aspergillus oryzae* catechol oxidase

AoCO4 was purified with a two-step ion-exchange chromatography. The buffer-exchanged culture filtrate was applied to cation-exchange chromatography, with the catechol-active protein eluted in two fractions, at 60 and 90 mM salt concentration. The

main activity was eluted at 90 mM salt concentration. Both fractions were further purified via strong anion-exchange chromatography. The MALDI-TOF MS analysis of purified AoCO4 from the fraction eluted at 90 mM resulted in a molecular weight (MW) of 39.3 kDa, and the fraction eluted at 60 mM in a mixture of MWs 39.3 and 40.5 kDa. The first amino acid in the N-terminus of the shorter form of AoCO4 was Gly45, whereas the fraction eluted at 60 mM salt concentration contained equimolar concentrations of proteins starting with Ala1 and Gly45. Interestingly, a Kex2/furin-type cleavage site was identified in AoCO4 (Lys43-Arg44). Kex2/furin-type proteases are known to be involved in the maturation of proteins in the Golgi apparatus of *T. reesei* (Goller et al. 1998). The processed form had the conserved Arg residue (Arg55) after the Kex2/furin-type cleavage site in the sequence. This conserved Arg residue is part of a short strand that forms a parallel β -sheet with the conserved “tyrosine motif”. The parallel β -sheet is structurally conserved in tyrosinases and catechol oxidases and it is important for keeping together the N- and C-terminal ends of the polypeptide chain (Flurkey & Inlow 2008). The results suggest that AoCO4 is a processed protein, from which the first 69 amino acids are cleaved. However, for some reasons the processing was not complete and also a small fraction (0.2%) of non-processed protein was found from the culture supernatant. It should be pointed out that both forms had similar specific activity on catechol. The work was continued with the processed form of AoCO4.

AoCO4 had a pH optimum in the acidic pH range (pH optimum 5–7), which is similar to the pH optimum of the fungal catechol oxidase from *Alternaria tenuis*, but different from the pH optima of catechol oxidases of plant origin, e.g., the catechol oxidase from *Ipomea batatas* (IbCO) has the pH optimum at 7.8 (Eicken et al. 1998). AoCO4 retained 50% of its activity after two hours incubation at 60 °C (pH 7.2). Thus, in the tested conditions AoCO4 was more thermostable than *A. tenuis* catechol oxidase, which is inactivated after 30 minutes of incubation at 60 °C (pH 5.2) (Motoda 1979a, Motoda 1979b).

AoCO4 was found to be active on the diphenolic substrates catechol, caffeic acid, hydrocaffeic acid and 4-*tert*-butylcatechol (TBC), and on the monophenolic substrates aminophenol and guaiacol. AoCO4 was found not to be active on L-tyrosine and L-DOPA. Furthermore, AoCO4 showed weak activity on phenol, tyrosol, *p*-creasol, and aniline. The affinity of AoCO4 for all tested substrates was generally low. AoCO4 showed the highest affinity to catechol and lower affinity to caffeic acid, hydrocaffeic acid and TBC. Similarly low affinity of plant catechol oxidases from *I. batatas* and *Lycopus europaeus* have been reported for catechol ($K_M=5$ mM for both catechol oxidases) (Eicken et al. 1998, Rompel et al. 1999b). The turnover number (k_{cat}) and the specificity constant (k_{cat}/K_M) of AoCO4 were significantly lower than the k_{cat} of *L. europaeus* and *I. batatas* for these substrates (data not shown). Hydrocaffeic acid is a structural analogue to caffeic acid, but it lacks the conjugation in the lateral chain. It has been suggested that substrates lacking this conjugation act as substrate analogues of tyrosinases and catechol oxidases and inhibit the enzyme (Fan & Flurkey 2004). Rompel et al. (1999b) reported that a catechol oxidase from *L. europaeus* has high affinity on hydrocaffeic acid ($K_M=4.3$ mM), which is lower than the K_M measured for AoCO4 by a factor ten. It is possible that hydrocaffeic acid is more a substrate analogue of AoCO4 rather than a substrate of AoCO4. A summary of the characteristics of AoCO4 is shown in **Table 9**.

Table 9. Characteristics of the *Aspergillus oryzae* catechol oxidase (AoCO4).

Property	Result	Methods
Molecular weight	39.3 kDa (40.5 kDa) ^a	MALDI TOF-MS
N terminus	Gly45 (Ala1) ^a	N-terminal sequencing
Isoelectric point	5.2	Isoelectric focusing
pH Optimum	pH 5–7	Activity measurements
pH Stability	> 75% Activity retained in the pH range 5–9 after 48 hours of incubation	Activity measurements
T_{1/2}	20 Hours at 50 °C (pH 7) 2 hours at 60 °C (pH 7)	Activity measurements
T_m	70 °C	Circular dichroism
Compounds with which AoCO4 showed activity	Catechol ($K_M=3.3\pm 0.9$ mM), caffeic acid ($K_M=7.9\pm 1.2$ mM), hydrocaffeic acid ($K_M=52.4\pm 6.5$ mM), TBC, aminophenol and guaiacol	Activity measurements
Compounds with which AoCO4 did not show activity	L-DOPA, D-DOPA, dopamine, L-tyrosine, tyramine, phloretic acid, 4-mercaptoethanol and ABTS	Activity measurements
Active site	Type 3 copper site Absorption maximum at 350 nm A dioxygen moiety bridged to CuA and CuB	UV/VIS spectroscopy; crystallography
Secondary structure	Negative peaks at 200 nm and 230 nm in the far-UV spectrum, indicating a helical structure Maximum intensity at 330 nm when AoCO4 was excited at 280 nm, indicating the presence of exposed aromatic residues on the surface of the protein	Circular dichroism Fluorescence spectroscopy
Tertiary structure	2.5 Å Resolution Monomer Four-helix-bundle core domain Three disulphide bridges Four glycosylation sites (Asn30, Asn104, Asn222, and Asn238)	X-ray data of crystals formed in hanging-drop method

^a The molecular weight and the N-terminus of the non-processed form of AoCO4 are shown in parenthesis.

4.1.3 Crystal structure and spectroscopic features of *Aspergillus oryzae* catechol oxidase

A crystal structure of AoCO4 was solved at 2.5 Å resolution from the crystals obtained from a preparation containing both the non-processed and the processed form of the enzyme. The overall structure of AoCO4 was mainly α -helical (**Figure 10**). The folding of AoCO4 was stabilised by the three disulphide bridges, which are conserved with the short tyrosinases (**Figure 9, Table 10**). The core of the enzyme was formed by a four-helix bundle (α 3, α 4, α 8 and α 9) where the catalytic site is found. The two copper ions in the catalytic centre each were co-ordinated each by three His residues. The first His residue that co-ordinates the CuA (HA1) was found to be His102, making the His pattern HA1-X(7)-HA2-X(8)-HA3, which is distinctive of the short-tyrosinase sequences. However, the sequence of AoCO4 contained two putative His residues (His86 and His102), and either of these His residues could hypothetically be the HA1 residue that co-ordinates the CuA copper ion. If the residue His86 co-ordinates CuA, the sequence of AoCO4 would be compatible with the long-tyrosinases.

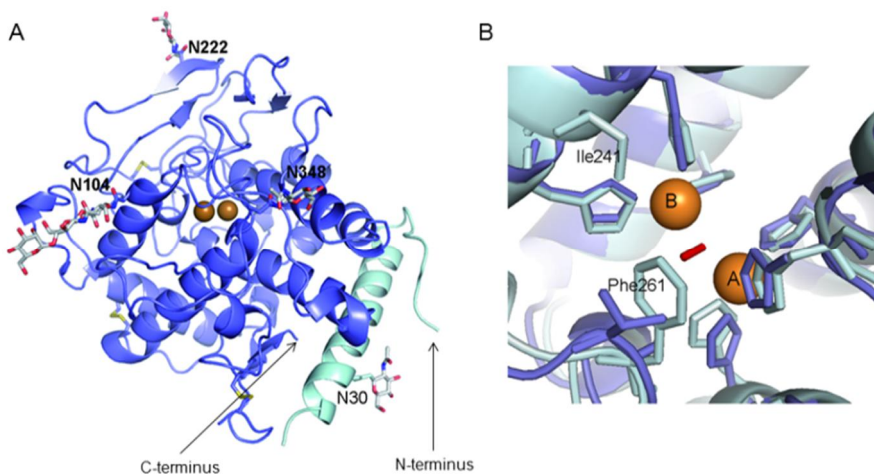


Figure 10. (A) A cartoon representation of the structure of the catechol oxidase from *Aspergillus oryzae* (AoCO4). The extra helix of the non-processed form of AoCO4 is shown in light blue. The copper ions at the active site are shown as orange spheres. (B) Comparison of the active site of *A. oryzae* catechol oxidase (blue) and *Ipomea batatas* catechol oxidase (light blue). The residues Phe241 and Ile241 of *I. batatas* catechol oxidase are also indicated. The copper ions in the active site are shown as orange spheres and the dioxygen moiety in red. (Unpublished results.)

The distance between CuA and CuB in the active site of AoCO4 was 4.1 Å and an elongated electron density was observed amidst CuA and CuB. A dioxygen moiety was found as bridging molecule between the two copper ions. The active site was studied also by spectroscopy. The UV/VIS absorption spectrum of AoCO4 showed a distinct maximum absorbance at 350 nm (**Figure 11**), suggesting that peroxide was present in the active

site of AoCO4 as reported for the *oxy*-forms (i.e., the enzyme form active on monophenols) of catechol oxidases and tyrosinases (Solomon et al. 1996). The *oxy*-form of catechol oxidases can be generated by addition of hydrogen peroxide (H₂O₂) to the enzyme, and it has been shown to give a maximum absorption at 350 nm, whereas the *met*-form of the enzyme does not show a clear maximum of absorbance at this wavelength (Jolley et al. 1974, Rompel et al. 1999a, Rompel et al. 2012). The UV/VIS absorption spectrum of AoCO4 showed a clear maximum at 350 nm without any H₂O₂ addition; however, addition of H₂O₂ transformed the enzyme totally to *oxy*-form. Five equivalents of H₂O₂ were needed for saturating AoCO4 to its oxidised form. From the ratio of the intensities of the absorbance at 350 nm of the untreated and treated enzyme, it was calculated that 35% of the untreated AoCO4 was in the *oxy*-form. This is significantly higher than the values reported for tyrosinases and catechol oxidases. For example, approximately 10–15% of AbT is in the *oxy*-form (Solomon et al. 1996). Despite 35% of the AoCO4 being in the *oxy*-form, AoCO4 did not have significant activity on monophenols, suggesting that the active site geometry and the essential amino acids around the active site determine the ability to oxidise monophenols.

The first three-dimensional structure of a catechol oxidase and of a tyrosinase were revealed from the plant *Ipomea batatas* (IbCO) (Klabunde et al. 1998) and the bacterium *Streptomyces castaneoglobisporus* (ScT) (Matoba et al. 2006), respectively. More recently, the three-dimensional structures of the bacterial tyrosinase from *Bacillus megaterium* (BmT) (Sendovski et al. 2011) and of the fungal tyrosinase from *Agaricus bisporus* (AbT) (Ismaya et al. 2011) were published. The reason catechol oxidases are not able to oxidise monophenols has been suggested to be related to a more restricted access of the substrates to the CuA site at the active site.

A Phe residue in IbCO (Phe261) clearly blocks the access of a substrate to the CuA at the active site, and it has been defined as a gatekeeper residue. Differently, in ScT the access to the active site is more open due to a smaller Gly residue (Gly203) instead of the Phe261 residue in IbCO. In the solved three-dimensional structure of ScT the active site was found to be occupied by a Tyr residue (Tyr98), which belongs to the co-crystallised caddie protein. This residue (Tyr98) was also suggested to function as a gatekeeper residue, keeping the active site of ScT occupied and thus preventing the binding of a substrate. A Val residue is present in BmT (Val218) and AbT (Val283) in the location of the gatekeeper residue (Phe261 in IbCO). A Val residue is less bulky than a Phe residue, so the active site of BmT and AbT is more accessible than the active site of IbCO. In the AoCO4 structure a Val residue (Val299) was found at the gatekeeper position, similarly to BmT and AbT. Despite of that, AoCO4 did not show a monophenolase activity on L-tyrosine, and it was classified as a catechol oxidase.

Klabunde et al. (1998) suggested that a conserved Glu residue (Glu236 in IbCO) may assist in deprotonating the substrate at the active site of catechol oxidases and tyrosinases (**Figure 12** and **Table 10**). Similarly to IbCO, a Glu residue is present in the structures of BmT (Sendovski et al. 2011), ScT (Matoba et al. 2006), and AbT (Ismaya et al. 2011) tyrosinases, whereas a Gln residue is present in the human tyrosinase and a Leu residue in *Neurospora crassa* tyrosinase (Klabunde et al. 1998). In AoCO4 a Gln residue (i.e., Gln273) was found, as in human tyrosinase, but unlike BmT, ScT, and AbT.

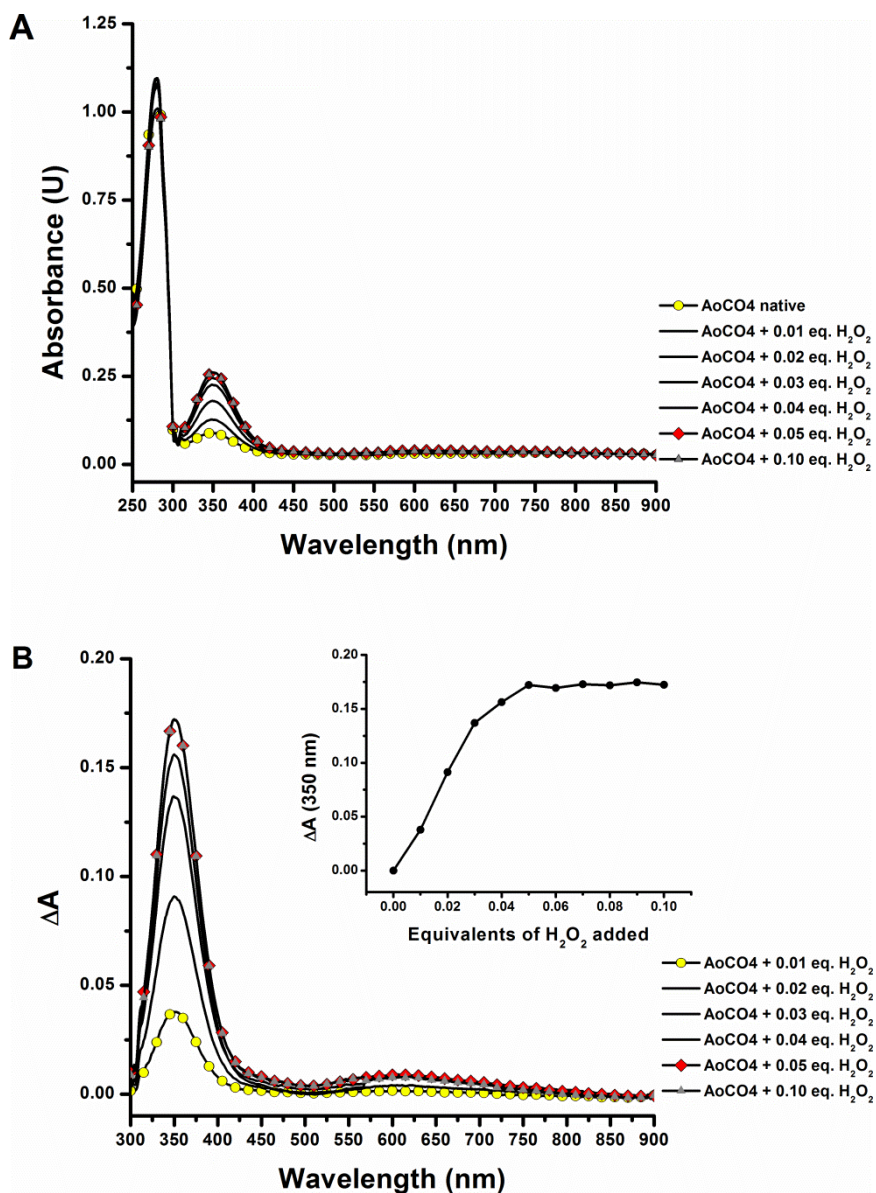


Figure 11. UV/VIS absorption spectra of *Aspergillus oryzae* catechol oxidase (AoCO4) and AoCO4 titrated with hydrogen peroxide (H₂O₂) (A) UV/VIS absorption spectra of the untreated AoCO4 and of the H₂O₂ treated AoCO4. The enzyme concentration was 30 μM and H₂O₂ was added to AoCO4 in 1–10 equivalents (eq.). Spectra were recorded in 10 mM Tris-HCl buffer, pH 7.2 by means of a Varian Cary 100 Bio spectrophotometer immediately after the addition of H₂O₂. (B) Difference spectra of AoCO4: H₂O₂ treated minus untreated enzyme. In the inset, the difference in absorbance (ΔA) at 350 nm is reported as a function of equivalents of H₂O₂ added. (Unpublished results)

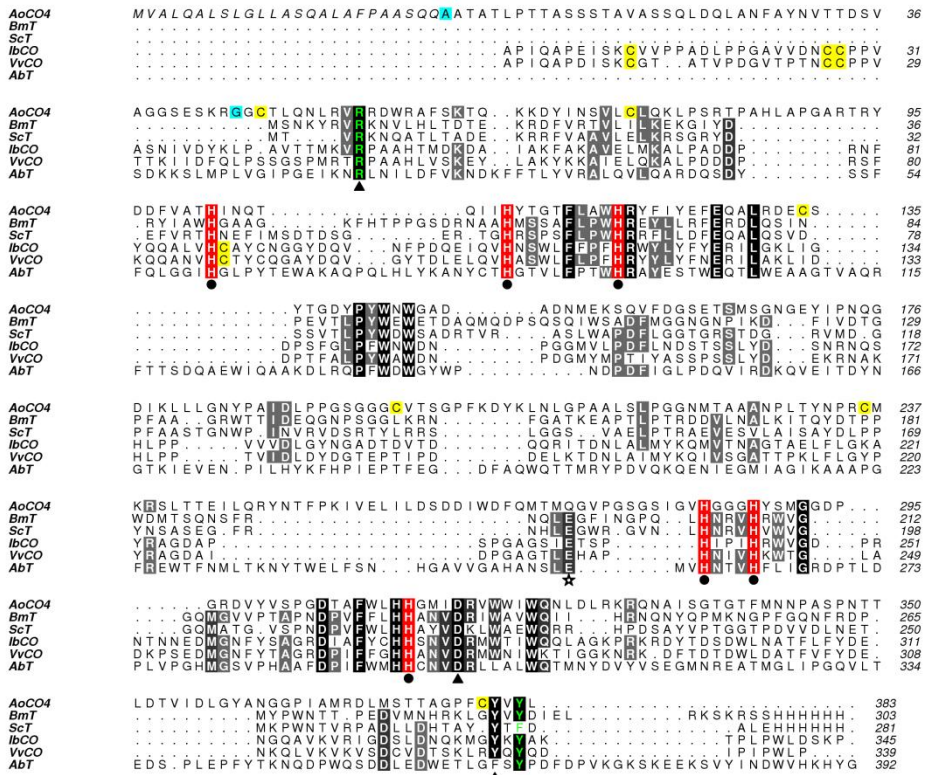


Figure 12. Amino acid sequence alignment of *Aspergillus oryzae* catechol oxidase (AoCO4; UniPROTKB: Q2UNF9), *Bacillus megaterium* tyrosinase (BmT; UniProtKB: B2ZB02), *Streptomyces castaneoglobisporus* tyrosinase (ScT; UniProtKB: Q83WS2), *Ipomea batatas* catechol oxidase (IbCO; UniProtKB: Q9ZP19), *Vitis vinifera* catechol oxidase (VvCO; UniProtKB: P43311), and *Agaricus bisporus* tyrosinase (AbT; UniProtKB: C7FF04). The copper-co-ordinating His residues are marked in red, the residues delimiting the core region in green, the disulphide bonds in yellow, the N-terminus in light blue. The triangles indicate the conserved residues involved in the interaction between C- and N-termini, the star the conserved proton donor residue. The numbering of the sequences was done according to their structures. The figure was produced by means of ALINE (Bond & Schuttelkopf 2009). (Unpublished results)

Siegbahn (2004) suggested a different reaction mechanism for catechol oxidases, wherein the oxygen could be bound to the active site as hydroperoxide during the catalytic cycle and in which no external base/acid is needed for proton acceptor and donor. The preliminary structure and the UV/VIS spectroscopic data for AoCO4 may support the reaction mechanism proposed by Siegbahn (2004). Further studies on the active site of AoCO4 are in progress and may elucidate the critical differences in the catalytic cycles of catechol oxidases and tyrosinases.

Table 10. Structural properties of *Aspergillus oryzae* catechol oxidase (AoCO4) as compared to the known structures of tyrosinases and catechol oxidases, i.e., *Bacillus megaterium* tyrosinase (BmT), *Streptomyces castaneoglobosporus* tyrosinase (ScT), *Ipomea batatas* (IbCO), *Vitis vinifera* catechol oxidase (VvCO) and *Agaricus bisporus* tyrosinase (AbT). (Unpublished results.)

Property	AoCO4	BmT	ScT	IbCO	VvCO	AbT
Sequence identity of AoCO4		27.2%	26.5%	21.8%	21.6%	21.6%
PDB ID		3NM8	1WX2	1BT1	2P3X	2Y9W
Core region	R55–Y382	R8–Y286	R4–Y333	R49–Y333	R48–Y330	R20–Y365
Four-helix bundle	α 3 (R94–Q105) α 4 (G113–C134) α 8 (I281–290) α 9 (T306–Q331)	α 2 (I34–G46) α 3 (F65–I83) α 7 (L203–V211) α 8 (V226–I244)	α 2 (R30–S44) α 3 (F59–V77) α 6 (H190–V197) α 7 (V211–R229)	α 2 (F81–C92) α 3 (F114–L132) α 6 (H240–V247) α 7 (I268–Q285)	α 4 (F80–C91) α 5 (F113–L131) α 12 (H239–T246) α 14 (F268–I285)	α 3 (F54–H61) α 4 (L89–R115) α 10 (L255–D269) α 11 (P290–M309)
His co-ordinating CuA	H102 (α 3) H110 H119 (α 4)	H42 (α 2) H60 H69 (α 3)	H38 (α 2) H54 H63 (α 3)	H88 (α 2) H109 H118 (α 3)	H87 (α 4) H108 H117 (α 5)	H61 (α 3) H85 H94 (α 4)
His co-ordinating CuB	H284 (α 8) H288 (α 8) H312 (α 9)	H204 (α 7) H208 (α 7) H231 (α 8)	H190 (α 6) H194 (α 6) H216 (α 7)	H240 (α 6) H244 (α 6) H274 (α 7)	H239 (α 12) H243 (α 12) H272 (α 14)	H259 (α 10) H263 (α 10) H296 (α 11)
Disulphide bonds	C39–C379 C75–C134 C198–C236	–	–	C11–C28 C27–C89	C11–C26 C25–C88	–
Thioether bond	–	–	–	C92–H109	C91–H108	C83–H85
Tyrosine motif	Y380–V381– Y382	Y284–V285– Y286	Y269–T270– F271	Y331–K332– Y333	Y328–Q329–Y330	F363–S364– Y365

Property	AoCO4	BmT	ScT	IbCO	VvCO	AbT
π Cation interaction	R55–Y380	R8–Y284	R4–Y269	R49–Y331	R48–Y328	R20–F363
Conserved R and residues forming a hydrogen bond with it	R55 D272	R8 D235	R4 D220	R49 D278	R48 D276	R20 D300, E102, Y365
Putative residues involved in assisting in the substrate deprotonation	Q273	E195	E181	E236	E235	E256

4.2 Detailed characterisation of the tyrosinase from *Trichoderma reesei* and comparison with the tyrosinase from *Agaricus bisporus* (Publications I and IV)

4.2.1 Characterisation of the substrate-specificity of tyrosinases from *Trichoderma reesei* and *Agaricus bisporus*

Among the studied tyrosinases, the extracellular tyrosinase from *Trichoderma reesei* (TrT) has been shown to have unique ability for cross-linking of proteins, and therefore TrT has potential application in protein cross-linking for industrial purposes (Selinheimo et al. 2007b). The fungal tyrosinase from *Pycnoporus sanguineus* can also cross-link proteins, but less efficiently than TrT. Unlike TrT, the commercial tyrosinase from *Agaricus bisporus* (AbT) and the plant tyrosinases from potato and apple can cross-link proteins only in the presence of a small diphenolic substrate acting as a cross-linking agent (Selinheimo et al. 2007b). A detailed characterisation of the substrate-specificity of TrT and AbT was carried out to increase understanding of the substrate-specificity of tyrosinases and thus also of the applicability of tyrosinase enzymes.

Tripeptides containing a Tyr residue in different positions (GGY, GYG, and YGG) and L-tyrosine (Y) were used as a model for peptide-bound Tyr residues. The K_M and V_{max} values for TrT and AbT for the tripeptides and L-tyrosine were determined by following of the consumption of the co-substrate molecular oxygen via polarography (**Table 11**). TrT and AbT performed differently on these model substrates. TrT showed very low affinity for Y and the kinetic parameters could not be determined (Figure 3 in Publication I), whereas the K_M values of AbT for the peptides were more than a factor ten lower than those of TrT. However, the turnover numbers (k_{cat}) were relatively similar between the two enzymes. TrT had lower affinity on YGG than on the GGY or GYG, and the highest k_{cat} was seen for GGY. With AbT the K_M and k_{cat} values were relatively similar to those with the three peptides. Clearly, therefore, the position of Y in the peptides affected the affinity and the reaction rate of TrT, whereas with AbT the position of Y in the peptide did not have a worthy effect. Furthermore, the lag periods (i.e., the time before the reaction products of monophenolase activity are produced at a linear/maximal rate) were shorter for TrT than for AbT and were not affected by the position of Y in the peptides.

The reaction end-products of the TrT- and AbT-catalysed oxidation of the three peptides were similar between the two tyrosinases. The reaction product of tyrosinase-catalysed oxidation of Y or YGG showed maximum absorbance at 475 nm, suggesting that the reaction end product is a dopachrome-related product. In contrast, the reaction product of tyrosinase-catalysed oxidation of GYG or GGY did not show a clear maximum at 475 nm, thus suggesting that a dopachrome-related product was not formed in significant quantities (Figure 4 in Publication I). The amino group of the Tyr residue of GYG and GGY is fixed in the peptide chain, so it is not free to take part in internal nucleophilic attack leading to the formation of a dopachrome-related product. However, it should be mentioned that analysis of the reaction end products based on the UV/VIS absorption spectra alone is not enough to elucidate the chemical structure of a reaction end product. Since the K_M of TrT for YGG was double the K_M of TrT for GGY and GYG,

the result suggested that the formation of a dopachrome-related product negatively affected the catalysis of TrT.

Overall, the oxidation capacity of TrT was lower than that of AbT on the peptide-bound tyrosine. Mattinen et al. (2008b) reported on the oxidation rates of TrT and AbT on a Tyr containing-peptide (EGVYVHPV) and GYG. The oxidation rate with TrT was faster on EGVYVHPV than on GYG, whereas with AbT it was the opposite. These results suggested that TrT can oxidise better Tyr residues in long peptides or proteins rather than short peptides, as also observed in the unique cross-linking ability of TrT (Selinheimo et al. 2007b).

Table 11. Kinetic parameters of the tyrosinases from *Trichoderma reesei* (TrT) and *Agaricus bisporus* (AbT) for L-tyrosine (Y) and the tripeptides GGY, GYG, and YGG, determined by oxygen consumption measurement. (Publication I).

Enzyme	Substrate	V_{\max} ($\text{mg L}^{-1} \text{s}^{-1}$) $\cdot 10^2$	K_M (mM)	k_{cat} (s^{-1})	k_{cat} / K_M ($\text{s}^{-1} \text{mM}^{-1}$)	Lag(s) with [S] 4 mM
TrT	Y		nd ^a			
TrT	GGY	11.9	3.1	7.2	2.4	120
TrT	GYG	6.9	3.9	4.2	1.1	120
TrT	YGG	5.2	6.0	3.2	0.5	120
AbT	Y		0.20			
AbT	GGY	2.7	0.11	3.0	26.5	600
AbT	GYG	2.8	0.18	3.1	17.1	240
AbT	YGG	3.6	0.21	4.0	19.0	180

^a Could not be determined due to insolubility of the substrate.

The K_M and V_{\max} values for TrT and AbT for small mono- and diphenolic substrates with different substitution of carboxyl and amino groups were determined by following of the oxidation products at specific wavelengths (**Table 12**). TrT and AbT were found to be very different in oxidation efficiency with small mono- and diphenolic substrates. Selinheimo et al. (2006b) reported on the K_M values of TrT for the substrates *p*-tyrosol ($K_M=1.3$ mM), *p*-coumaric acid ($K_M=1.6$ mM) and L-DOPA ($K_M=3.0$ mM), which were determined through monitoring of the consumption of the co-substrate molecular oxygen. In this work, in contrast, the K_M values were determined through following of the formation of the oxidation product at predetermined wavelengths. Slightly different K_M values were obtained. In general, the K_M values for AbT were observed to be the highest for those substrates whose structure contained a carboxyl group. The high K_M values of AbT for the substrates in which a carboxyl group was present in the structure suggest that these substrates are not real substrates for AbT (e.g., *p*-coumaric acid) but substrates analogues, as reported by several authors (Lim et al. 1999, Fan & Flurkey 2004, Kubo et al. 2004). A substrate analogue might bind the active site with the carboxylic group instead of with the hydroxyl group and thus compete with the substrate in binding of the active site of AbT (Fan & Flurkey 2004). In contrast, substrates in which a carboxyl group was present were real substrates for TrT. Again, unlike AbT, TrT showed low affinity for the substrates in which an amino group was present. A similar negative effect of an amine group on TrT was also found for the tripeptide YGG. In tyrosinases of fungi and

4. Results and discussion

plant origin, several residues are highly conserved in the sequence region containing the His residues that co-ordinate the CuB (Marusek et al. 2006). However, these residues are not highly conserved in TrT: for instance, a Met residue (Met280 in AbT) is a Phe residue in TrT (Phe284) (Selinheimo et al. 2007b). Therefore, it seems possible from the results that the binding of substrates at the active site is different in TrT as compared to AbT and other tyrosinases. However, in the absence of a three-dimensional structure of TrT, this remains as a hypothesis.

Table 12. K_M (mM) and V_{max} (Abs/min) values of tyrosinases from *Trichoderma reesei* (TrT) and *Agaricus bisporus* (AbT) for mono- and diphenolic compounds, determined by spectrophotometric assay with substrate-specific wavelengths (Abs/min). TrT and AbT enzyme dosages were 3.8 and 3.1 $\mu\text{g mL}^{-1}$ for the monophenols and 0.9 and 0.8 $\mu\text{g mL}^{-1}$ for the diphenols, respectively. (Publication I).

Substrate	Detection absorbance (nm)	K_M (mM)		V_{max} (Abs/min)	
		TrT	AbT	TrT	AbT
L-Tyrosine	475	–	0.20	6 ^a	13
L-DOPA	475	7.5	0.17	210	60
<i>p</i> -Coumaric acid	360	1.5	–	51	0
Caffeic acid	480	0.9	1.69	60	300
L-Tyramine	475	4.5	0.75	4	16
L-Dopamine	475	11	0.84	120	300
Phloretic acid	400	1.4	0.64	55	77
Hydrocaffeic acid	400/530 ^b	3.0	0.91	450	840
Phenol	390	3.8	0.33	9	14
Catechol	400/540 ^c	2.5	0.25	138	1500
<i>p</i> -Tyrosol	395	0.8	0.06	20	13

^a Oxidation rate determined with L-tyrosine concentration of 2.5 mM, not the V_{max} value.

^b Product formation followed at 400 and 530 nm with AbT and TrT, respectively.

^c Product formation followed at 400 and 540 nm with AbT and TrT, respectively.

The lag periods were detected in both the TrT- and AbT-catalysed oxidation of small monophenols. The lag period relates to the transformation of the *met*-form to the *oxy*-form of tyrosinase. In the AbT-catalysed oxidation the lag period increased when the substrate concentration increased for the substrates on which AbT showed the highest affinity, but the lag period decreased with L-tyramine and phloretic acid when substrate concentration increased (Table 3 in Publication I). It has been shown that when AbT has high affinity on a monophenolic substrate, the substrate binds also to the *met*-form of AbT leading the enzyme to a dead-end pathway. Thus the transition of the *met*-form into the *oxy*-form, which is the only active form on monophenols, is retarded (Espín et al. 1999). In contrast to AbT, TrT had generally lower affinity than AbT on the monophenolic substrates tested and the lag periods measured generally decreased when the substrate concentrations were increased with all of the monophenolic substrates. Therefore, the results are logical; with low affinity on substrates, an increased lag period related to the dead-end pathway was not observed with TrT. Correspondingly AbT showed the lowest affinity for L-tyramine and phloretic acid, and thus the binding of these substrates to the *met*-form of AbT was less favourable and, in consequence, no prolonged lag period was measured with the increased substrate concentration. The duration of the lag period of a specific

substrate was not directly related to the K_M , suggesting that there are also other reasons for the differences in the lag periods other than the affinity of the enzyme on the substrate.

The UV/VIS absorption spectra of the products formed by TrT- and AbT-catalysed oxidation of monophenolic and diphenolic substrates indicated that the primary product from most of the substrates was similar with both enzymes. Unexpectedly, different end products accumulated in TrT- and AbT-catalysed oxidation when catechol or hydrocaffeic acid was used as the substrate (**Figure 13**). When L-DOPA was the substrate, the spectrum revealed that the accumulation of dopachrome (i.e., the oxidation product from L-DOPA) was different with the two enzymes. In the TrT-catalysed reaction, the intensity of absorbance was lower than in the AbT-catalysed reaction (Figure 5 in Publication IV). It is known that dopachrome, the end product of the proximal phase, is not a stable compound, and it undergoes non-enzymatic reactions leading to the formation of melanins (the distal phase of melanogenesis). The distal phase starts immediately after the proximal phase and a mixture of products is formed (Cooksey et al. 1997). The linear formation of dopachrome, i.e., the proximal phase of melanogenesis lasted only five minutes in the TrT-catalysed oxidation, whereas it was 15 minutes with AbT, a result similar to that reported by Cooksey et al. (1997). However, the UV/VIS absorption spectra of the products formed in the distal phase were similar between TrT and AbT, suggesting that both TrT and AbT generate similar melanins.

4. Results and discussion

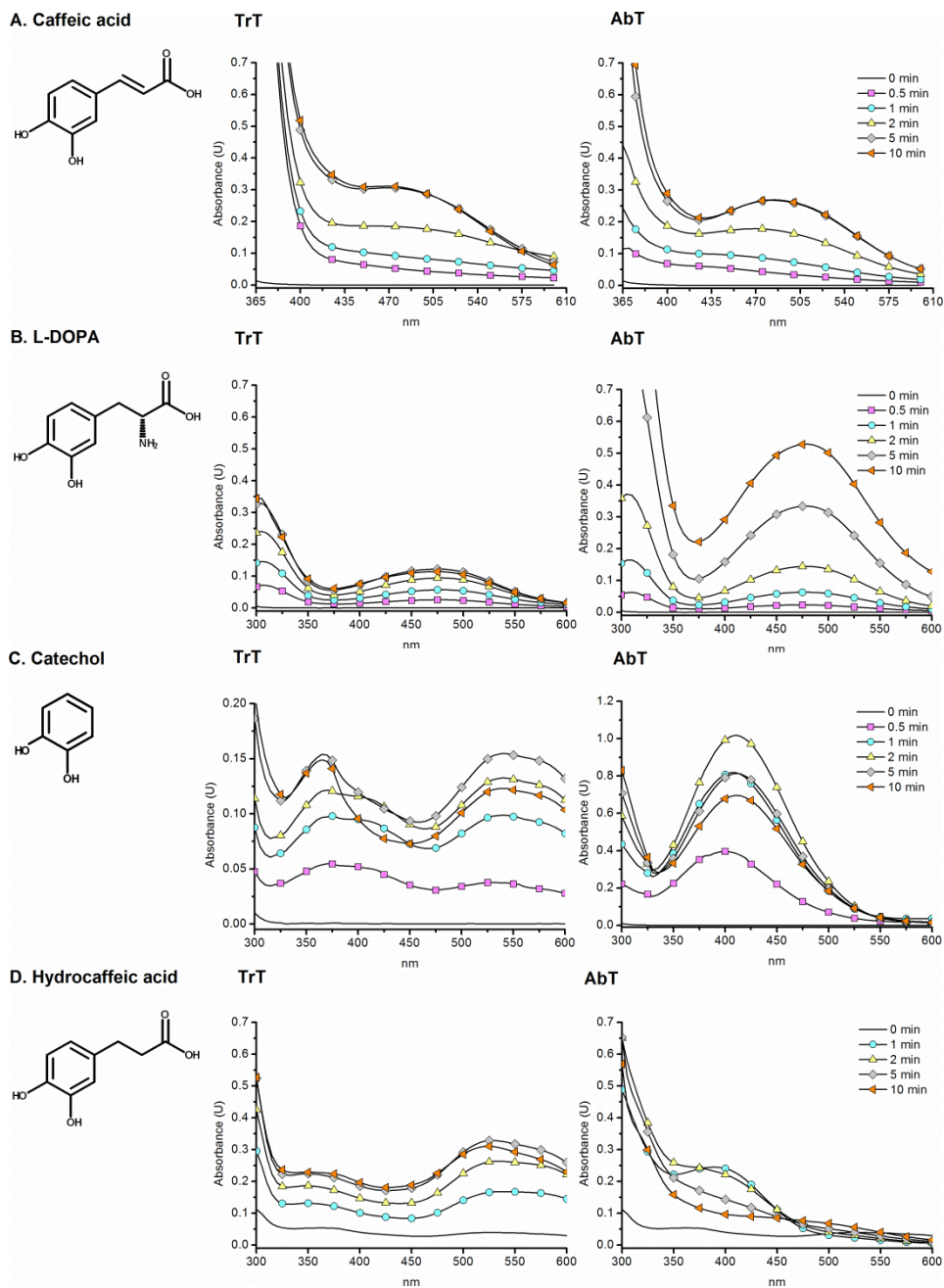


Figure 13. UV/VIS absorption product spectra of the oxidation of caffeic acid (A), L-DOPA (B), catechol (C) and hydrocaffeic acid (D) by tyrosinases from *Trichoderma reesei* (TrT) and *Agaricus bisporus* (AbT). Absorption spectra shown as a function of time.

4.2.2 *Trichoderma reesei* tyrosinase end product inhibition by dopachrome

The UV/VIS absorption spectra of products formed by TrT- and AbT-catalysed oxidation of L-DOPA suggested that TrT suffer from end product inhibition. It was detected that TrT produced dopachrome only in the first five minutes, despite the co-substrate molecular oxygen was still available in the reaction mixture. To confirm that dopachrome was the only product formed both by TrT- and AbT-catalysed oxidation of L-DOPA, the reaction end products of L-DOPA oxidation by the tyrosinases were analysed by means of ESI-FT-ICR mass spectrometry and through fragmentation analysis of the ions with IRMPD. Without enzyme, L-DOPA (MW 197 Da) gave an intense peak at m/z 196, corresponding to the $[M - H]^-$ ion. In the TrT- and AbT-catalysed reactions, a new peak at m/z 192 was observed, corresponding to dopachrome (MW 193 Da) (Figure 14, and Figure 4 in Publication IV). Dopachrome was the only end product detected in the conditions studied. TrT-catalysed oxidation of L-DOPA clearly plateaued after a few minutes of reaction, and less than 0.1% of the L-DOPA was oxidised to dopachrome, whereas AbT catalysed the complete conversion of L-DOPA to dopachrome within 20 minutes of reaction in these reaction conditions (Figure 14A and C).

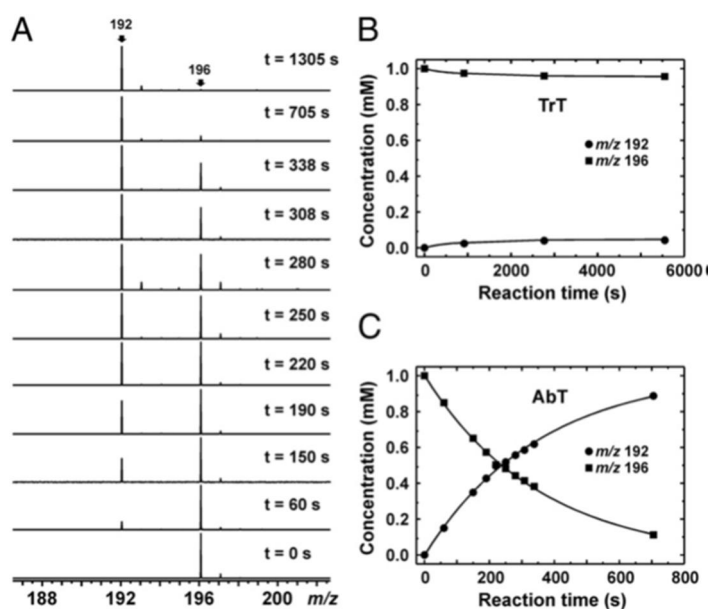


Figure 14. Negative mode ESI FT-ICR mass spectra from the oxidation of L-DOPA (m/z 196) to dopachrome (m/z 192) by *Agaricus bisporus* tyrosinase (AbT) at various time points (A). A plot of the respective ion intensities versus reaction time for *Trichoderma reesei* tyrosinase (TrT) (B) and AbT (C). (Publication IV).

The ESI-FT-ICR mass spectrometry result and the UV/VIS absorption spectra of products formed by TrT-catalysed oxidation of L-DOPA both suggested that TrT suffers from end product inhibition. With the aim of studying the TrT end product inhibition, dopachrome

4. Results and discussion

was produced by AbT-catalysed oxidation of L-DOPA in acidic conditions to ensure the stability of dopachrome. Reaction mixtures containing 8 mM L-DOPA and dopachrome in various concentrations (0, 0.25, 0.75, and 1.5 mM) were used for calculation of the degree of inhibition. The oxygen consumption rate of TrT on 8 mM L-DOPA in the presence of 1.5 mM dopachrome was reduced by 50% (**Table 13**), indicating that dopachrome clearly inhibited the TrT-catalysed oxidation of L-DOPA,

Table 13. Degree of inhibition of *Trichoderma reesei* tyrosinase (TrT) by dopachrome on L-DOPA (8 mM), Reaction mixture was prepared in 0.1 M sodium acetate buffer pH 5.6 and analysed by oxygen consumption measurement, determined by oxygen consumption measurement. (Publication IV).

Dopachrome (mM)	Oxygen consumption rate ($\mu\text{g L}^{-1} \text{min}^{-1}$)	Inhibition (%)
0	18.2 ± 3.5	0
0.25	17.9 ± 2.7	2
0.75	12.0 ± 1.0	34
1.5	8.4 ± 1.7	54

The end product inhibition of TrT elucidates why the oxidation capacity of TrT with L-DOPA was reduced relative to AbT. Furthermore, it suggests that end product inhibition of TrT occurs also with the structurally related substrates L-tyrosine and YGG. According to the analysis of the end product absorption spectra, the end product of a TrT-oxidation of L-tyrosine or YGG is a dopachrome-related product with a maximum absorbance at 475 nm. Selinheimo et al. (2007b) reported that the cross-linking ability of TrT decreased when L-DOPA was added to the reaction mixture. The dopachrome end product inhibition elucidated in this work is most probably the explanation of the reduced cross-linking ability of TrT in the presence of L-DOPA as a cross-linking agent. Thus far, TrT is the first tyrosinase shown to suffer from end product inhibition. Several substrates of AbT have been shown to act as suicide substrates leading AbT towards the suicide inactivation pathway (Muñoz-Muñoz et al. 2010b), accordingly, the possibility of L-DOPA to act as a suicide substrate for TrT was evaluated. A suicide diphenolic substrate cannot bind the oxy-form of tyrosinase in a coplanar binding geometry, and it leads the enzyme toward the suicide inactivation pathway, with the consequent loss of one reduced copper ion (Cu^0) and hydrogen peroxide together with the reaction product. The stronger the withdrawing effect of the group in the C-4 position of the diphenolic substrate is, the greater is the likelihood of leading to enzyme toward the suicide inactivation pathway (Muñoz-Muñoz et al. 2008). The ability of AoCO4 to recover its activity when dopachrome was removed from the reaction mixture was analysed by removing dopachrome by gel filtration. Interestingly, TrT retained its activity on L-DOPA (data not shown). The result indicated that dopachrome was not a suicide substrate of TrT.

4.2.3 Effect of inhibitors on the monophenolase and diphenolase activities of *Trichoderma reesei* tyrosinase

Since tyrosinases-catalysed browning reactions cause negative changes in organoleptic properties and in the appearance of fruits and vegetables, with subsequent shortening of product shelf life, research into inhibition of tyrosinases is of great interest. Among the large number of inhibitors of tyrosinases reported in the literature, kojic acid, arbutin, benzaldehyde, benzoic acid, potassium cyanide and sodium azide, were analysed as inhibitors of TrT with *p*-coumaric acid and caffeic acid used as monophenolic and diphenolic substrates (Table 2 in Publication IV). The inhibitory effect of the tested inhibitors on the monophenolase activity of TrT followed the order potassium cyanide > sodium azide > benzaldehyde > arbutin. No inhibitory effect was found for kojic acid or benzoic acid. However, kojic acid prolonged the lag period of TrT-catalysed oxidation of *p*-coumaric acid. The inhibitory effect of the tested inhibitors on the diphenolase activity of TrT followed the order kojic acid > potassium cyanide > sodium azide > arbutin. Benzaldehyde and benzoic acid did not have an effect on TrT-catalysed oxidation of caffeic acid, whereas they are known inhibitors for AbT (Wilcox et al. 1985, Chen et al. 1991, Cabanes et al. 1994, Conrad et al. 1994, Funayama et al. 1995, Espín & Wichers 1999). These results lend further support to the findings from the substrate-specificity determination that the amino acid residues close to the active sites of TrT and AbT are different.

The difference in the effect of kojic acid on mono- and diphenolase activity of TrT and AbT suggested that monophenols and diphenols bind differently to the active site of the tyrosinases. The three-dimensional structure of BmT in complex with kojic acid has recently shown that kojic acid is oriented with the hydroxymethyl group towards the CuB at the active site of *met*-tyrosinase and given rise to the hypothesis that monophenols bind to CuA whereas diphenols bind to CuB at the active site (Sendovski et al. 2011). Caffeic acid and kojic acid both bind to CuB, and indeed a clear competitive inhibition was observed for TrT. Differently, in the monophenolase cycle, *p*-coumaric acid binds to the CuA of TrT while kojic acid binds to the CuB, and no clear inhibition was observed. Furthermore, the lag time of TrT was greatly prolonged by kojic acid, suggesting that binding with the substrate is more difficult when the tyrosinase-kojic acid complex is present.

Interestingly, sodium azide was found to be a strong inhibitor of TrT, but it also had an effect on the reaction end products as analysed by UV/VIS absorption (Figure 6 in Publication IV). When catechol was used as a substrate, an absorption maximum at 400 nm was observed with AbT. In the presence of sodium azide the absorption maximum of products formed by AbT-catalysed oxidation of catechol was detected at 325 nm. Sugumaran (1995) reported on the formation of an azido-benzoquinone adduct at 325 nm after ten minutes of AbT-catalysed oxidation of catechol in the presence of sodium azide. The observed absorbance maximum at 325 nm indicated a formation of an azido-benzoquinone adduct with AbT. In contrast, the azido-benzoquinone adduct was not observed in product absorption spectra of TrT-catalysed oxidation of catechol in the presence of sodium azide. However, because the end-products formed by TrT- and AbT-catalysed oxidation of catechol were found to be different it is likely that the same adduct is not formed with TrT. A clear maximum at 375 nm was also observed in the product

absorption spectra of TrT- and AbT-catalysed oxidation of L-DOPA in the presence of sodium azide, suggesting that a dopachrome-adduct was formed with both the tyrosinases (Figure 5 in Publication IV).

4.3 Three-dimensional structure of a laccase from *Thielavia arenaria* and elucidation of the oxidation capacity of fungal laccases with different redox potential (Publication III)

4.3.1 Purification and three-dimensional structure of *Thielavia arenaria* laccase

The laccase 1 from the ascomycete fungus *Thielavia arenaria* (TaLcc1) has been shown to be an efficient enzyme in bleaching of denim at high temperatures, up to 80 °C and at neutral pH (Paloheimo et al. 2006). TaLcc1 was produced with *T. reesei* as a host at Roal Oy (Rajamäki, Finland). TaLcc1 was purified within a three-step purification procedure. First a culture supernatant was desalted and buffer-exchanged with gel filtration chromatography. Weak-affinity anion-exchange and subsequently high-affinity anion-exchange chromatography were used to purify TaLcc1 (Table 14).

Table 14. Purification of laccase 1 from *Thielavia arenaria*. Enzymatic activity was measured using 2,2'-azino-bis(3-ethylbenzthiazoline-6-sulphonic acid) (ABTS) as a substrate.

Purification step	Total activity (nkat)	Total protein (mg)	Specific activity (nkat mg ⁻¹)	Activity yield (%)	Purification factor
Culture filtrate	382690	700	547		1.0
Desalting	366910	585	627	96	1.1
Weak-affinity anion exchange chromatography	163660	174	940	43	1.7
High-affinity anion exchange chromatography	22120	27	813	6	1.5

TaLcc1 was crystallised with the hanging drop diffusion method at room temperature. The three-dimensional structure of TaLcc1 was solved by X-ray crystallography at 2.5 Å resolution at University of Eastern Finland (PDB ID 3PPS). The overall structure of TaLcc1 was rather similar to the structures of the known laccases and in particular to the structure of the ascomycete laccase from *Melanocarpus albomyces* (MaL, PDB ID 1GW0 and rMaL, PDB ID 2Q9O), which was the first published three-dimensional structure of an ascomycete laccase (Hakulinen et al. 2002, Hakulinen et al. 2008). However, also clear differences between the three-dimensional structures of TaLcc1 and rMaL were found, including the loops near the T1 copper site and the amino acid thought to be responsible for catalytic proton transfer.

TaLcc1 was found to be a monomer composed of three cupredoxin-like domains, called domain A (1–160), domain B (161–340) and domain C (340–564) (Figure 15). The mononuclear T1 copper was located in domain C and it was co-ordinated by His432, Cys504, His509, and two non-bonding residues (Ile506 and Leu214). The trinuclear

T2/T3 copper cluster was located at the interface between domains A and C. The three copper ions of the T2/T3 copper cluster were co-ordinated in total by eight His residues and one molecule of solvent. The T2 copper ion was coordinated by His94, His437, and one molecule of solvent. The T3 copper ion by His141, His437, and His503, and the T3' copper ion by His96, His139, and His505. Differently from TaLcc1, in the nearly atomic resolution structure of *rMaL* the T2 copper ion is co-ordinated by two His residue and one chloride ion (Hakulinen et al. 2008).

In three-dimensional structures of ascorbate oxidase two solvent channels leading to the T2/T3 copper centre have been described. The broad solvent channel, leading to the T3 copper ions is called the T3 solvent channel. The narrower solvent channel leads to the T2 copper site, and it is called the T2 channel (Messerschmidt et al. 1992). The T3 and the T2 channels have been reported also in basidiomycete laccases, e.g., in the laccase from *Trametes versicolor* (Piontek et al. 2002). On the contrary, in the ascomycete laccase *rMaL* the T3 channel is blocked by the last four C-terminal amino acids (i.e., Asp-Ser-Gly-Leu, known as the C-terminal plug) and the T2 channel is very tight, with the residues His98, Gln131, and Asp439 limiting the access of the solvent molecules. Furthermore, in *rMaL* a triangle of amino acids (Ser, Ser and Asp), called the SDS-gate is found, but it is absent in the laccases from basidiomycete fungi (Hakulinen et al. 2002, Hakulinen et al. 2002, Hakulinen et al. 2008). Differently from *rMaL*, the T2 channel was found also in TaLcc1 (Figure 3 in Publication III). The residue corresponding to His98 in *rMaL* is Arg99 in TaLcc1, which is oriented such that it forms the surface of the solvent channel. In TaLcc1, as in *rMaL*, the T3 solvent channel was blocked by a C-terminal plug. The C-terminal plug is highly conserved in the sequences of ascomycete laccases. Divergently, basidiomycete laccases generally do not have this type of C-terminus. In another similarity to *rMaL*, the SDS-gate was found in TaLcc1 (Ser143, Ser511, Asp561).

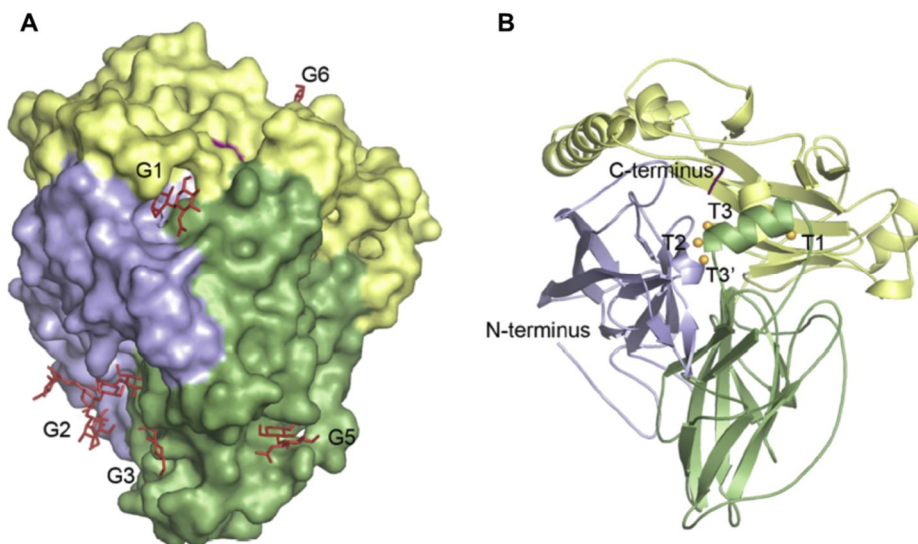


Figure 15. (A) The crystal structure of *Thielavia arenaria* laccase 1 (TaLcc1) as a surface model. Domain A is presented in blue, domain B in green, and domain C in yellow. The N-glycans are shown as red sticks. Glycans are named as G1 on Asn89, G2 on Asn202, G3 on Asn217, G4 on Asn247 (on the other side of the molecule), G5 on Asn290, and G6 on Asn376. (B) Cartoon representation of TaLcc1. The catalytic coppers are shown in orange, and the C-terminal plug in purple. (Publication III).

The substrate-binding site of TaLcc1 was found to be in a pocket between domains B and C, in a similarity to *rMaL*. The pocket was formed by ten hydrophobic residues (Ala193, Leu297, Leu363, Phe371, Trp373, Ile427, Val428, Leu430, Trp508, and His509) and one hydrophilic residue (Asp236). In general, the substrate-binding pocket of TaLcc1 was found to be similar to that one of *rMaL*. However, there are differences between the two enzymes, both in the shape and in the residues of the pocket. The pocket of TaLcc1 was found to be narrower than the pocket of *rMaL* in one direction, owing to the Leu297 in TaLcc1 (Ala297 in *rMaL*), and wider than the pocket of *rMaL* in the other direction, because of the Pro195 and Val428 in TaLcc1 (Phe194 and Phe427 in *rMaL*, respectively). The main difference between the substrate-binding pockets of TaLcc1 and *rMaL* was found to be in the residue Asp236 in TaLcc1, corresponding to Glu235 in *rMaL* (**Figure 16**).

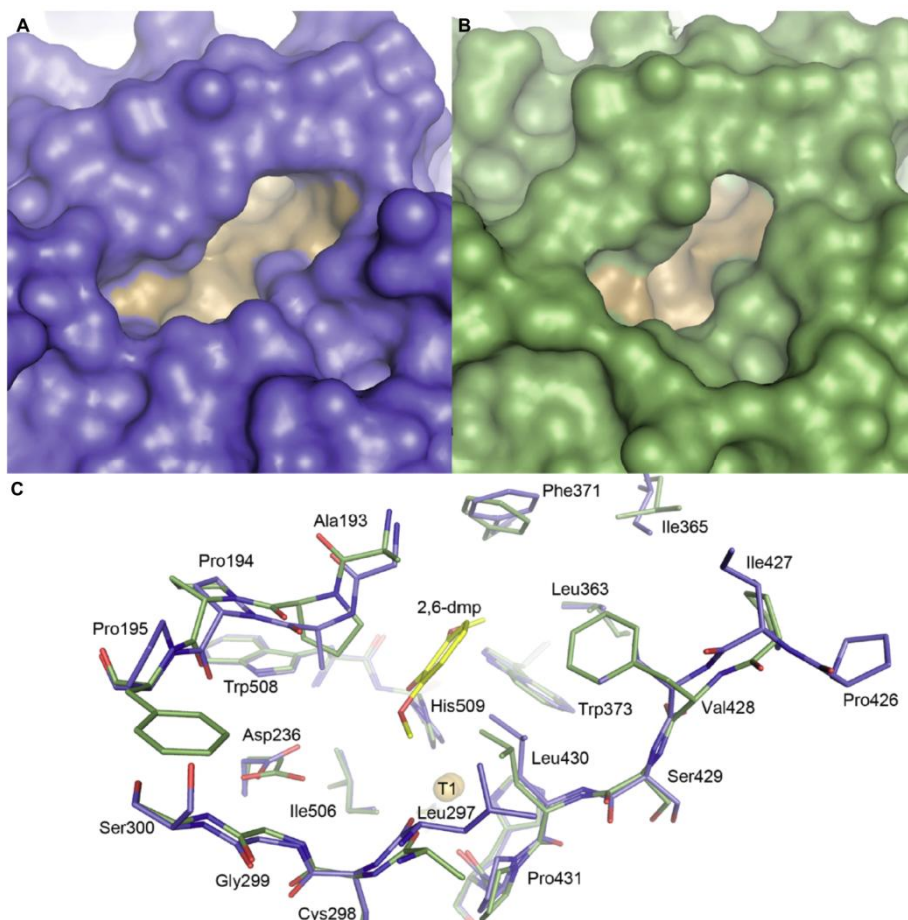


Figure 16. The substrate binding pockets of *Thielavia arenaria* laccase 1 (TaLcc1) (A) and the recombinant *Melanocarpus albomyces* laccase (rMaL) (B). (C) Superimposed amino acids forming the substrate-binding pockets. TaLcc1 is shown in blue, rMaL in green, and 2,6-dimethoxy phenol (2,6-DMP) from the complex structure (PDB ID 3FU8) in yellow. The amino acids of TaLcc1 are labelled. (Publication III).

The implications of the differences between the three-dimensional structures of TaLcc1, rMaL, and the basidiomycete laccase from *Trametes hirsuta* (ThL) for the capacity of these laccases to oxidise phenolic substrates is presented and discussed in the Subsection 4.3.2.

4.3.2 Elucidation of the oxidation capacity of fungal laccases with different redox potential as related to their available crystal structures

Both the affinity of the substrate to the enzyme and the difference in redox potential (ΔE°) between the T1 copper site of the laccase and the substrate affect the oxidation rate of the substrate in laccase-catalysed reactions (Xu 1996a, Xu 1997). The rate of laccase-catalysed reactions is assumed to increase as the ΔE° between the T1 copper site of the laccase and the substrate increases. In turn, the pH affects the laccase-catalysed oxidation of a phenolic substrate, either positively or negatively. At higher pH values, the hydroxyl group of the phenolic substrate dissociates and inhibits the laccase, thus the rate of laccase-catalysed reactions decreases. At higher pH values, the E° of the phenolic substrate is lower, whereas E° for the T1 copper site is not pH-dependent, thus ΔE° increases and the rate of laccase-catalysed reaction is also expected to increase (Xu 1996a, Xu et al. 1996).

The enzyme kinetics with different *p*-substituted dimethoxy phenolic substrates of different E° were analysed with three fungal laccases with different redox potential and examined in relation to their available three-dimensional structures. The novel laccase 1 from the ascomycete fungus *T. arenaria* (TaLcc1; $E^\circ = 0.51$ V) was compared to the other known laccase from ascomycete fungus *M. albomyces* (rMaL; $E^\circ = 0.48$ V) and to the high redox potential laccase from basidiomycete fungus *T. hirsuta* (ThL; $E^\circ = 0.78$ V). Three different *p*-substituted dimethoxy phenolic substrates, of different redox potential, were selected as substrates: 2,6-dimethoxy phenol (2,6-DMP), syringic acid and methyl syringate (Table 15). The kinetic of substrate oxidation by laccases was studied at two pHs, i.e., pH 4.5 and pH 6.0, where pH 4.5 is more optimal for ThL and pH 6.0 for TaLcc1 and rMaL (Figure 17).

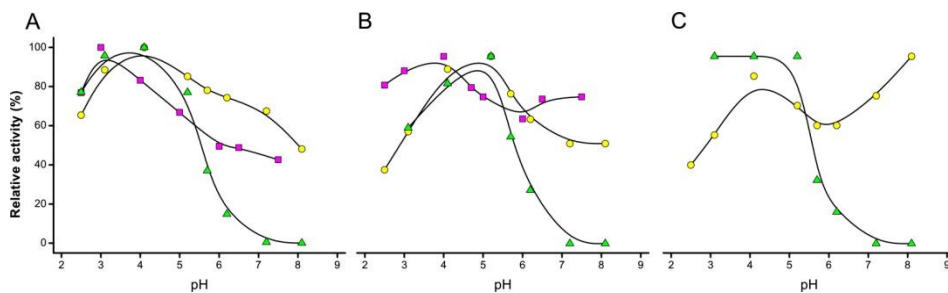
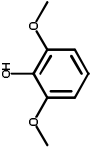
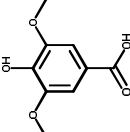
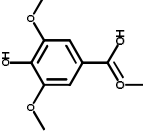


Figure 17. pH activity profiles of laccases from *Melanocarpus albomyces* (●), *Thielavia arenaria* (■), and *Trametes hirsuta* (▲), on 2,6-dimethoxy phenol (2,6-DMP) (A), syringic acid (B) and methyl syringate (C). (Publication III, supplementary data.)

Table 15. Kinetic parameters for laccases from *Melanocarpus albomyces* (MaL), *Thielavia arenaria* (TaLcc1), and *Trametes hirsuta* (ThL), measured with 2,6-dimethoxy phenol (2,6-DMP), syringic acid and methyl syringate in 25 mM succinate buffer at pH 4.5 and in 40 mM MES buffer at pH 6.0 (25 °C). Structural formulas of the substrates are presented. Redox potentials (E°) of type 1 copper centre of the laccases and redox potentials of the substrates at pH 4.5 and 6.0 are provided, together with the redox potential differences (ΔE°) between the type 1 copper centre of the laccases and the substrates. n.d. not determined. (Publication III.)

	2,6-DMP			Syringic acid			Methyl syringate		
	pH 4.5	pH 6		pH 4.5	pH 6		pH 4.5	pH 6	
	$E^\circ=0.53$ V	$E^\circ=0.40$ V		$E^\circ=0.57$ V	$E^\circ=0.51$ V		$E^\circ=0.69$ V	$E^\circ=0.65$ V	
MaL ($E^\circ=0.48$ V)									
ΔE° (V)	-0.05	0.08		-0.09	-0.03		-0.21	-0.17	
K_M (μ M)	18 ± 1	9.5 ± 0.9		122 ± 11	132 ± 22		n.d.	n.d.	
V_{max} (dA min ⁻¹ nmol ⁻¹)	126 ± 2	119 ± 1		3.5 ± 0.1	12.1 ± 0.6		n.d.	n.d.	
TaLcc1 ($E^\circ=0.51$ V)									
ΔE° (V)	-0.02	0.11		-0.06	0		-0.18	-0.14	
K_M (μ M)	45 ± 4	5.8 ± 0.6		128 ± 4	61 ± 4		n.d.	n.d.	
V_{max} (dA min ⁻¹ nmol ⁻¹)	99 ± 2	87 ± 1		3.5 ± 0.1	2.7 ± 0.1		n.d.	n.d.	
ThL ($E^\circ=0.78$ V)									
ΔE° (V)	0.25	0.38		0.21	0.27		0.09	0.13	
K_M (μ M)	18 ± 1	6.3 ± 1.3		35 ± 6	17 ± 4		168 ± 19	50 ± 16	
V_{max} (dA min ⁻¹ nmol ⁻¹)	193 ± 3	91 ± 2		8.3 ± 0.4	2.0 ± 0.1		21 ± 1	2.6 ± 0.2	
									

2,6-DMP and syringic acid were oxidised by all the three laccases in both of the pH conditions tested, while methyl syringate, the substrate of those tested that has the highest redox potential, was oxidised only by ThL. All three laccases were found to oxidise syringic acid at pH 6.0, despite the reaction not being facilitated by the ΔE° for TaLcc1 ($\Delta E^\circ = -0.03$) and rMaL ($\Delta E^\circ = 0$). However, in these reaction conditions (pH=6.0) TaLcc1 and rMaL were able to oxidise syringic acid at pH 6.0 mainly on account of the favourable pH. Differently, a pH of 6.0 was not the optimal pH for ThL (about 30% of residual activity on syringic acid) and thus the ThL-catalysed oxidation of syringic acid was favoured largely through a high ΔE° ($\Delta E^\circ = -0.27$). Nevertheless, the effect of ΔE° was found to prevail over the effect of pH for the substrates with high E° , i.e., in both pH conditions, methyl syringate was oxidised only by ThL, which is the laccase with the highest E° among the three laccases.

Despite TaLcc1 and rMaL having shown similar pH profiles and ΔE° values, the affinity of TaLcc1 to 2,6-DMP was lower than the affinity of rMaL for the same substrate at pH 4.5. Furthermore, a three-fold increase in the reaction rate with syringic acid at pH 6 as compared with pH 4.5 was observed for rMaL only, not for TaLcc1. These differences in the TaLcc1 and rMaL-catalysed oxidation of phenolic substrates must be attributable to the differences in the residues forming the binding pockets of the two laccases. The most evident difference between the substrate-binding pockets of TaLcc1 and rMaL was found to be in the hydrophilic residue, which is also the putative catalytic amino acid. In TaLcc1, an Asp236 is found, whereas rMaL has a Glu235 in the correspondent position (**Figure 16**, **Figure 18**). Kallio et al. (2009) reported that a single mutation in the Glu catalytic residue (Glu235->Asp) of rMaL increases the K_M value for phenolic substrates, suggesting that a carboxylic group is important for the catalytic activity. Bento et al. (2010) have shown that in the bacterial laccase from *Bacillus subtilis* a Glu residue (Glu498) near the dinuclear T3 copper centre participates in the proton transfer at the trinuclear T2/T3 copper cluster. Basidiomycete laccases have a conserved Asp residue close to the dinuclear T3 copper centre, and this residue might function similarly to the Glu residue. Differently in the ascomycete laccases, the only acidic residue that might assist in the proton transfer is the carboxylate group from the C-terminus (Leu459 in TaLcc1 and Leu559 in rMaL). Therefore, it is likely that the proton transfer is assisted by different residues in the basidiomycete laccases (the Glu residue) and the ascomycete laccases (the carboxylate group in the C-terminus). Still, it is also possible that in the ascomycete laccases only the proton transfer from the T1 copper site to the trinuclear copper centre is assisted by the residues in the SDS-gate. The kinetics of ThL showed clearly differences from those of TaLcc1 and rMaL. As related to their three-dimensional structures, the loops forming the substrate-binding pocket of ThL are completely different from those in TaLcc1 and rMaL, most likely accounting for the strong differences in the oxidation capacity of laccases from basidiomycete and ascomycete fungi, in addition to the different E° .

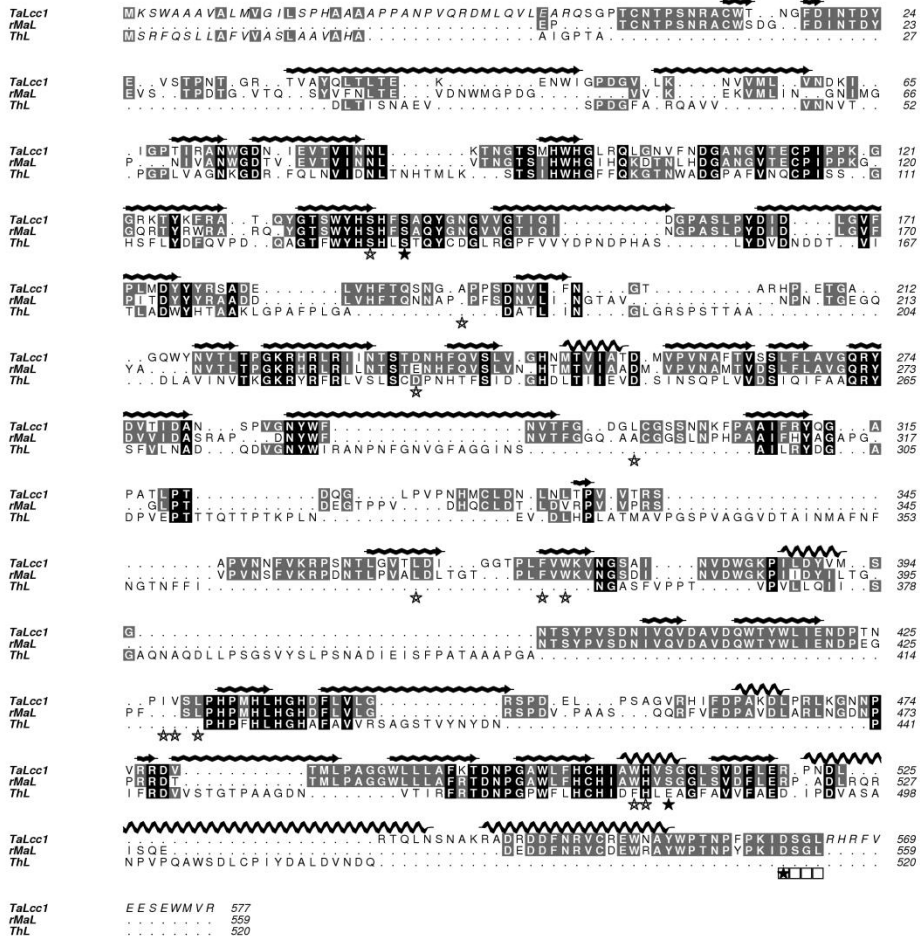


Figure 18. Amino acid sequence alignment of fungal laccases from *Thielavia arenaia* (TaLcc1, UniProtKB F6N9E7, PDB ID: 3PPS), *Melanocarpus albomyces* (rMaL, UniProtKB Q70KY3, PDB ID: 2Q9O), and *Trametes hirsuta* (ThL, UniProtKB Q02497). The N-terminally and C-terminally processed amino acid residues are indicated in italics. The secondary structure elements of TaLcc1 are also reported (α -helix as black helix, and strand as black strand). The hallow stars indicate the residues in the substrate binding pocket; the filled stars indicate the residues in the SDS-gate; the empty squares indicate the residues of the C-terminal tail. The figure was produced by means of ALINE (Bond & Schuttelkopf 2009). (Unpublished results)

4.4 Enzymatic cross-linking of α -casein proteins by means of catechol oxidase, tyrosinases, and laccases (Unpublished results)

All enzymes dealt with in this work were tested for their protein cross-linking ability with α -casein used as a model substrate with and without a cross-linking agent. Catechol was used as a cross-linking agent in the tyrosinases- and catechol oxidases-catalysed reactions, and *p*-coumaric acid in the laccases-catalysed reactions (**Figure 19**, **Figure 20**). *Trichoderma reesei* tyrosinase (TrT) efficiently cross-linked α -caseins without a cross-linking agent, whereas *Agaricus bisporus* tyrosinase (AbT) did not directly cross-link α -caseins, as also reported by Selinheimo et al. (2007b), nor was the newly discovered *Aspergillus oryzae* catechol oxidase (AoCO4) capable to cross-link α -caseins. AbT and AoCO4 clearly cross-linked α -caseins in the presence of the cross-linking agent; on the contrary, in the presence of catechol, the cross-linking ability of TrT was strongly reduced. Furthermore, AoCO4-catalysed (100 nkat g⁻¹ caseins) cross-linking of caseins in the presence of catechol was more efficient than was AbT-catalysed (100 nkat g⁻¹ caseins) cross-linking, as analysed by SDS-page. Selinheimo et al. (2007b) showed that tyrosinases from apple and potato have particularly low activity on L-tyrosine and are able to cross-link caseins in the presence of L-DOPA as a cross-linking agent. AoCO4 performed similarly to the tyrosinases from apple and potato in cross-linking of α -caseins. It is worthy of mention that, despite these enzymes from apple and potato being classified as tyrosinases, they have low activity on L-tyrosine and thereby resemble catechol oxidases more closely. In order to get a better understanding of the cross-linking abilities of catechol oxidases, more catechol oxidases should be discovered and characterised.

None of the three fungal laccases tested, i.e., those from *Thielavia arenaria* (TaLcc1), *Melanocarpus albomyces* (rMaL) and *Trametes hirsuta* (ThL), showed cross-linking ability of α -caseins without a cross-linking agent, in the reaction conditions studied. In the presence of *p*-coumaric acid (the cross-linking agent), the cross-linking efficiency of the three laccases tested followed the order TaLcc1 > rMaL > ThL. However, in contrast to the tyrosinases, none of the laccases were capable of fully cross-linking all of the α -caseins in the reaction conditions. The cross-linking abilities of rMaL and TaLcc1 had not been tested before. Previously, Selinheimo et al. (2008) reported on the cross-linking ability of ThL, showing that efficient cross-linking of α -caseins without any cross-linking agent was obtained with ThL (15000 nkat g⁻¹ caseins). However, this was a higher dosage than the one used in the present experiment conditions (i.e., 1000 nkat g⁻¹ caseins was the highest dosage tested). ThL was also found to cross-link α -caseins in the presence of *p*-coumaric acid, as already reported by Selinheimo et al. (2008).

Of the enzymes tested, TrT showed unique characteristics in protein cross-linking. The presence of a small diphenolic cross-linking agent (i.e., catechol) noticeably inhibited TrT-catalysed protein cross-linking. Similarly, TrT cross-linking

ability was greatly reduced when L-DOPA was used as a cross-linking agent, as reported by Selinheimo et al. (Selinheimo et al. 2007a, Selinheimo et al. 2007b, Mattinen et al. 2008a, Mattinen et al. 2008b, Selinheimo et al. 2008). The lower cross-linking efficiency of TrT in the presence of a cross-linking agent could be explained by the end product inhibition seen from the oxidation products of catechol and L-DOPA (Publication IV). Furthermore, it might be that the dopachrome formed by TrT-catalysed oxidation of L-DOPA could have reacted non-enzymatically with the protein-bound Tyr residues thus blocking these sites to further cross-linking of α -casein subunits.

4. Results and discussion

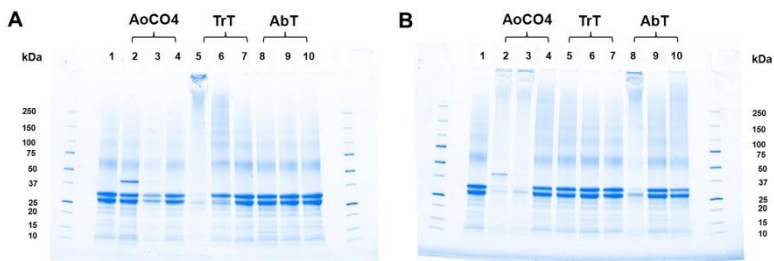


Figure 19. Cross-linking of α -casein proteins (3 g L^{-1}) by catechol oxidase from *Aspergillus oryzae* (AoCO4) and tyrosinases from *Trichoderma reesei* (TrT) and *Agaricus bisporus* (AbT) after 24 hours of incubation without a cross-linking agent (A) and with catechol (2 mM) as a cross-linking agent (B). The enzyme dosage were 1000, 100, and 10 nkat g^{-1} of α -caseins. Lanes for gel A: 1, α -caseins; 2, α -caseins + AoCO4 (1000 nkat); 3, α -caseins + AoCO4 (100 nkat); 4, α -caseins + AoCO4 (10 nkat); 5, α -caseins + TrT (1000 nkat); 6, α -caseins + TrT (100 nkat); 7, α -caseins + TrT (10 nkat); 8, α -caseins + AbT (1000 nkat); 9, α -caseins + AbT (100 nkat); 10, α -caseins + AbT (10 nkat). Lanes for gel B: the same as with gel A, except that catechol (2 mM) as a cross-linking agent was present in all of the experiments. (Unpublished results.)

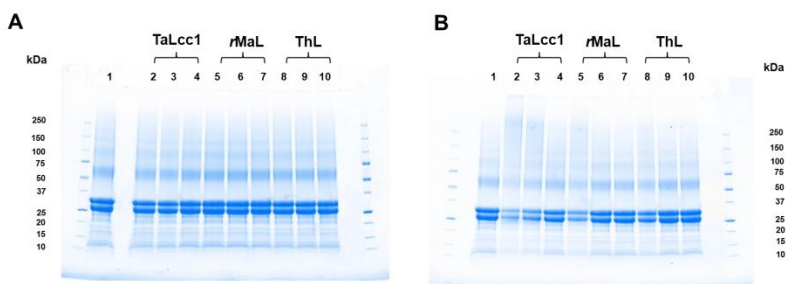


Figure 20. Cross-linking of α -casein proteins (3 g L^{-1}) by laccases from *Thielavia arenaria* (TaLcc1), *Melanocarpus albomyces* (rMaL) and *Trametes hirsuta* (ThL) after 24 hours of incubation without a cross-linking agent (A) and with *p*-coumaric acid (2 mM) as cross-linking agent (B). The enzyme dosage were 1000, 100 and 10 nkat g^{-1} of α -caseins. Lanes for gel A: 1, α -caseins; 2, α -caseins + TaLcc1 (1000 nkat); 3, α -caseins + TaLcc1 (100 nkat); 4, α -caseins + TaLcc1 (10 nkat); 5, α -caseins + rMaL (1000 nkat); 6, α -caseins + rMaL (100 nkat); 7, α -caseins + rMaL (10 nkat); 8, α -caseins + ThL (1000 nkat); 9, α -caseins + ThL (100 nkat); 10, α -caseins + ThL (10 nkat). Lanes for gel B: the same as with gel A, except that *p*-coumaric acid (2 mM) as a cross-linking agent was present in all of the experiments. (Unpublished results.)

5. Conclusions and future prospects

Food microstructure has an important role in the sensory perception of texture, water-binding, and rheological properties as well as in the digestibility and absorption of food components. Cross-linking enzymes may be used in food technology as specific tools for designed food properties and new products. This work was aimed at characterising copper-containing oxidative enzymes that can be utilised for cross-linking of proteins in food technology.

A novel family of short-tyrosinase sequences was identified in the available fungal genomes. Sequences belonging to this family are shorter in length and lack the C-terminal domain typical of long tyrosinase sequences. An extracellular catechol oxidase from *Aspergillus oryzae* (AoCO4) belonging to the newly discovered short-tyrosinase sequences was produced in *Trichoderma reesei* in high titre. AoCO4 was purified, and biochemically and structurally characterised. AoCO4 was observed to be a relatively thermostable enzyme, which is not typical for catechol oxidases and tyrosinases. AoCO4 was able to oxidise a limited range of diphenolic compounds, such as catechol, caffeic acid, hydrocaffeic acid, and 4-*tert*-butylcatechol. AoCO4 oxidised also the monophenolic compounds aminophenol and guaiacol. However, AoCO4 did not oxidise L-DOPA and L-tyrosine, which are the characteristic substrates of tyrosinase, therefore it was classified as a catechol oxidase. Since generally catechol oxidases of fungal origin are not well-characterised enzymes, the characterisation of AoCO4 could provide a new contribution to the knowledge of these enzymes.

A preliminary crystal structure of AoCO4 was solved at 2.5 Å resolution and it is thus far the only three-dimensional structure of a catechol oxidase of fungal origin. The overall structure of AoCO4 was found to be similar to the known structures of plant catechol oxidases and fungal tyrosinases. AoCO4 was a monomer. The two copper ions of the type-3 copper site were found in a four-helix bundle, which is conserved in catechol oxidases and tyrosinases. The UV/VIS spectroscopic features of the enzyme indicated that 35% of AoCO4 was in the *oxy*-form (i.e., the form of tyrosinases active on monophenols). Nevertheless, AoCO4 did not show significant activity on monophenols. From the three-dimensional structure of AoCO4 there is no definite explanation for the lack of monophenolase activity of this enzyme. However, it could be hypothesised that the residues involved in the oxidation of monophenols and diphenols are different in AoCO4 in comparison to tyrosinases and catechol oxidases. Future structural studies might elucidate the

reaction mechanism of AoCO4 and catechol oxidases and reveal the differences with tyrosinases.

The extracellular tyrosinase from *Trichoderma reesei* (TrT) has been shown to have exclusive cross-linking ability of proteins. In this work a detailed characterisation of TrT was performed and the well characterised commercial tyrosinase from *Agaricus bisporus* (AbT) was used as a reference enzyme. The ability of TrT and AbT to oxidise small molecular weight monophenolic and diphenolic substrates was found to be strongly influenced by the substitution of the substrate molecule. In general, TrT had higher affinity on the substrates in which a carboxyl group was present in the structure, whereas AbT had higher affinity for the substrates in which an amino group was present in the structure. Furthermore, TrT showed lower affinity than AbT on L-tyrosine alone and for tripeptides varying in the position of Tyr residue.

Dopachrome was found to be the only reaction end product of both tyrosinases-catalysed oxidation of L-DOPA, which was used as representative diphenolic substrate with an amino group in the structure. Dopachrome was found to inhibit the TrT-catalysed oxidation of L-DOPA, but not the AbT-catalysed oxidation of L-DOPA. Thus far, this is the first report on a tyrosinase end product inhibition.

The effect of the redox potential on the oxidation capacity of fungal laccases was elucidated using a set of laccases and substituted phenolic substrates and related to the available crystal structures of these enzymes. For this purpose, a novel laccase 1 from the ascomycete fungus *Thielavia arenaria* (TaLcc1) and the laccases from *Melanocarpus albomyces* and *Trametes hirsuta* were used. The laccase-catalysed oxidation of phenolic substrates was found to be dependent on the difference in redox potential between the enzyme and the substrate (ΔE°) and the pH. Indeed, the redox potential (E°) of a phenolic substrate is pH dependent and the laccase is inhibited by hydroxide ions. In general, both the ΔE° and the pH had an effect on the kinetics. However, the effect of ΔE° was found to prevail over the effect of the pH for substrates with high E° , such as methyl syringate.

The oxidative enzymes were shown to have potential cross-linking abilities. TrT was found to be the best enzyme for cross-linking of α -caseins, whereas AbT and AoCO4 were found to be the best enzymes for cross-linking α -caseins in the presence of catechol as a cross-linking agent. As a novel finding, AoCO4 was also found to cross-link α -caseins in the presence of catechol as a cross-linking agent.

References

- Aaslyng, D., Rorbaek, K. & Sorensen, N. 1996. An enzyme for dyeing keratinous fibres. Patent No: WO9719998.
- Abadulla, E., Tzanov, T., Costa, S., Robra, K., Cavaco-Paulo, A. & Gübitz, G.M. 2000. Decolorization and detoxification of textile dyes with a laccase from *Trametes hirsuta*. *Appl Environ Microbiol*, Vol. 66, No. 8, pp. 3357–3362.
- Ahmed, S.R., Lutes, A.T. & Barbari, T.A. 2006. Specific capture of target proteins by oriented antibodies bound to tyrosinase-immobilized Protein A on a polyallylamine affinity membrane surface. *J Memb Sci*, Vol. 282, No. 1–2, pp. 311–321.
- Akyilmaz, E., Kozgus, O., Türkmen, H. & Çetinkaya, B. 2010. A mediated polyphenol oxidase biosensor immobilized by electropolymerization of 1,2-diamino benzene. *Bioelectrochemistry*, Vol. 78, No. 2, pp. 135–140.
- Andberg, M., Hakulinen, N., Auer, S., Saloheimo, M., Koivula, A., Rouvinen, J. & Kruus, K. 2009. Essential role of the C-terminus in *Melanocarpus albomyces* laccase for enzyme production, catalytic properties and structure. *FEBS J*, Vol. 276, No. 21, pp. 6285–6300.
- Ando, H., Adachi, M., Umeda, K., Matsuura, A., Nonaka, M., Uchio, R., Tanaka, H. & Motoki, M. 1989. Purification and characteristics of a novel transglutaminase derived from microorganisms. *Agric Biol Chem*, Vol. 53, No. 10, pp. 2613–2617.
- Anghileri, A., Lantto, R., Kruus, K., Arosio, C. & Freddi, G. 2007. Tyrosinase-catalyzed grafting of sericin peptides onto chitosan and production of protein-polysaccharide bioconjugates. *J Biotechnol*, Vol. 127, No. 3, pp. 508–519.
- Arias, M.E., Arenas, M., Rodriguez, J., Soliveri, J., Ball, A.S. & Hernandez, M. 2003. Kraft pulp biobleaching and mediated oxidation of a nonphenolic substrate by laccase from *Streptomyces cyaneus* CECT 3335. *Appl Environ Microbiol*, Vol. 69, No. 4, pp. 1953–1958.
- Aroca, P., Solano, F., García-Borrón, J.C. & Lozano, J.A. 1990. A new spectrophotometric assay for dopachrome tautomerase. *J Biochem Biophys Methods*, Vol. 21, No. 1, pp. 35–46.

- Arvas, M., Kivioja, T., Mitchell, A., Saloheimo, M., Ussery, D., Penttila, M. & Oliver, S. 2007. Comparison of protein coding gene contents of the fungal phyla *Pezizomycotina* and *Saccharomycotina*. *BMC Genomics*, Vol. 8, pp. 325.
- Baldrian, P. 2006. Fungal laccases – occurrence and properties. *FEMS Microbiol Rev*, Vol. 30, No. 2, pp. 215–242.
- Bao, W., O'Malley, D.M., Whetten, R. & Sederoff, R.R. 1993. A laccase associated with lignification in loblolly pine xylem. *Science*, Vol. 260, No. 5108, pp. 672–674.
- Bar Nun, N., Tal Lev, A., Harel, E. & Mayer, A.M. 1988. Repression of laccase formation in *Botrytis cinerea* and its possible relation to phytopathogenicity. *Phytochemistry*, Vol. 27, No. 8, pp. 2505–2509.
- Baron, C.P., Børresen, T. & Jacobsen, C. 2007. Comparison of methods to reduce dioxin and polychlorinated biphenyls contents in fishmeal: extraction and enzymatic treatments. *J Agric Food Chem*, Vol. 55, No. 4, pp. 1620–1626.
- Basnar, B., Xu, J., Li, D. & Willner, I. 2007. Encoded and enzyme-activated nanolithography of gold and magnetic nanoparticles on silicon. *Langmuir*, Vol. 23, No. 5, pp. 2293–2296.
- Battistuzzi, G., Di Rocco, G., Leonardi, A. & Sola, M. 2003. ¹H NMR of native and azide-inhibited laccase from *Rhus vernicifera*. *J Inorg Biochem*, Vol. 96, No. 4, pp. 503–506.
- Bell, A.A. & Wheeler, M.H. 1986. Biosynthesis and functions of fungal melanins. *Annu Rev Phytopathol*, Vol. 24, pp. 411–451.
- Beltramini, M. & Lerch, K. 1982. Fluorescence properties of *Neurospora* tyrosinase. *Biochem J*, Vol. 205, No. 1, pp. 173–180.
- Bento, I., Silva, C.S., Chen, Z., Martins, L.O., Lindley, P.F. & Soares, C.M. 2010. Mechanisms underlying dioxygen reduction in laccases. Structural and modelling studies focusing on proton transfer. *BMC Struct Biol*, Vol. 10, pp. 28.
- Bergman, P.J., McKnight, J., Novosad, A., Charney, S., Farrelly, J., Craft, D., Wulderk, M., Jeffers, Y., Sadelain, M., Hohenhaus, A.E., et al. 2003. Long-term survival of dogs with advanced malignant melanoma after

- DNA vaccination with xenogeneic human tyrosinase: a phase I trial. *Clin Cancer Res*, Vol. 9, No. 4, pp. 1284–1290.
- Berka, R.M., Schneider, P., Golightly, E.J., Brown, S.H., Madden, M., Brown, K.M., Halkier, T., Mondorf, K. & Xu, F.F. 1997. Characterization of the gene encoding an extracellular laccase of *Myceliophthora thermophila* and analysis of the recombinant enzyme expressed in *Aspergillus oryzae*. *Appl Environ Microbiol*, Vol. 63, No. 8, pp. 3151–3157.
- Bernan, V., Filpula, D., Herber, W., Bibb, M. & Katz, E. 1985. The nucleotide sequence of the tyrosinase gene from *Streptomyces antibioticus* and characterization of the gene product. *Gene*, Vol. 37, No. 1–3, pp. 101–110.
- Bertrand, T., Jolival, C., Briozzo, P., Caminade, E., Joly, N., Madzak, C. & Mougin, C. 2002. Crystal structure of a four-copper laccase complexed with an arylamine: insights into substrate recognition and correlation with kinetics. *Biochemistry*, Vol. 41, No. 23, pp. 7325–7333.
- Bi, J.L. & Felton, G.W. 1995. Foliar oxidative stress and insect herbivory: primary compounds, secondary metabolites, and reactive oxygen species as components of induced resistance. *J Chem Ecol*, Vol. 21, pp. 1511–1530.
- Bittner, S. 2006. When quinones meet amino acids: chemical, physical and biological consequences. *Amino Acids*, Vol. 30, No. 3, pp. 205–224.
- Boer, H. & Koivula, A. 2003. The relationship between thermal stability and pH optimum studied with wild-type and mutant *Trichoderma reesei* cellobiohydrolase Cel7A. *Eur J Biochem*, Vol. 270, No. 5, pp. 841–848.
- Bollag, J.-M. & Leonowicz, A. 1984. Comparative studies of extracellular fungal laccases. *Appl Environ Microbiol*, Vol. 48, No. 4, pp. 849–854.
- Bond, C.S. & Schuttelkopf, A.W. 2009. ALINE: a WYSIWYG protein-sequence alignment editor for publication-quality alignments. *Acta Cryst*, Vol. D65, pp. 510–512.
- Borthakur, D., Lamb, J.W. & Johnston, A.W. 1987. Identification of two classes of *Rhizobium phaseoli* genes required for melanin synthesis, one of which is required for nitrogen fixation and activates the transcription of the other. *Mol Gen Genet*, Vol. 207, No. 1, pp. 155–160.

- Bourbonnais, R. & Paice, M.G. 1992. Demethylation and delignification of kraft pulp by *Trametes versicolor* laccase in the presence of 2,2'-azinobis-(3-ethylbenzthiazoline-6-sulphonate). *Appl Environ Microbiol*, Vol. 36, No. 6, pp. 823–827.
- Bourbonnais, R., Paice, M.G., Freiermuth, B., Bodie, E. & Borneman, S. 1997. Reactivities of various mediators and laccases with kraft pulp and lignin model compounds. *Appl Environ Microbiol*, Vol. 63, No. 12, pp. 4627–4632.
- Brändén, R. & Deinum, J. 1977. Type 2 copper(II) as a component of the dioxygen reducing site in laccase: evidence from EPR experiments with ^{17}O . *FEBS Lett*, Vol. 73, No. 2, pp. 144–146.
- Brändén, R., Deinum, J. & Coleman, M. 1978. A mass spectrometric investigation of the reaction between $^{18}\text{O}_2$ and reduced tree laccase. A differentiation between the two water molecules formed. *FEBS Lett*, Vol. 89, No. 1, pp. 180–182.
- Breathnach, A. 1996. Melanin hyperpigmentation of skin: melasma, topical treatment with azelaic acid, and other therapies. *Cutis*, Vol. 57, No. 1, pp. 36–45.
- Bubacco, L., Van Gastel, M., Groenen, E.J., Vijgenboom, E. & Canters, G.W. 2003. Spectroscopic characterization of the electronic changes in the active site of *Streptomyces antibioticus* tyrosinase upon binding of transition state analogue inhibitors. *J Biol Chem*, Vol. 278, No. 9, pp. 7381–7389.
- Buchert, J., Selinheimo, E., Kruus, K., Mattinen, M.-L., Lantto, R. & Autio, K. 2007. Using crosslinking enzymes to improve textural and other properties of food. In: Rastall, R. (ed.) *Novel enzyme technology for food applications*. CRC press, pp. 101–139.
- Buchert, J., Ercili Cura, D., Ma, H., Gasparetti, C., Monogioudi, E., Faccio, G., Boer, H., Partanen, R., Selinheimo, E., Lantto, R., et al. 2010. Cross linking food proteins for improved functionality. *Annu Rev Food Sci Technol*, Vol. 1, No. 1, pp. 113–138.
- Busch, J.L.H.C., Hrnčirik, K., Bulukin, E., Boucon, C. & Mascini, M. 2006. Biosensor measurements of polar phenolics for the assessment of the bitterness and pungency of virgin olive oil. *J Agric Food Chem*, Vol. 54, No. 12, pp. 4371–4377.

- Cabanes, J., Chazarra, S. & García Carmona, F. 1994. Kojic acid, a cosmetic skin whitening agent, is a slow-binding inhibitor of catecholase activity of tyrosinase. *J Pharm Pharmacol*, Vol. 46, pp. 982–985.
- Call, H.P. & Mücke, I. 1997. History, overview and applications of mediated lignolytic systems, especially laccase-mediator-systems (Lignozym[®]-process). *J Biotechnol*, Vol. 53, No. 2–3, pp. 163–202.
- Camarero, S., Ibarra, D., Martínez, Á.T., Romero, J., Gutiérrez, A. & del Río, J.C. 2007. Paper pulp delignification using laccase and natural mediators. *Enzyme Microb Technol*, Vol. 40, No. 5, pp. 1264–1271.
- Canfora, L., Iamarino, G., Rao, M.A. & Gianfreda, L. 2008. Oxidative transformation of natural and synthetic phenolic mixtures by *Trametes versicolor* laccase. *J Agric Food Chem*, Vol. 56, No. 4, pp. 1398–1407.
- Canovas, F.G., García-Carmona, F., Sanchez, J.V., Pastor, J.L. & Teruel, J.A. 1982. The role of pH in the melanin biosynthesis pathway. *J Biol Chem*, Vol. 257, No. 15, pp. 8738–8744.
- Carvalho, G.M., Alves, T.L. & Freire, D.M. 2000. L-DOPA production by immobilized tyrosinase. *Appl Biochem Biotechnol*, Vol. 84–86, pp. 791–800.
- Chang, T.S. 2009. An updated review of tyrosinase inhibitors. *Int J Mol Sci*, Vol. 10, No. 6, pp. 2440–2475.
- Chao, A., Shyu, S., Lin, Y. & Mi, F. 2004. Enzymatic grafting of carboxyl groups on to chitosan – to confer on chitosan the property of a cationic dye adsorbent. *Bioresour Technol*, Vol. 91, No. 2, pp. 157–162.
- Chedekel, M.R., Agin, P.P. & Sayre, R.M. 1980. Photochemistry of pheomelanin: action spectrum for superoxide production. *Photochem Photobiol*, Vol. 31, pp. 553–555.
- Chefetz, B., Chen, Y. & Hadar, Y. 1998. Purification and characterization of laccase from *Chaetomium thermophilum* and its role in humification. *Appl Environ Microbiol*, Vol. 64, No. 9, pp. 3175–3179.
- Chen, J.S., Wei, C. & Marshall, M.R. 1991. Inhibition mechanism of kojic acid on polyphenol oxidase. *J Agric Food Chem*, Vol. 39, pp. 1897–1901.
- Chen, Y.T., Stockert, E., Tsang, S., Coplan, K.A. & Old, L.J. 1995. Immunophenotyping of melanomas for tyrosinase: implications for

- vaccine development. Proc Natl Acad Sci U S A, Vol. 92, No. 18, pp. 8125–8129.
- Chen, S., Ge, W. & Buswell, J.A. 2004. Biochemical and molecular characterization of a laccase from the edible straw mushroom, *Volvariella volvacea*. Eur J Biochem, Vol. 271, No. 2, pp. 318–328.
- Choi, M. & Davidson, V.L. 2011. Cupredoxins-A study of how proteins may evolve to use metals for bioenergetic processes. Metallomics, Vol. 2, pp. 140–151.
- Claus, H. & Decker, H. 2006. Bacterial tyrosinases. Syst Appl Microbiol, Vol. 29, No. 1, pp. 3–14.
- Coll, P.M., Fernandez-Abalos, J.M., Villanueva, J.R., Santamaria, R. & Perez, P. 1993. Purification and characterization of a phenoloxidase (laccase) from the lignin-degrading basidiomycete PM1 (CECT 2971). Appl Environ Microbiol, Vol. 59, No. 8, pp. 2607–2613.
- Conrad, J.S., Dawso, S.R., Hubbard, E.R., Meyers, T.E. & Strothkamp, K.G. 1994. Inhibitor binding to the binuclear active site of tyrosinase: temperature, pH, and solvent deuterium isotope effects. Biochemistry, Vol. 33, No. 19, pp. 5739–5744.
- Conrad, L.S., Sponholz, W.R. & Berker, O. 2000. Treatment of cork with a phenol oxidizing enzyme. USA. Patent No: US 6152966.
- Cooksey, C.J., Garratt, P.J., Land, E.J., Pavel, S., Ramsden, C.A., Riley, P.A. & Smit, N.P. 1997. Evidence of the indirect formation of the catecholic intermediate substrate responsible for the autoactivation kinetics of tyrosinase. J Biol Chem, Vol. 272, No. 42, pp. 26226–26235.
- Coyne, V.E. & Al-Harhi, L. 1992. Induction of melanin biosynthesis in *Vibrio cholerae*. Appl Environ Microbiol, Vol. 58, No. 9, pp. 2861–2865.
- Cuff, M.E., Miller, K.I., van Holde, K.E. & Hendrickson, W.A. 1998. Crystal structure of a functional unit from *Octopus* hemocyanin. J Mol Biol, Vol. 278, No. 4, pp. 855–870.
- D'Annibale, A., Stazi, S.R., Vinciguerra, V. & Giovannozzi Sermanni, G. 2000. Oxirane-immobilized *Lentinula edodes* laccase: stability and phenolics removal efficiency in olive mill wastewater. J Biotechnol, Vol. 77, No. 2–3, pp. 265–273.

- Dawley, R.M. & Flurkey, W.H. 1993. Differentiation of tyrosinase and laccase using 4-hexyl-resorcinol, a tyrosinase inhibitor. *Phytochemistry*, Vol. 33, No. 2, pp. 281–284.
- De La Mora, E., Valderrama, B., Horjales, E. & Rudino-Pinera, E. 2008. Crystal structure of *Corioloropsis gallica* laccase at 1.7 Å resolution. DOI:10.2210/pdb2vdz/pdb.
- De Leeuw, S.M., Smit, N.P., Van Veldhoven, M., Pennings, E.M., Pavel, S., Simons, J.W. & Schothorst, A.A. 2001. Melanin content of cultured human melanocytes and UV-induced cytotoxicity. *J Photochem Photobiol B*, Vol. 61, No. 3, pp. 106–113.
- de Marco, A. & Roubelakis-Angelakis, K.A. 1997. Laccase activity could contribute to cell-wall reconstitution in regenerating protoplasts. *Phytochemistry*, Vol. 46, No. 3, pp. 421–425.
- Decker, H., Schweikardt, T. & Tucek, F. 2006. The first crystal structure of tyrosinase: all questions answered? *Angew Chem Int Ed Engl*, Vol. 45, No. 28, pp. 4546–4550.
- Dedeyan, B., Klonowska, A., Tagger, S., Tron, T., Iacazio, G., Gil, G. & Le Petit, J. 2000. Biochemical and molecular characterization of a laccase from *Marasmius quercophilus*. *Appl Environ Microbiol*, Vol. 66, No. 3, pp. 925–929.
- Dervall, B.J. 1961. Phenolase and peptic enzyme activity in the chocolate spot disease of beans. *Nature*, Vol. 189, p. 311.
- Dinckaya, E., Akyilmaz, E., Akgol, S., Tatar Önal, S., Zihnioglu, F. & Telefoncu, A. 1998. A novel catechol oxidase enzyme electrode for the specific determination of catechol. *Biosci Biotechnol Biochem*, Vol. 62, No. 11, pp. 2098–2100.
- DiSpirito, A.A., Taaffe, L.R., Lipscomb, J.D. & Hooper, A.B. 1985. A 'blue' copper oxidase from *Nitrosomonas europaea*. *Biochim Biophys Acta*, Vol. 827, No. 3, pp. 320–326.
- Dittmer, N.T., Suderman, R.J., Jiang, H., Zhu, Y., Gorman, M.J., Kramer, K.J. & Kanost, M.R. 2004. Characterization of cDNAs encoding putative laccase-like multicopper oxidases and developmental expression in the tobacco hornworm, *Manduca sexta*, and the malaria mosquito, *Anopheles gambiae*. *Insect Biochem Mol Biol*, Vol. 34, No. 1, pp. 29–41.

- Dong, S. & Chen, X. 2002. Some new aspects in biosensors. *J Biotechnol*, Vol. 82, No. 4, pp. 303–323.
- Draelos, Z.D. 2007. Skin lightening preparations and the hydroquinone controversy. *Dermatol Ther*, Vol. 20, No. 5, pp. 308–313.
- Dubé, E., Shareck, F., Hurtubise, Y., Daneault, C. & Beauregard, M. 2008. Homologous cloning, expression, and characterisation of a laccase from *Streptomyces coelicolor* and enzymatic decolourisation of an indigo dye. *Appl Microbiol Biotechnol*, Vol. 79, No. 4, pp. 597–603.
- Duckworth, H.W. & Coleman, J.E. 1970. Physicochemical and kinetic properties of mushroom tyrosinase. *J Biol Chem*, Vol. 245, No. 7, pp. 1613–1625.
- Ducros, V., Brzozowski, A.M., Wilson, K.S., Brown, S.H., Ostergaard, P., Schneider, P., Yaver, D.S., Pedersen, A.H. & Davies, G.J. 1998. Crystal structure of the type-2 Cu depleted laccase from *Coprinus cinereus* at 2.2 Å resolution. *Nat Struct Biol*, Vol. 5, No. 4, pp. 310–316.
- Dwivedi, U.N., Singh, P., Pandey, V.P. & Kumar, A. 2011. Structure-function relationship among bacterial, fungal and plant laccases. *J Molec Catal B*, Vol. 68, No. 2, pp. 117–128.
- Eggert, C., Temp, U. & Eriksson, K.-E.L. 1996. The ligninolytic system of the white rot fungus *Pycnoporus cinnabarinus*: purification and characterization of the laccase. *Appl Environ Microbiol*, Vol. 62, No. 4, pp. 1151–1158.
- Eicken, C., Zippel, F., Büldt-Karentzopoulos, K. & Krebs, B. 1998. Biochemical and spectroscopic characterization of catechol oxidase from sweet potatoes (*Ipomoea batatas*) containing a type-3 dicopper center. *FEBS Lett*, Vol. 436, No. 2, pp. 293–299.
- Eickman, N.C., Solomon, E.I., Larrabee, J.A., Spiro, T.G. & Lerch, K. 1978. Ultraviolet resonance Raman study of oxytyrosinase. Comparison with oxyhemocyanins. *J Am Chem Soc*, Vol. 100, No. 20, pp. 6529–6531.
- Enguita, F.J., Martins, L.O., Henriques, A.O. & Carrondo, M.A. 2003. Crystal structure of a bacterial endospore coat component. A laccase with enhanced thermostability properties. *J Biol Chem*, Vol. 278, No. 21, pp. 19416–19425.

- Ercili Cura, D., Lille, M., Partanen, R., Kruus, K., Buchert, J. & Lantto, R. 2010. Effect of *Trichoderma reesei* tyrosinase on rheology and microstructure of acidified milk gels. *Int Dairy J*, Vol. 20, No. 12, pp. 830–837.
- Espín, J.C., García-Ruíz, P.A., Tudela, J. & García-Cánovas, F.G. 1998. Study of stereospecificity in mushroom tyrosinase. *Biochem J*, Vol. 331, No. 2, pp. 547–551.
- Espín, J.C., Jolivet, S. & Wichers, H.J. 1999. Kinetic study of the oxidation of γ -L-glutaminyl-4-hydroxybenzene catalyzed by mushroom (*Agaricus bisporus*) tyrosinase. *J Agric Food Chem*, Vol. 47, No. 9, pp. 3495–3502.
- Espín, J.C. & Wichers, H.J. 1999. Slow-binding inhibition of mushroom (*Agaricus bisporus*) tyrosinase isoforms by tropolone. *J Agric Food Chem*, Vol. 47, No. 7, pp. 2638–2644.
- Espín, J.C., Varón, R., Fenoll, L.G., Gilabert, M.A., García-Ruíz, P.A., Tudela, J. & García-Cánovas, F.G. 2000. Kinetic characterization of the substrate specificity and mechanism of mushroom tyrosinase. *Eur J Biochem*, Vol. 267, No. 5, pp. 1270–1279.
- Færgemand, M., Otte, J. & Qvist, K.B. 1998. Cross-linking of whey proteins by enzymatic oxidation. *J Agric Food Chem*, Vol. 46, pp. 1326–1333.
- Fan, Y. & Flurkey, W.H. 2004. Purification and characterization of tyrosinase from gill tissue of *Portabella* mushrooms. Vol. 65, No. 6, pp. 671–678.
- Fatibello-Filho, O. & da Cruz Vieira, I. 1997. Flow injection spectrophotometric determination of L-dopa and carbidopa in pharmaceutical formulations using a crude extract of sweet potato root [*Ipomoea batatas* (L.) Lam.] as enzymatic source. *Analyst*, Vol. 122, No. 4, pp. 345–350.
- Faure, D., Bouillant, M.L. & Bally, R. 1994. Isolation of *Azospirillum lipoferum* 4T Tn5 mutants affected in melanization and laccase activity. *Appl Environ Microbiol*, Vol. 60, No. 9, pp. 3413–3415.
- Faure, D., Bouillant, M. & Bally, R. 1995. Comparative study of substrates and inhibitors of *Azospirillum lipoferum* and *Pyricularia oryzae* laccases. *Appl Environ Microbiol*, Vol. 61, No. 3, pp. 1144–1146.
- Felton, G.W., Donato, K., Del Vecchio, R.J. & Duffey, S.S. 1989. Activation of plant foliar oxidases by insect feeding reduces nutritive quality of foliage for noctuid herbivores. *J Chem Ecol*, Vol. 15, pp. 2267–2694.

- Fenoll, L.G., Rodríguez-López, J.N., Garcia-Molina, F.J., García-Cánovas, F.G. & Tudela, J. 2002. Michaelis constants of mushroom tyrosinase with respect to oxygen in the presence of monophenols and diphenols. *Int J Biochem Cell Biol*, Vol. 34, No. 4, pp. 332–336.
- Fernandez-Larrea, J. & Stahl, U. 1996. Isolation and characterization of a laccase gene from *Podospora anserina*. *Mol Gen Genet*, Vol. 252, No. 5, pp. 539–551.
- Ferraroni, M., Myasoedova, N., Schmatchenko, V., Leontievsky, A., Golovleva, L., Scozzafava, A. & Briganti, F. 2007. Crystal structure of a blue laccase from *Lentinus tigrinus*: evidences for intermediates in the molecular oxygen reductive splitting by multicopper oxidases. *BMC Struct Biol*, Vol. 7, No. 60.
- Fling, M., Horowitz, N.H. & Heinenmann, S.F. 1963. The isolation and properties of crystalline tyrosinase from *Neurospora*. *J Biol Chem*, Vol. 238, pp. 2045–2053.
- Flurkey, W.H., Ratcliff, B., Lopez, L., Kuglin, J. & Dawley, R.M. 1995. Differentiation of fungal tyrosinases and laccases using selective inhibitors and substrates. In: Lee, C. & Whitaker, J.R. (eds.) *Enzymatic browning and its prevention*. ACS Symposium Series; American Chemical Society, Washington, DC, pp. 81–89.
- Flurkey, W.H. & Inlow, J.K. 2008. Proteolytic processing of polyphenol oxidase from plants and fungi. *J Inorg Biochem*, Vol. 102, No. 12, pp. 2160–2170.
- Folk, J.E. & Finlayson, J.S. 1977. The epsilon-(gamma-glutamyl)lysine crosslink and the catalytic role of transglutaminases. *Adv Protein Chem*, Vol. 31, pp. 1–133.
- Freddi, G., Anghileri, A., Sampaio, S., Buchert, J., Monti, P. & Taddei, P. 2006. Tyrosinase-catalyzed modification of *Bombyx mori* silk fibroin: grafting of chitosan under heterogeneous reaction conditions. *J Biotechnol*, Vol. 125, No. 2, pp. 281–294.
- Froehner, S.C. & Eriksson, K.-E.L. 1974. Purification and properties of *Neurospora crassa* laccase. *J Bacteriol*, Vol. 120, No. 1, pp. 458–465.
- Funayama, M., Arakawa, H., Yamamoto, R., Nishino, T., Shin, T. & Murao, S. 1995. Effects of alpha- and beta-arbutin on activity of tyrosinases from

- mushroom and mouse melanoma. *Biosci Biotechnol Biochem*, Vol. 59, No. 1, pp. 143–144.
- Galante, Y.M. & Formantici, C. 2003. Enzyme applications in detergency and in manufacturing industries. *Curr Org Chem*, Vol. 7, No. 13, pp. 1399–1422.
- Galhaup, C., Wagner, H., Hinterstoisser, B. & Haltrich, D. 2002. Increased production of laccase by the wood-degrading basidiomycete *Trametes pubescens*. *Enzyme Microb Technol*, Vol. 30, No. 4, pp. 529–536.
- Garavaglia, S., Cambria, M.T., Miglio, M., Ragusa, S., Iacobazzi, V., Palmieri, F., D'Ambrosio, C., Scaloni, A. & Rizzi, M. 2004. The structure of *Rigidoporus lignosus* laccase containing a full complement of copper ions, reveals an asymmetrical arrangement for the T3 copper pair. *J Mol Biol*, Vol. 342, No. 5, pp. 1519–1531.
- Garzillo, A.M., Colao, M.C., Buonocore, V., Oliva, R., Falcigno, L., Saviano, M., Santoro, A.M., Zappala, R., Bonomo, R.P., Bianco, C., et al. 2001. Structural and kinetic characterization of native laccases from *Pleurotus ostreatus*, *Rigidoporus lignosus*, and *Trametes trogii*. *J Protein Chem*, Vol. 20, No. 3, pp. 191–201.
- Gasowska, B., Kafarski, P. & Wojtasek, H. 2004. Interaction of mushroom tyrosinase with aromatic amines, *o*-diamines and *o*-aminophenols. *Biochim Biophys Acta*, Vol. 1673, No. 3, pp. 170–177.
- van Gastel, M., Bubacco, L., Groenen, E.J.J., Vijgenboom, E. & Canters, G.W. 2000. EPR study of the dinuclear active copper site of tyrosinase from *Streptomyces antibioticus*. *FEBS Lett*, Vol. 474, No. 2-3, pp. 228-232.
- Gavnholt, B. & Larsen, K. 2002. Molecular biology of plant laccases in relation to lignin formation. *Physiol Plant*, Vol. 116, pp. 273–280.
- Ge, H., Gao, Y., Hong, Y., Zhang, M., Xiao, Y., Teng, M. & Niu, L. 2010. Structure of native laccase B from *Trametes* sp. AH28-2. *Acta Crystallogr Sect F Struct Biol Cryst Commun*, Vol. 66, pp. 254–258.
- Gerdemann, C., Eicken, C. & Krebs, B. 2002. The crystal structure of catechol oxidase: new insight into the function of type-3 copper proteins. *Acc Chem Res*, Vol. 35, No. 3, pp. 183–191.
- Germann, U.A. & Lerch, K. 1986. Isolation and partial nucleotide sequence of the laccase gene from *Neurospora crassa*: amino acid sequence homology

- of the protein to human ceruloplasmin. Proc Natl Acad Sci U S A, Vol. 83, No. 23, pp. 8854–8858.
- Gheibi, N., Saboury, A.A., Haghbeen, K. & Moosavi-Movahedi, A.A. 2005. Activity and structural changes of mushroom tyrosinase induced by *n*-alkyl sulfates. Colloids Surf B Biointerfaces, Vol. 45, No. 2, pp. 104–107.
- Giardina, P., Palmieri, G., Scaloni, A., Fontanella, B., Faraco, V., Cennamo, G. & Sanna, G. 1999. Protein and gene structure of a blue laccase from *Pleurotus ostreatus*1. Biochem.J, Vol. 341 (Pt 3), No. Pt 3, pp. 655–663.
- Gill, R., Freeman, R., Xu, J., Willner, I., Winograd, S., Shweky, I. & Banin, U. 2006. Probing biocatalytic transformations with CdSe-ZnS QDs. J Am Chem Soc, Vol. 128, No. 48, pp. 15376–15377.
- Goller, S.P., Schoisswohl, D., Baron, M., Parriche, M. & Kubicek, C.P. 1998. Role of endoproteolytic dibasic proprotein processing in maturation of secretory proteins in *Trichoderma reesei*. Appl Environ Microbiol, Vol. 64, No. 9, pp. 3202–3208.
- Griffin, M., Casadio, R. & Bergamini, C.M. 2002. Transglutaminases: nature's biological glues. Biochem J, Vol. 368, No. 2, pp. 377–396.
- Gukasyan, G.S. 1999. Purification and some properties of tyrosinase from *Aspergillus flavipes* 56003. Biokhimiya, Vol. 64, No. 4, pp. 497–501.
- Gutiérrez, A., Rencoret, J., Ibarra, D., Molina, S., Camarero, S., Romero, J., del Río, J.C. & Martínez, Á.T. 2007. Removal of lipophilic extractives from paper pulp by laccase and lignin-derived phenols as natural mediators. Environ Sci Technol, Vol. 41, No. 11, pp. 4124–4129.
- Hakulinen, N., Kiiskinen, L.-L., Kruus, K., Saloheimo, M., Paananen, A., Koivula, A. & Rouvinen, J. 2002. Crystal structure of a laccase from *Melanocarpus albomyces* with an intact trinuclear copper site. Nat Struct Biol, Vol. 9, No. 8, pp. 601–605.
- Hakulinen, N., Kruus, K., Koivula, A. & Rouvinen, J. 2006. A crystallographic and spectroscopic study on the effect of X-ray radiation on the crystal structure of *Melanocarpus albomyces* laccase. Biochem Biophys Res Commun, Vol. 350, No. 4, pp. 929–934.

- Hakulinen, N., Andberg, M., Kallio, J., Koivula, A., Kruus, K. & Rouvinen, J. 2008. A near atomic resolution structure of a *Melanocarpus albomyces* laccase. *J Struct Biol*, Vol. 162, No. 1, pp. 29–39.
- Halaban, R., Patton, R.S., Cheng, E., Svedine, S., Trombetta, E.S., Wahl, M.L., Ariyan, S. & Hebert, D.N. 2002. Abnormal acidification of melanoma cells induces tyrosinase retention in the early secretory pathway. *J Biol Chem*, Vol. 277, No. 17, pp. 14821–14828.
- Halaoui, S., Asther, M., Kruus, K., Guo, L., Hamdi, M., Sigoillot, J.C., Asther, M. & Lomascolo, A. 2005. Characterization of a new tyrosinase from *Pycnoporus* species with high potential for food technological applications. *J Appl Microbiol*, Vol. 98, No. 2, pp. 332–343.
- Halaoui, S., Asther, M., Sigoillot, J.C., Hamdi, M. & Lomascolo, A. 2006a. Fungal tyrosinases: new prospects in molecular characteristics, bioengineering and biotechnological applications. *J Appl Microbiol*, Vol. 100, No. 2, pp. 219–232.
- Halaoui, S., Record, E., Casalot, L., Hamdi, M., Sigoillot, J.C., Asther, M. & Lomascolo, A. 2006b. Cloning and characterization of a tyrosinase gene from the white-rot fungus *Pycnoporus sanguineus*, and overproduction of the recombinant protein in *Aspergillus niger*. *Appl Environ Microbiol*, Vol. 70, No. 5, pp. 580–589.
- Harjinder, S. 1991. Modification of food proteins by covalent crosslinking. *Trends Food Sci Technol*, Vol. 2, No. 0, pp. 196–200.
- Hepp, A.F., Himmelwright, R.S., Eickman, N.C. & Solomon, E.I. 1979. Ligand displacement reactions of oxyhemocyanin: comparison of reactivities of arthropods and molluscs. *Biochem Biophys Res Commun*, Vol. 89, No. 4, pp. 1050–1057.
- Hildén, K., Hakala, T.K. & Lundell, T. 2009. Thermotolerant and thermostable laccases. *Biotechnol Lett*, Vol. 31, No. 8, pp. 1117–1128.
- Himmelwright, R.S., Eickman, N.C., LuBien, C.D., Lerch, K. & Solomon, E.I. 1980. Chemical and spectroscopic studies of the binuclear copper active site of *Neurospora* tyrosinase: comparison to hemocyanins. *J Am Chem Soc*, Vol. 102, pp. 7339–7344.
- Hoegger, P.J., Kilaru, S., James, T.Y., Thacker, J.R. & Kues, U. 2006. Phylogenetic comparison and classification of laccase and related

- multicopper oxidase protein sequences. Vol. 273, No. 10, pp. 2308–2326.
- Hoffmann, P.F. & Esser, K. 1977. The phenol oxidases of the ascomycete *Podospora anserina*. XII. Affinity of laccases II and III to substrates with different substitution patterns. Arch Microbiol, Vol. 112, pp. 111–114.
- Huang, K.X., Fujii, I., Ebizuka, Y., Gomi, K. & Sankawa, U. 1995. Molecular cloning and heterologous expression of the gene encoding dihydrogeodin oxidase, a multicopper blue enzyme from *Aspergillus terreus*. J Biol Chem, Vol. 270, No. 37, pp. 21495–21502.
- Ismaya, W.T., Rozeboom, H.J., Weijn, A., Mes, J.J., Fusetti, F., Wichers, H.J. & Dijkstra, B.W. 2011. Crystal structure of *Agaricus bisporus* mushroom tyrosinase: identity of the tetramer subunits and interaction with tropolone. Biochemistry, Vol. 50, No. 24, pp. 5477–5486.
- Ito, S., Kato, T., Shinpo, K. & Fujita, K. 1984. Oxidation of tyrosine residues in proteins by tyrosinase. Biochem J, Vol. 222, pp. 407–411. Itoh, S., Kumei, H., Taki, M., Nagatomo, S., Kitagawa, T. & Fukuzumi, S. 2001. Oxygenation of phenols to catechols by a (μ - η^2 : η^2 -peroxo)dycopper(II) complex: mechanistic insight into the phenolase activity of tyrosinase. J Am Chem Soc, Vol. 123, No. 27, pp. 6708–6709.
- Ito, S. & Wakamatsu, K. 2008. Chemistry of mixed melanogenesis-pivotal roles of dopaquinone. Photochem Photobiol, Vol. 84, No. 3, pp. 582–592.
- Jacobson, E.S. 2000. Pathogenic roles for fungal melanins. Clin Microbiol Rev, Vol. 13, No. 4, pp. 708–717.
- Johnson, D.L., Thompson, J.L., Brinkmann, S.M., Schuller, K.A. & Martin, L.L. 2003. Electrochemical characterization of purified *Rhus vernicifera* laccase: voltammetric evidence for a sequential four-electron transfer. Biochemistry, Vol. 42, No. 34, pp. 10229–10237.
- Jolley, R.L., Jr., Evans, L.H., Makino, N. & Mason, H.S. 1974. Oxytyrosinase. J Biol Chem, Vol. 249, No. 2, pp. 335–345.
- Jordan, A.M., Khan, T.H., Osborn, H.M., Photiou, A. & Riley, P.A. 1999. Melanocyte-directed enzyme prodrug therapy (MDEPT): development of a targeted treatment for malignant melanoma. Bioorg Med Chem, Vol. 7, No. 9, pp. 1775–1780.

- Jordan, A.M., Khan, T.H., Malkin, H., Osborn, H.M., Photiou, A. & Riley, P.A. 2001. Melanocyte-directed enzyme prodrug therapy (MDEPT): development of second generation prodrugs for targeted treatment of malignant melanoma. *Bioorg Med Chem*, Vol. 9, No. 6, pp. 1549–1558.
- Jung, H., Xu, F.F. & Li, K. 2002. Purification and characterization of laccase from wood-degrading fungus *Trichophyton rubrum* LKY-7. *Enzyme Microb Technol*, Vol. 30, No. 2, pp. 161–168.
- Jus, S., Kokol, V. & Gübitz, G.M. 2008. Tyrosinase-catalysed coupling of functional molecules onto protein fibres. Vol. 42, No. 7, pp. 535–542.
- Käärik, A. 1965. The identification of the mycelia of wood-decay fungi by their oxidation reactions with phenolic compounds. *Studia forestalia suecica*, Vol. 31, pp. 1–80.
- Kaljunen, H., Gasparetti, C., Kruus, K., Rouvinen, J. & Hakulinen, N. 2011. Crystallization and preliminary X-ray analysis of *Aspergillus oryzae* catechol oxidase. *Acta Crystallogr Sect F Struct Biol Cryst Commun*, Vol. 67, No. 6, pp. 672–674.
- Kallio, J.P., Auer, S., Jänis, J., Andberg, M., Kruus, K., Rouvinen, J., Koivula, A. & Hakulinen, N. 2009. Structure-function studies of a *Melanocarpus albomyces* laccase suggest a pathway for oxidation of phenolic compounds. *J Mol Biol*, Vol. 392, No. 4, pp. 895–909.
- Kanda, K., Sato, T., Ishii, S., Enei, H. & Ejiri, S. 1996. Purification and properties of tyrosinase isozymes from the gill of *Lentinus edodes* fruiting body. *Biosci Biotechnol Biochem*, Vol. 60, No. 8, pp. 1273–1278.
- Karahanian, E., Corsini, G., Lobos, S. & Viciña, R. 1998. Structure and expression of a laccase gene from the ligninolytic basidiomycete *Ceriporiopsis subvermispora*. *Biochim Biophys Acta*, Vol. 1443, No. 1–2, pp. 65–74.
- Kato, A., Wada, T., Kobayashi, K., Seguro, K. & Motoki, M. 1991. Ovomulcin-food protein conjugates prepared through the transglutaminase reaction. *Agric Biol Chem*, Vol. 55, pp. 1027–1031.
- Kato, A., Minaki, K. & Kobayashi, K. 1993. Improvement of emulsifying properties of egg white proteins by the attachment of polysaccharide through maillard reaction in a dry state. Vol. 41, No. 4, pp. 540–543.

- Kiiskinen, L.-L., Viikari, L. & Kruus, K. 2002. Purification and characterisation of a novel laccase from the ascomycete *Melanocarpus albomyces*. *Appl Environ Microbiol*, Vol. 59, No. 2–3, pp. 198–204.
- Kiiskinen, L.-L., Kruus, K., Bailey, M., Ylösmäki, E., Siika-Aho, M. & Saloheimo, M. 2004. Expression of *Melanocarpus albomyces* laccase in *Trichoderma reesei* and characterization of the purified enzyme. *Microbiology*, Vol. 150, No. 9, pp. 3065–3074.
- Kim, Y.J. & Uyama, H. 2005. Tyrosinase inhibitors from natural and synthetic sources: structure, inhibition mechanism and perspective for the future. *Cell Mol Life Sci*, Vol. 62, No. 15, pp. 1707–1723.
- Klabunde, T., Eicken, C., Sacchettini, J.C. & Krebs, B. 1998. Crystal structure of a plant catechol oxidase containing a dicopper center. *Nat Struct Biol*, Vol. 5, No. 12, pp. 1084–1090.
- Klonowska, A., Gaudin, C., Fournel, A., Asso, M., Le Petit, J., Giorgi, M. & Tron, T. 2002. Characterization of a low redox potential laccase from the basidiomycete C30. *Eur J Biochem*, Vol. 269, No. 24, pp. 6119–6125.
- Knowles, W.S. 2003. Asymmetric hydrogenations (Nobel Lecture 2001). Vol. 345, No. 1–2, pp. 3–13.
- Ko, E.M., Leem, Y.E. & Choi, H.T. 2001. Purification and characterization of laccase isozymes from the white-rot basidiomycete *Ganoderma lucidum*. *Appl Microbiol Biotechnol*, Vol. 57, No. 1–2, pp. 98–102.
- Komori, H., Miyazaki, K. & Higuchi, Y. 2009. X-ray structure of a two-domain type laccase: A missing link in the evolution of multi-copper proteins. *FEBS Lett*, Vol. 583, No. 7, pp. 1189–1195.
- Kong, K.-H., Lee, J., Park, H. & Cho, S. 1998. Purification and characterization of the tyrosinase isozymes of pine needles. *Biochem Mol Biol Int*, Vol. 45, No. 4, pp. 717–724.
- Kong, K.-H., Hong, M.P., Choi, S.S., Kim, Y.T. & Cho, S.H. 2000. Purification and characterization of a highly stable tyrosinase from *Thermomicrobium roseum*. *Biotechnol Appl Biochem*, Vol. 31, No. 2, pp. 113–118.
- Kubo, I., Nihei, K. & Tsujimoto, K. 2004. Methyl *p*-coumarate, a melanin formation inhibitor in B16 mouse melanoma cells. Vol. 12, No. 20, pp. 5349–5354.

- Kupper, U., Niedermann, D.M., Travaglini, G. & Lerch, K. 1989. Isolation and characterization of the tyrosinase gene from *Neurospora crassa*. *J Biol Chem*, Vol. 264, No. 29, pp. 17250–17258.
- Kwon, B.S., Haq, A.K., Pomerantz, S.H. & Halaban, R. 1987. Isolation and sequence of a cDNA clone for human tyrosinase that maps at the mouse c-albino locus. *Proc Natl Acad Sci U S A*, Vol. 84, No. 21, pp. 7473–7477.
- Labat, E., Morel, M.H. & Rouau, X. 2000. Effects of laccase and ferulic acid on wheat flour doughs. *Cereal Chem*, Vol. 77, No. 6, pp. 823–828.
- Labat, E., Morel, M.H. & Rouau, X. 2001. Effect of laccase and manganese peroxidase on wheat gluten and pentosans during mixing. *Food Hydrocoll*, Vol. 15, No. 1, pp. 47–52.
- Laemmli, U.K. 1970. Cleavage of structural proteins during the assembly of the head of bacteriophage T4. *Nature*, Vol. 227, No. 5259, pp. 680–685.
- Land, E.J., Ramsden, C.A. & Riley, P.A. 2007. The mechanism of suicide-inactivation of tyrosinase: a substrate structure investigation. *Tohoku J Exp Med*, Vol. 212, No. 4, pp. 341–348.
- Lang, G. & Cotteret, J. 1998. Hair dye composition containing a laccase. Patent No: WO9936036.
- Langfelder, K., Streibel, M., Jahn, B., Haase, G. & Brakhage, A.A. 2003. Biosynthesis of fungal melanins and their importance for human pathogenic fungi. *Fungal Genet Biol*, Vol. 38, No. 2, pp. 143–158.
- Lantto, R., Heine, E., Freddi, G., Lappalainen, A., Miettinen-Oinonen, A., Niku-Paavola, M. & Buchert, J. 2005a. Enzymatic modification of wool with tyrosinase and peroxidase. *J Textile Inst*, Vol. 96, No. 2, pp. 109–116.
- Lantto, R., Puolanne, E., Kalkkinen, N., Buchert, J. & Autio, K. 2005b. Enzyme-aided modification of chicken-breast myofibril proteins: effect of laccase and transglutaminase on gelation and thermal stability. *J Agric Food Chem*, Vol. 53, No. 23, pp. 9231–9237.
- Lantto, R., Puolanne, E., Kruus, K., Buchert, J. & Autio, K. 2007. Tyrosinase-aided protein cross-linking: effects on gel formation of chicken breast myofibrils and texture and water-holding of chicken breast meat homogenate gels. *J Agric Food Chem*, Vol. 55, No. 4, pp. 1248–1255.

- Lawton, T.J., Sayavedra-Soto, L.A., Arp, D.J. & Rosenzweig, A.C. 2009. Crystal structure of a two-domain multicopper oxidase: implications for the evolution of multicopper blue proteins. *J Biol Chem*, Vol. 284, No. 15, pp. 10174–10180.
- Lee, S.-K., George, S.D., Antholine, W.E., Hedman, B., Hodgson, K.O. & Solomon, E.I. 2002. Nature of the intermediate formed in the reduction of O₂ to H₂O at the trinuclear copper cluster active site in native laccase. *J Am Chem Soc*, Vol. 124, No. 21, pp. 6180–6193.
- Lee, Y., Whittaker, M. & Whittaker, J. 2008. The electronic structure of the Cys-Tyr(*) free radical in galactose oxidase determined by EPR spectroscopy. *Biochemistry (N.Y.)*, Vol. 47, No. 25, pp. 6637–6649.
- Lerch, K. & Ettinger, L. 1972. Purification and characterization of a tyrosinase from *Streptomyces glaucescens*. *Eur J Biochem*, Vol. 31, No. 3, pp. 427–437.
- Lerch, K. 1982. Primary structure of tyrosinase from *Neurospora crassa*. II. Complete amino acid sequence and chemical structure of a tripeptide containing an unusual thioether. *J Biol Chem*, Vol. 257, No. 11, pp. 6414–6419.
- Lerch, K. 1983. *Neurospora* tyrosinase: structural, spectroscopic and catalytic properties. *Mol Cell Biochem*, Vol. 52, No. 2, pp. 125–138.
- Lertsiri, S., Phontree, K., Thepsingha, W. & Bhumiratana, A. 2003. Evidence of enzymatic browning due to laccase-like enzyme during mash fermentation in Thai soybean paste. *Food Chem*, Vol. 80, No. 2, pp. 171–176.
- Li, X., Wei, Z., Zhang, M., Peng, X., Yu, G., Teng, M. & Gong, W. 2007. Crystal structures of *E. coli* laccase CueO at different copper concentrations. *Biochem Biophys Res Commun*, Vol. 354, No. 1, pp. 21–26.
- Liao, J.C., Gregor, P., Wolchok, J.D., Orlandi, F., Craft, D., Leung, C., Houghton, A.N. & Bergman, P.J. 2006. Vaccination with human tyrosinase DNA induces antibody responses in dogs with advanced melanoma. *Cancer Immun*, Vol. 6, p. 8.
- Lim, J.Y., Ishiguro, K. & Kubo, I. 1999. Tyrosinase inhibitory *p*-coumaric acid from ginseng leaves. *Phytother Res*, Vol. 13, No. 5, pp. 371–375.

- Lim, K.G. & Palmore, G.T.R. 2007. Microfluidic biofuel cells: The influence of electrode diffusion layer on performance. *Biosens Bioelectron*, Vol. 22, No. 6, pp. 941–947.
- Littoz, F. & McClements, D.J. 2008. Bio-mimetic approach to improving emulsion stability: Cross-linking adsorbed beet pectin layers using laccase. *Food Hydrocoll*, Vol. 22, No. 7, pp. 1203–1211.
- Litvintseva, A.P. & Henson, J.M. 2002. Cloning, characterization, and transcription of three laccase genes from *Gaeumannomyces graminis* var. *tritici*, the take-all fungus. *Appl Environ Microbiol*, Vol. 68, No. 3, pp. 1305–1311.
- Liu, Y. & Dong, S. 2007. A biofuel cell with enhanced power output by grape juice. *Vol. 9, No. 7, pp. 1423–1427.*
- Lundell, T.K., Mäkelä, M.R. & Hildén, K. 2010. Lignin-modifying enzymes in filamentous basidiomycetes – ecological, functional and phylogenetic review. *J Basic Microbiol*, Vol. 50, No. 1, pp. 5–20.
- Lyashenko, A.V., Zhukhlistova, N.E., Gabdoulkhakov, A.G., Zhukova, Y.N., Voelter, W., Zaitsev, V.N., Bento, I., Stepanova, E.V., Kachalova, G.S., Koroleva, O.V., Betzel, C., Lindley, P.F., Mikhailov, A.M., Tishkov, V.I. & Morgunova, E.Y. 2007. Crystal structure of laccase from *Coriolus zonatus* at 2.6 Å resolution. 10.2210/pdb2hzh/pdb.
- Marbach, I., Harel, E. & Mayer, A.M. 1984. Molecular properties of extracellular *Botrytis cinerea* laccase. *Phytochemistry*, Vol. 23, No. 12, pp. 2713–2717.
- Martin, C., Moeder, M., Daniel, X., Krauss, G. & Schlosser, D. 2007. Biotransformation of the polycyclic musks HHCB and AHTN and metabolite formation by fungi occurring in freshwater environments. *Environ Sci Technol*, Vol. 41, No. 15, pp. 5395–5402.
- Martins, L.O., Soares, C.M., Pereira, M.M., Teixeira, M., Costa, T., Jones, G.H. & Henriques, A.O. 2002. Molecular and biochemical characterization of a highly stable bacterial laccase that occurs as a structural component of the *Bacillus subtilis* endospore coat. *J Biol Chem*, Vol. 277, No. 21, pp. 18849–18859.
- Marusek, C.M., Trobaugh, N.M., Flurkey, W.H. & Inlow, J.K. 2006. Comparative analysis of polyphenol oxidase from plant and fungal species. *J Inorg Biochem*, Vol. 100, No. 1, pp. 108–123.

- Mason, H.S. 1948. The chemistry of melanin; mechanism of the oxidation of dihydroxyphenylalanine by tyrosinase. *J Biol Chem*, Vol. 172, No. 1, pp. 83–99.
- Masse, M.-O., Duvallet, V., Borremans, M. & Goeyens, L. 2001. Identification and quantitative analysis of kojic acid and arbutine in skin-whitening cosmetics. *Int J Cosmet Sci*, Vol. 23, No. 4, pp. 219–232.
- Matera, I., Gullotto, A., Tilli, S., Ferraroni, M., Scozzafava, A. & Briganti, F. 2008. Crystal structure of the blue multicopper oxidase from the white-rot fungus *Trametes trogii* complexed with *p*-toluate. *Inorganica Chim Acta*, Vol. 361, No. 14–15, pp. 4129–4137.
- Matoba, Y., Kumagai, T., Yamamoto, A., Yoshitsu, H. & Sugiyama, M. 2006. Crystallographic evidence that the dinuclear copper center of tyrosinase is flexible during catalysis. *J Biol Chem*, Vol. 281, No. 13, pp. 8981–8990.
- Matoba, Y., Bando, N., Oda, K., Noda, M., Higashikawa, F., Kumagai, T. & Sugiyama, M. 2011. A molecular mechanism for copper transportation to tyrosinase that is assisted by a metallochaperone, caddie protein. *J Biol Chem*, Vol. 286, No. 34, pp. 30219–30231.
- Mattinen, M.-L., Hellman, M., Steffensen, C.L., Selinheimo, E., Permi, P., Kalkkinen, N., Kruus, K. & Buchert, J. 2008a. Laccase and tyrosinase catalysed polymerization of proteins and peptides. *J Biotechnol*, Vol. 136, No. 1, pp. S318–S318.
- Mattinen, M.-L., Lantto, R., Selinheimo, E., Kruus, K. & Buchert, J. 2008b. Oxidation of peptides and proteins by *Trichoderma reesei* and *Agaricus bisporus* tyrosinases. *J Biotechnol*, Vol. 133, No. 3, pp. 395–402.
- Mayer, A.M. & Harel, E. 1979. Polyphenol oxidases in plants. *Phytochemistry*, Vol. 18, No. 2, pp. 193–215.
- Mayer, A.M. 1987. Polyphenol oxidases in plants-recent progress. *Phytochemistry*, Vol. 26, No. 1, pp. 11–20.
- Mayer, A.M. & Staples, R.C. 2002. Laccase: new functions for an old enzyme. *Phytochemistry*, Vol. 60, No. 6, pp. 551–565.
- McMahon, A.M., Doyle, E.M., Brooks, S. & O'Connor, K.E. 2007. Biochemical characterisation of the coexisting tyrosinase and laccase in the soil

- bacterium *Pseudomonas putida* F6. *Enzyme Microb Technol*, Vol. 40, pp. 1435–1441.
- Melo, G.A., Shimizu, M.M. & Mazzafera, P. 2006. Polyphenoloxidase activity in coffee leaves and its role in resistance against the coffee leaf miner and coffee leaf rust. *Phytochemistry*, Vol. 67, No. 3, pp. 277–285.
- Mensah, C.A., Adamafio, N.A., Amaning-Kwarteng, K. & Rodrigues, F.K. 2012. Reduced tannin content of laccase-treated cocoa (*Theobroma cacao*) pod husk. *IJBC*, Vol. 6, pp. 31–36.
- Messerschmidt, A., Ladenstein, R., Huber, R., Bolognesi, M., Avigliano, L., Petruzzelli, R., Rossi, A. & Finazzi-Agro, A. 1992. Refined crystal structure of ascorbate oxidase at 1.9 Å resolution. *J Mol Biol*, Vol. 224, No. 1, pp. 179–205.
- Mikolasch, A., Niedermeyer, T.H., Lalk, M., Witt, S., Seefeldt, S., Hammer, E., Schauer, F., Gesell, M., Hessel, S., Julich, W.D., et al. 2006. Novel penicillins synthesized by biotransformation using laccase from *Trametes* spec. *Chem Pharm Bull (Tokyo)*, Vol. 54, No. 5, pp. 632–638.
- Mikolasch, A., Wurster, M., Lalk, M., Witt, S., Seefeldt, S., Hammer, E., Schauer, F., Julich, W.D. & Lindequist, U. 2008. Novel beta-lactam antibiotics synthesized by amination of catechols using fungal laccase. *Chem Pharm Bull (Tokyo)*, Vol. 56, No. 7, pp. 902–907.
- Minussi, R.C., Pastore, G.M. & Durán, N. 2002. Potential applications of laccase in the food industry. *Trends Food Sci Technol*, Vol. 13, No. 6–7, pp. 205–216.
- Minussi, R.C., Rossi, M., Bologna, L., Rotilio, D., Pastore, G.M. & Durán, N. 2007. Phenols removal in musts: strategy for wine stabilization by laccase. *J Molec Catal B*, Vol. 45, No. 3–4, pp. 102–107.
- Mita, D.G., Attanasio, A., Arduini, F., Diano, N., Grano, V., Bencivenga, U., Rossi, S., Amine, A. & Moscone, D. 2007. Enzymatic determination of BPA by means of tyrosinase immobilized on different carbon carriers. *Biosens Bioelectron*, Vol. 23, No. 1, pp. 60–65.
- Monogioudi, E., Creusot, N., Kruus, K., Gruppen, H., Buchert, J. & Mattinen, M.,-L. 2009. Cross-linking of β -casein by *Trichoderma reesei* tyrosinase and *Streptovorticillium mobaraense* transglutaminase followed by SEC-MALLS. *Food Hydrocoll*, Vol. 23, No. 7, pp. 2008–2015.

- Montiel, A.M., Fernandez, F.J., Marcial, J., Soriano, J., Barrios-Gonzalez, J. & Tomasini, A. 2004. A fungal phenoloxidase (tyrosinase) involved in pentachlorophenol degradation. *Biotechnol Lett*, Vol. 26, No. 17, pp. 1353–1357.
- Morpurgo, L., Graziani, M.T., Desideri, A. & Rotilio, G. 1980. Titrations with ferrocyanide of japanese-lacquer-tree (*Rhus vernicifera*) laccase and of the type 2 copper-depleted enzyme. Interrelation of the copper sites. *Biochem J*, Vol. 187, No. 2, pp. 367–370.
- Morrison, M.E., Yagi, M.J. & Cohen, G. 1985. In vitro studies of 2,4-dihydroxyphenylalanine, a prodrug targeted against malignant melanoma cells. *Proc Natl Acad Sci U S A*, Vol. 82, No. 9, pp. 2960–2964.
- Motoda, S. 1979a. Properties of polyphenol oxidase from *Alternaria tenuis*. *J Ferment Technol*, Vol. 57, No. 2, pp. 79–85.
- Motoda, S. 1979b. Purification and some properties of polyphenol oxidase from *Alternaria tenuis*. *J Ferment Technol*, Vol. 57, No. 2, pp. 71–78.
- Muñoz-Muñoz, J.L., Garcia-Molina, F.J., García-Ruíz, P.A., Molina-Alarcón, M., Tudela, J., García-Cánovas, F.G. & Rodríguez-López, J.N. 2008. Phenolic substrates and suicide inactivation of tyrosinase: kinetics and mechanism. *Biochem J*, Vol. 416, No. 3, pp. 431–440.
- Muñoz-Muñoz, J.L., Acosta-Motos, J.R., Garcia-Molina, F.J., Varón, R., García-Ruíz, P.A., Tudela, J., García-Cánovas, F.G. & Rodríguez-López, J.N. 2010a. Tyrosinase inactivation in its action on dopa. *Biochim Biophys Acta*, Vol. 1804, No. 7, pp. 1467–1475.
- Muñoz-Muñoz, J.L., Garcia-Molina, F.J., Varón, R., García-Ruíz, P.A., Tudela, J., García-Cánovas, F.G. & Rodríguez-López, J.N. 2010b. Suicide inactivation of the diphenolase and monophenolase activities of tyrosinase. *IUBMB Life*, Vol. 62, No. 7, pp. 539–547.
- Muñoz-Muñoz, J.L., Garcia-Molina, F., García-Ruíz, P.A., Varon, R., Tudela, J., Rodríguez-López, J.N. & García-Cánovas, F. 2011. Catalytic oxidation of *o*-aminophenols and aromatic amines by mushroom tyrosinase. *Biochim Biophys Acta*, Vol. 1814, No. 12, pp. 1974–1983.
- Nagai, M., Sato, T., Watanabe, H., Saito, K., Kawata, M. & Enei, H. 2002. Purification and characterization of an extracellular laccase from the

edible mushroom *Lentinula edodes*, and decolorization of chemically different dyes. *Appl Environ Microbiol*, Vol. 60, No. 3, pp. 327–335.

- Nagai, M., Kawata, M., Watanabe, H., Ogawa, M., Saito, K., Takesawa, T., Kanda, K. & Sato, T. 2003. Important role of fungal intracellular laccase for melanin synthesis: purification and characterization of an intracellular laccase from *Lentinula edodes* fruit bodies. *Microbiology*, Vol. 149, No. 9, pp. 2455–2462.
- Nakamura, M., Nakajima, T., Ohba, Y., Yamauchi, S., Lee, B.R. & Ichishima, E. 2000. Identification of copper ligands in *Aspergillus oryzae* tyrosinase by site-directed mutagenesis. *Biochem J*, Vol. 350, No. 2, pp. 537–545.
- Nakamura, T., Sho, S. & Ogura, Y. 1966. On the purification and properties of mushroom tyrosinase. *J Biochem*, Vol. 59, No. 5, pp. 481–486.
- Niku-Paavola, M.L., Karhunen, E., Salola, P. & Raunio, V. 1988. Ligninolytic enzymes of the white-rot fungus *Phlebia radiata*. *Biochem J*, Vol. 254, No. 3, pp. 877–884.
- Niladevi, K.N., Jacob, N. & Prema, P. 2008. Evidence for a halotolerant-alkaline laccase in *Streptomyces psammoticus*: purification and characterization. *Process Biochem*, Vol. 43, No. 6, pp. 654–660.
- Niladevi, K.N. 2009. Ligninolytic enzymes. In: Singh nee' Nigam, P. & Pandey, A. (eds.) *Biotechnology for agro-industrial residues utilisation*. Springer Netherlands, The Netherlands. pp. 397–414.
- Nishizawa, Y., Nakabayashi, K. & Shinagawa, E. 1995. Purification and characterization of laccase from white rot fungus *Trametes sanguinea* M85-2. *J Ferment Bioeng*, Vol. 80, No. 1, pp. 91–93.
- Olivares, C. & Solano, F. 2009. New insights into the active site structure and catalytic mechanism of tyrosinase and its related proteins. *Pigment Cell Melanoma Res*, Vol. 22, No. 6, pp. 750–760.
- O'Malley, D.M., Whetten, R., Bao, W., Chen, C.-L. & Sederoff, R.R. 1993. The role of laccase in lignification. Vol. 4, No. 5, pp. 751–757.
- Ossola, M. & Galante, Y.M. 2004. Scouring of flax rove with the aid of enzymes. *Enzyme Microb Technol*, Vol. 34, No. 2, pp. 177–186.
- Palmer, A.E., Randall, D.W., Xu, F.F. & Solomon, E.I. 1999. Spectroscopic studies and electronic structure description of the high potential type 1 copper

- site in fungal laccase: Insight into the effect of the axial ligand. *J Am Chem Soc*, Vol. 121, No. 30, pp. 7138–7149.
- Palmieri, G., Giardina, P., Marzullo, L., Desiderio, B., Nitti, G., Cannio, R. & Sanna, G. 1993. Stability and activity of a phenol oxidase from the ligninolytic fungus *Pleurotus ostreatus*. *Appl Microbiol Biotechnol*, Vol. 39, No. 4–5, pp. 632–636.
- Palmieri, G., Giardina, P., Bianco, C., Fontanella, B. & Sanna, G. 2000. Copper induction of laccase isoenzymes in the ligninolytic fungus *Pleurotus ostreatus*. *Appl Environ Microbiol*, Vol. 66, No. 3, pp. 920–924.
- Palmieri, G., Cennamo, G., Faraco, V., Amoresano, A., Sanna, G. & Giardina, P. 2003. Atypical laccase isoenzymes from copper supplemented *Pleurotus ostreatus* cultures. *Enzyme Microb Technol*, Vol. 33, No. 2–3, pp. 220–230.
- Palmore, G.T.R. & Kim, H.-H. 1999. Electro-enzymatic reduction of dioxygen to water in the cathode compartment of a biofuel cell. *J Electroanal Chem*, Vol. 464, No. 1, pp. 110–117.
- Paloheimo, M., Valtakari, L., Puranen, T., Kruus, K., Kallio, J., Mäntylä, A., Fagerström, R., Ojapalo, P. & Vehmaanperä, J. 2006. Novel laccase enzyme and use thereof. Patent No: WO 2006 032723 A1.
- Palonen, H. & Viikari, L. 2004. Role of oxidative enzymatic treatments on enzymatic hydrolysis of softwood. *Biotechnol Bioeng*, Vol. 86, No. 5, pp. 550–557.
- Palumbo, A., d'Ischia, M., Misuraca, G. & Protà, G. 1987. Effect of metal ions on the rearrangement of dopachrome. *Biochim Biophys Acta*, Vol. 925, No. 2, pp. 203–209.
- Parrish, F.W., Wiley, B.J., Simmons, E.G. & Long, L., Jr 1966. Production of aflatoxins and kojic acid by species of *Aspergillus* and *Penicillium*. *Appl Microbiol*, Vol. 14, No. 1, p. 139.
- Parsons, M.R., Convery, M.A., Wilmot, C.M., Yadav, K.D., Blakeley, V., Corner, A.S., Phillips, S.E., McPherson, M.J. & Knowles, P.F. 1995. Crystal structure of a quinoenzyme: copper amine oxidase of *Escherichia coli* at 2 Å resolution. *Structure*, Vol. 3, No. 11, pp. 1171–1184.

- Parvez, S., Kang, M., Chung, H., Cho, C., Hong, M., Shin, M. & Bae, H. 2006. Survey and mechanism of skin depigmenting and lightening agents. *Phytother Res*, Vol. 20, No. 11, pp. 921–934.
- Pazarlioğlu, N.K., Sarişik, M. & Telefoncu, A. 2005. Laccase: production by *Trametes versicolor* and application to denim washing. *Process Biochem*, Vol. 40, pp. 1673–1678.
- Penttilä, M., Nevalainen, H., Ratto, M., Salminen, E. & Knowles, J. 1987. A versatile transformation system for the cellulolytic filamentous fungus *Trichoderma reesei*. *Gene*, Vol. 61, No. 2, pp. 155–164.
- Peralta-Zamora, P., Pereira, C.M., Tiburtius, E.R.L., Moraes, S.G., Rosa, M.A., Minussi, R.C. & Durán, N. 2003. Decolorization of reactive dyes by immobilized laccase. *Appl Catal B*, Vol. 42, No. 2, pp. 131–144.
- Philipp, S., Held, T. & Kutzner, H.J. 1991. Purification and characterization of the tyrosinase of *Streptomyces michiganensis* DSM 40015. *J Basic Microbiol*, Vol. 31, pp. 293–300.
- Piontek, K., Antorini, M. & Choinowski, T. 2002. Crystal structure of a laccase from the fungus *Trametes versicolor* at 1.90 Å resolution containing a full complement of coppers. *J Biol Chem*, Vol. 277, No. 40, pp. 37663–37669.
- Polyakov, K.M., Fedorova, T.V., Stepanova, E.V., Cherkashin, E.A., Kruzeev, S.A., Strokopytov, B.V., Lamzin, V.S. & Koroleva, O.V. 2009. Structure of native laccase from *Trametes hirsuta* at 1.8 Å resolution. *Acta Crystallogr Sect F Struct Biol Cryst Commun*, Vol. 65, pp. 611–617.
- Poppius-Levlin, K., Wang, W., Tamminen, T., Hortling, B., Viikari, L. & Niku-Paavola, M. 1999. Effects of laccase/HBT treatment on pulp and lignin structures. *J Pulp Pap Sci*, Vol. 25, No. 3, pp. 90–94.
- Prota, G. 1980. Recent advances in the chemistry of melanogenesis in mammals. *J Investig Dermatol*, Vol. 75, No. 1, pp. 122–127.
- Prota, G. 1988. Progress in the chemistry of melanins and related metabolites. *Med Res Rev*, Vol. 8, No. 4, pp. 525–556.
- Ramirez, E.D., Whitaker, J.R. & Virador, V.M. 2004. Polyphenol oxidase. In: Whitaker, J.R., Voragen, A.G.J. & Wong, D.W.S. (eds.) *Handbook of food enzymology*. CRC Press, pp. 509–523.

- Raper, H.S. 1927. The tyrosinase-tyrosine reaction: production from tyrosine of 5:6-dihydroxyindole and 5:6-dihydroxyindole-2-carboxylic acid – the precursors of melanin. *Biochem J*, Vol. 21, No. 1, pp. 89–96.
- Rescigno, A., Sanjust, E., Soddu, G., Rinaldi, A.C., Sollai, F., Curreli, N. & Rinaldi, A. 1998. Effect of 3-hydroxyanthranilic acid on mushroom tyrosinase activity. *Biochim Biophys Acta*, Vol. 1384, No. 2, pp. 268–276.
- Reyes, P., Pickard, M.A. & Vazquez-Duhalt, R. 1999. Hydroxybenzotriazole increases the range of textile dyes decolorized by immobilized laccase. *Biotechnol Lett*, Vol. 21, No. 10, pp. 875–880.
- Rigling, D. & Van Alfen, N.K. 1993. Extra- and intracellular laccases of the chestnut blight fungus, *Cryphonectria parasitica*. *Appl Environ Microbiol*, Vol. 59, No. 11, pp. 3634–3639.
- Rittstieg, K., Suurnäkki, A., Suortti, T., Kruus, K., Gübitz, G.M. & Buchert, J. 2002. Investigations on the laccase-catalyzed polymerization of lignin model compounds using size-exclusion HPLC. *Enzyme Microb Technol*, Vol. 31, No. 4, pp. 403–410.
- Robb, D.A. 1984. Tyrosinase. In: Lontie, R. (ed.) *Copper proteins and copper enzymes*. CRC Press, Inc., Boca Raton, FL, pp. 207–241.
- Rodgers, C.J., Blanford, C.F., Giddens, S.R., Skamnioti, P., Armstrong, F.A. & Gurr, S.J. 2009. Designer laccases: a vogue for high-potential fungal enzymes? *Trends Biotechnol*, Vol. 28, No. 2, pp. 63–72.
- Rodríguez Couto, S. & Toca Herrera, J.L. 2006. Laccases in the textile industry. *BMBR*, Vol. 1, No. 4, pp. 115–120.
- Rodríguez-López, J.N., Tudela, J., Varón, R. & García-Cánovas, F.G. 1991. Kinetic study on the effect of pH on the melanin biosynthesis pathway. *Biochim Biophys Acta*, Vol. 1076, No. 3, pp. 379–386.
- Rodríguez-López, J.N., Fenoll, L.G., García-Ruiz, P.A., Varon, R., Tudela, J., Thorneley, R.N. & García-Cánovas, F. 2000. Stopped-flow and steady-state study of the diphenolase activity of mushroom tyrosinase. *Biochemistry*, Vol. 39, No. 34, pp. 10497–10506.
- Rogers, M.S. & Dooley, D.M. 2003. Copper-tyrosyl radical enzymes. *Curr Opin Chem Biol*, Vol. 7, No. 2, pp. 189–196.

- Rokhsana, D., Howells, A.E., Dooley, D.M. & Szilagyí, R.K. 2012. Role of the Tyr-Cys cross-link to the active site properties of galactose oxidase. *Inorg Chem*, Vol. 51, pp. 3513–3524.
- Rompel, A., Fischer, H., Meiwes, D., Büldt-Karentzopoulos, K., Dillinger, R., Tuzcek, F., Witzel, H. & Krebs, B. 1999a. Purification and spectroscopic studies on catechol oxidases from *Lycopus europaeus* and *Populus nigra*: evidence for a dinuclear copper center of type 3 and spectroscopic similarities to tyrosinase and hemocyanin. *J Biol Inorg Chem*, Vol. 4, No. 1, pp. 56–63.
- Rompel, A., Fischer, H., Meiwes, D., Büldt-Karentzopoulos, K., Magrini, A., Eicken, C., Gerdemann, C. & Krebs, B. 1999b. Substrate specificity of catechol oxidase from *Lycopus europaeus* and characterization of the bioproducts of enzymic caffeic acid oxidation. *FEBS Lett*, Vol. 445, No. 1, pp. 103–110.
- Rompel, A., Büldt-Karentzopoulos, K., Molitor, C. & Krebs, B. 2012. Purification and spectroscopic studies on catechol oxidase from lemon balm (*Melissa officinalis*). *Phytochemistry*, Vol. 81, pp. 19–23.
- Roure, M., Delattre, P. & Froger, H. 1992. Composition for an enzymic coloration of keratin fibres, especially for hair and its use in a dyeing process. Patent No: EP0504005.
- Samokhvalov, A., Hong, L., Liu, Y., Garguilo, J., Nemanich, R.J., Edwards, G.S. & Simon, J.D. 2005. Oxidation potentials of human eumelanosomes and pheomelanosomes. *Photochem Photobiol*, Vol. 81, No. 1, pp. 145–148.
- Sanchez-Amat, A. & Solano, F. 1997. A pluripotent polyphenol oxidase from the melanogenic *Marine alteromonas* sp. shares catalytic capabilities of tyrosinases and laccases. *Biochem Biophys Res Commun*, Vol. 240, No. 3, pp. 787–792.
- Sanjust, E., Cecchini, G., Sollai, F., Curreli, N. & Rescigno, A. 2003. 3-Hydroxykynurenine as a substrate/activator for mushroom tyrosinase. *Arch Biochem Biophys*, Vol. 412, No. 2, pp. 272–278.
- Sannia, G., Giardina, P. & Luna, M. 1986. Laccase from *Pleurotus ostreatus*. *Biotechnol Lett*, Vol. 8, No. 11, pp. 797–800.
- Schneider, P., Caspersen, M.B., Mondorf, K., Halkier, T., Skov, L.K., Østergaard, P.R., Brown, K.M., Brown, S.H. & Xu, F.F. 1999. Characterization of a

- Coprinus cinereus* laccase. *Enzyme Microb Technol*, Vol. 25, No. 6, pp. 502–508.
- Schoot Uiterkamp, A.J.M., Evans, L.H., Jolley, R.L., Jr. & Mason, H.S. 1976. Absorption and circular dichroism spectra of different forms of mushroom tyrosinase. *Biochim Biophys Acta*, Vol. 453, No. 1, pp. 200–204.
- Schouten, A., Wagemakers, L., Stefanato, F.L., van der Kaaij, R.M. & van Kan, J.A.L. 2002. Resveratrol acts as a natural antifungicide and induces self-intoxication by a specific laccase. *Mol Microbiol*, Vol. 43, No. 4, pp. 883–894.
- Selamat, M.J., Bakar, J. & Nazamid, S. 2002. Oxidation of polyphenols in unfermented and partly fermented cocoa beans by cocoa polyphenol oxidase and tyrosinase. *J Sci Food Agric*, Vol. 82, No. 5, pp. 559–566.
- Selinheimo, E., Kruus, K., Buchert, J., Hopia, A. & Autio, K. 2006a. Effects of laccase, xylanase and their combination on the rheological properties of wheat doughs. Vol. 43, No. 2, pp. 152–159.
- Selinheimo, E., Saloheimo, M., Ahola, E., Westerholm-Parvinen, A., Kalkkinen, N., Buchert, J. & Kruus, K. 2006b. Production and characterization of a secreted, C-terminally processed tyrosinase from the filamentous fungus *Trichoderma reesei*. *FEBS J*, Vol. 273, No. 18, pp. 4322–4335.
- Selinheimo, E., Autio, K., Kruus, K. & Buchert, J. 2007a. Elucidating the mechanism of laccase and tyrosinase in wheat bread making. *J Agric Food Chem*, Vol. 55, No. 15, pp. 6357–6365.
- Selinheimo, E., NiEidhin, D., Steffensen, C., Nielsen, J., Lomascolo, A., Halaouli, S., Record, E., O’Beirne, D., Buchert, J. & Kruus, K. 2007b. Comparison of the characteristics of fungal and plant tyrosinases. *J Biotechnol*, Vol. 130, No. 4, pp. 471–480.
- Selinheimo, E., Lampila, P., Mattinen, M.-L. & Buchert, J. 2008. Formation of protein-oligosaccharide conjugates by laccase and tyrosinase. *J Agric Food Chem*, Vol. 56, No. 9, pp. 3118–3128.
- Sendovski, M., Kanteev, M., Ben-Yosef, V.S., Adir, N. & Fishman, A. 2011. First structures of an active bacterial tyrosinase reveal copper plasticity. *J Mol Biol*, Vol. 405, No. 1, pp. 227–237.

- Seo, S.Y., Sharma, V.K. & Sharma, N. 2003. Mushroom tyrosinase: recent prospects. *J Agric Food Chem*, Vol. 51, No. 10, pp. 2837–2853.
- Sethuraman, A., Akin, D.E. & Eriksson, K.-E.L. 1999. Production of ligninolytic enzymes and synthetic lignin mineralization by the bird's nest fungus *Cyathus stercoreus*. *Appl Environ Microbiol*, Vol. 52, No. 5, pp. 689–697.
- Setti, L., Giuliani, S., Spinozzi, G. & Pifferi, P.G. 1999. Laccase catalyzed-oxidative coupling of 3-methyl 2-benzothiazolinone hydrazone and methoxyphenols. *Enzyme Microb Technol*, Vol. 25, No. 3–5, pp. 285–289.
- Shin, W., Sundaram, U.M., Cole, J.L., Zhang, H.H., Hedman, B., Hodgson, K.O. & Solomon, E.I. 1996. Chemical and spectroscopic definition of the peroxide-level intermediate in the multicopper oxidases: relevance to the catalytic mechanism of dioxygen reduction to water. *J Am Chem Soc*, Vol. 118, No. 13, pp. 3202–3215.
- Shuster Ben-Yosef, V., Sendovski, M. & Fishman, A. 2010. Directed evolution of tyrosinase for enhanced monophenolase/diphenolase activity ratio. *Enzyme Microb Technol*, Vol. 47, No. 7, pp. 372–376.
- Si, J.Q. 1994. Use of laccase in baking industry. Patent No: PCT/DK94/00232.
- Siegbahn, P.E. 2004. The catalytic cycle of catechol oxidase. *J Biol Inorg Chem*, Vol. 9, No. 5, pp. 577–590.
- Sigoillot, J.-C., Herpoël, I., Frasse, P., Moukha, S., Lesage-Messen, L. & Marcel, A. 1999. Laccase production by a monokaryotic strain of *Pycnoporus cinnabarinus* derived from a dikaryotic strain. *World J Microbiol Biotechnol*, Vol. 15, No. 4, pp. 481–484.
- Sjoblad, R. & Bollag, J. 1981. Oxidative coupling of aromatic compounds by enzymes from soil microorganisms. In: Paul, E. & Ladd, J. (eds.) *Soil biochemistry*. Marcel Dekker, New York. Pp. 113–152.
- Skálová, T., Dohnálek, J., Østergaard, L.H., Østergaard, P.R., Kolenko, P., Dušková, J., Štěpánková, A. & Hašek, J. 2009. The structure of the small laccase from *Streptomyces coelicolor* reveals a link between laccases and nitrite reductases. *J Mol Biol*, Vol. 385, No. 4, pp. 1165–1178.
- Skálová, T., Duskova, J., Hasek, J., Stepankova, A., Koval, T., Ostergaard, L.H. & Dohnalek, J. 2011. Structure of laccase from *Streptomyces coelicolor*

- after soaking with potassium hexacyanoferrate and at an improved resolution of 2.3 Å. *Acta Crystallogr Sect F Struct Biol Cryst Commun*, Vol. 67, pp. 27–32.
- Smolander, M., Boer, H., Valkiainen, M., Roozeman, R., Bergelin, M., Eriksson, J.-E., Zhang, X.-C., Koivula, A. & Viikari, L. 2008. Development of a printable laccase-based biocathode for fuel cell applications. *Enzyme Microb Technol*, Vol. 43, No. 2, pp. 93–102.
- Soler-Rivas, C., Arpin, N., Olivier, J.M. & Wichers, H.J. 1997. Activation of tyrosinase in *Agaricus bisporus* strains following infection by *Pseudomonas tolaasii* or treatment with a tolaasin-containing preparation. *Mycol Res*, Vol. 101, No. 3, pp. 375–382.
- Solomon, E.I., Sundaram, U.M. & Machonkin, T.E. 1996. Multicopper oxidases and oxygenases. *Chem Rev*, Vol. 96, No. 7, pp. 2563–2606.
- Solomon, E.I., Chen, P., Metz, M., Lee, S.-K. & Palmer, A.E. 2001. Oxygen binding, activation, and reduction to water by copper proteins. *Angew Chem Int Ed Engl*, Vol. 40, No. 24, pp. 4570–4590.
- Streffer, K., Vijgenboom, E., Tepper, A.W.J.W., Makower, A., Scheller, F.W., Canters, G.W. & Wollenberger, U. 2001. Determination of phenolic compounds using recombinant tyrosinase from *Streptomyces antibioticus*. *Anal Chim Acta*, Vol. 427, No. 2, pp. 201–210.
- Subramanian, N., Venkatesh, P., Ganguli, S. & Sinkar, V.P. 1999. Role of polyphenol oxidase and peroxidase in the generation of black tea theaflavins. *J Agric Food Chem*, Vol. 47, No. 7, pp. 2571–2578.
- Sugumaran, M., Giglio, L., Kundzicz, H., Saul, S. & Semensi, V. 1992. Studies on the enzymes involved in puparial cuticle sclerotization in *Drosophila melanogaster*. *Arch Insect Biochem Physiol*, Vol. 19, No. 4, pp. 271–283.
- Sugumaran, M. 1995. A caution about the azide inhibition of enzymes associated with electrophilic metabolites. *Biochem Biophys Res Commun*, Vol. 212, No. 3, pp. 834–839.
- Sugumaran, M. 2002. Comparative biochemistry of eumelanogenesis and the protective roles of phenoloxidase and melanin in insects. *Pigment Cell Res*, Vol. 15, No. 1, pp. 2–9.

- Suzuki, T., Endo, K., Ito, M., Tsujibo, H., Miyamoto, K. & Inamori, Y. 2003. A thermostable laccase from *Streptomyces lavendulae* REN-7: purification, characterization, nucleotide sequence, and expression. *Biosci Biotechnol Biochem*, Vol. 67, No. 10, pp. 2167–2175.
- Swan, G.A. & Waggott, A. 1970. Studies related to the chemistry of melanins. X. Quantitative assessment of different types of units present in dopa-melanin. *J Chem Soc Perkin 1*, Vol. 10, pp. 1409–1418.
- Swan, G.A. 1974. Structure, chemistry, and biosynthesis of the melanins. *Fortschr Chem Org Naturst*, Vol. 31, No. 0, pp. 521–582.
- Takada, K., Uozumi, T., Kimurja, A., Someya, K. & Yoshino, T. 2003. Influence of oxidative and/or reductive treatment on human hair (III) oxidative reaction of polyphenol oxidase (laccase) to hair dyeing. *J Oleo Sci*, Vol. 52, No. 10, pp. 557–563.
- Takeuchi, S., Zhang, W., Wakamatsu, K., Ito, S., Hearing, V.J., Kraemer, K.H. & Brash, D.E. 2004. Melanin acts as a potent UVB photosensitizer to cause an atypical mode of cell death in murine skin. *Proc Natl Acad Sci U S A*, Vol. 101, No. 42, pp. 15076–15081.
- Tepper, A.W.J.W. 2005. Structure and mechanism of the type-3 copper protein tyrosinase. Doctoral Thesis Leiden University. Pp. 1–165.
- Thalman, C.R. & Lötzbeyer, T. 2002. Enzymatic cross-linking of proteins with tyrosinase. *Eur Food Res Technol*, Vol. 214, pp. 276–281.
- Torres, E., Bustos-Jaimes, I. & Le Borgne, S. 2003. Potential use of oxidative enzymes for the detoxification of organic pollutants. *Appl Catal B*, Vol. 46, No. 1, pp. 1–15.
- Toussaint, O. & Lerch, K. 1987. Catalytic oxidation of 2-aminophenols and ortho hydroxylation of aromatic amines by tyrosinase. *Biochemistry*, Vol. 26, No. 26, pp. 8567–8571.
- Tsukamoto, K., Jackson, I.J., Urabe, K., Montague, P.M. & Hearing, V.J. 1992. A second tyrosinase-related protein, TRP-2, is a melanogenic enzyme termed DOPAchrome tautomerase. *EMBO J*, Vol. 11, No. 2, pp. 519–526.
- Valderrama, B., Oliver, P., Medrano-Soto, A. & Vazquez-Duhalt, R. 2003. Evolutionary and structural diversity of fungal laccases. Vol. 84, No. 4,

- pp. 289–299. Virador, V.M., Reyes Grajeda, J.P., Blanco-Labra, A., Mendiola-Olaya, E., Smith, G.M., Moreno, A. & Whitaker, J.R. 2009. Cloning, sequencing, purification, and crystal structure of grenache (*Vitis vinifera*) polyphenol oxidase. *J Agric Food Chem*, Vol. 58, pp. 1189–1201.
- Wahleithner, J.A., Xu, F., Brown, K.M., Brown, S.H., Golightly, E.J., Halkier, T., Kauppinen, S., Pederson, A. & Schneider, P. 1996. The identification and characterization of four laccases from the plant pathogenic fungus *Rhizoctonia solani*. *Curr Genet*, Vol. 29, No. 4, pp. 395–403.
- Waite, J.H. 1976. Calculating extinction coefficients for enzymatically produced o-quinones. *Anal Biochem*, Vol. 75, No. 1, pp. 211–218.
- Walker, J.R. & Ferrar, P.H. 1998. Diphenol oxidases, enzyme-catalysed browning and plant disease resistance. *Biotechnol Genet Eng Rev*, Vol. 15, pp. 457–498.
- Wang, N. & Hebert, D.N. 2006. Tyrosinase maturation through the mammalian secretory pathway: bringing color to life. *Pigment Cell Res*, Vol. 19, No. 1, pp. 3–18.
- Wilcox, D.E., Porras, A.G., Hwang, Y.T., Lerch, K., Winkler, M.E. & Solomon, E.I. 1985. Substrate analogue binding to the coupled binuclear copper active site in tyrosinase. *J Am Chem Soc*, Vol. 107, pp. 4015–4027.
- Williamson, P.R. 1994. Biochemical and molecular characterization of the diphenol oxidase of *Cryptococcus neoformans*: identification as a laccase. *J Bacteriol*, Vol. 176, No. 3, pp. 656–664.
- Wong, Y. & Yu, J. 1999. Laccase-catalyzed decolorization of synthetic dyes. *Water Res*, Vol. 33, No. 16, pp. 3512–3520.
- Wood, D.A. 1980a. Production, purification and properties of extracellular laccase of *Agaricus bisporus*. *J Gen Microbiol*, Vol. 117, pp. 327–338.
- Wood, D.A. 1980b. Inactivation of extracellular laccase during fruiting of *Agaricus bisporus*. *J Gen Microbiol*, Vol. 117, No. 2, pp. 339–345.
- Xiao, Y.Z., Chen, Q., Hang, J., Shi, Y.Y., Xiao, Y.Z., Wu, J., Hong, Y.Z. & Wang, Y.P. 2004. Selective induction, purification and characterization of a laccase isozyme from the basidiomycete *Trametes* sp. AH28-2. *Mycologia*, Vol. 96, pp. 26–35.

- Xie, J., Song, K., Qiu, L., He, Q., Huang, H. & Chen, Q. 2007. Inhibitory effects of substrate analogues on enzyme activity and substrate specificities of mushroom tyrosinase. *Food Chem*, Vol. 103, No. 4, pp. 1075–1079.
- Xu, F.F. 1996a. Oxidation of phenols, anilines, and benzenethiols by fungal laccases: correlation between activity and redox potentials as well as halide inhibition. *Biochemistry*, Vol. 35, No. 23, pp. 7608–7614.
- Xu, F.F. 1996b. Catalysis of novel enzymatic iodide oxidation by fungal laccase. *Appl Biochem Biotechnol*, Vol. 59, No. 3, pp. 221–230.
- Xu, F.F., Shin, W., Brown, S.H., Wahleithner, J.A., Sundaram, U.M. & Solomon, E.I. 1996. A study of a series of recombinant fungal laccases and bilirubin oxidase that exhibit significant differences in redox potential, substrate specificity, and stability. *Biochim Biophys Acta*, Vol. 1292, No. 2, pp. 303–311.
- Xu, F.F. 1997. Effects of redox potential and hydroxide inhibition on the pH activity profile of fungal laccases. *J Biol Chem*, Vol. 272, No. 2, pp. 924–928.
- Xu, F.F., Palmer, A.E., Yaver, D.S., Berka, R.M., Gambetta, G.A., Brown, S.H. & Solomon, E.I. 1999. Targeted mutations in a *Trametes villosa* laccase. Axial perturbations of the T1 copper. *J Biol Chem*, Vol. 274, No. 18, pp. 12372–12375.
- Xu, F.F., Kulys, J.J., Duke, K., Li, K., Krikstopaitis, K., Deussen, H.J., Abbate, E., Galinyte, V. & Schneider, P. 2000. Redox chemistry in laccase-catalyzed oxidation of N-hydroxy compounds. *Appl Environ Microbiol*, Vol. 66, No. 5, pp. 2052–2056.
- Xu, F.F., Deussen, H.J., Lopez, B., Lam, L. & Li, K. 2001. Enzymatic and electrochemical oxidation of N-hydroxy compounds. Redox potential, electron-transfer kinetics, and radical stability. *Eur J Biochem*, Vol. 268, No. 15, pp. 4169–4176.
- Yagi, A., Kanbara, T. & Morinobu, N. 1987. Inhibition of mushroom tyrosinase by *Aloe* extract. *Planta Medica*, Vol. 53, No. 6, pp. 515–517.
- Yagüe, S., Terrón, M.C., González, T., Zapico, E., Bocchini, P., Galletti, G.C. & González, A.E. 2000. Biotreatment of tannin-rich beer-factory wastewater with white-rot basidiomycete *Coriolopsis gallica* monitored by pyrolysis/gas chromatography/mass spectrometry. *Rapid Commun Mass Spectrom*, Vol. 14, No. 10, pp. 905–910.

- Yaropolov, A.I., Kharybin, A.N., Emnéus, J., Marko-Varga, G. & Gorton, L. 1995. Flow-injection analysis of phenols at a graphite electrode modified with co-immobilised laccase and tyrosinase. *Anal Chim Acta*, Vol. 308, No. 1–3, pp. 137–144.
- Yaver, D.S., Xu, F., Golightly, E.J., Brown, K.M., Brown, S.H., Rey, M.W., Schneider, P., Halkier, T., Mondorf, K. & Dalboge, H. 1996. Purification, characterization, molecular cloning, and expression of two laccase genes from the white rot basidiomycete *Trametes villosa*. *Appl Environ Microbiol*, Vol. 62, No. 3, pp. 834–841.
- Yaver, D.S., Overjero, M.D., Xu, F., Nelson, B.A., Brown, K.M., Halkier, T., Bernauer, S., Brown, S.H. & Kauppinen, S. 1999. Molecular characterization of laccase genes from the basidiomycete *Coprinus cinereus* and heterologous expression of the laccase lcc1. *Appl Environ Microbiol*, Vol. 65, No. 11, pp. 4943–4948.
- Yoon, J., Liboiron, B.D., Sarangi, R., Hodgson, K.O., Hedman, B. & Solomon, E.I. 2007. The two oxidized forms of the trinuclear Cu cluster in the multicopper oxidases and mechanism for the decay of the native intermediate. *Proc Natl Acad Sci U S A*, Vol. 104, No. 34, pp. 13609–13614.
- Yoruk, R. & Marshall, M.R. 2003. Physicochemical properties and function of plant polyphenol oxidase: a review. *J Food Biochem*, Vol. 27, No. 5, pp. 361–422.
- Yoshida, H. 1883. Chemistry of lacquer (Urushi), part 1. *J Chem Soc*, Vol. 43, pp. 472–486.
- Zhukova, Y.N., Lyashenko, A.V., Zhukhlistova, N.E., Voelter, W., Gabdoulkhakov, A.G., Bento, I., Zaitsev, V.N., Stepanova, E.V., Kachalova, G.S., Koroleva, O.V., et al. 2006. Purification, crystallization and preliminary X-ray study of the fungal laccase from *Cerrena maxima*. *Acta Crystallogr Sect F Struct Biol Cryst Commun*, Vol. 62, No. 10, pp. 954–957.
- Zille, A., Gornacka, B., Rehorek, A. & Cavaco-Paulo, A. 2005. Degradation of azo dyes by *Trametes villosa* laccase over long periods of oxidative conditions. *Appl Environ Microbiol*, Vol. 71, No. 11, pp. 6711–6718.

*Publications II is not included in the PDF version.
Please order the printed version to get the complete publication
(<http://www.vtt.fi/publications/index.jsp>).*

PUBLICATION I

**Comparison of substrate
specificity of tyrosinases
from *Trichoderma reesei* and
*Agaricus bisporus***

In: Enzyme and Microbial Technology 44(2009),
pp. 1–10.

Copyright 2012 Elsevier.

Reprinted with permission from the publisher.



Comparison of substrate specificity of tyrosinases from *Trichoderma reesei* and *Agaricus bisporus*

Emilia Selinheimo^{a,*}, Chiara Gasparetti^a, Maija-Liisa Mattinen^a,
Charlotte L. Steffensen^b, Johanna Buchert^a, Kristiina Kruus^a

^a VTT Technical Research Centre of Finland, P.O. Box 1000, Espoo FIN-02044 VTT, Finland

^b Department of Food Science, Faculty of Agricultural Sciences, Aarhus University, Research Centre Foulum, P.O. Box 50, DK-8830 Tjele, Denmark

ARTICLE INFO

Article history:

Received 5 May 2008

Received in revised form 4 September 2008

Accepted 26 September 2008

Keywords:

Tyrosinase

Fungal

Substrate specificity

Kinetic constants

ABSTRACT

Understanding the substrate specificity of tyrosinases (EC 1.14.18.1) as well as their capability to oxidize peptide-bound tyrosine residues is important in a view of applicability of tyrosinases. In the present study, two fungal tyrosinases, an extracellular enzyme from the filamentous fungus *Trichoderma reesei* (TrT) and an intracellular enzyme from the edible mushroom *Agaricus bisporus* (AbT) were compared. Oxidation of various mono- and diphenolic compounds and tyrosine-containing tripeptides was examined and kinetic constants determined using spectrophotometric and oxygen consumption measurements. TrT and AbT were found to show notable differences in their substrate specificity. TrT generally showed 10-fold higher K_m values than AbT. The presence of a carboxylic and amine group in the substrate influenced the enzymes differently. While the substrates with a carboxyl group were observed not to be effectively oxidized by AbT, the amine group seemed to hinder the oxidation in the TrT-catalyzed reactions. Moreover, the UV-visible absorption spectra on the oxidation of catechol and hydrocaffeic acid showed that the product patterns were different between the enzymes. The result is interesting as the primary products from tyrosinase-catalyzed reactions were assumed to be identical with both enzymes. Furthermore, a nucleophilic 3-methyl-2-benzothiazolinone hydrazone (MBTH) affected differently on the activity of the tyrosinases: the lag period related to the oxidation of monophenols was prolonged by MBTH with TrT, whereas with AbT the lag was shortened.

© 2008 Elsevier Inc. All rights reserved.

1. Introduction

Tyrosinases (monophenol, *o*-diphenol:oxygen oxidoreductase, EC 1.14.18.1) are copper-containing metalloproteins and widely found in microbes, plants and mammals. These enzymes are known as type 3 copper proteins having a diamagnetic spin-coupled copper pair in the active centre [1]. Tyrosinases catalyze the *o*-hydroxylation of monophenols and subsequent oxidation of *o*-diphenols to quinones [2,3]. Molecular oxygen is used as an electron acceptor in the catalysis, with subsequent reduction of oxygen to water. The binuclear active site of tyrosinases is known to exist in three states: *oxy*-tyrosinase, *met*-tyrosinase and *deoxy*-tyrosinase. Both *met*- and *oxy*-states of tyrosinases can catalyze diphenolase

reaction, whereas the hydroxylation reaction that is involved in the monophenolase catalytic cycle requires the *oxy*-form of the active site, in which dioxygen is bound as a peroxide [7,8]. *Deoxy*-tyrosinase is a reduced and instable form and binds oxygen to give the *oxy*-form [4–6].

Even though many tyrosinase proteins and the corresponding genes have been characterized from bacteria, fungi, plants and mammals, the protein structures of the different tyrosinases are still largely unrevealed. However, the crystal structure of the *Streptomyces castaneoglobisporus* tyrosinase was recently resolved [8]. The *S. castaneoglobisporus* tyrosinase was shown to have similarities with the crystal structures of the catechol oxidase from *Ipomoea batatas* [9] and hemocyanin, an oxygen carrier protein from *Octopus dofleini* [10]. Furthermore, the identical catalytic mechanism between the tyrosinases of different origin has been postulated [8,11,12].

Characteristics of various fungal tyrosinases, especially the enzymes from *Agaricus bisporus* [13,14] and *Neurospora crassa* [2], have been investigated comprehensively. The fungal tyrosinase from the edible mushroom *A. bisporus* (AbT) [13,15,16] is reported to be composed of two monomeric subunits [13,14]. Based on the

Abbreviations: TrT, tyrosinase from *Trichoderma reesei*; AbT, tyrosinase from *Agaricus bisporus*; Y, tyrosine; G, glycine; MBTH, 3-methyl-2-benzothiazolinone hydrazone; [S], substrate concentration.

* Corresponding author at: P.O. Box 1500, Espoo FIN-02044 VTT, Finland. Tel.: +358 20 722 7135 fax: +358 20 722 7071.

E-mail address: emilia.selinheimo@vtt.fi (E. Selinheimo).

cDNAs the predicted molecular weight of AbT is 64 kDa. The mature protein, however, show a molecular mass of 43 kDa with a putative cleavage site in the C-terminus [14]. Recently Selinheimo et al. [17] reported the production and purification of a novel tyrosinase from *Trichoderma reesei* (TrT). Similarly to AbT, the mature protein of TrT was processed from C-terminus and TrT showed a molecular mass of 43.2 kDa [17]. Unlike the intracellular plant, fungal and animal tyrosinases studied thus far, the gene *tyr2* of *T. reesei* was found to contain a signal sequence, and the gene product was verified to be secreted. Moreover, the extracellular TrT enzyme was produced at high amount, which is rather exceptional within this class of enzymes. The tyrosinases from *Gibberella zeae*, *N. crassa* and *Magnaporthe grisea* also contain putative signal sequences, suggesting extracellular enzymes [17]. However, they have not been characterized at a protein level. The reported *Streptomyces* tyrosinases are also secreted, but the secretion of the bacterial tyrosinases is assisted by another protein, which has a signal sequence [18,19].

Comparison of biochemical characteristics of the intracellular AbT and the extracellular TrT has recently been performed by Selinheimo et al. [20]. AbT and TrT were found to differ, especially, in their protein crosslinking ability, and in the efficiency to oxidize substrates substituted with amine and carboxyl acid group [20]. In the present study, the aim was to further elucidate the influence of the substitution of mono- and diphenolic compounds on the affinity and the catalytic efficiency of AbT and TrT.

2. Materials and methods

2.1. Enzymes

TrT was produced, purified as described by Selinheimo et al. [17]. AbT was obtained from Fluka, and it was dissolved in 0.1 M sodium phosphate buffer, pH 7.0. For some experiments, AbT was further purified as described by Duckworth and Coleman [21].

2.2. Chemicals

L-Tyrosine, 3,4-dihydroxy-L-phenylalanine (L-dopa), L-tyramine, L-dopamine, *p*-coumaric acid, were from Sigma, *p*-tyrosol 3-(4-hydroxyphenyl)propanoic acid (phloretic acid) and 3-(3,4-dihydroxyphenyl)propanoic acid (hydrocaffeic acid) were from Aldrich, caffeic acid and pyrocatechol were from Fluka, phenol and benzoic acid were from Merck, and the peptides glycine-glycine-tyrosine (GGY), glycine-tyrosine-glycine (GYG) and tyrosine-glycine-glycine (YGG) from Bachem. 3-methyl-2-benzothiazolinone hydrazone (MBTH) and aniline were from Sigma.

2.3. Enzyme activity assays

Tyrosinase activity was measured as described by Robb [3], with few modifications, using 15 mM L-dopa and 2 mM L-tyrosine as substrates. Activity assays were carried out in 0.1 M sodium phosphate buffer (pH 7.0) at 25 °C either by monitoring dopachrome formation at 475 nm ($\epsilon_{\text{dopachrome}} = 3400 \text{ M}^{-1} \text{ cm}^{-1}$) or by monitoring the consumption of the co-substrate oxygen, with a single channel fibre-optic oxygen meter for mini-sensors (Precision sensing GmbH, Regensburg, Germany). The oxygen consumption assay was performed as described by Selinheimo et al. [17]. Furthermore, the enzymatic activities on L-dopa (15 mM) and L-tyrosine (2 mM) were detected by a spectrophotometric assay in the presence of chromogenic nucleophile 3-methyl-2-benzothiazolinone hydrazone (MBTH). A coupling reaction between MBTH and *o*-quinones that are generated during the oxidation of monophenols and *o*-diphenols leads to the formation a MBTH-quinone adduct absorbing at 510 nm ($\epsilon = 22 \text{ 300 M}^{-1} \text{ cm}^{-1}$) [22–25]. In the activity assay with MBTH, concentrations of 0.25–10 mM of MBTH were used, and 2% (v/v) *N,N*-dimethylformamide was added to the reaction mixture to keep the MBTH-quinone adducts in solution.

2.4. Determination of kinetic parameters K_m and V_{max}

Monophenolic compounds, L-tyrosine, phenol, L-tyramine, *p*-coumaric acid, phloretic acid and their corresponding diphenols L-dopa, catechol, L-dopamine, caffeic acid, hydrocaffeic acid, and additionally monophenolic *p*-tyrosol (Fig. 1), were dissolved at a concentration of 0.1–20 mM in 0.1 M sodium phosphate buffer (pH 7.0). TrT and AbT dosages per 1 ml of substrate were 3.8 and 3.1 μg for the monophenols and 0.9 and 0.8 μg for the diphenols, respectively. Kinetic assays were carried out by monitoring the enzymatic reactions by measuring the product formation at the

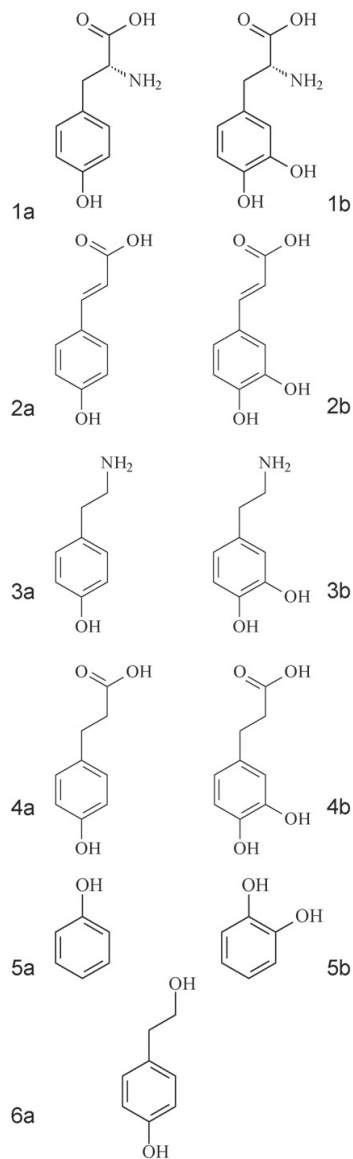


Fig. 1. Chemical structures of the substrates used in the study: **1a** L-tyrosine, **1b** L-dopa, **2a** *p*-coumaric acid, **2b** caffeic acid, **3a** L-tyramine, **3b** L-dopamine, **4a** 3-(4-hydroxyphenyl) propanoic acid (phloretic acid), **4b** 3,4-dihydroxycinnamic acid (hydrocaffeic acid), **5a** phenol, **5b** catechol, **6a** *p*-tyrosol.

selected wavelengths at 25 °C. Specific wavelengths for the product formation from substrates were determined according to the UV-visible absorption spectrum of the oxidation products from the particular substrates by the enzymes. Formation of the UV-visible absorption spectra were monitored as a function of enzyme reaction time. For the tripeptides, GGY, GYG and YGG, the kinetic constants were analyzed by the oxygen consumption assay. Peptides were dissolved in 0.1 M sodium phosphate buffer (pH 7), reaction volume was 1.8 ml, and TrT and AbT doses were 40 and 30 μg , respectively. Kinetic constants K_m , V_{max} and k_{cat} were obtained with the Graph Pad Prism 3.02 program (Graph Pad Software Inc., San Diego, CA, USA). Additionally, the absorption spectra of the oxidation products of the tripeptides by TrT and AbT were determined.

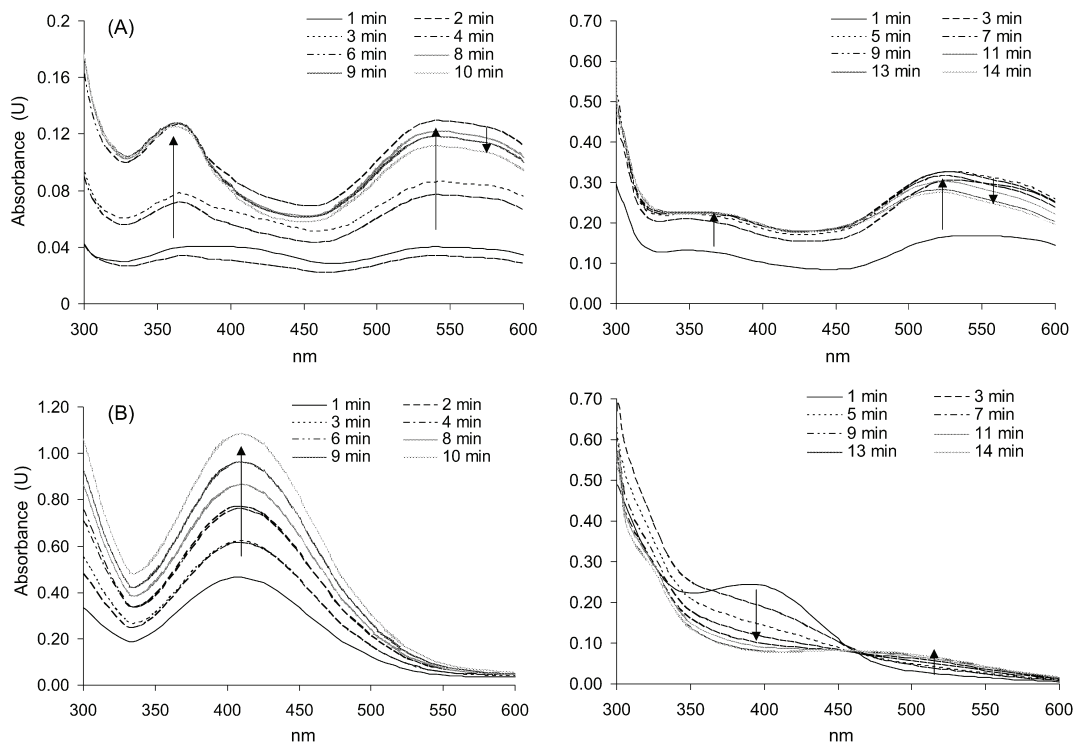


Fig. 2. Absorption product spectra from the oxidation of catechol (left side) and hydrocaffeic acid (right side) by TrT (A) and AbT (B). Absorption spectra of products shown as a function of reaction time.

2.5. ESR experiment

ESR experiment for semiquinone detection from the oxidation of the tripeptides, GGY, GYG and YGG, was performed on a Bruker EMX X-band ESR spectrometer equipped with an ER4119HS cavity (Bruker Analytische Messtechnik, Rheinstetten, Germany). The operating conditions were as follows: microwave power, 20 mW; modulation frequency, 100 kHz; field modulation amplitude, 0.2 G; receiver gain, 2×10^3 ; time constant, 2.56 ms; and conversion time, 2.56 ms. After initiation of the enzymatic reaction, reaction mixture was immediately transferred to an ESR flat cell, mounted within the ESR cavity, after which the measurement was started instantly. ESR signal appearance and disappearance was monitored as a function of time: one measurement, a sum of 34 successive scans, took 3.5 min, after which the ESR was restarted without a delay. GGY, GYG and YGG (2.5 mM) were dissolved in 0.2 M acetate buffer (pH 6.5) containing 0.05 M Zn^{2+} . Zn^{2+} was included in the reaction mixtures to stabilize the *o*-semiquinones [26]. Reactions were made at ambient temperature and in a volume of 0.5 ml. Dosing of the enzymes (0.55 nkat/mg peptide) was based on the determined activity of the enzymes on *L*-tyrosine (2 mM). To elucidate the effect of Zn^{2+} on the enzymatic activity, the oxidation of the peptides in presence of Zn^{2+} was also monitored by oxygen consumption measurement, and by following the UV–visible absorption spectrum formation during oxidation of the substrates.

3. Results

3.1. Product formation by TrT and AbT by determination of the UV–visible absorption spectrum

UV–visible absorption spectra of the oxidation products by TrT and AbT from different mono- and diphenolic compounds were measured. Based on the absorption spectra of product formation, specific wavelengths were established for determination of the kinetic constants K_m and V_{max} on the substrates. When catechol and hydrocaffeic acid were used as substrates, the UV–visible

absorption spectrum obtained by TrT and AbT was completely different. AbT-catalyzed oxidation reaction led to an absorption maximum at 400 nm for both substrates, whereas in the TrT reactions the UV–visible absorption spectrum showed two maxima: one at 360 nm and another at 540–560 nm (Fig. 2). For the other substrates studied, the absorption spectra of the oxidation products of mono- and diphenolic compounds were similar between the enzymes. Tyrosinase-catalyzed oxidation products from phenol and phloretic acid, i.e. the corresponding monophenols for catechol and hydrocaffeic acid, with both enzymes resulted in absorption spectra similar to that of catechol and hydrocaffeic acid catalyzed by AbT, i.e. absorption maximum of product at 400 nm.

Table 1

Absorption maxima (nm) in the UV/Vis absorption spectrum of the primary product formation by TrT and AbT from the mono- and diphenolic substrates.

Substrate	Wavelength (nm)	
	TrT	AbT
<i>L</i> -Tyrosine	475	475
<i>L</i> -Dopa	475	475
<i>p</i> -Coumaric acid	360	360
Caffeic acid	480	480
<i>L</i> -Tyramine	475	475
<i>L</i> -Dopamine	475	475
Phloretic acid	400	400
Hydrocaffeic acid	530 (360) ^a	400
Phenol	390	390
Catechol	540 (360) ^a	400
<i>p</i> -Tyrosol	395	395

^a Two products were detectable in TrT-catalyzed reactions. The absorption maximum of the second primary product is shown in parentheses.

Table 2
 K_m (mM) and V_{max} (Abs/min) values of tyrosinases from TrT and AbT for mono- and diphenolic compounds, determined by spectrophotometric assay with substrate-specific wavelengths (Abs/nm).

Substrate	Detection absorbance (nm)	K_m (mM)		V_{max} (Abs/min)	
		TrT	AbT	TrT	AbT
L-Tyrosine	475	–	0.20	6 ^a	13
L-Dopa	475	7.5	0.17	210	60
<i>p</i> -Coumaric acid	360	1.5	–	51	0
Caffeic acid	480	0.9	1.69	60	300
L-Tyramine	475	4.5	0.75	4	16
L-Dopamine	475	11	0.84	120	300
Phloretic acid	400	1.4	0.64	55	77
Hydrocaffeic acid	400/530 ^b	3.0	0.91	450	840
Phenol	390	3.8	0.33	9	14
Catechol	400/540 ^c	2.5	0.25	138	1500
<i>p</i> -Tyrosol	395	0.8	0.06	20	13

^a Oxidation rate determined using tyrosine concentration of 2.5 mM, not the V_{max} value.

^b Product formation followed at 400 and 530 nm with AbT and TrT, respectively.

^c Product formation followed at 400 and 540 nm with AbT and TrT, respectively.

The absorption maxima selected for determining kinetic constants for the substrates were as follows: phenol 390 nm; catechol 400 (AbT) and 540 nm (TrT); *p*-coumaric acid 360 nm; caffeic acid 480 nm; L-tyramine, L-dopamine, L-tyrosine and L-dopa 475 nm; phloretic acid 400 nm; hydrocaffeic acid 400 (AbT) and 530 nm (TrT); and *p*-tyrosol 395 nm (Table 1).

3.2. Substrate specificity of TrT and AbT on mono- and diphenolic compounds

The ability of TrT and AbT to oxidize mono and diphenolic substrates with different substitution of carboxyl and amino groups was elucidated by determining the kinetic parameters, K_m and V_{max} (Table 2). The maximum reaction rate V_{max} is expressed as a change in absorbance as a function of time (Abs/min). The molar extinction coefficients (ϵ) for calculation of V_{max} (mol/s) and k_{cat} (s^{-1}) were not possible to determine. It was observed that different oxidation products were formed in the AbT and TrT catalyzed reactions. In addition, although the primary product from many substrates was same with both enzymes, different end products accumulated in TrT and AbT catalyzed reactions. For instance, in the oxidation of L-dopa, the dopachrome (λ_{max} at 475 nm) was the primary product with both enzymes, but with TrT the accumulation of dopachrome stopped, and other products accumulating at 370–460 nm appeared after initiating the reaction (data not shown).

The determined K_m values were approximately ten times lower for AbT than for TrT (Table 2). On the other hand, the maximum reaction rates V_{max} of corresponding mono- and diphenols varied between the enzymes depending on the substrates (Table 2). For instance, with L-dopa, V_{max} was clearly higher with TrT than AbT, whereas with caffeic acid and L-dopamine the outcome was opposite.

Under the conditions studied, AbT showed the highest affinity on monophenolic *p*-tyrosol (K_m 0.06 mM) and L-tyrosine (K_m 0.2 mM), and diphenolic L-dopa (K_m 0.17 mM) and catechol (K_m 0.25 mM). The highest K_m values for AbT were detected for caffeic acid, 1.61 mM and hydrocaffeic acid, 0.91 mM. Generally, AbT had higher affinity on monophenols than on the corresponding diphenols, except phenol, which showed slightly lower affinity when compared to catechol (Table 2). *p*-Coumaric acid was not oxidized by AbT. It was also seen that V_{max} was reached by AbT at certain substrate concentration with phenol, catechol, caffeic acid, phloretic acid, hydrocaffeic acid and *p*-tyrosol, above which the V_{max} began to decrease (data not shown). The decrease in the maximum reaction rate with increasing substrate concentrations is presumably related to inhibition of AbT by an excess of substrate.

TrT showed the highest affinity on *p*-tyrosol (K_m 0.8 mM), caffeic acid (K_m 0.9 mM), phloretic acid (K_m 1.4 mM) and *p*-coumaric acid (K_m 1.5 mM), whereas the affinity on L-dopamine (K_m 11 mM), L-dopa (K_m 7.5 mM) and L-tyramine (K_m 4.5 mM) was low (Table 2). The K_m value for L-tyrosine could not be determined due to insolubility of the substrate at concentrations above 2.5 mM. This concentration was not high enough to reach the V_{max} (Fig. 3). From the shape of the reaction rate vs. substrate concentration plot, the decrease in the maximum rate with increasing [S] was clearly seen in the TrT reactions with hydrocaffeic acid and caffeic acid, and also faintly with phloretic acid, referring to the inhibition of TrT by an excess of the substrate. Additionally, with catechol the corresponding substrate inhibition was detected for the product formation at 360 nm, but interestingly, not for the product formation at 540 nm (data not shown).

With monophenolic substrates a lag period prior to the oxidation reactions were detected by both enzymes. The lag periods for the oxidation reactions by AbT were longest with phenol (400 s), *p*-tyrosol (200–300 s) and L-tyrosine (200 s), with a substrate concentration of 15 mM (Table 3). The lag period increased as a function of substrate concentration for phenol, *p*-tyrosol and L-tyrosine, whereas for L-tyramine and phloretic acid the lag period decreased when substrate concentration was increased. The lag periods prior

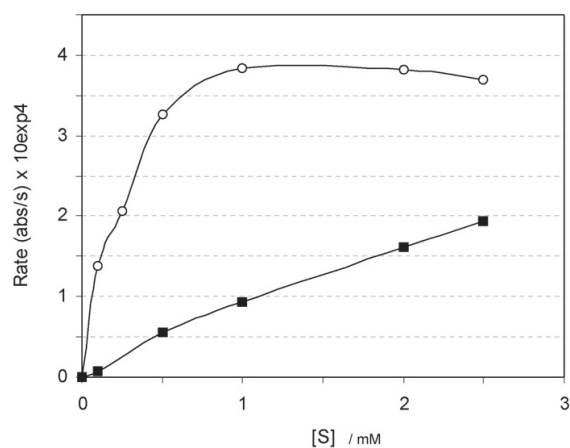


Fig. 3. Reaction rate as a function of substrate concentration [S], using L-tyrosine as substrate. Legends: AbT (○), TrT (■).

Table 3

Duration of lag periods (s) of tyrosinases from TrT and AbT for monophenolic compounds, determined by spectrophotometric assay.

Substrate	Detection absorbance (nm)	Lag (s) with [S] 15 mM		Lag (s) with [S] 1 mM	
		TrT	AbT	TrT	AbT
L-Tyrosine	475	0 ^a	200 ^a	0–100 ^b	50–100 ^b
<i>p</i> -Coumaric acid	360	100–150	–	300	–
L-Tyramine	475	0	0	400	100–150
Phloretic acid	400	25–50	0–25	100–150	50–100
Phenol	390	200	400	500	300
<i>p</i> -Tyrosol	395	0	200–300	200	100–200

^a Substrate concentration 2.5 mM.^b Substrate concentration 0.25 mM.**Table 4**

Kinetic parameters of tyrosinases from TrT and AbT for the peptides GGY, GYG and YGG, determined by oxygen consumption measurement.

Enzyme	Substrate	V_{max} (mg L ⁻¹ s ⁻¹) × 10 ²	K_m (mM)	k_{cat} (s ⁻¹)	k_{cat}/K_m (s ⁻¹ mM ⁻¹)	Lag phase (s) with [S] 4 mM
TrT	Y		nd ^a			
TrT	GGY	11.9	3.1	7.2	2.4	120
TrT	GYG	6.9	3.9	4.2	1.1	120
TrT	YGG	5.2	6.0	3.2	0.5	120
AbT	Y		0.20			
AbT	GGY	2.7	0.11	3.0	26.5	600
AbT	GYG	2.8	0.18	3.1	17.1	240
AbT	YGG	3.6	0.21	4.0	19.0	180

^a Could not be determined due to insolubility of the substrate.

to the oxidation of monophenols by TrT were longest with phenol (200 s), *p*-coumaric acid (100–150 s) and phloretic acid (25–50 s) with a substrate concentration of 15 mM (Table 3). Duration of the lag period decreased when substrate concentration increased with all of the tested monophenols in the TrT-catalyzed reactions.

3.3. Kinetic parameters for the tyrosine-containing tripeptides

The K_m and V_{max} values of AbT and TrT for the tripeptides varying in the position of tyrosine residue, GGY, GYG and YGG, were determined by an oxygen consumption assay. Similarly to the results obtained with mono- and diphenols, the K_m values of AbT for the peptides were over 10-fold lower than those of TrT (Table 4). AbT

showed the highest apparent affinity on GGY (K_m 0.11 mM) and lowest on YGG (K_m 0.21 mM), whereas the highest catalytic efficiency k_{cat} was on YGG (4.0 s⁻¹) and lowest on GGY (3.0 s⁻¹). With YGG the affinity for AbT was rather similar to L-tyrosine (K_m 0.20 mM). TrT also showed the highest affinity on GGY (K_m 3.1 mM) and lowest on YGG (K_m 6 mM). However, contrary to AbT, the best catalytic efficiency was observed on GGY (7.2 s⁻¹) and lowest on YGG (3.2 s⁻¹). Interestingly, although there was a clear difference in K_m values, the k_{cat} values were relatively similar between AbT and TrT (Table 4). The lag periods prior to the oxidation reactions were shorter for TrT than AbT. The duration of the lag periods between the peptides was rather similar in the TrT-catalyzed reactions. However, the closer to the C-terminus the tyrosine residue was the longer

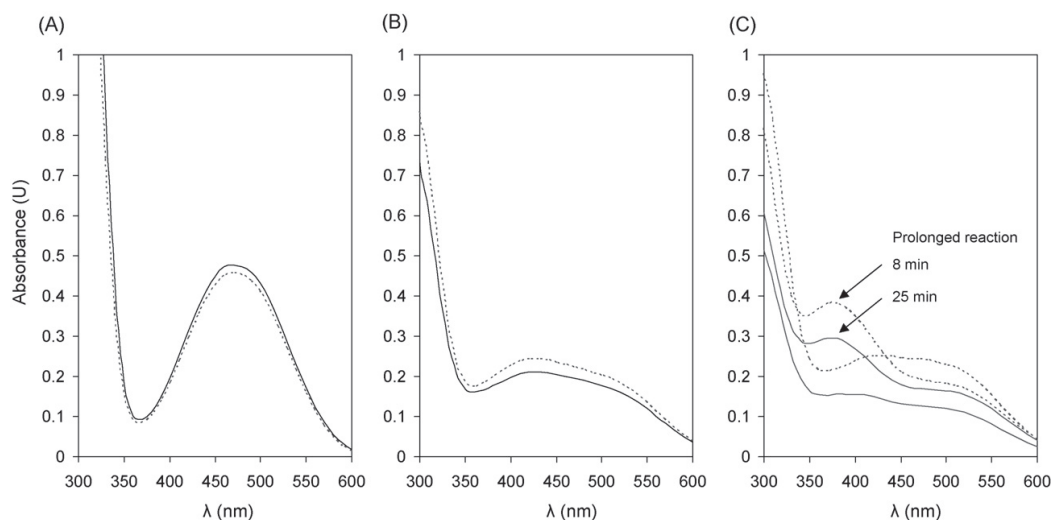


Fig. 4. Product spectra from the oxidation of the tripeptides YGG (A), GYG (B) and GGY (C) by TrT and AbT. Patterns: solid line for TrT, dashed line for AbT. In C arrows show the absorbance lines that represent prolonged reactions with TrT (at 8 min) and AbT (at 25 min), respectively.

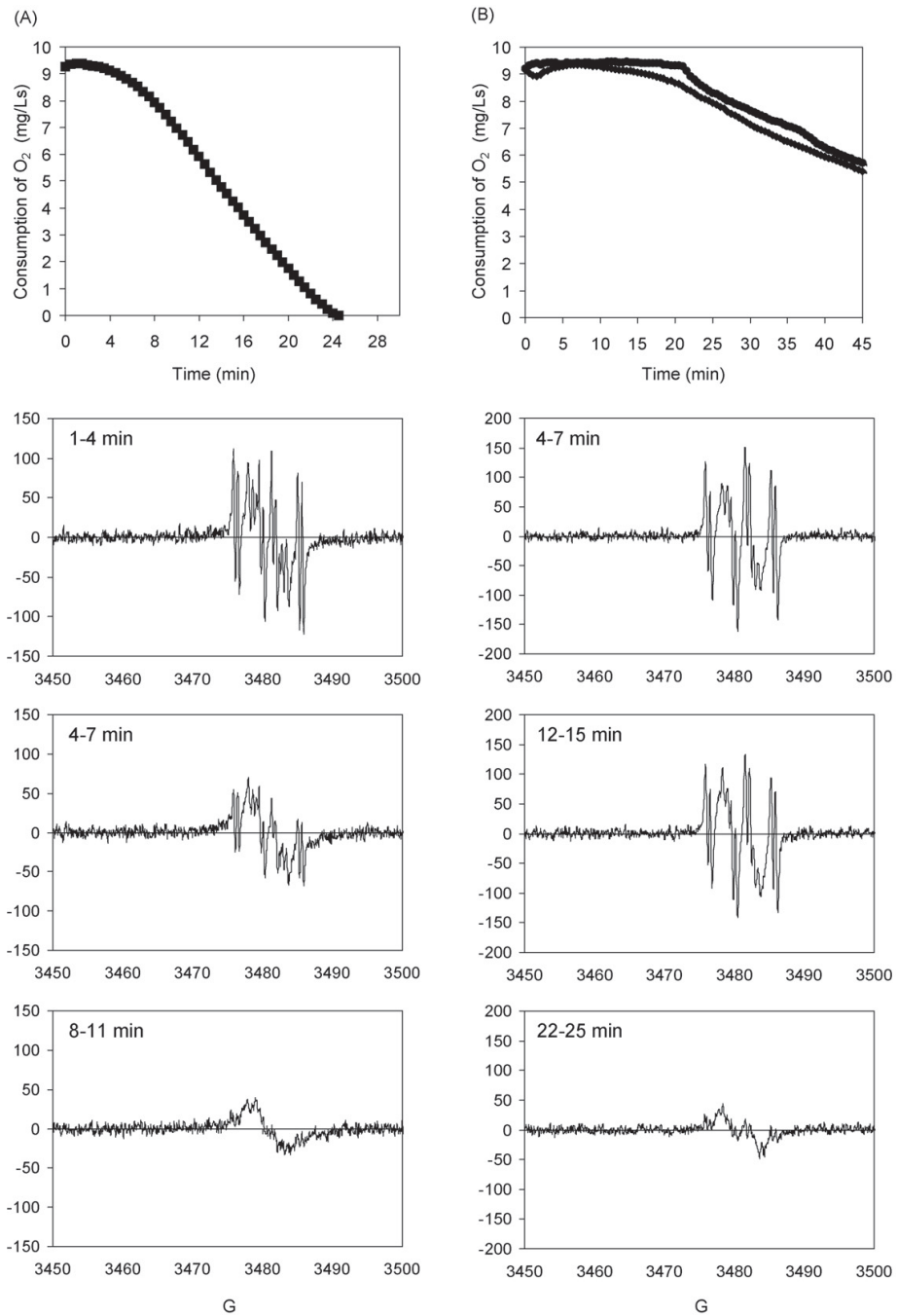


Fig. 5. Semiquinone-derived ESR signals and consumption of oxygen ($\text{mg L}^{-1} \text{s}^{-1}$) by TrT in presence of 1 mM GGY and GYG. Reaction conditions for oxygen consumption measurements correspond to the detection times of ESR signals as a function of reaction time. GGY (A) and GYG (B).

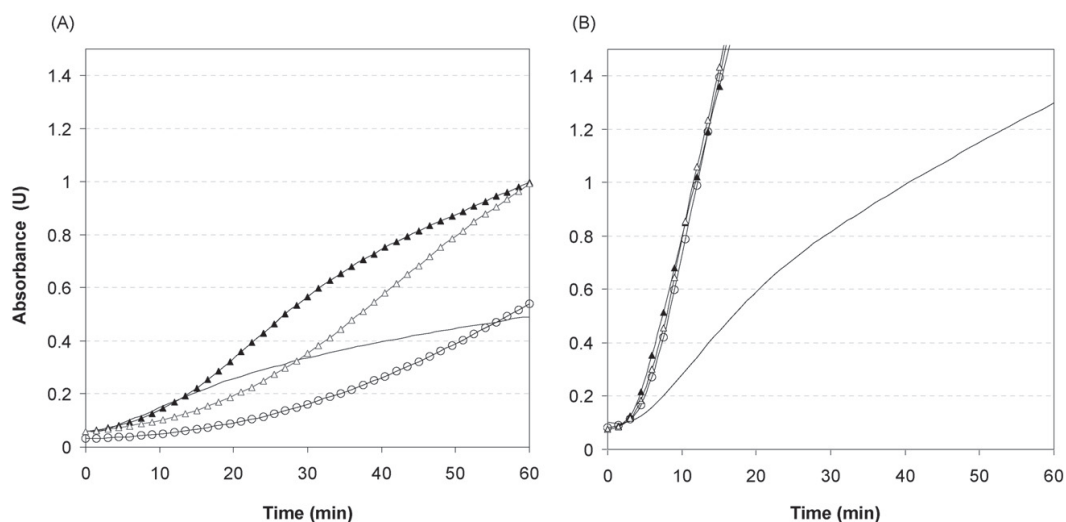


Fig. 6. Enzymatic activities of TrT and AbT on oxidation of L-dopa (15 mM) in presence of MBTH (0–10 mM). Formation rate for the MBTH-quinone adduct followed as an increase in absorbance at 510 nm as a function of time. Legends: MBTH concentration of 0 mM (—), 2.0 mM (Δ), 3.5 mM (\circ), 5.0 mM (\blacktriangle).

the lag period was with AbT. The UV–visible absorption spectra for the oxidation products from the peptides were similar between the enzymes (Fig. 4). However, the product patterns differed clearly between the peptides. Oxidation product from YGG (Fig. 4A) corresponded to dopachrome-related product, showing a maximum at 475 nm, whereas with GYG (Fig. 4B) there was no clear absorption maximum and the product pattern was broad showing absorption maximum around 400–500 nm. Similarly with GGY the oxidation products gave broad absorption maximum at 400–500 nm. During a prolonged reaction (8 min for TrT, 25 min for AbT) absorption maximum with GGY shifted from 400–500 nm to 380 nm (Fig. 4C).

3.4. ESR measurements

Oxidation of GGY, GYG and YGG peptides by TrT and AbT was also monitored with ESR experiment in order to measure semiquinone radical production. The oxidation of the tripeptides GGY and GYG resulted in ESR spectra with two overlapping low intensity multiline ESR signals (Fig. 5A) by both enzymes (data on AbT not shown), corresponding to L-tyrosine-derived signal defined previously by Selinheimo et al. [20]. Signals were not detected by the enzymes or the substrates alone. Maximum signal intensities from GGY and GYG were relatively similar. When YGG was used as substrate, semiquinone-derived signal could not be detected in ESR. Oxidation of the tripeptides in the presence of Zn^{2+} , which was included in the reaction mixture to stabilize the semiquinones, was also monitored by an oxygen consumption assay (Fig. 5B) and by measuring the UV–visible absorption spectrum for the oxidation products (data not shown) in the conditions analogous to the ESR experiment. From the oxygen consumption measurements it was detected that the lag periods increased in presence of Zn^{2+} for all peptides and with both enzymes. With an oxygen consumption assay it was confirmed that the oxidation of YGG in presence of Zn^{2+} occurred by TrT and AbT (data not shown), although ESR signal was not detected from YGG. When the consumption of oxygen as a function of reaction time, and especially, the duration of the lag periods prior to the oxidation were compared to the appearance time of the semiquinone-derived signals, the outcome was

unexpected. The semiquinone-derived ESR signal from GGY and GYG was observed to be present mainly during the lag period as detected by the oxygen consumption measurements (Fig. 5A and B). In other words, when the oxygen consumption was initiated, and thus, oxidation reaction accelerated, the ESR signal seemed to disappear. The result was also supported by the UV–visible absorption spectrum scanning measurements, monitored as a function of reaction time, in which the product formation accelerated when the ESR signal started to vanish (data not shown). However, some product formation was detected also during the lag period.

3.5. Effect of MBTH

Tyrosinase activity is often determined in presence of nucleophile MBTH, which is an efficient quinone binder [22–25]. Activities of TrT and AbT on L-dopa (15 mM) and L-tyrosine (2 mM) were determined in the presence of MBTH as well. Interestingly, when the monophenolase activities of AbT and TrT were determined using L-tyrosine in presence of MBTH, the lag period increased significantly as a function of MBTH concentration in the TrT-catalyzed reactions (Fig. 6A). On the other hand, with AbT the lag period was constant with varying MBTH concentrations (Fig. 6B). When the absorption spectra for the reaction products were determined on L-dopa and L-tyrosine in the presence of MBTH, absorbance intensity at 510 nm increased, referring to the MBTH-quinone adduct (data not shown). However, lowering the MBTH concentration a shift towards the dopachrome product (475 nm) was detected. For instance, when L-tyrosine was used as substrate, with MBTH concentration of ≤ 0.5 mM, a clear shift towards dopachrome was observed during the reaction with both enzymes. Apparently, with lower MBTH concentrations, not all of the formed quinones could be trapped.

4. Discussion

Detailed information on the substrate specificity of tyrosinases is essential for development of tyrosinase-based applications. The aim in the present study was to compare the substrate specificity of

the recently characterized tyrosinase TrT to the commercial tyrosinase preparation AbT. AbT is a well characterized enzyme, and for instance, the substrate specificity of AbT has been studied by Espín et al. [27,28], Fenoll et al. [29], Rodríguez-López et al. [30] and Xie et al. [31]. There is variation in the results of kinetic parameters for AbT, depending on both the level of purification of AbT and the assay method used [21,25–27]. Espín et al. [27] determined kinetic parameters by a spectrophotometric method using a purified AbT preparation, and reported for L-tyrosine a K_m value of 0.21 ± 0.01 mM, and for L-dopa a K_m value of 0.8 ± 0.04 mM. For the major isoform of AbT (Mw 43 kDa) Espín et al. [25] reported for L-tyrosine a K_m value of 0.021 ± 0.001 mM, and for L-dopa a K_m value of 0.038 ± 0.003 mM. Regarding hydrocaffeic acid (**4b**), Xie et al. [31] reported a K_m value of 1.24 mM for non-purified AbT, whereas Espín et al. [27] determined a K_m value of 1.89 mM for purified AbT. In the present work the experiments were made with the commercial AbT enzyme preparation, which has been reported to contain several isoforms of tyrosinase [13,14,31]. AbT was also further purified according to Duckworth and Coleman [21] for some of the experiments. For instance, the different location of tyrosine in the tripeptide, and its subsequent influence on the catalysis was studied with both crude and purified AbT, and the results were analogous (data not shown).

TrT and AbT showed notable differences in the affinity of the substrates studied. The K_m values for AbT were observed to be the highest for the substrates, in which an acid group was present in the structure (i.e. caffeic (**2b**) and hydrocaffeic acid (**4b**)). Furthermore, *p*-coumaric acid (**2a**) was not oxidized by AbT. It has been proposed that carboxylic aromatic structures can act as substrate analogues for tyrosinase, and they are believed to bind to both the *oxy*-form and the *met*-form of the coupled binuclear copper site [32–34]. Specifically *p*-coumaric acid and benzoic acid have been hypothesized to bind to the binuclear copper centre preferentially with the more acidic carboxylic group and compete with the substrate [32,34–37]. Rompel et al. [38] suggested that the blocking of active site could be based on either the coordination of the carboxylic group to the copper atoms or the binding of carboxylic acid group at a positively charged amino acid residue near the catalytic site. Since phloretic acid is oxidized by AbT, it has been suggested that particularly the conjugation of carboxylic group into the aromatic ring that is missing in phloretic acid is essential for binding of the acid group [32]. In contrast to AbT, TrT was observed to have clearly higher K_m values for substrates with amine substitution when compared to the substrates with carboxylic acid substitution. It appears particularly interesting that while AbT was not able to oxidize *p*-coumaric acid and showed the lowest affinity on caffeic acid among the tested substrates, TrT showed high affinity on caffeic acid and *p*-coumaric acid. Previously, Selinheimo et al. [17] reported for TrT the K_m values of 1.3, 1.6 and 3.0 mM for *p*-tyrosol, *p*-coumaric acid and L-dopa, respectively, determined by monitoring consumption of oxygen which differ to some extent from the K_m values of the present study, assayed by a spectrophotometric method.

The negative effect of proximity of an amine group on TrT was also detected in the K_m values of the tripeptides, as the highest K_m value and lowest catalytic efficacy (k_{cat}) was on YGG, in which tyrosine residue is in the amino-terminal end of the peptide. With AbT the lowest K_m value was detected, when the tyrosine residue located in the carboxyl-terminal end, i.e. for the GGY tripeptide. However, with GGY the k_{cat} was the lowest and the lag period longest for AbT, suggesting high affinity, but poorer catalytic efficacy as compared to the other peptides. Although the exact reasons for the differences in the K_m values between TrT and AbT remain to be resolved, it could be that the coordinating amino acids of enzymes, which assist substrates to the active site, differ between the enzymes. Hence, varying polarity and acidity of the phenolic

hydroxyl group of the substrate could cause different orientation of the substrate to the active site of AbT and TrT. Determining the tertiary structure of AbT and TrT and the detailed construction of active site is essential to elicit the explanation for the result.

The activity assay using a nucleophilic quinone binder MBTH has been reported to be relatively sensitive and accurate for determining tyrosinase activity, as with this nucleophile a relatively stable quinone adduct can be formed [22–25]. It has also been reported that the lag period, which is typically present in the tyrosinase-catalyzed monophenol oxidation, could be shortened by using nucleophilic coupling reactions through quick generation of *o*-diphenols [23]. During the lag period, the *oxy*-form of tyrosinase, which is capable for the hydroxylation of monophenols, is generated by indirect *o*-diphenol formation from the *met*-form of tyrosinase, which can perform only the oxidation of diphenols [7,39]. In the TrT-catalyzed reactions with L-tyrosine and MBTH, the duration of the lag period was unexpectedly increased as a function of MBTH concentration, referring that MBTH retarded the initiation of the catalytic cycle by TrT. However, the maximum reaction rate was not significantly changed by MBTH. Hence, it seemed that MBTH retarded principally the transformation of TrT from the *met*- to the *oxy*-form. With AbT the effect of MBTH was as reported previously [24,25]: the lag was constant and even decreased when compared to the reactions without MBTH.

The lag periods for TrT and AbT were measured for all the monophenolic substrates studied (without MBTH). It has been proposed that a monophenolic substrate with high affinity saturates the *met*-form of enzyme [25]. Hence, if most of the enzyme is in a form, in which monophenols are bound to the *met*-tyrosinase, the transformation from the *met*- to the *oxy*-form is delayed because there is less free enzyme for diphenol oxidation. Espín et al. [25] reported that lag period increased when substrate concentration ($[S]$) was increased, suggesting that the *met*-form of the enzyme was increasingly saturated with monophenol when $[S]$ was increased. When the lag periods were monitored in the AbT-catalyzed reactions, the lag period increased as a function of $[S]$ with *p*-tyrosol, L-tyrosine and phenol, but with L-tyramine and phloretic acid the situation was opposite. On the other hand, with TrT, the lag period was invariably shortened with increasing $[S]$. However, the K_m values for TrT were relatively high which might partly explain the lag durations. If the reactions with lower $[S]$ were still clearly beyond V_{max} , the lag could be expected to increase by increasing $[S]$, as with lower $[S]$ there is not enough substrate to occupy the active site. This might also partly explain the incoherence in the duration of the lag periods with AbT, as L-tyramine and phloretic acid, which showed decreasing lag with increasing $[S]$, were also the substrates with highest K_m values. However, the difference between the K_m values was not very significant between the substrates with different changes in lag duration, suggesting that there are also other factors behind.

The product formation in the tyrosinase catalysis was determined by monitoring the changes in UV-visible absorption spectrum as a function of reaction time. Unpredictably, diphenols catechol (**5b**) and hydrocaffeic acid (**4b**) gave different product pattern by AbT and TrT, whereas the products from the corresponding monophenols (phenol (**5a**) and phloretic acid (**4a**)) did not differ between the enzymes. The dissimilarity in the diphenol catalysis between the enzymes seemed to be specific only for these substrates, as for the other diphenols studied, i.e. L-dopa, L-dopamine and caffeic acid, the product spectrum was similar between the enzymes. Although there is not clear explanation for the found differences in the oxidation products from catechol and hydrocaffeic acid, it could be hypothesized that the observations could

relate to the differences of the enzymes in their affinity to the non-enzymatic quinone-derived products. It is known that the quinones formed in the catalysis will quickly react further and also act as substrates for tyrosinase. Typically oxidation of catechol by tyrosinases is known to generate products absorbing at 390–400 nm [40], which was also detected with AbT. Interestingly these products were not detected with TrT. It could be anticipated that TrT immediately further oxidized the product resulting from the non-enzymatic reactions of *o*-quinone. Hence, the primary product at 390–400 nm could not have accumulated in the TrT-catalyzed reactions.

When enzymatic oxidation of tripeptides was examined, the position of tyrosine residue in the tripeptide was observed to influence differently on the TrT- and AbT-catalyzed reactions. The reaction products were different depending on whether the tyrosine was located in the carboxyl- or amino-terminus or in the middle of the peptide; however, differences in the reaction products between AbT and TrT were not detected. Land et al. [41,42] have shown that increasing the chain length of catecholamines leads to unachievable cyclization of these amines due to a steric hindrance. Based on the product accumulation from the tripeptides GGY, GYG and YGG by the tyrosinases, only oxidation of YGG was observed to lead to the formation of dopachrome-type cyclization product. Probably in the case of GGY and GYG, cyclization of peptide via reaction of quinone with nucleophilic amine was unfavourable due to the steric hindrance. When the semiquinone radical formation during the oxidation of the peptides was studied by ESR, Zn^{2+} was included in the reaction solution to stabilize the semiquinones [26]. Zn^{2+} was observed to influence on the oxidation readiness of the peptides by lengthening the lag phase prior to the oxidation. The presence of transition metal ions, such as Zn^{2+} , has been reported to affect the lag period related to oxidation of monophenols either by prolonging or by diminishing the lag phase [43–45]. The transition metal ions can also affect the chemical properties of melanins formed by the tyrosinase-catalyzed oxidation of L-dopa. Particularly, the non-carboxylative rearrangement of dopachrome to 5,6-dihydroxyindole-2-carboxylic acid may occur in the presence of metal ions [46–48]. In actual fact, the UV-visible absorption spectra on the oxidation products of the tripeptides clearly changed in presence of Zn^{2+} . With YGG an absorption maximum was at 430 nm instead of 475 nm, and with GYG and GGY the maximum was around 300–450 nm (data not shown). Unexpectedly, semiquinone-derived ESR signal was not detected for YGG oxidation by the tyrosinases. This could be due to the inability of Zn^{2+} to stabilize the YGG-derived oxidation product, which differed from that of GGY and GYG.

Based on the results of the oxygen consumption of the tripeptides by AbT and TrT in presence of the Zn^{2+} , the ESR signal was noted to appear during the lag period, and disappear when the oxidation reaction accelerated. The results clearly indicate that the semiquinone-derived ESR signal was present in the very beginning of the catalysis. However, after indirect generation of diphenols during enzymatic catalysis, semiquinones should be detectable due to auto-oxidation. After formation of quinines, semiquinones are generated by inverse disproportionation between diphenol and quinone [49]. Because in this study the semiquinone-derived ESR signals were mostly detected during the lag period, it is intriguing to suggest that the semiquinone formation relates specifically to the reaction catalyzed by the *met*-form of tyrosinase.

5. Conclusions

The extracellular fungal tyrosinase TrT and the intracellular tyrosinase AbT were found to clearly differ in their substrate specificity. The product pattern from catechol and hydrocaffeic acid was

also observed to be different between these enzymes. Although the detailed catalytic mechanisms of the enzymes are still to be explicated, the noted contrasts in the determined K_m values for the substrates could suggest differences in the distribution of acid/base residues and orientation of the substrates in the active site of TrT and AbT.

Acknowledgements

This paper has been carried out with financial support from the Research Foundation of Raisiigroup (Raisio, Finland), the Consortium Cresci belonging to University of Perugia (Italy), and the STReP-project (HIPERMAX/NMP-3-CT-2003-505790) funded by the European Commission; the contents of the publication reflects only the views of the authors. Dr. Markku Saloheimo is acknowledged for the expression construct for TrT production, BSc. Michael Bailey for the TrT production, and Heljä Heikkinen for technical assistance.

References

- [1] Lerch K, Huber M, Schneider H, Drexler R, Linzen B. Different origins of metal binding sites in binuclear copper proteins, tyrosinase and hemocyanin. *J Inorg Biochem* 1986;26:213–7.
- [2] Lerch K. *Neurospora* tyrosinase: structural, spectroscopic and catalytic properties. *Mol Cell Biochem* 1983;52:125–38.
- [3] Robb DA. Tyrosinase. In: Lontie R, editor. Copper proteins and copper enzymes. Boca Raton, FL: CRC Press Inc.; 1984. p. 207–40.
- [4] Jolley RL, Evans LH, Mason HS. Reversible oxygenation of tyrosinase. *Biochem Biophys Res Commun* 1972;46:878–84.
- [5] Makino N, Mason HS. Reactivity of oxytyrosinase towards substrates. *J Biol Chem* 1973;248:5731–5.
- [6] Jolley RL, Evans LH, Makino N, Mason HS. Oxytyrosinase. *J Biol Chem* 1974;249:335–45.
- [7] Solomon EI, Sundaram UM, Machonkin TE. Multicopper oxidases and oxygenases. *Chem Rev* 1996;96:2563–606.
- [8] Matoba Y, Kumagai T, Yamamoto A, Yoshitsu H, Sugiyama M. Crystallographic evidence that the dinuclear copper center of tyrosinase is flexible during catalysis. *J Biol Chem* 2006;281:8981–90.
- [9] Klabunde T, Eicken C, Sacchetti JM, Krebs B. Crystal structure of a plant catechol oxidase containing a dicopper center. *Nat Struct Biol* 1998;5:1084–90.
- [10] Cuff ME, Miller KI, van Holde KE, Hendrickson WA. Crystal structure of a functional unit from *Octopus dofleini hemocyanin*. *J Mol Biol* 1998;278:855–70.
- [11] Decker H, Schweikardt T, Tucek F. The first crystal structure of tyrosinase: all questions answered? *Angew Chem Int Ed* 2006;45:4546–50.
- [12] Marusek CM, Trobaugh NM, Flurkey WH, Inlow JK. Comparative analysis of polyphenol oxidase from plant & fungal species. *J Inorg Biochem* 2006;100:108–23.
- [13] Wichers HJ, Gerritse YA, Chapelon CGJ. Tyrosinase isoforms from the fruitbodies of *Agaricus bisporus*. *Phytochemistry* 1996;43:333–7.
- [14] Wichers HJ, Recourt K, Hendriks M, Ebbelaar CEM, Biancone G, Hoeberichts FA, et al. Cloning, expression and characterisation of two tyrosinase cDNAs from *Agaricus bisporus*. *Appl Microbiol Biotechnol* 2003;61:336–41.
- [15] Nakamura T, Sho S, Ogura Y. On the purification and properties of mushroom tyrosinase. *J Biochem* 1966;59:481–6.
- [16] Robb DA, Gutteridge S. The polypeptide composition of two fungal tyrosinases. *Phytochemistry* 1981;20:1481–5.
- [17] Selinheimo E, Saloheimo M, Ahola E, Westerholm-Parvinen A, Kalkkinen N, Buchert J, et al. Production and characterization of a secreted, C-terminally processed tyrosinase from the filamentous fungus *Trichoderma reesei*. *FEBS J* 2006;273:4322–35.
- [18] Leu W, Chen L, Liaw L, Lee Y. Secretion of the *Streptomyces* tyrosinase is mediated through its trans-activator. *Mol Cell Biol* 1992;267:20108–13.
- [19] Tsai TT, Lee YH. Roles of copper ligands in the activation and secretion of *Streptomyces* tyrosinase. *J Biol Chem* 1998;273:19243–50.
- [20] Selinheimo E, NiEidhin D, Steffensen C, Nielsen J, Lomascolo A, Halaoui S, et al. Comparison of the characteristics of fungal and plant tyrosinases. *J Biotechnol* 2007;130:471–80.
- [21] Duckworth HW, Coleman JE. Kinetic properties of mushroom tyrosinase. *J Biol Chem* 1970;245:1613–25.
- [22] Rodríguez-López JN, Escribano J, García-Canovas F. A continuous spectrophotometric method for the determination of monophenolase activity of tyrosinase using 3-methyl 2-benzothiazolinone hydrazone. *Anal Biochem* 1994;216:205–12.
- [23] Espin JC, Morales M, Varón R, Tudela J, García-Canovas F. A continuous spectrophotometric method for determining the monophenolase and diphenolase activities of apple polyphenol oxidase. *Anal Biochem* 1995;231:237–46.

- [24] Espín JC, Morales M, García-Ruiz PA, Tudela J, García-Cánovas F. Improvement of a continuous spectrophotometric method for determining the monophenolase and diphenolase activities of mushroom polyphenol oxidase. *J Agric Food Chem* 1997;45:1084–90.
- [25] Espín JC, Jolivet S, Wichers HJ. Kinetic study of the oxydation of γ -L-glutaminy-4-hydroxybenzene catalyzed by mushroom (*A. bisporus*) tyrosinase. *J Agric Food Chem* 1999;47:3495–502.
- [26] Yamasaki H, Grace SC. EPR detection of phytophenoxyl radicals stabilized by zinc ions: evidence for the redox coupling of plant phenolics with ascorbate in the H_2O_2 -peroxidase system. *FEBS Lett* 1998;422:377–80.
- [27] Espín JC, García-Ruiz PA, Tudela J, García-Cánovas F. Study of stereospecificity in mushroom tyrosinase. *Biochem J* 1998;331:547–51.
- [28] Espín JC, Varon R, Fenoll LG, Gilabert MA, García-Ruiz PA, Tudela J, et al. Kinetic characterization of the substrate specificity and mechanism of mushroom tyrosinase. *Eur J Biochem* 2000;267:1270–9.
- [29] Fenoll LG, Rodríguez-Lopez JN, García-Molina F, García-Canovas F, Tudela J. Michaelis constants of mushroom tyrosinase with respect to oxygen in the presence of monophenols and diphenols. *Int J Biochem Cell B* 2002;34:332–6.
- [30] Rodríguez-López JN, Fenoll LG, García-Ruiz PA, Varón R, Tudela J, Thorneley RN, et al. Stopped-flow and steady-state study of the diphenolase activity of mushroom tyrosinase. *Biochemistry* 2000;39:10497–506.
- [31] Xie J-J, Song K-K, Qiu L, He Q, Huang H, Chen Q-X. Inhibitory effects of substrate analogues on enzyme activity and substrate specificities of mushroom tyrosinase. *Food Chemistry* 2007;103:1075–9.
- [32] Fan Y, Flurkey WH. Purification and characterization of tyrosinase from gill tissue of *Portabella* mushroom. *Phytochemistry* 2004;65:671–8.
- [33] Lim JY, Ishiguro K, Kubo I. Tyrosinase inhibitory *p*-coumaric acid from ginseng leaves. *Phytother Res* 1999;13:371–5.
- [34] Kubo I, Nihei K, Tsujimoto K. Methyl *p*-coumarate, a melanin formation inhibitor in B16 mouse melanoma cells. *Bioorg Med Chem* 2004;12:5349–54.
- [35] Conrad JS, Dawson SR, Hubbard ER, Meyers TE, Strothkamp KG. Inhibitor binding to the binuclear active site of tyrosinase: temperature, pH, and solvent deuterium isotope effects. *Biochemistry* 1994;33:5739–44.
- [36] Winkler ME, Lerch K, Solomon EI. Competitive inhibitor binding to the binuclear copper active site in tyrosinase. *J Am Chem Soc* 1981;103:7001–3.
- [37] Wilcox DE, Porras AG, Hwang YT, Lerch K, Winkler ME, Solomon EI. Substrate analogue binding to the coupled binuclear copper active site in tyrosinase. *J Am Chem Soc* 1985;107:4015–27.
- [38] Rompel A, Fischer H, Meiwes D, Buldt-Karentzopoulos K, Magrini A, Eicken C, et al. Substrate specificity of catechol oxidase from *Lycopus europaeus* and characterization of the bioproducts of enzymic caffeic acid oxidation. *FEBS Lett* 1999;445:103–10.
- [39] Cooksey CJ, Garratt PJ, Land EJ, Pavel S, Ramsden CA, Riley PA, et al. Evidence of the indirect formation of the catecholic intermediate substrate responsible for the autoactivation kinetics of tyrosinase. *J Biol Chem* 1997;272:26226–35.
- [40] Mason H. The chemistry of melanin. VI. Mechanism of the oxidation of catechol by tyrosinase. *J Biol Chem* 1949;181:803–12.
- [41] Land EJ, Ramsden CA, Riley PA. Quinone chemistry and melanogenesis. *Methods Enzymol* 2004;378:88–109.
- [42] Land EJ, Ramsden CA, Riley PA, Yoganathan G. Formation of *para*-quinomethanes via 4-aminobutylcatechol oxidation and *ortho*-quinone tautomerism. *Org Biomol Chem* 2003;1:3120–4.
- [43] Palumbo A, Misuraca G, d'Ischia M, Protá G. Effect of metal ions on the kinetics of tyrosine oxidation catalysed by tyrosinase. *Biochem J* 1985;228:647–51.
- [44] Ros JR, Rodríguez-López JN, García-Cánovas F. Effect of ferrous ions on the monophenolase activity of tyrosinase. *Biochim Biophys Acta* 1993;1163:303–8.
- [45] Sánchez-Ferrer A, Rodríguez-López JN, García-Cánovas F, García-Carmona F. Tyrosinase: a comprehensive review of its mechanism. *Biochimica et Biophysica Acta* 1995;1247:1–11.
- [46] Bowness JM, Morton RA. The association of zinc and other metals with melanin and melanin-protein complex. *Biochem J* 1953;53:620–6.
- [47] Palumbo A, d'Ischia M, Misuraca G, Protá G. Effect of metal ions on the rearrangement of dopachrome. *Biochim Biophys Acta* 1987;925:203–9.
- [48] Palumbo A, d'Ischia M, Misuraca G, Protá G, Schultz TM. Structural modifications in biosynthetic melanins induced by metal ions. *Biochim Biophys Acta* 1988;964:193–9.
- [49] Kalyanaraman B. Characterization of *o*-semiquinone radicals in biological systems. *Methods Enzymol* 1990;186:333–43.

PUBLICATION III

**Crystal structure of an
ascomycete fungal laccase
from *Thielavia arenaria*
– common structural features
of asco-laccases**

In: FEBS Journal 278(2011), pp. 2283–2295.
Copyright 2011 John Wiley and Sons.
Reprinted with permission from the publisher.

Crystal structure of an ascomycete fungal laccase from *Thielavia arenaria* – common structural features of asco-laccases

Juha P. Kallio¹, Chiara Gasparetti², Martina Andberg², Harry Boer², Anu Koivula², Kristiina Kruus², Juha Rouvinen¹ and Nina Hakulinen¹

¹ Department of Chemistry, University of Eastern Finland, Joensuu, Finland

² VTT Technical Research Centre of Finland, Espoo, Finland

Keywords

ascomycete; C-terminal plug; laccase; proton transfer; redox potential

Correspondence

N. Hakulinen, Department of Chemistry, University of Eastern Finland, Joensuu Campus, P.O. Box 111, FIN-80101 Joensuu, Finland

Fax: +358 13 2513390

Tel: +358 13 2513359

E-mail: nina.hakulinen@uef.fi

(Received 8 March 2011, revised 20 April 2011, accepted 27 April 2011)

doi:10.1111/j.1742-4658.2011.08146.x

Laccases are copper-containing enzymes used in various applications, such as textile bleaching. Several crystal structures of laccases from fungi and bacteria are available, but ascomycete types of fungal laccases (asco-laccases) have been rather unexplored, and to date only the crystal structure of *Melanocarpus albomyces* laccase (MaL) has been published. We have now solved the crystal structure of another asco-laccase, from *Thielavia arenaria* (TaLcc1), at 2.5 Å resolution. The loops near the T1 copper, forming the substrate-binding pockets of the two asco-laccases, differ to some extent, and include the amino acid thought to be responsible for catalytic proton transfer, which is Asp in TaLcc1, and Glu in MaL. In addition, the crystal structure of TaLcc1 does not have a chloride attached to the T2 copper, as observed in the crystal structure of MaL. The unique feature of TaLcc1 and MaL as compared with other laccases structures is that, in both structures, the processed C-terminus blocks the T3 solvent channel leading towards the trinuclear centre, suggesting a common functional role for this conserved 'C-terminal plug'. We propose that the asco-laccases utilize the C-terminal carboxylic group in proton transfer processes, as has been suggested for Glu498 in the CotA laccase from *Bacillus subtilis*. The crystal structure of TaLcc1 also shows the formation of a similar weak homodimer, as observed for MaL, that may determine the properties of these asco-laccases at high protein concentrations.

Database

Structural data are available in the Protein Data Bank database under the accession numbers [3PPS](#) and [2VDZ](#)

Structured digital abstract

• [laccase](#) [binds](#) to [laccase](#) by [x-ray crystallography](#) ([View interaction](#))

Introduction

Laccases (benzenediol oxygen oxidoreductases) are enzymes belonging to the group of blue multicopper

oxidases, along with ascorbate oxidases [1], mammalian plasma ceruloplasmin [2], *Escherichia coli* copper

Abbreviations

ABTS, 2,2'-azinobis(3-ethylbenzo-6-thiazolinesulfonic acid); BsL, *Bacillus subtilis* laccase; 2,6-DMP, 2,6-dimethoxyphenol; MaL, *Melanocarpus albomyces* laccase; PDB, Protein Data Bank; RiL, *Rigidoporus lignosus* laccase; rMaL, recombinant *Melanocarpus albomyces* laccase; TaLcc1, *Thielavia arenaria* laccase; ThL, *Trametes hirsuta* laccase; TvL, *Trametes versicolor* laccase.

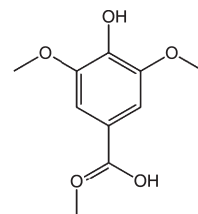
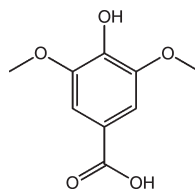
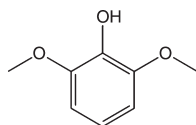
efflux operon, which is involved in copper homeostasis [3], a yeast plasma membrane-bound Fet3p that catalyses iron oxidation [4], and phenoxazinone synthase from *Streptomyces antibioticus* [5]. Laccases are common in fungi, and are also found in some higher plants and bacteria. These enzymes are capable of oxidizing various organic and even inorganic substrates; however, in general, their substrates are phenolic compounds (such as those presented in Table 1). Phenolics are oxidized near the T1 copper to phenoxy radicals, which can then form a large variety of oxidation products by radical reactions. The substrate variety can be increased by the use of redox mediators, such as 2,2'-azinobis(3-ethylbenzo-6-thiazolinesulfonic acid) (ABTS). In addition, direct electron exchange between laccase and, for example, graphite electrodes [6,7] has been reported. The broad substrate range, wide pH optimum and thermostability of some laccases, as well as their use of oxygen as the terminal electron acceptor, mean that these enzymes have great potential for several applications, such as pulp bleaching, textile dye decolorization, delignification, bioremediation, fuel cells, and sensors [8,9].

Laccases have recently been extensively studied by X-ray crystallography. The first complete laccase structures were published in 2002, and crystal structures from at least 10 different organisms have now been reported. Most of the structures are from sporophoral basidiomycota fungi: *Coprinus cinereus* [10], *Trametes versicolor* [11,12], *Rigidoporus lignosus* [13], *Cerrena maxima* [14], *Coriolus zonatus* [15], *Lentinus tigrinus* [16], *Trametes trogii* [17], *Trametes hirsuta* [18], and *Coriolopsis gallica*. Structures of bacterial laccases or multicopper oxidases are also available, including the spore coat protein A from *Bacillus subtilis* [20], a copper efflux operon from *E. coli* [21], and the more recently published novel two-domain laccases [22–24]. The other phylum of the fungi, the Ascomycota or sac fungi, is much less studied, and only the crystal structure of *Melanocarpus albomyces* laccase (MaL) has been solved [25].

The fold of the three-domain laccases is composed of three β -barrel domains that are assembled around two catalytic copper-binding sites (Fig. 1). The active sites are formed by four copper cations, which are divided into three different types – type 1 (T1), type 2 (T2), and type 3 (T3) – by their characteristic spectro-

Table 1. Kinetic parameters for rMaL, TaLcc1, and ThL, measured with 2,6-DMP, syringic acid and methyl syringate in 25 mM succinate buffer at pH 4.5 and in 40 mM Mes buffer at pH 6.0 (25 °C). Structural formulas of the substrates are presented. Redox potentials (E°) of T1 coppers of the laccases and redox potentials of the substrates at pH 4.5 and pH 6.0 are provided, together with the redox potential differences (ΔE°) between the T1 coppers of the laccases and the substrates. ND, not determined.

	2,6-DMP		Syringic acid		Methyl syringate	
	pH 4.5 $E^\circ = 0.53$ V	pH 6 $E^\circ = 0.40$ V	pH 4.5 $E^\circ = 0.57$ V	pH 6 $E^\circ = 0.51$ V	pH 4.5 $E^\circ = 0.69$ V	pH 6 $E^\circ = 0.65$ V
rMaL ($E^\circ = 0.48$ V)						
ΔE° (V)	-0.05	0.08	-0.09	-0.03	-0.21	-0.17
K_m (μ M)	18 \pm 1	9.5 \pm 0.9	122 \pm 11	132 \pm 22	ND	ND
V_{max} (dA min ⁻¹ ·nmol ⁻¹)	126 \pm 2	119 \pm 1	3.5 \pm 0.1	12.1 \pm 0.6	ND	ND
TaLcc1 ($E^\circ = 0.51$ V)						
ΔE° (V)	-0.02	0.11	-0.06	0	-0.18	-0.14
K_m (μ M)	45 \pm 4	5.8 \pm 0.6	128 \pm 4	61 \pm 4	ND	ND
V_{max} (dA min ⁻¹ ·nmol ⁻¹)	99 \pm 2	87 \pm 1	3.5 \pm 0.1	2.7 \pm 0.1	ND	ND
ThL ($E^\circ = 0.78$ V)						
ΔE° (V)	0.25	0.38	0.21	0.27	0.09	0.13
K_m (μ M)	18 \pm 1	6.3 \pm 1.3	35 \pm 6	17 \pm 4	168 \pm 19	50 \pm 16
V_{max} (dA min ⁻¹ ·nmol ⁻¹)	193 \pm 3	91 \pm 2	8.3 \pm 0.4	2.0 \pm 0.1	21 \pm 1	2.6 \pm 0.2



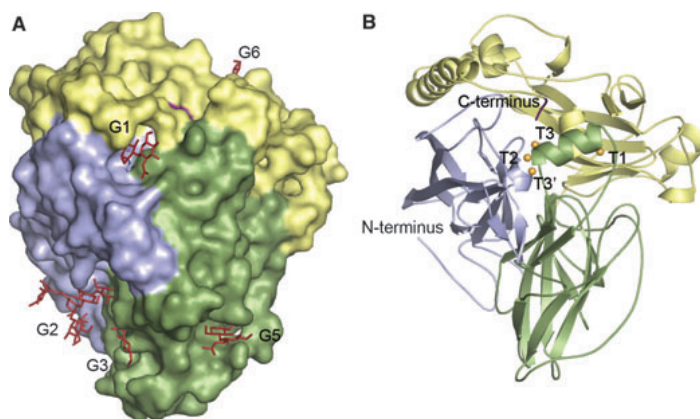


Fig. 1. (A) The crystal structure of TaLcc1 as a surface model. Domain A is presented in blue, domain B in green, and domain C in yellow. The N-glycans are shown as red sticks. Glycans are named as G1 on Asn89, G2 on Asn202, G3 on Asn217, G4 on Asn247 (on the other side of the molecule), G5 on Asn290, and G6 on Asn376. (B) Cartoon representation of TaLcc1. The catalytic coppers are shown in orange, and the C-terminal plug in purple.

scopic features. The T1 copper is responsible for the characteristic blue colour of these enzymes, and has strong absorption at 600 nm. The T1 and T2 coppers are paramagnetic, and can be detected by EPR spectroscopy. The T3 coppers form an antiferromagnetically coupled dinuclear copper–copper pair, and are therefore EPR silent, although these coppers cause absorbance at 330 nm. The loops surrounding the T1 copper form the phenolic substrate-binding site of the enzyme, whereas the T2 and the T3-pair coppers form the trinuclear site that is responsible for binding and reduction of the molecular oxygen. The reduction of oxygen to two water molecules requires the transfer of four electrons [26,27]. The rate-limiting step for the catalysis is apparently the transfer of the first electron from the substrate to the T1 copper in laccase. The suitability of a chemical compound as a laccase substrate depends on two factors. First, the substrate must dock at the T1 copper site, which is mainly determined by the nature and position of substituents on the phenolic ring of the substrate. Second, the redox potential (E°) of the substrate must be low enough, as the rate of the reaction has been shown to depend on the difference between the redox potentials of the enzyme and the substrate (ΔE°) [28–31].

This study presents the crystal structure of a novel laccase (TaLcc1) from the ascomycete fungus *Thielavia arenaria* [32]. The molecular mass of the enzyme is ~ 80 kDa (based on SDS/PAGE), and it shows multiple bands in IEF. The pH optimum is 5.5, but the enzyme retains substantial activity at pH 7. The three-dimensional structure of TaLcc1 shows both similarities to and differences from the analogous structures of the ascomycete laccase (asco-laccase) MaL, thus giving a comprehensive view of the structure and function of asco-laccases.

Results and Discussion

Overall structure

The crystal structure of TaLcc1 was solved to 2.5-Å resolution from pseudomerohedrally twinned crystals by molecular replacement, using the recombinant MaL expressed in *Trichoderma reesei* [rMaL; Protein Data Bank (PDB) code [2Q9O](#)] [33] as a model. The real space group was $P2_1$, and it was mimicking orthorhombic ($\beta = 90.3^\circ$). This led us to the solution with four molecules in an asymmetric unit, with a Matthews coefficient probability of $2.61 \text{ \AA}^3 \cdot \text{Da}^{-1}$ and a solvent content of 52.9%. Interestingly, molecules A and B (and C and D) formed a similar weak dimer as previously reported for rMaL [33]. Thus, the asymmetric unit contained two weak TaLcc1 dimers (Fig. 1).

The crystal structure of TaLcc1 contained 564 amino acids. The overall structure was similar to that of other fungal laccases, especially the only known asco-laccase structure from *M. albomyces* [25]. Protein monomers of the two asco-laccases could be superimposed with an rmsd of 0.65 Å for 558 C α atoms. The fold is composed of three cupredoxin-like domains, called A (1–160), B (161–340), and C (340–564) (Fig. 1A,B), or sometimes referred to in the literature as domains I, II, and III. In TaLcc1, three disulfide bridges located in domain A (Cys5–Cys13), in domain B (Cys298–Cys332) and between domains A and C (Cys115–Cys545) stabilize the fold.

Most laccases are glycoproteins, with typically 3–10 glycosylation sites per monomer, although the functional role of the carbohydrates is not clear. Glycosylation has been suggested to be involved, for example, in the stabilization of the catalytic centre, giving protection against hydrolysis, and improving the

thermostability of the enzyme [34]. On the basis of the sequence of TaLcc1, there are eight putative N-glycosylation sites (Asn89, Asn202, Asn217, Asn247, Asn290, Asn337, Asn376, and Asn396), and carbohydrate residues were found on six of these sites (Asn89, Asn202, Asn217, Asn247, Asn290, and Asn376) in our crystal structure (Fig. 1A). The carbohydrate composition slightly varied between the molecules in the asymmetric unit; however, the glycans attached to Asn89 (G1 in Fig. 1A) and to Asn202 (G2 in Fig. 1A) were consistent in all four molecules. These two glycans seem to have a clear stabilizing effect on the multidomain protein structure. The glycan on Asn89 was located alongside the C-terminal tail between all three domains (Fig. 2A), and had two hydrogen bonds with Ser180 and Asn555. The glycan on Asn202 was in the groove between the β -barrels of domains A and B (Fig. 2B), and had six hydrogen bonds, three to the main chain carbonyls at Asn6, Leu168, and Val170, and three to the side chains of Arg11, Arg71, and Tyr216.

The catalytic centres were arranged in similar way as previously reported for MaL [25]. In the mononuclear centre, the T1 copper was coordinated to two ND1 atoms of His residues. The residues in the axial positions of the mononuclear centre were Leu and Ile. The trinuclear centre had two type 3 coppers (T3 and T3'), each being coordinated to three nitrogen atoms of His residues. The T2 copper was coordinated to two nitrogens of His residues. On the basis of the electron density, we refined one oxygen atom (probably a hydroxide) between the type 3 coppers in molecules B, C and D in the asymmetric unit of the crystal structure. However, the electron density among the coppers in molecule A was stronger than in the other molecules, and had a slightly elliptic shape towards the T2 copper. On the basis of these observations, we decided to refine a dioxygen molecule at this site. Another oxygen atom (most likely a hydroxide or a water molecule) was coordinated to the T2 copper on the opposite side (in the T2 solvent channel). No chloride was observed, even though the purified enzyme was in Tris/HCl buffer. In the crystal structure of MaL/rMaL, a chloride is bound to the T2 copper, whereas in other published laccase crystal structures, an oxygen atom, most likely in a hydroxide ion, is reported to be here.

T2 solvent channel

The water channel leading to the trinuclear centre from the side of the T2 copper, between domains A and C, can be found in all fungal laccases except in in rMaL, where His98 blocks the access. The T2 cavity is

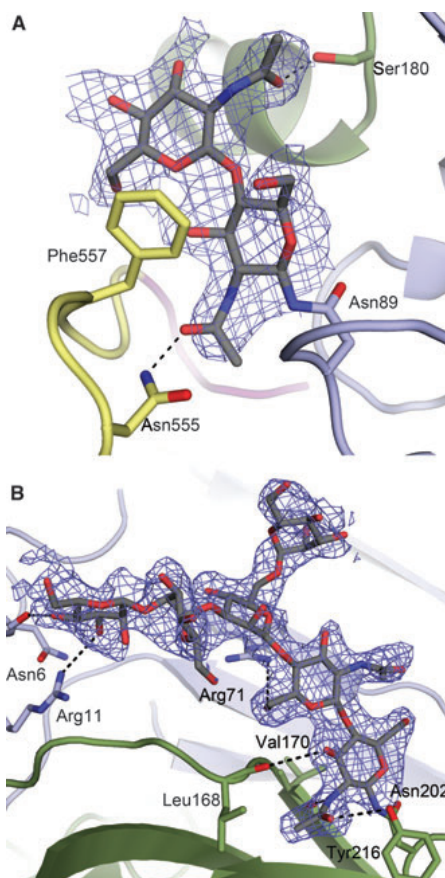


Fig. 2. Stabilizing carbohydrates of TaLcc1. Domain A is presented in blue, domain B in green, and domain C in yellow. (A) The glycan on Asp89 stabilizes the C-terminal tail (marked in purple). (B) The glycan on Asp202 is located on the groove between domain A and domain B. The $2F_o - F_c$ electron density for the carbohydrates is presented in cyan, contoured at 1σ .

surrounded by acidic Asp residues (Fig. 3), which have been suggested to provide the protons required for dioxygen reduction in Fet3p multicopper oxidase [35]. In our TaLcc1 structure, His98 was replaced by Arg99, orientated such that it formed the surface of the solvent channel. Therefore, the access through the channel was unhindered in TaLcc1 (Fig. 3A). It is possible that His98 in rMaL may also rotate to another conformation to open the T2 channel (Fig. 3B). On the basis of protein structure libraries, the 'open conformation' would be the second most favoured conformation. On the other hand, we did not observe any trace of the movements on the His98 residue in our MaL/rMaL

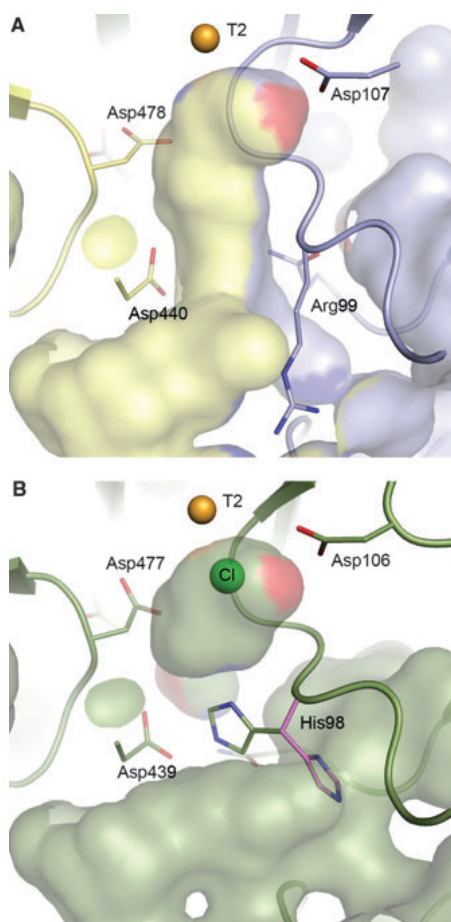


Fig. 3. T2 solvent channels leading into the trinuclear centre of asco-laccases. (A) The open solvent channel in TaLcc1. The cavity is formed between domain A (blue) and domain C (yellow). (B) The closed solvent channel in rMaL. His98 (corresponding to Arg99 in TaLcc1) blocks the solvent channel in rMaL. The putative open conformation of His98 is shown in purple. In the rMaL structure, the chloride is located in the upper cavity.

crystal structures. In our near-atomic crystal structure of rMaL, His98 exists in its oxidized form, possibly because of the oxidative stress [33]. The oxidation of the His residues probably affects its ability to change the side chain conformation, which may have implications for the catalytic function of this laccase.

Role of the C-terminus

In addition to the T2 solvent channel, a so-called T3 solvent channel is generally reported in basidiomycete

laccases. The T3 solvent channel gives the solvent access to the trinuclear centre. However, the channel is blocked by the C-terminal end of the amino acid chain in MaL/rMaL [25,33]. Similarly, in the structure of TaLcc1, the last four amino acids (DSGL) penetrate inside the channel. This is known as a C-terminal plug or a C-terminal tail. On the basis of the crystal structure, the mature TaLcc1 enzyme lacks 40 residues at the N-terminus and 13 residues at the C-terminus as compared with the coded sequence. It has been previously reported that the gene sequence of rMaL codes for 623 residues, but the secreted mature enzyme lacks 50 residues at the N-terminus and 14 residues at the C-terminus [36]. The C-terminal extension containing the last 14 (13 in TaLcc1) residues is post-translationally cleaved, and thus the active forms of both enzymes have DSGL as the last four amino acids penetrating into the channel.

The C-terminal processing has been reported for asco-laccases of different origins [37–39]; furthermore, the C-terminus of the mature asco-laccases is highly conserved, suggesting that the DSGL/V/I plug is most likely a characteristic feature of asco-laccases. Basidiomycete laccases do not generally have this type of C-terminus. However, *R. lignosus* laccase (RIL) [13] has a C-terminal DSGLA sequence. Among the known basidiomycete laccases, RIL is phylogenetically the closest to asco-laccases. Although the last amino acids of RIL are not visible in the crystal structure, it is unlikely that the C-terminus of RIL would be long enough to form such a plug, as the last visible amino acid (Asn494) is located on the surface of the molecule and is rather far away from the trinuclear site. Therefore, the C-terminal sequence of RIL might be more of an evolutionary relic than a functional feature of the enzyme.

The actual role of the C-terminus in asco-laccases has been unclear. However, we have recently shown that a mutation in the C-terminus of rMaL affects both the activity and the stability of the enzyme [40]. The Leu559 → Ala mutation greatly reduced the turnover number for ABTS, whereas the turnover number for the phenolic substrates was not significantly altered. In addition, deletion of the four last amino acids (delDSGL) of rMaL resulted in a practically inactive form of the enzyme [40]. Therefore, it is obvious that the C-terminal amino acids are critical for the function of asco-laccases. Furthermore, the C-terminal extension (the amino acids after the cleavage site) has been shown to affect the secretion process and folding of asco-laccases [41].

Very recently, studies on a CotA laccase from *B. subtilis* (BsL) have provided evidence for Glu498 near the T3 coppers participating in the catalytic

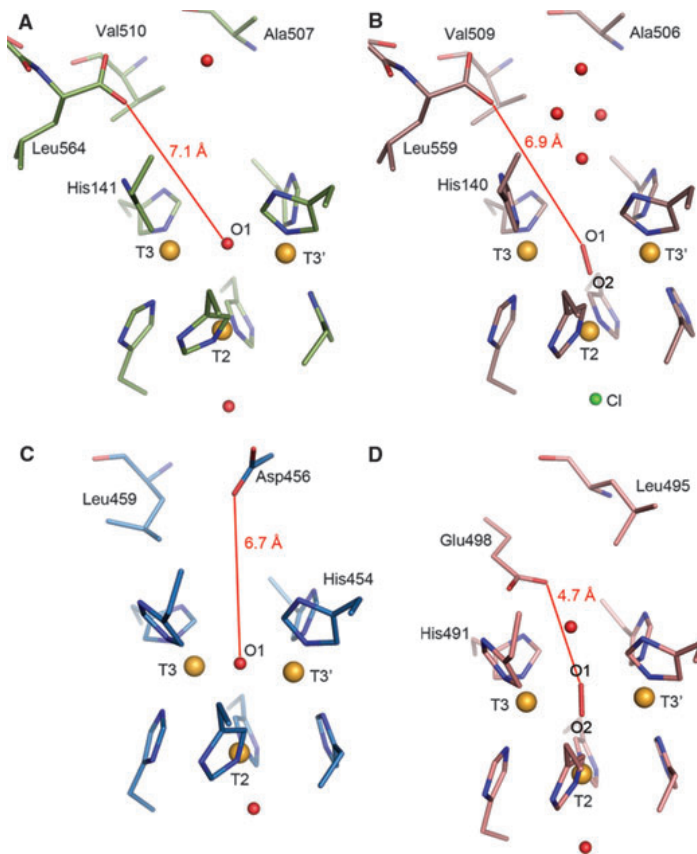


Fig. 4. The trinuclear centres of (A) TaLcc1, (B) rMaL, (C) TvL, and (D) BsL. The distance of the putative catalytic carboxyl group from the oxygen species between the T3 coppers is shown.

function of the enzyme, possibly by promoting proton transfer [42,43]. The fungal laccase structures have no Glu or Asp in this position, but basidiomycete fungal laccases have a conserved Asp in close proximity, i.e. Asp456 in *T. versicolor* laccase. In asco-laccases, the only acidic residue in the T3 solvent cavity that is close enough to assist in the proton transfer is the carboxylate from the C-terminus. The C-terminal carboxylate group of asco-laccases and the conserved Asp of the basidiomycete laccases are both ~ 7 Å from the oxygen species located between the T3 coppers. Glu498 of BsL is 4.7 Å from this oxygen (Fig. 4). It is plausible that asco-laccases use the C-terminal carboxylate group and basidiomycete laccases use the conserved Asp to assist proton transfer for reducing the molecular oxygen. Nevertheless, the continuous flow of protons from the phenolic substrate might come through the so-called SDS gate, which is conserved in asco-laccases but not detected in basidiomycete laccases or the

B. subtilis CotA laccase. The SDS gate is formed by two Ser residues and one Asp residue, and it is thought to be involved in proton transfer from the T1 site to the trinuclear centre [33]. In TaLcc1, Ser143, Ser511 and Asp561 form the SDS gate, which possibly assists the proton flow. Laccases from different organisms might thus have adopted different strategies to facilitate proton transfer for the dioxygen reduction.

Oxidation of phenolic substrates

The substrate-binding pocket of TaLcc1 is similar to that in MaL, but there are clear differences in both the size and the shape of the pocket (Fig. 5A,B). Leu297 in TaLcc1 (Ala297 in MaL) narrows the cavity as compared with MaL, whereas Pro195 and Val428 (Phe194 and Phe427 in MaL) make the cavity in TaLcc1 wider in the other direction. In addition, the loop with Val428 has an additional Ile427 in TaLcc1. This

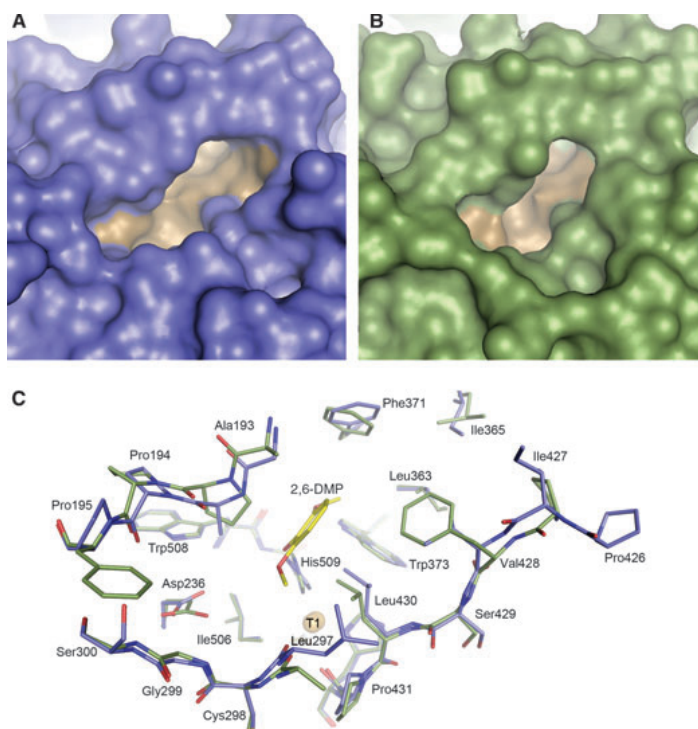


Fig. 5. (A, B) The substrate-binding pockets of (A) TaLcc1 and (B) rMaL. (C) Superimposed amino acids forming the substrate-binding pockets. TaLcc1 is shown in blue, rMaL in green, and 2,6-DMP from the complex structure (PDB code 3FU8) in yellow. The amino acids of TaLcc1 are labelled.

loop resembles ‘the extended jut’ reported in LacB of *Trametes* sp., which was also suggested to be involved in substrate recognition [44].

In TaLcc1, 10 hydrophobic residues (Ala193, Leu297, Leu363, Phe371, Trp373, Ile427, Val428, Leu430, Trp508, and His509) and one hydrophilic residue, Asp236, form the binding pocket. The most evident difference between MaL and TaLcc1 is in this putative catalytic amino acid: TaLcc1 has an Asp236, instead of the Glu235 observed in MaL. Most basidiomycete laccases, such as *T. versicolor*, *L. tigrinus* and *C. cinereus* laccases, have Asp residues here. In the crystal structure of the basidiomycete *T. hirsuta* laccase (PDB code 3FPX), the corresponding residue is an Asn, and it has been suggested that this contributes to the high catalytic constants of *T. hirsuta* [18]. However, the purified laccase from *T. hirsuta* (ThL) (UniProt Knowledgebase accession number Q02497) used in our experiments has an Asp here [45].

In order to understand the oxidation of phenolic compounds in the binding pockets of laccases, the kinetic behaviour of TaLcc1, rMaL and ThL on three phenolic compounds [2,6-dimethoxyphenol (2,6-DMP), syringic acid, and methyl syringate] was studied (Table 1). The dimethoxy phenolic substrates have dif-

ferent *para*-substituents and different redox potentials. On the basis of our crystal structure of rMaL with 2,6-DMP [46], and the *T. versicolor* laccase (TvL) complex structure with 2,5-xylidine [11], the *para*-substituents would point out from the binding pocket and therefore not affect the substrate binding. The rate of laccase-catalysed reactions is thought to increase as the redox potential difference (ΔE°) between the T1 copper and the substrate increases. In TaLcc1, the redox potential of the T1 copper is slightly higher (0.51 V) than that in rMaL (0.48 V), but not as high as in ThL (0.78 V); thus, it would be expected that the kinetic data for TaLcc1 would fit in between the data of rMaL and ThL. However, our kinetic data clearly show that this is not the case, suggesting that the redox potential difference is not the only factor contributing to the rate of substrate oxidation (Table 1).

The kinetics of substrate oxidation by laccases has also been shown to be pH-dependent [47]. At higher pH values, phenolic substrates have lower E° values, whereas E° for the T1 copper of laccases seems to be unaffected by varying pH [28]. As consequence, when ΔE° increases at the higher pH, the reaction rate is increased, but the inhibitory effect of hydroxide also increases. A typical feature of basidiomycete laccases is

their acidic pH optima, whereas asco-laccases generally work in a more neutral range with phenolic compounds [48,49]. Therefore, kinetic studies were carried out at pH 4.5, which is more optimal for ThL, and at pH 6.0, which is, in general, more optimal for TaLcc1 and rMaL (Fig. S1). Because both the pH dependence and the difference in redox potential affect the kinetics of the laccases, we concluded that rMaL and TaLcc1 were able to oxidize syringic acid at pH 6.0, mainly owing to the favourable pH, whereas ThL could oxidize the same substrate, mainly because of the large difference in redox potential. However, the effect of the difference in redox potential outweighs the effect of pH for substrates with high E° , such as methyl syringate. Oxidation of methyl syringate was only possible with the high redox potential ThL, whereas the kinetic parameters for this substrate could not be determined with TaLcc1 or rMaL at either pH value (Table 1).

Interestingly, TaLcc1 showed a lower K_m for 2,6-DMP at pH 6.0 than at pH 4.5 (Table 1). Despite the small difference in redox potentials of the two asco-laccases and their very similar pH optimum profiles, the affinity of TaLcc1 for 2,6-DMP was lower than the affinity of rMaL for the same substrate at pH 4.5. The similar pH profiles and ΔE° values for the two asco-laccases do not explain the three-fold increase in reac-

tion rate of rMaL with syringic acid at pH 6 as compared with pH 4.5. These differences in kinetic behaviour between TaLcc1 and rMaL must therefore be attributable to the variations in several residues forming the binding pocket, most likely Asp236, Ala193 and Val428 observed in TaLcc1 instead of Glu235, Pro192 and Phe427 observed in rMaL. Our mutagenesis studies with MaL have demonstrated that Glu235 \rightarrow Asp mutation of the catalytic residue clearly increases the K_m value for phenolic substrates while not affecting the k_{cat} value. Furthermore, both the K_m and k_{cat} values were clearly affected by the Glu235 \rightarrow Thr mutation, suggesting the importance of the carboxylic group for the catalytic activity [46]. In addition, Phe427 in rMaL (Val428 in TaLcc1) might be involved in placing substrate molecules into the correct orientation for oxidation. In *T. hirsuta*, the loops forming the substrate-binding pocket are completely different, possibly accounting for the clear differences in reaction kinetics between basidiomycete laccases and asco-laccases.

Dimerization

In the TaLcc1 crystal structure, molecules A and B (and C and D) of the asymmetric unit form a weak dimer (Fig. 6). On the basis of calculations performed

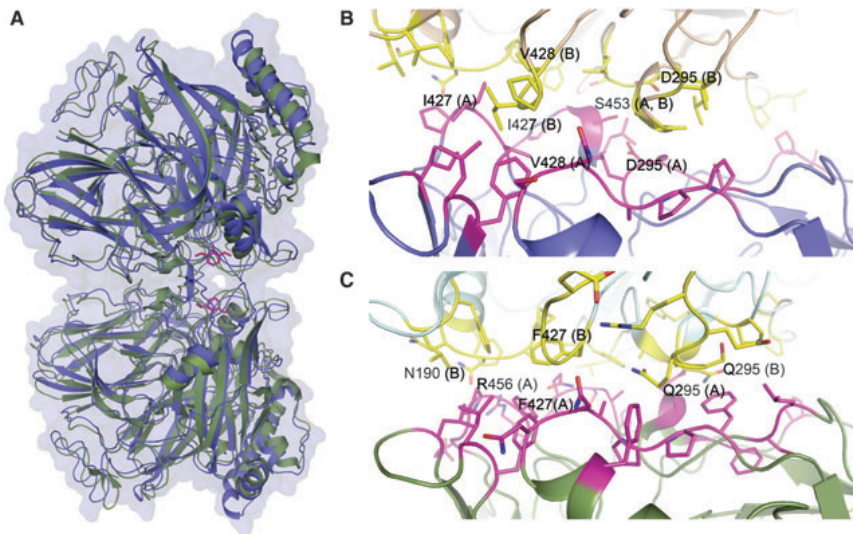


Fig. 6. (A) Cartoon representation of dimers of TaLcc1 (blue) and rMaL (green). 2,6-DMP ligands (purple) are presented as they are in the rMaL complex structure (PDB code 3FU8). A surface representation of TaLcc1 (light blue) shows a small central channel that provides access for the substrates. (B, C) The contact amino acids at the dimeric interface in TaLcc1 (B) and rMaL (C). The residues from molecule A are shown in purple, and those from molecule B in yellow. The hydrogen bonding residues (according to Protein Interfaces, Surfaces and Assemblies) have been labelled, as have the hydrophobic residues with the closest contacts.

with the Protein Interfaces, Surfaces and Assemblies service [50–52], the buried surface area for the weak dimers, AB and CD, is 3.2% (658 Å²) and 3.3% (667 Å²) of the total surface area, respectively. In this weak dimer, the loop areas surrounding the phenolic substrate-binding pockets are packed together (Fig. 6A). Similar dimerization has been reported in the crystal structure of MaL [33]. In MaL, one of the key residues for the dimeric interaction is Phe427, located at the edge of the substrate-binding pocket. This residue might be involved in the orientation or the docking of the substrate molecules. In MaL, the Phe residues from two molecules are packed face-to-face. In TaLcc1, the corresponding loop is longer, and the interacting residues are Ile427 and Val428 (Fig. 6B). As a consequence, the T1–T1 copper distance is slightly longer in TaLcc1 (28 Å) than in MaL (27 Å), and the surface contact area is also slightly smaller (667 Å²) than that on MaL (796 Å² for [2Q9O](#)).

It is possible that the weak dimers of MaL and TaLcc1 are the so-called ‘transient dimers’, which exist in solution as a mixture of monomers and dimers in a concentration-dependent manner [53]. It is noteworthy that the dimeric composition in MaL and TaLcc1 is very similar, suggesting that the ability to form dimers may have functional meaning. Interestingly, the two substrate-binding sites are packed against each other, and there is a shared cavity in the interface of the dimer. This cavity is enclosed in the MaL structure, whereas in the TaLcc1 structure there is a clear solvent channel in the interface between protein molecules that provides free access of the substrate molecules to the binding sites (Fig. 6A). However, the cavity itself is more compact in TaLcc1 than in MaL, owing to the loop containing Ile427 and Val428. The other narrow solvent channel reported earlier for rMaL is also visible in TaLcc1 [46]. The observed dimer in the crystalline state favours smaller phenolic substrates without large substituents in the *para*-position. The docking simulations based on the crystal structure for TaLcc1 reveal that substrates with large groups at the *para*-position clash with the loop containing Ile427 and Leu428. The corresponding loop is shorter in MaL, and the cavity is also more spacious.

Industrial utilization

Laccases have wide reaction capabilities and possess great biotechnological potential, because of their broad substrate specificity. Laccases can be utilized in many industrial applications, including biopulping, textile

dye bleaching, bioremediation, biological fuel cells, and sensors. The stability and activity over broad pH and temperature ranges are desired properties for industrial enzymes. With respect to industrial applications, the ascomycete fungal laccase TaLcc1 is an efficient enzyme, particularly in denim bleaching, even at high temperatures and at neutral pH [32].

In general, asco-laccases possess a wider optimal pH range than basidiomycete laccases; however, the catalytic ability of asco-laccases in less acidic conditions has not yet been fully clarified on the basis of the available laccase structures. It could be that the adaptation of slightly different methods for proton transfer in asco-laccases and basidiomycete laccases (and in bacterial laccases) is responsible for the differences in the pH optimum range of laccases. In addition, the trinuclear site in asco-laccases is more protected, owing to the C-terminal plug; this might reduce the effect of hydroxide inhibition. Both TaLcc1 and MaL are also rather thermostable as compared with many other laccases. The stabilization of both the N-termini and C-termini of TaLcc1 and MaL might be a reason for the higher thermal stability. The extended C-terminus of asco-laccases is buried inside the solvent channel, and the extended N-terminus is stabilized by an additional disulfide bridge. In addition, both termini interact with carbohydrates bound to the protein structure.

Asco-laccases typically have middle redox potentials (TaLcc1, 0.51 V), whereas many basidiomycete laccases have very high redox potentials (ThL, 0.78 V), resulting in enhanced oxidation power. In the future, rational design methods could be used for tuning the redox potential of asco-laccases, or to increase the stability and the optimal pH range of high redox potential basidiomycete laccases. However, more studies are needed to understand how the enzyme structure contributes to the industrially desired properties.

Experimental procedures

Purification

TaLcc1 was produced at Roal Oy (Rajamäki, Finland), with *Tr. reesei* as host [32]. The culture supernatant was concentrated, buffer-exchanged, applied to a weak anion exchange column (DEAE Sepharose FF) in 5 mM Tris/HCl buffer (pH 8.5), and eluted with a linear 0–100 mM sodium sulfate gradient. Active fractions were pooled on the basis of ABTS activity, and were concentrated and desalted (Vivaspin, MWCO 10 000 Da). Typically, the laccase was further purified with a high-resolution anion exchange column (Resource Q) pre-equilibrated in 5 mM Tris/HCl

buffer (pH 8.5). The bound proteins were eluted with a linear sodium sulfate gradient (0–100 mM). Active fractions were eluted at sodium sulfate concentrations between 5 and 40 mM, and concentrated. Subsequently, the buffer was changed to Tris/HCl (20 mM, pH 7.2). The protein yield from the purification was 6%, and the purification factor was 1.5.

MaL was overproduced in *Tr. reesei*, and purified basically as described previously [54]. ThL, assigned with UniProt Knowledgebase accession number Q02497 [45], was produced in its native host and purified in two chromatographic steps, as described previously [55].

Crystallization

TaLcc1 was crystallized at room temperature with the hanging drop vapour diffusion method. Two microlitres of protein solution at a concentration of 9 mg mL⁻¹ and 2 μL of crystallization solution were equilibrated against 500 μL of reservoir solution. Initial screens were made with Crystal Screen I by Hampton Research. Optimization of the molecular weight of poly(ethylene glycol) and its concentration, together with pH, led us to the final crystallization condition of 7.5% poly(ethylene glycol) 3350, 0.2 M ammonium sulfate, and 0.1 M sodium acetate (pH 4.4). The streak seeding method with an equilibration time of ~ 10 h was used to obtain better-quality crystals. The crystals grew as thin plates, which made them difficult to handle. The crystals were approximately 0.3–1 mm long and 0.15–0.5 mm wide, and the thickness of the crystals was always under 0.1 mm.

Data collection and structure refinement

Before data collection, TaLcc1 crystals were quickly soaked in a cryoprotectant solution containing the reservoir solution with 25% glycerol. The crystal was then picked up with nylon loops and flash-frozen in liquid nitrogen. Data were collected at 100 K with synchrotron radiation at the European Synchrotron Radiation Facility (Grenoble) on beamline ID14-1, using an ADSC Q210 charge-coupled device detector. The data were indexed and integrated in MOSFLM [56], and scaled to 2.5-Å resolution in SCALA [57] from CCP4 [58]. The structure factors were created with TRUNCATE [59] from CCP4. A summary of the processing statistics is given in Table 2. The rather high R_{merge} might be attributable to twinning or, additionally, to anisotropic diffraction patterns of the crystal.

The data were analysed with XTRIAGE from the PHENIX package [60]. The suggested lattice was monoclinic, but the highest possible lattice seemed to be orthorhombic. The multivariate *L*-tests strongly indicated that the data were twinned. The *Z*-score was 10.9, whereas the value should be under 3.5 for good-quality to reasonable-quality data. The twin operator for this case was (*h*, -*k*, -*l*), and the estimated twin fraction was about 0.3 (Table 2). In addition, we

Table 2. Summary of processing and refinement statistics. Values in parentheses are for highest-resolution shells. $R_{\text{merge}} = \sum_h \sum_l |M_{hl} - \langle I_h \rangle| / \sum_h \sum_l \langle I_h \rangle$. $R_{\text{pim}} = \sum_h (1/n_h - 1)^{1/2} \sum_l |M_{hl} - \langle I_h \rangle| / \sum_h \sum_l \langle I_h \rangle$.

Data collection	
Wavelength (Å)	0.934
No. of images	360
Crystal–detector distance (mm)	239.3
Oscillation range (°)	0.5
Space group	P2 ₁
Unit cell	<i>a</i> = 61.3, <i>b</i> = 178.9, 118.1, <i>b</i> = 90.3
Resolution range (Å)	42.6–2.5 (2.6–2.5)
No. of reflections	334 560 (49 270)
No. of unique reflections	87 766 (12 787)
Completeness (%)	99.9 (99.9)
<i>I</i> /σ (<i>I</i>)	5.8 (2.9)
Multiplicity	3.8 (3.9)
R_{merge}	25.8 (44.1)
R_{pim}	15.3 (26.0)
Analysis	
Statistics independent of twin laws	
< <i>I</i> ² > / < <i>I</i> > ²	1.99
< <i>F</i> ² > / < <i>F</i> > ²	0.83
< <i>E</i> ² -1 >	0.67
< <i>L</i> >, < <i>L</i> ² >	0.38, 0.20
<i>Z</i> -score <i>L</i> -test	10.9
Twin fraction estimated	0.30
Twin law	<i>h</i> , - <i>k</i> , - <i>l</i>
Refined twin fraction	0.36
Refinement	
R_{work}	18.1
R_{free}	22.4
rmsd bond length from ideal (Å)	0.009
rmsd bond angles from ideal (°)	1.053
Ramachandran plot	
Favoured (%)	92.9
Allowed (%)	7.0
Outlier (%)	0.1

also noticed a rather large off-origin peak, indicating some pseudotranslational symmetry that is most likely involved in the twinning with noncrystallographic symmetry.

The structure was solved by molecular replacement with the rMaL structure (75% sequence identity) as a model. Molecular replacement was performed with PHASER [61] from the CCP4 package and the rMaL (PDB code [2Q90](#)) coordinates as a model. Only in space group P2₁ were rotation and translation solutions found that showed reasonable crystal packing. The *R*-values for the first round of refinement were *R* = 26.7% and R_{free} = 34.9%. When a twin operator was included, *R*-value and R_{free} -value were decreased to 19.2% and 25.2%, respectively. Refinement of the model and twin fraction were carried out with PHENIX, and model building in COOT [62]. The final *R*-values after the refinement were *R* = 18.1% and R_{free} = 22.4%, and the twin fraction was refined to 0.36. Despite the twinning,

a surprisingly good-quality and continuous electron density map was observed. Noncrystallographic symmetry restraints were used during the refinement, and we also tried to release them, but this resulted in high *B*-factors for atoms in molecules C and D. Validation was performed with SFCHECK [63] from the CCP4 package, with 92.9% of all residues being in the most favourable region of the Ramachandran plot (Table 2).

Kinetic data

Kinetic constants (K_m and V_{max}) for rMaL, TaLcc1 and ThL were determined on 2,6-DMP, syringic acid, and methyl syringate, at both pH 4.5 and pH 6.0, in 25 mM succinate buffer and 40 mM Mes buffer, respectively (Table 1). Kinetic measurements were performed in microtitre plates with a Varioskan kinetic plate reader (Thermo Electron Corporation, Waltham, MA, USA). The reactions were started by addition of substrate, and the rate of substrate oxidation was measured by monitoring the change in absorbance over 5 min. All of the measurements were performed in duplicate, with eight substrate concentrations (0.008–1.333 mM for 2,6-DMP and syringic acid; 0.008–2.800 mM for methyl syringate). The kinetic parameters were obtained by curve-fitting analysis with GRAPHPAD PRISM 4.01 (GraphPad Software). The pH optima of the three laccases were measured, with a substrate concentration of 1.7 mM, for 2,6-DMP, syringic acid and methyl syringate in McIlvaine's buffer system at pH levels ranging from 2 to 8.

Acknowledgements

We are grateful to M. Paloheimo from Roal Oy for providing us with samples of TaLcc1. The ESRF is thanked for provision of synchrotron facilities. We also thank the staff members at beamline ID14-1 for their skilled assistance, and B. Hillebrant-Chellaoui at VTT for skilful help with the TaLcc1 purification. Roal Oy and the Academy of Finland (Project 115085) supported the work at Joensuu, and part of the VTT work was carried out with financial support from the Marie Curie EU-project 'Enzymatic tailoring of protein interactions and functionalities in food matrix', PRO-ENZ (MEST-CT-2005-020924), and from the National Technology Agency of Finland, Tekes project 40522/02.

References

- Messerschmidt A, Ladenstein R & Huber R (1992) Refined crystal structure of ascorbate oxidase at 1.9 Å resolution. *J Mol Biol* **224**, 179–205.
- Lindley PF, Card G, Zaitseva I, Zaitsev V, Reinhammar B, Selin-Lindgren B & Yoshida K (1997) An X-ray structural study of human ceruloplasmin in relation to ferroxidase activity. *J Biol Inorg Chem* **2**, 454–463.
- Roberts SA, Wildner GF, Grass G, Weichsel A, Ambrus A, Rensing C & Montfort WR (2003) A labile regulatory copper ion lies near the T1 copper site in the multicopper oxidase CueO. *J Biol Chem* **278**, 31958–31963.
- Taylor A, Stoj CS, Ziegler L, Kosman DJ & Hart J (2005) The copper–iron connection in biology: structure of a metallo-oxidase Fet3p. *Proc Natl Acad Sci USA* **102**, 15459–15464.
- Smith AW, Camara-Artigas A, Wang M, Allen JP & Francisco WA (2006) Structure of phenoxazinone synthase from *Streptomyces antibioticus* reveals a new type 2 copper center. *Biochemistry* **45**, 4378–4387.
- Thuesen MH, Farver O, Reinhammar B & Ulstrup J (1998) Cyclic voltammetry and electrocatalysis of the blue copper oxidase *Polyporus versicolor* laccase. *Acta Chem Scand* **52**, 555–562.
- Blanford CF, Heath RS & Armstrong FA (2007) A stable electrode for high-potential, electrocatalytic O₂ reduction based on rational attachment of a blue copper oxidase to a graphite surface. *Chem Commun* **17**, 1710–1712.
- Xu F (2005) Applications of oxidoreductases: recent progress. *Ind Biotechnol* **1**, 38–50.
- Rodríguez Couto S & Toca Herrera JL (2006) Industrial and biotechnological applications of laccases: a review. *Biotechnol Adv* **24**, 500–513.
- Ducros V, Brzozowski AM, Wilson KS, Brown SH, Ostergaard P, Schneider P, Yaver DS, Pedersen AH & Davies GJ (1998) Crystal structure of the type-2 Cu depleted laccase from *Coprinus cinereus* at 2.2 Å resolution. *Nat Struct Biol* **5**, 310–316.
- Bertrand T, Jolivald C, Briozzo P, Caminade E, Joly N, Madzak C & Mougin C (2002) Crystal structure of a four-copper laccase complexed with an arylamine: insights into substrate recognition and correlation with kinetics. *Biochemistry* **41**, 7325–7333.
- Piontek K, Antorini M & Choinowski T (2002) Crystal structure of a laccase from the fungus *Trametes versicolor* at 1.90 Å resolution containing a full complement of coppers. *J Biol Chem* **277**, 37663–37669.
- Garavaglia S, Cambria MT, Miglio M, Ragusa S, Iacobazzi V, Palmieri F, D'Ambrosio C, Scaloni A & Rizzi M (2004) The structure of *Rigidoporus lignosus* laccase containing a full complement of copper ions, reveals an asymmetrical arrangement for the T3 copper pair. *J Mol Biol* **342**, 1519–1531.
- Lyashenko AV, Bento I, Zaitsev VN, Zhukhlistova NE, Zhukova YN, Gabdoulkhakov AG, Morgunova EY, Voelter W, Kachalova GS, Stepanova EV *et al.* (2006) X-ray structural studies of the fungal laccase from *Cerrena maxima*. *J Biol Inorg Chem* **11**, 963–973.

- 15 Lyashenko AV, Zhukova Y, Zhukhlistova N, Zaitsev V, Stepanova E, Kachalova G, Koroleva O, Voelter W, Betzel C, Tishkov V *et al.* (2006) Three-dimensional structure of laccase from *Coriolus zonatus* at 2.6 Å resolution. *Crystallogr Rep* **51**, 817–823.
- 16 Ferraroni M, Myasoedova NM, Schmatchenko V, Leontievsky AA, Golovleva LA, Scozzafava A & Briganti F (2007) Crystal structure of a blue laccase from *Lentinus tigrinus*: evidences for intermediates in the molecular oxygen reductive splitting by multicopper oxidases. *BMC Struct Biol* **7**, 60, doi:10.1186/1472-6807-7-6.
- 17 Matera I, Gullotto A, Tilli S, Ferraroni M, Scozzafava A & Briganti F (2008) Crystal structure of the blue multicopper oxidase from the whiterot fungus *Trametes trogii* complexed with p-toluolate. *Inorg Chim Acta* **361**, 4129–4137.
- 18 Polyakov KM, Fedorova TV, Stepanova EV, Cherkashin EA, Kurzeev SA, Strokopytov BV, Lamzin VS & Koroleva OV (2009) Structure of native laccase from *Trametes hirsuta* at 1.8 Å resolution. *Acta Crystallogr D* **65**, 611–617.
- 19 Reference withdrawn
- 20 Enguita FJ, Marçal D, Martins LO, Grenha R, Henriques AO, Lindley PF & Carrondo MA (2004) Substrate and dioxygen binding to the endospore coat laccase from *Bacillus subtilis*. *J Biol Chem* **279**, 23472–23476.
- 21 Li X, Wei Z, Zhang M, Peng X, Yu G, Teng M & Gong W (2007) Crystal structures of *E. coli* laccase CueO at different copper concentrations. *Biochem Biophys Res Commun* **354**, 21–26.
- 22 Komori H, Miyazaki K & Higuchi Y (2009) X-ray structure of a two-domain type laccase: a missing link in the evolution of multi-copper proteins. *FEBS Lett* **583**, 1189–1195.
- 23 Lawton TJ, Sayavedra-Soto LA, Arp DJ & Rosenzweig AC (2009) Crystal structure of a two-domain multicopper oxidase: implications for the evolution of multicopper blue proteins. *J Biol Chem* **284**, 10174–10180.
- 24 Skálová T, Dohnálek J, Østergaard LH, Østergaard PR, Kolenko P, Dusková J, Štěpánková A & Hasek J (2009) The structure of the small laccase from *Streptomyces coelicolor* reveals a link between laccases and nitrite reductases. *J Mol Biol* **385**, 1165–1178.
- 25 Hakulinen N, Kiiskinen L-L, Kruus K, Saloheimo M, Paananen A, Koivula A & Rouvinen J (2002) Crystal structure of a laccase from *Melanocarpus albomyces* with an intact trinuclear site. *Nat Struct Biol* **9**, 601–605.
- 26 Solomon EI, Sundaram UM & Machonkin TE (1996) Multicopper oxidases and oxygenases. *Chem Rev* **96**, 2563–2606.
- 27 Solomon EI, Chen P, Metz M, Lee S-K & Palmer AE (2001) Oxygen binding, activation, and reduction to water by copper enzymes. *Angew Chem Int Ed* **40**, 4570–4590.
- 28 Xu F (1996) Oxidation of phenols, anilines, and benzenethiols by fungal laccases: correlation between activity and redox potentials as well as halide inhibition. *Biochemistry* **35**, 7608–7614.
- 29 Xu F, Shin W, Brown SH, Wahleithner JA, Sundaram UM & Solomon EI (1996) A study of a series of recombinant fungal laccases and bilirubin oxidase that exhibit significant differences in redox potential, substrate specificity, and stability. *Biochim Biophys Acta Protein Struct Mol Enzymol* **1292**, 303–311.
- 30 Xu F, Kulus JJ, Cuke K, Li K, Kristopaitis K, Deussen HW, Abbate E, Galinyte V & Schneider P (2000) Redox chemistry in laccase-catalyzed oxidation of N-hydroxy compounds. *Appl Environ Microbiol* **66**, 2052–2056.
- 31 Xu F, Deussen HW, Lopez B, Lam L & Li K (2001) Enzymatic and electrochemical oxidation of N-hydroxy compounds: redox potential, electron transfer kinetics, and radical stability. *Eur J Biochem* **268**, 4169–4176.
- 32 Paloheimo M, Valtakari L, Puranen T, Kruus K, Kallio J, Mäntylä A, Fagerström R, Ojapalo P & Vehmaanperä J (2006) Novel laccase enzyme and use thereof. European patent application WO/2006/032723.
- 33 Hakulinen N, Andberg M, Kallio J, Koivula A, Kruus K & Rouvinen J (2008) A near atomic resolution structure of a *Melanocarpus albomyces* laccase. *J Struct Biol* **162**, 29–39.
- 34 Rodger CJ, Blanford CF, Giddens SR, Skamnioti P, Armstrong FA & Gurr SJ (2010) Designer laccases: a vogue for high-potential fungal enzymes? *Trends Biotechnol* **28**, 63–72.
- 35 Quintanar L, Stoj C, Wang T-P, Kosman DJ & Solomon EI (2005) Role of aspartate 94 in the decay of the peroxide intermediate in the multicopper oxidase Fet3p. *Biochemistry* **44**, 6081–6091.
- 36 Kiiskinen L-L & Saloheimo M (2004) Molecular cloning and expression in *Saccharomyces cerevisiae* of a laccase gene from the ascomycete *Melanocarpus albomyces*. *Appl Environ Microbiol* **70**, 137–144.
- 37 Germann U, Muller G, Hunziker P & Lerch K (1988) Characterization of two allelic forms of *Neurospora crassa* laccase. Amino- and carboxyl-terminal processing of a precursor. *J Biol Chem* **263**, 885–896.
- 38 Fernandez-Larrea J & Stahl U (1996) Isolation and characterization of a laccase gene from *Podospora anserina*. *Mol Gen Genet* **252**, 539–551.
- 39 Bulter T, Alcalde M, Sieber V, Meinhold P, Schlachtbauer C & Arnold FH (2003) Functional expression of a fungal laccase in *Saccharomyces cerevisiae* by directed evolution. *Appl Environ Microbiol* **69**, 987–995.
- 40 Andberg M, Hakulinen N, Auer S, Saloheimo M, Koivula A, Rouvinen J & Kruus K (2009) Essential role of the C-terminus in *Melanocarpus albomyces* laccase for enzyme production, catalytic properties and structure. *FEBS J* **276**, 6285–6300.

- 41 Zumárraga M, Camarero S, Shleev S, Martínez-Arias A, Ballesteros A, Plou FJ & Alcalde M (2008) Altering the laccase functionality by in vivo assembly of mutant libraries with different mutational spectra. *Proteins* **71**, 250–260.
- 42 Chen Z, Durão P, Silva CS, Pereira MM, Todorovic S, Hildebrandt P, Bento I, Lindley PF & Martins LO (2010) The role of Glu⁴⁹⁸ in the dioxygen reactivity of CotA-laccase from *Bacillus subtilis*. *Dalton Trans* **39**, 2875–2882.
- 43 Bento I, Silva CS, Chen Z, Martins LO, Lindley PF & Soares CM (2010) Mechanisms underlying dioxygen reduction in laccases. Structural and modelling studies focusing on proton transfer. *BMC Struct Biol* **10**, 28, doi:10.1186/1472-6807-10-28.
- 44 Ge H, Gao Y, Hong Y, Zhang M, Xiao Y, Teng M & Niu L (2010) Structure of native laccase B from *Trametes* sp. AH28-2. *Acta Crystallogr F* **66**, 254–258.
- 45 Frascioni M, Favero G, Boer H, Koivula A & Mazzei F (2010) Bio-electrochemical characterisation of high and low redox potential laccases from fungal and plant origin. *Biochim Biophys Acta Proteins Proteom* **1804**, 899–908.
- 46 Kallio JP, Auer S, Jänis J, Andberg M, Kruus K, Rouvinen J, Koivula A & Hakulinen N (2009) Structure–function studies of a *Melanocarpus albomyces* laccase suggest a pathway for oxidation of phenolic compounds. *J Mol Biol* **392**, 895–909.
- 47 Xu F (1997) Effects of redox potential and hydroxide inhibition on the pH activity profile of fungal laccases. *J Biol Chem* **272**, 924–928.
- 48 Kiiskinen L-L, Viikari L & Kruus K (2002) Purification and characterization of a novel laccase from the ascomycete *Melanocarpus albomyces*. *Appl Microbiol Biotechnol* **59**, 198–204.
- 49 Chakroun H, Mechichi T, Martinez MJ, Dhoubi A & Sayadi S (2010) Purification and characterization of a novel laccase from the ascomycete *Trichoderma atroviride*: application on bioremediation of phenolic compounds. *Process Biochem* **45**, 507–513.
- 50 Krissinel E & Henrick K (2005) Detection of protein assemblies in crystals. In *Lecture Notes in Computer Science* (Berthold MR ed), pp 163–174. Springer-Verlag, Berlin.
- 51 Krissinel E & Henrick K (2007) Inference of macromolecular assemblies from crystalline state. *J Mol Biol* **372**, 774–797.
- 52 Krissinel E (2009) Crystal contacts as nature's docking solutions. *J Comput Chem* **31**, 133–143.
- 53 Nooren MA & Thornton JM (2003) Structural characterization and functional significance of transient protein–protein interactions. *J Mol Biol* **325**, 991–1018.
- 54 Kiiskinen L-L, Kruus K, Bailey M, Ylosmaki E, Siikaho M & Saloheimo M (2004) Expression of *Melanocarpus albomyces* laccase in *Trichoderma reesei* and characterization of the purified enzyme. *Microbiology* **150**, 3065–3074.
- 55 Rittstieg K, Suurnäkki A, Suortti T, Kruus K, Guebitz G & Buchert J (2002) Investigations on the laccase-catalyzed polymerization of lignin model compounds using size-exclusion HPLC. *Enzyme Microbiol Technol* **31**, 403–410.
- 56 Leslie AGW (1992) Joint CCP4+ ESF-EAMCB. *Newslett Protein Crystallogr* **26**, 27–33.
- 57 Weiss M (2001) Global indicators of X-ray data quality. *J Appl Crystallogr* **34**, 130–135.
- 58 Collaborative Computational Project, Number 4 (1994) The CCP4 Suite: programs for protein crystallography. *Acta Crystallogr D* **50**, 760–763.
- 59 French GS & Wilson KS (1978) On the treatment of negative intensity observations. *Acta Crystallogr A* **34**, 517–525.
- 60 Adams PD, Grosse-Kunstleve RW, Hung L-W, Ioerger TR, McCoy AJ & Moriarty NW (2002) PHENIX: building new software for automated crystallographic structure determination. *Acta Crystallogr D* **58**, 1948–1954.
- 61 McCoy AJ, Grosse-Kunstleve RW, Adams PD, Winn MD, Storoni LC & Read RJ (2007) Phaser crystallographic software. *J Appl Crystallogr* **40**, 658–674.
- 62 Emsley P, Lohkamp B, Scott WG & Cowtan K (2010) Features and development of Coot. *Acta Crystallogr D* **66**, 486–501.
- 63 Vaguine AA, Richelle J & Wodak SJ (1999) SFCHECK: a unified set of procedures for evaluating the quality of macromolecular structure-factor data and their agreement with the atomic model. *Acta Crystallogr D* **55**, 191–205.

Supporting information

The following supplementary material is available:

Fig. S1. The pH activity profiles of rMaL, TaL and ThL for 1.7 mM 2,6-DMP, syringic acid and methyl syringate.

This supplementary material can be found in the online version of this article.

Please note: As a service to our authors and readers, this journal provides supporting information supplied by the authors. Such materials are peer-reviewed and may be re-organized for online delivery, but are not copy-edited or typeset. Technical support issues arising from supporting information (other than missing files) should be addressed to the authors.

PUBLICATION IV

**Extracellular tyrosinase from
the fungus *Trichoderma reesei*
shows product inhibition and
different inhibition mechanism
from the intracellular
tyrosinase from *Agaricus
bisporus***

In: BBA – Proteins and Proteomics 1824(2012),
pp. 598–607.

Copyright 2012 Elsevier.

Reprinted with permission from the publisher.



Extracellular tyrosinase from the fungus *Trichoderma reesei* shows product inhibition and different inhibition mechanism from the intracellular tyrosinase from *Agaricus bisporus*

Chiara Gasparetti ^{a,*}, Emilia Nordlund ^a, Janne Jänis ^b, Johanna Buchert ^a, Kristiina Kruus ^a

^a VTT Technical Research Centre of Finland P.O. Box 1000, Espoo FIN-02044 VTT, Finland

^b Department of Chemistry, University of Eastern Finland, P.O. Box 111, Joensuu FIN-80101, Finland

ARTICLE INFO

Article history:

Received 28 October 2011

Received in revised form 20 December 2011

Accepted 23 December 2011

Available online 14 January 2012

Keywords:

Tyrosinase

Trichoderma reesei

Agaricus bisporus

End product inhibition

Dopachrome

K_i

ABSTRACT

Tyrosinase (EC 1.14.18.1) is a widely distributed type 3 copper enzyme participating in essential biological functions. Tyrosinases are potential biotools as biosensors or protein crosslinkers. Understanding the reaction mechanism of tyrosinases is fundamental for developing tyrosinase-based applications. The reaction mechanisms of tyrosinases from *Trichoderma reesei* (TrT) and *Agaricus bisporus* (AbT) were analyzed using three diphenolic substrates: caffeic acid, L-DOPA (3,4-dihydroxy-L-phenylalanine), and catechol. With caffeic acid the oxidation rates of TrT and AbT were comparable; whereas with L-DOPA or catechol a fast decrease in the oxidation rates was observed in the TrT-catalyzed reactions only, suggesting end product inhibition of TrT. Dopachrome was the only reaction end product formed by TrT- or AbT-catalyzed oxidation of L-DOPA. We produced dopachrome by AbT-catalyzed oxidation of L-DOPA and analyzed the TrT end product (i.e. dopachrome) inhibition by oxygen consumption measurement. In the presence of 1.5 mM dopachrome the oxygen consumption rate of TrT on 8 mM L-DOPA was halved. The type of inhibition of potential inhibitors for TrT was studied using *p*-coumaric acid (monophenol) and caffeic acid (diphenol) as substrates. The strongest inhibitors were potassium cyanide for the TrT-monophenolase activity, and kojic acid for the TrT-diphenolase activity. The lag period related to the TrT-catalyzed oxidation of monophenol was prolonged by kojic acid, sodium azide and arbutin; contrary it was reduced by potassium cyanide. Furthermore, sodium azide slowed down the initial oxidation rate of TrT- and AbT-catalyzed oxidation of L-DOPA or catechol, but it also formed adducts with the reaction end products, i.e., dopachrome and *o*-benzoquinone.

© 2012 Elsevier B.V. All rights reserved.

1. Introduction

Tyrosinases (EC 1.14.18.1) belong to type 3 copper proteins, which also include catechol oxidases (EC 1.10.3.1) and oxygen carrier proteins hemocyanins [1]. Tyrosinase catalyzes the *o*-hydroxylation of monophenols and the subsequent oxidation to quinones (cresolase or monophenolase activity). Tyrosinase also catalyzes the direct oxidation of *o*-diphenols to quinones (catecholase or diphenolase activity), which are colorful and highly reactive compounds [1,2]. Tyrosinases exist widely in plants, animals, fungi and bacteria. Tyrosinases are involved in many biologically essential functions such as biosynthesis of melanin pigments, sclerotization, primary immune response and host defense [3–9]. The best characterized tyrosinases are derived from species of *Streptomyces* bacteria, and from the fungi *Neurospora crassa* and *Agaricus bisporus* [2,10–16]. At today, the intracellular enzyme from *A. bisporus* is the only tyrosinase commercially available. *A. bisporus*

tyrosinase is highly homologous to the mammalian tyrosinases, thus it has been used as a model in most of the studies on melanogenesis [17]. The binuclear active site of tyrosinase consists of two copper ions, coordinated each by three highly conserved histidines [2]. The active site of tyrosinase exists in three forms: *oxy*-, *met*- and *deoxy*-form [18]. Both *met*- and *oxy*-forms show a diphenolase activity, whereas only the *oxy*-form shows a monophenolase activity [11,19]. The *deoxy*-form is a reduced and an instable form and binds oxygen to give the *oxy*-form [20–22]. Tyrosinase can accept a wide range of *p*-substituted monophenolic and diphenolic substrates. Among them, *L*-tyrosine and L-DOPA (3,4-dihydroxy-L-phenylalanine) are the natural precursors of melanins. The direct product of a tyrosinase-catalyzed reaction on *L*-tyrosine or L-DOPA is dopaquinone (Fig. 1). In the absence of sulphhydryl residues dopaquinone undergoes an intramolecular addition of an amino group to produce leukodopachrome, known also as cyclodopa. A redox reaction between leukodopachrome and dopaquinone forms L-DOPA and dopachrome [23–25]. The spontaneous non-enzymatic reactions yielding to the formation of dopachrome are fast, and tyrosinase activity can be measured spectrophotometrically by following the formation of the product dopachrome at 475 nm. Dopachrome is a relatively stable orange–red intermediate and is the final

* Corresponding author. Tel.: +358 40 849 1073; fax: +358 20 722 7071.

E-mail addresses: ext-Chiara.Gasparetti@vtt.fi (C. Gasparetti),

Emilia.Nordlund@vtt.fi (E. Nordlund), Janne.Janis@uef.fi (J. Jänis),

Johanna.Buchert@vtt.fi (J. Buchert), Kristiina.Kruus@vtt.fi (K. Kruus).

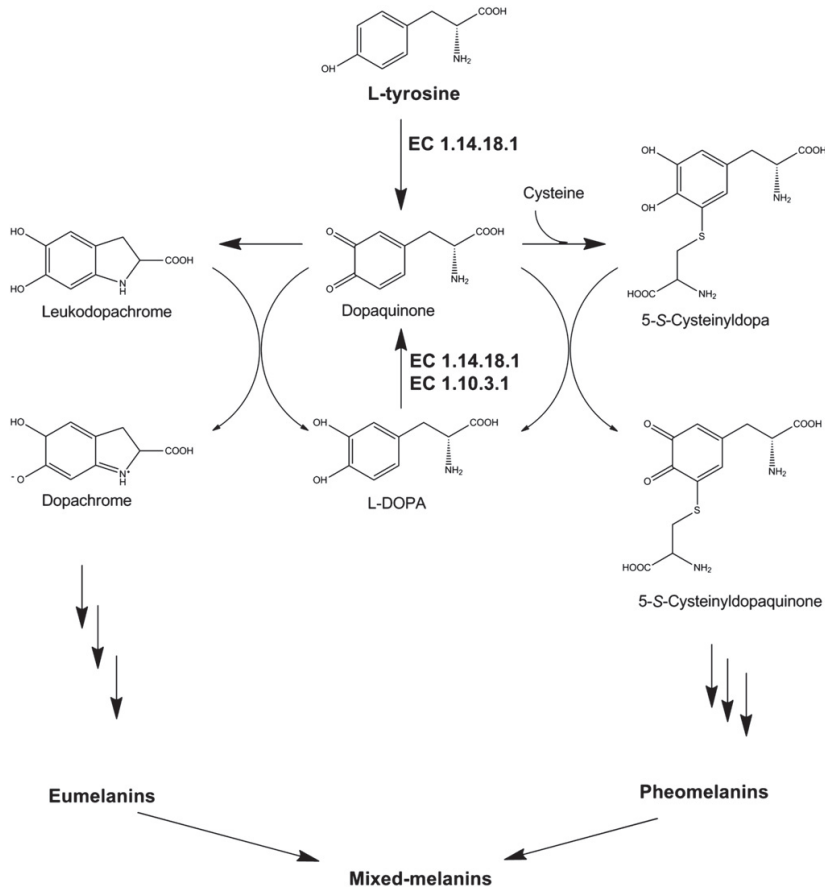


Fig. 1. Early stages of biosynthetic pathways leading to melanin production (modified from [28]).

product of the proximal phase of melanogenesis [23,24]. Dopachrome is the precursor of eumelanins, which are formed in the distal phase of melanogenesis via chemical and enzymatic reactions [26]. In the presence of sulphhydryl residues, i.e., a cysteinyl residue or glutathione, the thiol group causes a nucleophilic attack to the dopaquinone and cysteinyl-dopa or glutathionyl-dopa are formed. Cysteinyl-dopa and glutathionyl-dopa are the precursors of the reddish pheomelanins [26]. Eumelanins and pheomelanins polymerize via enzymatic and non-enzymatic crosslinking reactions to form mixed melanins [27,28].

The occurrence of the above mentioned reactions in fruits and vegetables or in skin is responsible of food browning or of hyperpigmentation in human skin. Because such reactions are not desirable, food and cosmetic industries are constantly interested in novel tyrosinase inhibitors to be used as antibrowning agents of foods and as skin whiteners [17]. Currently, sulfite is the most commonly applied inhibitor in the discoloration process, while arbutin and aloesin, isolated from plants, are the tyrosinase inhibitors used in the cosmetic industry [29]. A number of tyrosinase inhibitors from both natural and synthetic sources have been identified [17,26,30,31]. The effect of many potential tyrosinase inhibitors has been examined directly monitoring the tyrosinase-catalyzed oxidation of tyrosine or L-DOPA [17]. Differently, other compounds have been classified as tyrosinase inhibitors because they interfere in the further non-enzymatic reactions involved in the melanin formation; however, the direct interaction of those compounds with tyrosinase has not been elucidated

[17]. Rescigno et al. [31] divided tyrosinase inhibitors in two groups: copper chelators and substrate analogs. Copper chelators compete with the oxygen at the binding site while substrate analogs compete with the monophenolic or diphenolic substrate of the enzyme. Tropolone, cyanide, azide and halide ions are copper chelators; resorcinol, benzoic acid, and naphthalene are examples of substrate analogs. More recently Chang [17] divided true tyrosinase inhibitors as specific tyrosinase inactivators and specific tyrosinase inhibitors. Specific tyrosinase inactivators are also called suicide substrates; they can bind covalently to tyrosinase and irreversibly inactivate the enzyme. On the contrary, specific tyrosinase inhibitors reversibly bind to tyrosinase and reduce its catalytic capacity [17].

Tyrosinase activity can also be beneficial for instance to improve the sensory properties of some products, such as dark raisins and fermented tea leaves. In particular, fungal tyrosinases can form covalent bonds between peptides, proteins and carbohydrates, thus these enzymes have been studied as crosslinking agents in food and non-food applications [32–35]. Tyrosinases have been proposed for structure engineering of meat-derived food products, as well for baking applications [36,37]. Tailoring polymers, e.g., grafting of silk proteins onto chitosan via tyrosinase reactions has also been reported [33,38].

The fungal tyrosinases characterized so far are typically intracellular enzymes and the first extracellular fungal tyrosinase has been characterized from the filamentous fungus *Trichoderma reesei* [39]. This tyrosinase showed distinctive characteristics in terms of

substrate specificity and food protein crosslinking ability as compared to tyrosinases from fungal and plant origins [40]. In our previous work we compared the substrate specificity of *T. reesei* (TrT) and *A. bisporus* (AbT) tyrosinases utilizing different small monophenols and diphenols as substrates. The presence of an amine group in the substrate, e.g., L-DOPA, was suggested to hinder the oxidation in the TrT-catalyzed reactions; differently, substrates with a carboxyl group were observed not to be effectively oxidized by AbT [41]. In this work the aim was to study the product inhibition of TrT and the inhibition mechanism of potential inhibitors of TrT.

2. Material and methods

2.1. Enzymes

T. reesei tyrosinase (TrT) was produced and purified as described by Selinheimo et al. [39]. *A. bisporus* tyrosinase (AbT) was obtained from Fluka; a stock solution of AbT (5 mg mL⁻¹) was prepared in 0.1 M sodium phosphate buffer, pH 7.0.

2.2. Chemicals

L-tyrosine, L-DOPA, arbutin, and *p*-coumaric acid were from Sigma; caffeic acid, catechol, and benzaldehyde were from Fluka; phenol, sodium azide, potassium cyanide, kojic acid, and benzoic acid were from Merck.

2.3. Enzyme activity assays

Tyrosinase activity was measured using 15 mM L-DOPA as a substrate. Activity assays were performed in 0.1 M sodium phosphate buffer pH 7.0 at 25 °C either by monitoring dopachrome formation at 475 nm ($\epsilon_{\text{dopachrome}} = 3400 \text{ M}^{-1} \text{ cm}^{-1}$) or by measuring the consumption of the co-substrate oxygen, with a single channel fiber-optic oxygen meter for mini-sensors (Precision sensing GmbH, Regensburg, Germany) as described by Selinheimo et al. [41].

2.4. UV-visible spectroscopy measurements

Formation of the absorption product spectra from the oxidation of diphenolic substrates, i.e., caffeic acid, L-DOPA and catechol, by tyrosinases was monitored spectrophotometrically at 300–600 nm at periodic intervals of 0.5 min during the first 10 min of the reaction, and afterwards at periodic intervals of 10 min. A fresh solution of diphenolic substrate was prepared in sodium phosphate buffer pH 7.0 and the reaction was started by addition of tyrosinase. Solutions of the diphenolic substrate and sodium azide were separately prepared in sodium phosphate buffer pH 7.0. The reaction mixture containing the diphenolic substrate (15 mM) and sodium azide (10 mM) was freshly prepared before starting the reaction by adding the tyrosinase.

2.5. Mass spectrometry

A 4.7-T Bruker APEX-Qe Fourier transform ion cyclotron resonance (FT-ICR) mass spectrometer (Bruker Daltonics, Billerica, MA, USA) described by Jänis et al. [42] was used. Negative ions were produced in an Apollo-II electrospray ion (ESI) source and externally accumulated for 1–2 s in a hexapole collision cell before transferred to the Infinity ICR cell for trapping, excitation and detection. For infrared multiphoton dissociation (IRMPD) experiments, ions of interest were further isolated by mass-selective quadrupole. The isolated precursor ions were irradiated with IR-photons from a Synrad 48-Series 40-W, 10.6- μm cw-CO₂ laser (Synrad, Mulkitoo, WA, USA). The focused laser beam was directed to the ICR cell through a BaF window, located near the rear trapping plate electrode. Duration of laser irradiation was 100 ms and 250 ms, for L-DOPA and dopachrome, respectively;

the laser power was set to 90% of the maximal laser power. For each spectrum, one to four co-added 128-kWord time-domain transients (sweep width 833 kHz, acquisition time 0.079 s per transient) were recorded and zero-filled once prior to Gaussian apodization, magnitude calculation and Fast Fourier transformation. Bruker XMASS software (version 6.0.2) was used for data acquisition and processing. Kinetic analyses of L-DOPA to dopachrome conversion by tyrosinases were performed in Eppendorf tubes using 1 mM L-DOPA in ammonium acetate pH 7.0 at 25 °C. The reaction was started by addition of tyrosinase (3.6 nkat mL⁻¹ reaction) and the sample was injected into the mass spectrometer at determined time intervals for a total time of 20 min. The relative ion intensities were directly converted to the respective solution concentrations given the virtually same ion transmission and ionization efficiencies for L-DOPA (*m/z* 196) and dopachrome (*m/z* 192).

2.6. Inhibition of *T. reesei* tyrosinase by dopachrome

Since dopachrome was not commercially available, we produced dopachrome enzymatically using L-DOPA as substrate and AbT as enzyme. Two milligrams of AbT preparation was added to 2.5 mL of 5 mM L-DOPA dissolved in sodium acetate buffer, pH 5.6. The reaction was vigorously mixed in a small baker for 30 min at 25 °C, after which the enzyme was removed by ultracentrifugation (Vivaspin tubes, 5000 Da cut-off). The concentration of dopachrome in the obtained solution was calculated from the intensity of absorbance at 475 nm using the extinction coefficient $\epsilon_{\text{dopachrome}} = 3400 \text{ M}^{-1} \text{ cm}^{-1}$. The stability of dopachrome produced by AbT was monitored by the polarography. Reaction mixtures of L-DOPA (8 mM) and dopachrome (from 0 to 1.5 mM) were prepared. Activity of TrT was measured on L-DOPA in the presence of different concentrations of freshly prepared dopachrome by following the consumption of the co-substrate oxygen in the time interval of 1–3 min after addition of TrT (0.9 nkat mL⁻¹ of reaction mixture).

2.7. Determination of K_i parameters

Fresh solutions of the inhibitors (0–60 mM) and substrates (0.1–15 mM) were prepared in 0.1 M sodium phosphate buffer pH 7.0, and the reaction was started by an addition of the enzyme. Enzyme dosages were 6 $\mu\text{g mL}^{-1}$ and 3 $\mu\text{g mL}^{-1}$ of reaction mixture for the monophenolic substrate (*p*-coumaric acid) and the diphenolic substrate (caffeic acid), respectively. The initial rate of product formation from the reaction mixture was determined at 25 °C as the increase of absorbance at wavelength 360 nm and 480 nm per min for *p*-coumaric acid and caffeic acid, respectively. The type of inhibition and the K_i parameters for each inhibitor were determined plotting the data to the Lineweaver–Burk and Dixon plots. Furthermore, the Cornish plot was used to determine the K_i' parameter.

3. Results

3.1. Oxidation of diphenolic substrates by *T. reesei* and *A. bisporus* tyrosinases

UV-visible spectroscopy was used to monitor the product formation and polarography was used to measure the consumption of the co-substrate oxygen in the *T. reesei* and *A. bisporus* tyrosinase-catalyzed oxidation of caffeic acid and L-DOPA. When caffeic acid was used as a substrate, the products were similar between the two tyrosinases, according to their product spectra showing a maximum of absorbance at 480 nm. In addition, in these experimental conditions both enzymes were capable of consuming all oxygen present in the reaction mixture within 10 min (Fig. 2A and B). When L-DOPA was used as a substrate, the product spectra of both enzymes showed a maximum absorbance at 475 nm, but the intensities of

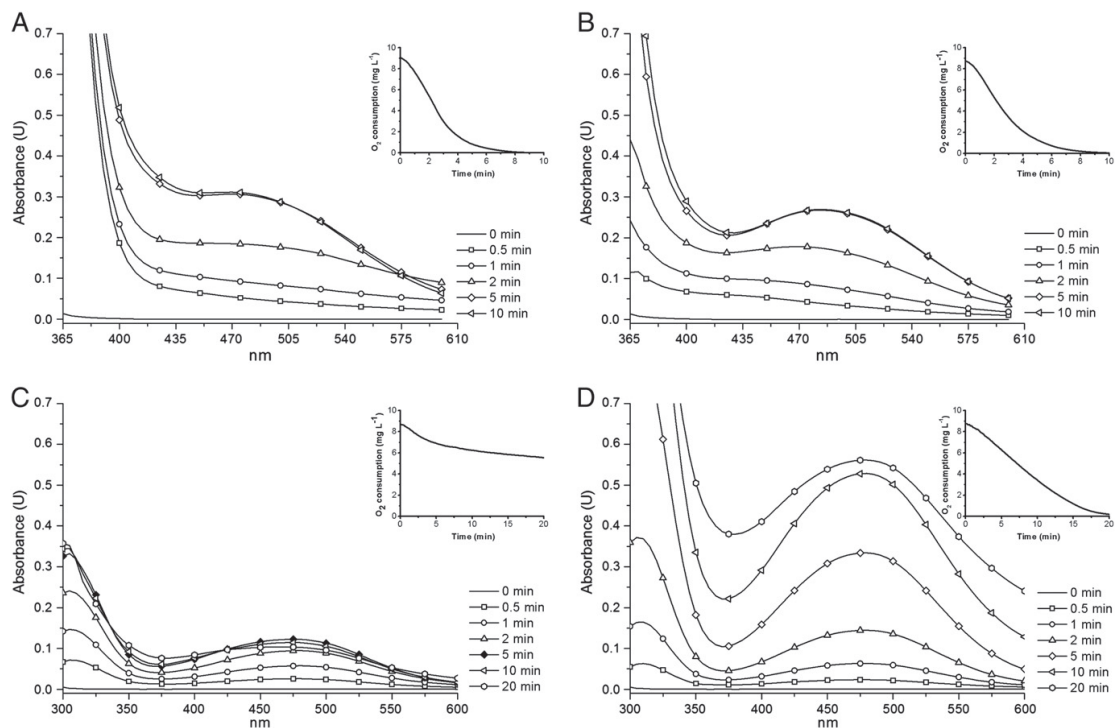


Fig. 2. Absorption product spectra from the oxidation of caffeic acid (15 mM) by *Trichoderma reesei* (TrT) tyrosinase (A) and *Agaricus bisporus* (AbT) tyrosinase (B) and absorption product spectra from the oxidation of L-DOPA (15 mM) by TrT (C) and AbT (D). Oxygen consumption for each reaction is reported in the inset.

the $A_{475\text{ nm}}$ were different. In the TrT-catalyzed reaction the maximum intensity of $A_{475\text{ nm}}$ was recorded after 5 min ($A_{475\text{ nm}}=0.13$ units), after which the absorbance at 475 nm did not increase any more. Also the oxygen consumption measurement indicated that after the first 5 min the oxygen consumption rate was retarded, and after 20 min most of the oxygen was still not consumed (Fig. 2C). In the AbT-catalyzed reaction the maximum absorbance at 475 nm was recorded after 15 min ($A_{475\text{ nm}}=0.57$ units) and all the oxygen in the reaction mixture was consumed within 20 min of reaction (Fig. 2D).

3.2. ESI-FT-ICR detection of the end products formed in *T. reesei* and *A. bisporus* tyrosinase-catalyzed oxidation of L-DOPA

The reaction end products of L-DOPA oxidation by the tyrosinases were analyzed with ESI-FT-ICR mass spectrometry. The reactions were performed in 10 mM ammonium acetate using 1 mM L-DOPA as a substrate. Alternatively, reactions were performed in 20 mM sodium phosphate, pH 7.0 or pure water with qualitative similar results (data not shown). Without enzyme, L-DOPA (197 Da) gave an intense peak at m/z 196, corresponding to the $[M - H]^-$ ion. In the presence of TrT, the signal for L-DOPA (m/z 196) decreased by approximately 10% within the first 2000 s of reaction while a new peak at m/z 192 was observed (spectra not presented), suggesting a formation of dopachrome (193 Da). The ions at m/z 192 and at m/z 196 did not change in intensity at prolonged reaction time. No other ions were detected. In the presence of AbT, the signal for L-DOPA (m/z 196) decreased over time while a new peak at m/z 192 was observed (Fig. 3A), suggesting a formation of dopachrome (193 Da). The ion at m/z 192 was the only ion detected at prolonged reaction times. Fig. 3B and C shows the reaction progress for L-DOPA oxidation by

TrT and AbT, respectively, as determined with mass spectrometry. In the case of TrT the production of dopachrome clearly plateaued after a few minutes of reaction time and the reaction did not go to

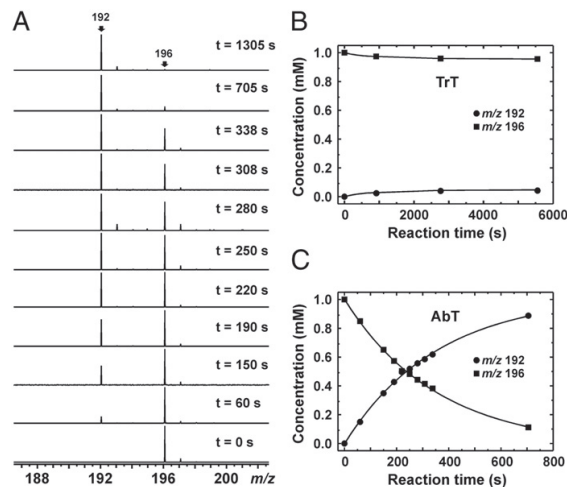


Fig. 3. Negative mode ESI FT-ICR mass spectra from the oxidation of L-DOPA (m/z 196) to dopachrome (m/z 192) by *Agaricus bisporus* tyrosinase (AbT) at various time points (A). A plot of the respective ion intensities versus reaction time for *Trichoderma reesei* tyrosinase (TrT) (B) and AbT (C); the y-axis is converted to the solution concentrations (see Materials and methods for details) and solid lines are the best fits for the first order exponential.

completion, suggesting that the reaction was inhibited by the end product. Instead, complete conversion of 1 mM L-DOPA to 1 mM dopachrome occurred within 20 min of AbT-catalyzed reaction, following a pseudo first-order kinetics (i.e., $[L-DOPA] < K_M$) (Fig. 3C). The two ions at m/z 196 and m/z 192 were further subjected to fragmentation analysis by IRMPD (Fig. 4). IRMPD spectrum of the deprotonated L-DOPA (m/z 196) showed three fragment ions, consistent with the losses of NH_3 (m/z 179), CO_2 (m/z 152) or both (m/z 135) (Fig. 4B). The IRMPD spectrum of the reaction product (m/z 192), showed four fragment ions, accounting for eliminations of H_2O (m/z 174), H_2CO (m/z 162) or CO_2 (m/z 148) followed by elimination of CO (m/z 120) (Fig. 4D). Decarboxylation (loss of CO_2) is highly characteristic for carboxylate group, while the losses of H_2O , H_2CO and CO are typical for quinone structures. This confirms the product to be dopachrome for both TrT and AbT-catalyzed oxidation of L-DOPA.

3.3. Product inhibition of *T. reesei* tyrosinase

The product inhibition was analyzed by monitoring the TrT-catalyzed oxidation of L-DOPA in the presence of dopachrome. Dopachrome was prepared oxidizing 5 mM L-DOPA in 0.2 M acetate buffer pH 5.6 by AbT. In these conditions, the conversion yield of dopachrome production was 70%. Dopachrome was detected to be stable in this buffer solution for at least 1.5 h when stored in dark and on ice. Reaction mixtures containing 8 mM L-DOPA and different dopachrome concentrations (0; 0.25; 0.75 and 1.5 mM) were used to calculate the degree of inhibition. The oxygen consumption rate of TrT on 8 mM L-DOPA in the presence of 1.5 mM dopachrome was clearly reduced, and TrT activity was inhibited by 54% (Table 1).

3.4. Determination of the type of inhibition and K_i constants of the selected inhibitors for *T. reesei* tyrosinase

The inhibition of TrT was further analyzed with known tyrosinase inhibitors. Six selected inhibitors were used to determine the thermodynamic constants (K_i) for TrT using *p*-coumaric acid as a

Table 1
Degree of inhibition of *Trichoderma reesei* tyrosinase (TrT) by dopachrome on L-DOPA (8 mM). Reaction mixture was prepared in 0.2 M sodium acetate buffer pH 5.6 and analyzed by oxygen consumption measurement.

Dopachrome (mM)	Oxygen consumption rate ($\mu\text{g L}^{-1} \text{min}^{-1}$)	Inhibition (%)
0	18.2 ± 3.5	0
0.25	17.9 ± 2.7	2
0.75	12.0 ± 1.0	34
1.5	8.4 ± 1.7	54

monophenolic substrate and caffeic acid as a diphenolic substrate (Table 2). Potassium cyanide was the strongest inhibitor ($K_i = 0.14$ mM) of the TrT-monophenolase activity. Sodium azide, benzaldehyde and arbutin were also strong inhibitors with K_i values of 0.97 mM, 1.95 mM and 6.66 mM, respectively. In the tested conditions, benzoic acid and kojic acid did not have an inhibitory effect on the monophenolase activity of TrT. However, kojic acid had a strong influence on the duration of the lag time (i.e., a timeframe prior to the oxidation reactions of monophenolic substrates); in the presence of 0.1 mM kojic acid the lag time was six folds longer than in the condition without the inhibitor (400–450 s). The lag time in the oxidation of *p*-coumaric acid by TrT was differently affected by the tested inhibitors. While kojic acid, sodium azide and arbutin prolonged the lag time, potassium cyanide reduced the lag time, and benzaldehyde did not have an effect on the lag time in the TrT-catalyzed oxidation of *p*-coumaric acid.

Kojic acid was the strongest inhibitor ($K_i = 0.01$ mM) and the only competitive inhibitor of the TrT-diphenolase activity. Both potassium cyanide and sodium azide showed mixed noncompetitive type of inhibition when caffeic acid was used as a substrate. Potassium cyanide ($K_i = 0.16$ mM) was a stronger inhibitor than sodium azide ($K_i = 0.96$ mM) of the TrT-diphenolase activity. Arbutin was detected to be an uncompetitive inhibitor of the TrT-diphenolase activity, thus the K_i' value was calculated ($K_i' = 15.31$ mM) instead of the K_i value, according to Cornish-Bowden [43]. In the tested conditions, benzaldehyde and benzoic acid did not inhibit the diphenolase activity of TrT.

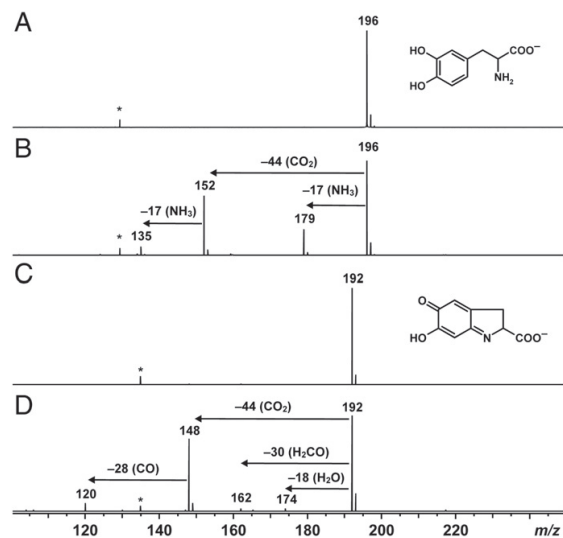


Fig. 4. Negative mode ESI FT-ICR mass spectra of the substrate L-DOPA (1 mM) without tyrosinase (A) and the reaction product dopachrome (C) obtained after 20 min of reaction with *Agaricus bisporus* (AbT) tyrosinase. Infrared multiple-photon dissociation (IRMPD) spectra of L-DOPA (B) and dopachrome (D). Ions marked with an asterisk correspond to the known instrument noise peaks.

Table 2
Kinetic constants (K_i) and types of inhibition of selected inhibitors towards the monophenolase (*p*-coumaric acid) and the diphenolase (caffeic acid) activities of *Trichoderma reesei* tyrosinase (TrT).

Inhibitor	Type of inhibition towards <i>p</i> -coumaric acid	K_i (mM)	Lag time (s) ^a
Potassium cyanide	Mixed noncompetitive	0.14 ± 0.09	0–50
Sodium azide	Noncompetitive	0.97 ± 0.08	2200–2250
Arbutin ^b	Competitive	6.66 ± 0.32	1200–1250
Kojic acid	No effect	n.d.	2450–2500
Benzaldehyde	Competitive	1.95 ± 0.20	400–450
Benzoic acid	No effect	n.d.	400–450

Inhibitor	Type of inhibition towards caffeic acid	K_i (mM)
Potassium cyanide	Mixed noncompetitive	0.16 ± 0.01
Sodium azide	Mixed noncompetitive	0.96 ± 0.03
Arbutin ^b	Uncompetitive	15.31 ± 1.68
Kojic acid	Competitive	0.01 ± 0.00
Benzaldehyde	No effect	n.d.
Benzoic acid	No effect	n.d.

Notes:

n.d.: not determined.

^a Lag time was measured on 15 mM *p*-coumaric acid concentration with the highest inhibitor concentration tested.

^b Reported values for arbutin are K_i and K_i' for *p*-coumaric acid and caffeic acid, respectively.

3.5. Effect of sodium azide on the *T. reesei* and *A. bisporus* tyrosinases-catalyzed oxidation of L-DOPA and catechol

Spectrophotometry and polarography were used to analyze the effect of sodium azide (10 mM) on the TrT- and AbT-catalyzed oxidation of the diphenolic substrates L-DOPA and catechol (15 mM) (Fig. 5). The absorption spectrum of product formed during the TrT-catalyzed oxidation of L-DOPA (15 mM) could be divided in three phases: phase Ia (0–5 min) where the oxidation rate of L-DOPA was linear as followed at 475 nm; phase Ib (5–30 min) where the oxidation rate of L-DOPA started to decrease; and phase II (30–120 min) where an increase in absorbance at wavelengths 300–600 nm was observed (Fig. 5A). When the corresponding reaction was analyzed by monitoring the consumption of the co-substrate oxygen, the oxygen consumption rate within the first 5 min was $5.4 \mu\text{g L}^{-1} \text{s}^{-1}$. After the first 5 min of reaction the oxygen consumption rate was clearly decreased, and all the oxygen present in the reaction mixture was consumed after 4 h of reaction (data not shown). The absorption spectrum of AbT-catalyzed oxidation of L-DOPA could also be divided in three phases, but the length of phases Ia and Ib was different as compared to the TrT-catalyzed reaction (Fig. 5B). As analyzed by monitoring oxygen consumption, the oxygen consumption rate within the first 5 min was $7.6 \mu\text{g L}^{-1} \text{s}^{-1}$, and it did not change significantly after the first 5 min of reaction. After 20 min the concentration of oxygen in the reaction mixture was only 0.4 mg L^{-1} (Fig. 5B), whereas in the corresponding TrT-catalyzed oxidation of L-DOPA without sodium azide the concentration of oxygen in the reaction mixture after 20 min was still 5.5 mg L^{-1} (Fig. 5A).

When 10 mM sodium azide was added into the reaction mixture of L-DOPA with TrT, the accumulation of the reaction product at 475 nm (dopachrome) continued also during the time interval of 5–30 min, and the three phases detected with the TrT-catalyzed oxidation of L-

DOPA only were not observed (Fig. 5C). Furthermore, in the presence of sodium azide the oxygen consumption rate calculated on the first 5 min of TrT-catalyzed oxidation of L-DOPA was halved, but all the oxygen present in the reaction mixture was consumed within 2 h (Fig. 5C). After 20 min of TrT-catalyzed oxidation of L-DOPA with sodium azide, the concentration of oxygen in the reaction mixture was 4.9 mg L^{-1} . Similar to the TrT-catalyzed reaction, in the AbT-catalyzed oxidation of L-DOPA with 10 mM sodium azide the accumulation of the reaction product at 475 nm continued also during the time interval 15–30 min (Fig. 5D). As for TrT, the oxygen consumption rate calculated on the first 5 min of AbT-catalyzed oxidation of L-DOPA with sodium azide was halved, and the time needed for the consumption of all oxygen in the reaction mixture was doubled (Fig. 5D). After 20 min of AbT-catalyzed oxidation of L-DOPA with sodium azide, the concentration of oxygen in the reaction mixture was 2.9 mg L^{-1} .

When catechol (15 mM) was used as a substrate, the products formed by TrT- and AbT-catalyzed reaction were different, as we already reported in our previous study [41]. The *o*-benzoquinone (400 nm) produced by AbT-catalyzed oxidation of catechol was not clearly observed in the TrT-catalyzed oxidation of the same substrate (Fig. 6A and B). As for L-DOPA, the oxygen consumption rate was high ($8.9 \mu\text{g L}^{-1} \text{s}^{-1}$) in the first 5 min of reaction, and it clearly decreased after that. Again, the oxygen consumption rate calculated on the first 5 min of TrT-catalyzed oxidation of catechol with sodium azide was halved (Fig. 6A and C). Similar to L-DOPA oxidation, the consumption of all the oxygen present in the reaction by TrT occurred earlier when sodium azide was added in the reaction mixture with catechol (data not shown). The absorption spectrum of products formed by TrT-catalyzed oxidation of catechol with sodium azide showed a clear maximum at 500 nm (Fig. 6C). Different from TrT, AbT was capable to use all the oxygen in the reaction mixture within 5 min when

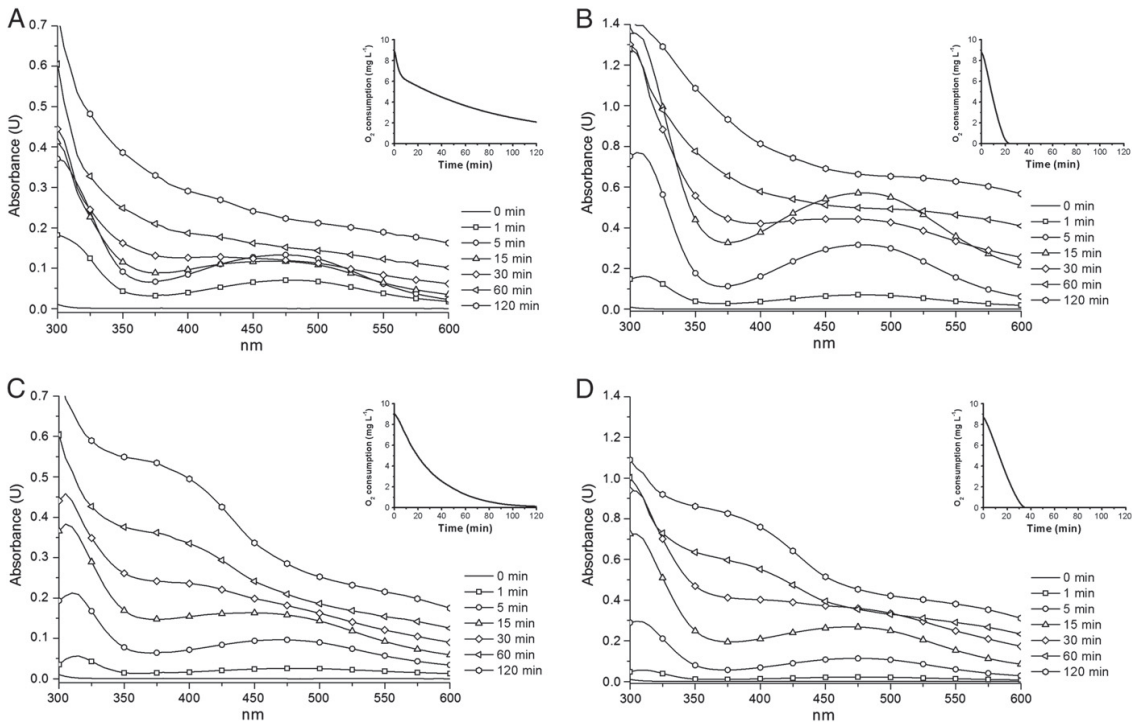


Fig. 5. Absorption product spectra from the oxidation of L-DOPA (15 mM) by *Trichoderma reesei* (TrT) tyrosinase (A) and *Agaricus bisporus* (AbT) tyrosinase (B), and absorption product spectra from the oxidation of L-DOPA (15 mM) in the presence of sodium azide (10 mM) by TrT (C) and AbT (D). Tyrosinase was added as 0.4 nkat mL^{-1} of reaction mixture. Oxygen consumption for each reaction is reported in the inset.

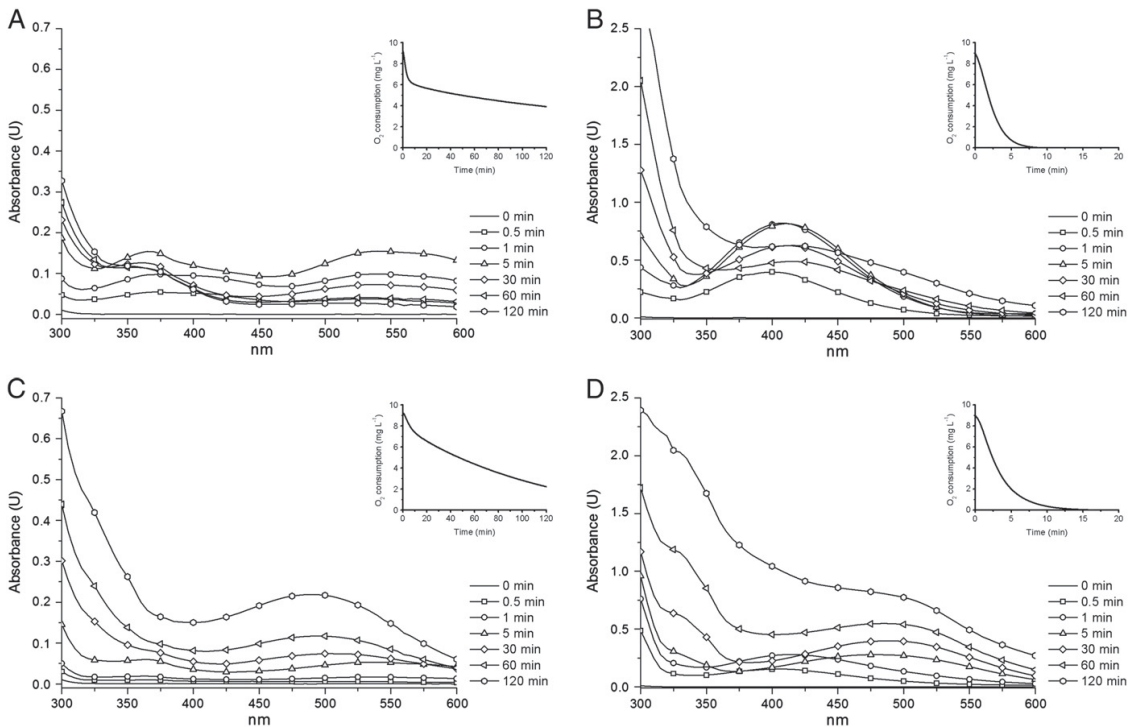


Fig. 6. Absorption product spectra from the oxidation of catechol (15 mM) by *Trichoderma reesei* (TrT) tyrosinase (A) and *Agaricus bisporus* (AbT) tyrosinase (B), and absorption product spectra from the oxidation of catechol (15 mM) in the presence of sodium azide (10 mM) by TrT (C) and AbT (D). Tyrosinase was added as 1 nkat mL⁻¹ of reaction mixture. Oxygen consumption for each reaction is reported in the inset.

oxidizing catechol (without sodium azide). In the presence of sodium azide the oxygen consumption rate of AbT-catalyzed oxidation of catechol was reduced only by 10%, but the absorption spectrum of products formed was strongly affected. A clear and fast shift of the maximum absorbance from 400 nm to 500 nm was observed already in the first 5 min of AbT-catalyzed reaction. Furthermore, in the AbT-catalyzed oxidation of catechol with sodium azide a maximum at 330 nm was observed after 30 min of reaction (Fig. 6D).

4. Discussion

Detailed information on the reaction mechanism and the inhibition mechanism of tyrosinases is fundamental when developing applications for tyrosinases. The intracellular tyrosinase from *Agaricus bisporus* (AbT) has been extensively studied both from biochemical and structural points of view [1,15,44–47]. Also applications for tyrosinases have been proposed, e.g., in tailoring silk fibroin and special peptides [33,38]. Recently Selinheimo et al. [39] reported on an extracellular tyrosinase produced by the ascomycete *Trichoderma reesei* (TrT). We have homologously overexpressed this enzyme in high yields, thus, enabling characterization and testing the enzyme in applications. In particular, the enzyme has been shown to have good abilities to crosslink food protein matrices [36,37]. Furthermore, differences in substrate specificity between TrT and AbT have been reported by Selinheimo et al. [41]. TrT has higher affinity (K_M) on caffeic acid than AbT and it can also catalyze the oxidation of the corresponding monophenol *p*-coumaric acid to *o*-quinone corresponding to caffeic acid whereas *p*-coumaric acid cannot be oxidized by AbT, in fact it has been suggested as an inhibitor for AbT [41,48]. On the contrary, TrT has lower affinity on L-DOPA than AbT [41]. We observed in this work a fast decrease in the reaction rate of TrT-

catalyzed oxidation of L-DOPA and catechol, as analyzed both by UV-visible spectroscopy and oxygen consumption measurements. Cooksey et al. [49] reported the reaction kinetics of AbT on L-DOPA and they divided the reactions in three phases: in phase Ia dopaquinone is produced by AbT, in phase Ib dopaquinone is rapidly converted to dopachrome via a spontaneous reductive cyclization, and in phase II the tautomerization of dopachrome to 5,6-dihydroxyindole-2-carboxylic acid (DHICA) takes place. The phases Ia and Ib represent the proximal phase of melanogenesis where dopachrome is the reaction end product; and phase II represents the distal phase of melanogenesis where the chemical and enzymatic reactions leading to eumelanins occur [26,49]. In our experiment conditions the proximal phase in AbT-catalyzed reaction had duration of 15 min (as also reported by Cooksey et al. [49]), while with TrT the proximal phase lasted only for 5 min, and the total amount of formed dopachrome remained low. In the distal phase of both the TrT- and AbT-catalyzed reactions the concentration of dopachrome decreased and new undefined products absorbing at 300–600 nm were observed. Furthermore, the oxygen consumption rate in TrT-catalyzed oxidation of L-DOPA clearly decreased in the distal phase (i.e. 5–120 min for TrT) despite the co-substrate oxygen was still available in the reaction mixture, thus suggesting product inhibition. On the contrary, in the AbT-catalyzed oxidation of L-DOPA the oxygen available in the reaction mixture was totally consumed during the proximal phase (i.e. 0–15 min) and the product dopachrome was linearly produced. The AbT-catalyzed oxidation of L-DOPA could not proceed in the distal phase (i.e. 15–120 min) since there was no oxygen available in the reaction mixture. Because with TrT the proximal phase was very short the reactions of the distal phase of melanogenesis occurred earlier than in AbT-catalyzed reactions.

The formation of end product dopachrome in L-DOPA oxidation was confirmed by high-resolution mass spectrometry measurements (ESI-FT-ICR) and no other end products were detected in the proximal and distal phases of reaction. In these conditions (i.e. 1 mM L-DOPA) a fast decrease in the TrT-catalyzed oxidation rate of L-DOPA to dopachrome was also observed, while the AbT-catalyzed oxidation of L-DOPA to dopachrome occurred linearly within 20 min, in accordance to what observed by oxygen consumption and UV-visible spectroscopy measurements. To analyze the suggested product inhibition, dopachrome was produced by AbT-catalyzed oxidation of L-DOPA in acidic conditions (sodium acetate buffer pH 5.6) to assure stability of dopachrome [50]. The inhibitory effect of dopachrome on TrT was clear; the 1.5 mM dopachrome concentration was enough to reduce by 50% the rate of L-DOPA oxidation in the reaction conditions. Inhibition by dopachrome was reversible since the TrT activity was recovered after removal of dopachrome from the reaction mixture using gel filtration (data not shown). Although the substrate inhibition and the inhibition by various inhibitors of tyrosinase have been widely studied, no studies have earlier reported about end product inhibition [51,52]. Similar to L-DOPA, the oxygen consumption rate of a TrT-catalyzed oxidation of catechol clearly decreased after the first 5 min of reaction, suggesting also the end product inhibition. Furthermore, several products (300–600 nm) were formed and the known tyrosinase reaction product *o*-benzoquinone (400 nm) was not accumulated during the TrT-catalyzed oxidation of catechol. On the contrary, with the AbT-catalyzed oxidation of catechol, the oxygen consumption rate was linear and the product *o*-benzoquinone (400 nm) clearly accumulated in the first 5 min of the reaction.

Inhibition of AbT by various inhibitors, i.e., kojic acid, arbutin, benzaldehyde, benzoic acid, potassium cyanide, and sodium azide is thoroughly reported [53–59]. In this work, the various known tyrosinase inhibitors, and the inhibition mechanism for TrT were analyzed using *p*-coumaric acid and caffeic acid as monophenolic and diphenolic substrates. Kojic acid was found to be a strong inhibitor of diphenolase, but did not inhibit the monophenolase activity of TrT although prolonged the lag period. Chen et al. [53] reported on the inhibition mechanism of kojic acid, and recently also the three-dimensional structure of the tyrosinase from *Bacillus megaterium* in complex with kojic acid has been reported [60]. Kojic acid is oriented with the hydroxymethyl towards the CuB in the active site of *met*-tyrosinase, different from the suggested bidentate fashion binding to both the CuA and CuB through its hydroxyl and *o*-positioned carbonyl groups [60]. According to Sendovski et al. [60], monophenols bind to CuA of tyrosinase, instead diphenols bind to CuB. Our results are in accordance with this mechanism: it would be possible to explain the effect of kojic acid towards TrT, assuming that *p*-coumaric acid (monophenol) binds to the CuA while caffeic acid (diphenol) binds to the CuB in the active site of TrT. Caffeic acid (diphenol) and kojic acid competed in binding to CuB, and a clear competitive inhibition was observed. Differently, in the monophenolase cycle, *p*-coumaric acid binds to the CuA while kojic acid binds to the CuB and no clear inhibition was observed. The lag time of TrT was, however, strongly prolonged by kojic acid; most probably the binding of substrate is more difficult when the complex tyrosinase-kojic acid is present.

Arbutin is a hydroquinone glycoside of plant origin used in cosmetic industry as skin-whitening agent. Nihei and Kubo [61] suggested that arbutin covalently binds to the *met*-form of tyrosinase as a monophenol substrate analog and leads the enzyme to a dead-end pathway [62]. In our experimental conditions arbutin was a competitive inhibitor of the TrT monophenolase activity and prolonged the lag time, probably leading TrT towards the dead-end pathway. In the case of the TrT diphenolase activity, arbutin was a noncompetitive inhibitor, while it has been reported that it is a noncompetitive or mixed noncompetitive inhibitor of AbT [56]. Uncompetitive inhibitors can bind only the enzyme–substrate complex [17], thus the K_i value cannot be determined; instead, the K_i' value can be calculated

from the Cornish plot, where the K_i' value is the dissociation constant of the enzyme–substrate–inhibitor complex [43]. The high K_i and K_i' values of arbutin determined for TrT indicated that arbutin was not a strong inhibitor of TrT, and suggested that the caffeic acid–TrT complex must be formed before the binding of arbutin.

Benzaldehyde and benzoic acid were selected for the inhibition studies of TrT, since they are well known tyrosinase inhibitors [57,58]. In our experimental conditions, benzaldehyde efficiently inhibited only the oxidation of *p*-coumaric acid by TrT with a competitive mechanism similar to arbutin. Benzaldehyde was a stronger inhibitor than arbutin to the monophenolase activity of TrT; however, different from arbutin benzaldehyde did not affect the lag time, which is in accordance with previous studies where it has been reported that unsaturated aldehydes do not affect the lag time of AbT [48,63]. Benzoic acid did not strongly inhibit the TrT-catalyzed oxidation of caffeic acid or *p*-coumaric acid, while it has been reported that benzoic acid is a strong competitive inhibitor ($K_i = 18 \mu\text{M}$) of AbT monophenolase activity [58]. Nevertheless, when we analyzed spectrophotometrically the inhibitory effect of benzoic acid (10 mM) on the TrT-catalyzed oxidation of phenol and *l*-tyrosine as monophenolic substrates (10 mM), the reaction rate was inhibited by 52% and 34% for phenol and *l*-tyrosine, respectively. The TrT-catalyzed oxidation of the corresponding diphenolic substrates (10 mM), i.e., catechol and L-DOPA was also inhibited in the presence of 10 mM benzoic acid by 31% and 55% for catechol and L-DOPA, respectively (data not shown).

The type of inhibition of small chemicals used as copper chelators such as potassium cyanide and sodium azide has been extensively studied with respect to AbT and tyrosinase from *N. crassa* [59,64]. Wilcox et al. [59] proposed that potassium cyanide binds the reduced form of tyrosinase (*deoxy*-form) and stabilizes it, thus functioning as a competitive inhibitor of tyrosinase with respect to oxygen binding to the *deoxy*-form and as a noncompetitive inhibitor to respect of L-DOPA oxidation. Accordingly, in our experimental conditions the K_i values of potassium cyanide for TrT-catalyzed oxidation of *p*-coumaric acid and caffeic acid were in the same order of magnitude, suggesting that potassium cyanide competes with oxygen in binding the *deoxy*-form of TrT that is involved in both monophenolase and diphenolase catalytic cycles. TrT and AbT showed distinctive characteristics also when the reactions catalyzed by the enzymes were studied in the presence of sodium azide. It has been reported that sodium azide binds the *deoxy*-form of tyrosinase, but also to the oxidized forms (*met*- and *oxy*-forms) displacing the peroxide from the *oxy*-form of tyrosinase. Furthermore, Wilcox et al. [59] proposed that sodium azide can bind also to the *met*-form in complex with the diphenol. The diphenol can further dissociate from this complex and subsequently molecular oxygen can bind to it; eventually sodium azide can dissociate and the *oxy*-form of tyrosinase is generated. Altogether the type of inhibition of sodium azide has been explained as noncompetitive towards AbT for the oxidation of *l*-tyrosine and L-DOPA. Similarly, we found that TrT is inhibited by sodium azide with a noncompetitive and a mixed noncompetitive type of inhibition for the monophenolic and diphenolic substrates, respectively.

Effect of sodium azide on the tyrosinases was also studied by monitoring the UV-visible spectrum of product accumulation during enzymatic oxidation of L-DOPA and catechol as diphenolic substrates. In our experimental conditions (i.e. 15 mM L-DOPA or catechol and 10 mM sodium azide), sodium azide clearly slowed down the initial reaction rate of TrT- and AbT-catalyzed oxidation of L-DOPA as well of catechol, but it also had an effect on the reaction end products. Previously Sugumaran [65] used UV-visible spectroscopy and HPLC to study the effect of sodium azide (20 mM) on the AbT-catalyzed oxidation of catechol (1 mM) and the end product (*o*-benzoquinone), and reported on an azido-benzoquinone adduct detected at 330 nm. In our study, the formation of the azido-benzoquinone adduct was not detected in the TrT-catalyzed oxidation of 15 mM catechol in

the presence of sodium azide (10 mM), probably because the production of *o*-benzoquinone was limited due to end product inhibition. In the same conditions the azido-benzoquinone adduct was clearly formed after 2 h of AbT-catalyzed reaction. Furthermore, we observed a clear maximum at 500 nm in the absorption spectrum of products formed by TrT- and AbT-catalyzed oxidation of catechol in the presence of sodium azide. No azido-dopachrome adduct has been reported in literature; however, the clear maximum at 375 nm observed in the product absorption spectra of TrT- and AbT-catalyzed oxidation of L-DOPA in the presence of sodium azide suggest that a dopachrome-adduct was formed. Interestingly, we also found that the sodium azide affected the detected end product inhibition of TrT in the reaction mixture of L-DOPA and catechol. The product inhibition seemed to be diminished when sodium azide was present and thus the oxygen was consumed to higher degree than without sodium azide. The reason for the result is not clear, but suggests a very complex inhibition mechanism of sodium azide for tyrosinases.

5. Conclusions

The extracellular fungal tyrosinase TrT was revealed to suffer of end product inhibition when L-DOPA or catechol were used as a diphenolic substrate, whereas corresponding inhibition was not observed with the intracellular fungal tyrosinase AbT. Sodium azide, in addition to retardation of the initial oxygen consumption rate of the TrT- and AbT-catalyzed oxidation of L-DOPA or catechol and formation azido-quinone adducts with the end product, was also found to play so far an inexplicable role in the detected product inhibition of TrT.

Among the studied potential inhibitors of TrT, potassium cyanide and kojic acid were the strongest inhibitors for the monophenolase and diphenolase activities, respectively. Although the detailed inhibition mechanisms of the selected inhibitors are still poorly understood, the differences in the type of inhibition could suggest differences in the reaction mechanism of TrT and AbT. A possible complex crystal structure in the future, especially between TrT and L-DOPA, could provide better insights into the inhibitory mechanism of TrT.

Acknowledgements

The work was carried out with financial support from the Marie Curie EU-project "Enzymatic tailoring of protein interactions and functionalities in food matrix" PRO-ENZ (MEST-CT-2005-020924) and from the Research Foundation of Raisiogroup (Raisio, Finland). Markku Saloheimo is acknowledged for the expression construct for TrT production, Michael Bailey for the TrT production, and Birgit Hillebrandt-Chellaoui for the skillful help in enzyme purification.

References

- [1] D.A. Robb, Tyrosinase, in: R. Lontie (Ed.), *Copper Proteins and Copper Enzymes*, Vol. 2, CRC Press Inc., Boca Raton, FL, 1984, pp. 207–241.
- [2] K. Lerch, *Neurospora* tyrosinase: structural, spectroscopic and catalytic properties, *Mol. Cell. Biochem.* 52 (1983) 125–138.
- [3] A.A. Bell, M.H. Wheeler, Biosynthesis and functions of fungal melanins, *Annu. Rev. Phytopathol.* 24 (1986) 411–451.
- [4] C. Soler-Rivas, N. Arpin, J.M. Olivier, H.J. Wichers, Activation of tyrosinase in *Agaricus bisporus* strains following infection by *Pseudomonas tolaasii* or treatment with a tolaasin-containing preparation, *Mycol. Res.* 101 (1997) 375–382.
- [5] C.W.G. van Gelder, W.H. Flurkey, H.J. Wichers, Sequence and structural features of plant and fungal tyrosinases, *Phytochemistry* 45 (1997) 1309–1323.
- [6] A.M. Mayer, Polyphenol oxidases in plants—recent progress, *Phytochemistry* 26 (1987) 11–20.
- [7] M. Sugumaran, Comparative biochemistry of eumelanogenesis and the protective roles of phenoloxidase and melanin in insects, *Pigment Cell Res.* 15 (2002) 2–9.
- [8] M. Sugumaran, Molecular mechanisms for mammalian melanogenesis: comparison with insect cuticular sclerotization, *FEBS Lett.* 295 (1991) 233–239.
- [9] J.D. Nosanchuk, A. Casadevall, The contribution of melanin to microbial pathogenesis, *Cell. Microbiol.* 5 (2003) 203–223.
- [10] K. Lerch, L. Ettinger, Purification and characterization of a tyrosinase from *Streptomyces glaucescens*, *Eur. J. Biochem.* 31 (1972) 427–437.

- [11] Y. Matoba, T. Kumagai, A. Yamamoto, H. Yoshitsu, M. Sugiyama, Crystallographic evidence that the dinuclear copper center of tyrosinase is flexible during catalysis, *J. Biol. Chem.* 281 (2006) 8981–8990.
- [12] M. Fling, N.H. Horowitz, S.F. Heinenmann, The isolation and properties of crystalline tyrosinase from *Neurospora*, *J. Biol. Chem.* 238 (1963) 2045–2053.
- [13] U. Kupper, D.M. Niedermann, G. Travaglini, K. Lerch, Isolation and characterization of the tyrosinase gene from *Neurospora crassa*, *J. Biol. Chem.* 264 (1989) 17250–17258.
- [14] T. Nakamura, S. Sho, Y. Ogura, On the purification and properties of mushroom tyrosinase, *J. Biochem.* 59 (1966) 481–486.
- [15] H.J. Wichers, Y.A.M. Gerritsen, C.G.J. Chapelon, Tyrosinase isoforms from the fruit-bodies of *Agaricus bisporus*, *Phytochemistry* 43 (1996) 333–337.
- [16] D.A. Robb, S. Gutteridge, Polypeptide composition of two fungal tyrosinases, *Phytochemistry* 20 (1981) 1481–1485.
- [17] T.S. Chang, An updated review of tyrosinase inhibitors, *Int. J. Mol. Sci.* 10 (2009) 2440–2475.
- [18] H. Decker, T. Schweikardt, D. Nillius, U. Salzbrunn, E. Jaenicke, F. Tuzcek, Similar enzyme activation and catalysis in hemocyanins and tyrosinases, *Gene* 398 (2007) 183–191.
- [19] E.I. Solomon, U.M. Sundaram, T.E. Machonkin, Multicopper oxidases and oxygenases, *Chem. Rev.* 96 (1996) 2563–2606.
- [20] R.L. Jolley Jr., L.H. Evans, H.S. Mason, Reversible oxygenation of tyrosinase, *Biochem. Biophys. Res. Commun.* 46 (1972) 878–884.
- [21] R.L. Jolley Jr., L.H. Evans, N. Makino, H.S. Mason, Oxytyrosinase, *J. Biol. Chem.* 249 (1974) 335–345.
- [22] N. Makino, H.S. Mason, Reactivity of oxytyrosinase toward substrates, *J. Biol. Chem.* 248 (1973) 5731–5735.
- [23] H.S. Raper, The tyrosinase-tyrosine reaction: production from tyrosine of 5,6-dihydroxyindole and 5,6-dihydroxyindole-2-carboxylic acid—the precursors of melanin, *Biochem. J.* 21 (1927) 89–96.
- [24] H.S. Mason, The chemistry of melanin; mechanism of the oxidation of dihydroxyphenylalanine by tyrosinase, *J. Biol. Chem.* 172 (1948) 83–99.
- [25] J.N. Rodriguez-Lopez, J. Tudela, R. Varón, F.G. García-Cánovas, Kinetic study on the effect of pH on the melanin biosynthesis pathway, *Biochim. Biophys. Acta* 1076 (1991) 379–386.
- [26] Y.J. Kim, H. Uyama, Tyrosinase inhibitors from natural and synthetic sources: structure, inhibition mechanism and perspective for the future, *Cell. Mol. Life Sci.* 62 (2005) 1707–1723.
- [27] H. Claus, H. Decker, Bacterial tyrosinases, *Syst. Appl. Microbiol.* 29 (2006) 3–14.
- [28] S. Ito, K. Wakamatsu, Chemistry of mixed melanogenesis—pivotal roles of dopa-quinone, *Photochem. Photobiol.* 84 (2008) 582–592.
- [29] S.Y. Seo, V.K. Sharma, N. Sharma, Mushroom tyrosinase: recent prospects, *J. Agric. Food Chem.* 51 (2003) 2837–2853.
- [30] S. Parvez, M. Kang, H.S. Chung, H. Bae, Naturally occurring tyrosinase inhibitors: mechanism and applications in skin health, cosmetics and agriculture industries, *Phytother. Res.* 21 (2007) 805–816.
- [31] A. Rescigno, F. Sollai, B. Pisu, A. Rinaldi, E. Sanjust, Tyrosinase inhibition: general and applied aspects, *J. Enzyme Inhib. Med. Chem.* 17 (2002) 207–218.
- [32] M. Mattinen, R. Lantto, E. Selinheimo, K. Kruus, J. Buchert, Oxidation of peptides and proteins by *Trichoderma reesei* and *Agaricus bisporus* tyrosinases, *J. Biotechnol.* 133 (2008) 395–402.
- [33] G. Freddi, A. Anghileri, S. Sampaio, J. Buchert, P. Monti, P. Taddei, Tyrosinase-catalyzed modification of *Bombyx mori* silk fibroin: grafting of chitosan under heterogeneous reaction conditions, *J. Biotechnol.* 125 (2006) 281–294.
- [34] S. Halalouli, M. Asther, K. Kruus, L. Guo, M. Hamdi, J.C. Sigoiilot, M. Asther, A. Lomascolo, Characterization of a new tyrosinase from *Pycnoporus* species with high potential for food technological applications, *J. Appl. Microbiol.* 98 (2005) 332–343.
- [35] C.M. Aberg, T. Chen, A. Olumide, S.R. Raghavan, G.F. Payne, Enzymatic grafting of peptides from casein hydrolysate to chitosan. Potential for value-added byproducts from food-processing wastes, *J. Agric. Food Chem.* 52 (2004) 788–793.
- [36] R. Lantto, E. Puolanne, K. Kruus, J. Buchert, K. Autio, Tyrosinase-aided protein cross-linking: effects on gel formation of chicken breast myofibrils and texture and water-holding of chicken breast meat homogenate gels, *J. Agric. Food Chem.* 55 (2007) 1248–1255.
- [37] E. Selinheimo, K. Autio, K. Kruus, J. Buchert, Elucidating the mechanism of laccase and tyrosinase in wheat bread making, *J. Agric. Food Chem.* 55 (2007) 6357–6365.
- [38] A. Anghileri, R. Lantto, K. Kruus, C. Arosio, G. Freddi, Tyrosinase-catalyzed grafting of selenic peptides onto chitosan and production of protein-polysaccharide bioconjugates, *J. Biotechnol.* 127 (2007) 508–519.
- [39] E. Selinheimo, M. Saloheimo, E. Ahola, A. Westerholm-Parvinen, N. Kalkkinen, J. Buchert, K. Kruus, Production and characterization of a secreted, C-terminally processed tyrosinase from the filamentous fungus *Trichoderma reesei*, *FEBS J.* 273 (2006) 4322–4335.
- [40] E. Selinheimo, D. NiEdidin, C. Steffensen, J. Nielsen, A. Lomascolo, S. Halalouli, E. Record, D. O'Beirne, J. Buchert, K. Kruus, Comparison of the characteristics of fungal and plant tyrosinases, *J. Biotechnol.* 130 (2007) 471–480.
- [41] E. Selinheimo, C. Gasparetti, M. Mattinen, C.L. Steffensen, J. Buchert, K. Kruus, Comparison of substrate specificity of tyrosinases from *Trichoderma reesei* and *Agaricus bisporus*, *Enzyme Microb. Technol.* 44 (2009) 1–10.
- [42] J. Jänis, P. Pulkkinen, J. Rouvinen, P. Vainiotalo, Determination of steady-state kinetic parameters for a xylanase-catalyzed hydrolysis of neutral underivatized xylooligosaccharides by mass spectrometry, *Anal. Biochem.* 365 (2007) 165–173.

- [43] A. Cornish-Bowden, A simple graphical method for determining the inhibition constants of mixed, uncompetitive and non-competitive inhibitors, *Biochem. J.* 137 (1974) 143–144.
- [44] J.C. Espín, P.A. García-Ruiz, J. Tudela, F.G. García-Cánovas, Study of stereospecificity in mushroom tyrosinase, *Biochem. J.* 331 (1998) 547–551.
- [45] J.C. Espín, R. Varón, L.G. Fenoll, M.A. Gilibert, P.A. García-Ruiz, J. Tudela, F.G. García-Cánovas, Kinetic characterization of the substrate specificity and mechanism of mushroom tyrosinase, *Eur. J. Biochem.* 267 (2000) 1270.
- [46] H.J. Wichers, K. Recourt, M. Hendriks, C.E. Ebbelaar, G. Biancone, F.A. Hoeberichts, H. Mooibroek, C. Soler-Rivas, Cloning, expression and characterisation of two tyrosinase cDNAs from *Agaricus bisporus*, *Appl. Environ. Microbiol.* 61 (2003) 336–341.
- [47] W.T. Ismaya, H.J. Rozeboom, A. Weijn, J.J. Mes, F. Fusetti, H.J. Wichers, B.W. Dijkstra, Crystal structure of *Agaricus bisporus* mushroom tyrosinase: identity of the tetramer subunits and interaction with tropolone, *Biochemistry* 50 (2011) 5477–5486.
- [48] J.Y. Lim, K. Ishiguro, I. Kubo, Tyrosinase inhibitory *p*-coumaric acid from ginseng leaves, *Phytother. Res.* 13 (1999) 371–375.
- [49] C.J. Cooksey, P.J. Garratt, E.J. Land, S. Pavel, C.A. Ramsden, P.A. Riley, N.P. Smit, Evidence of the indirect formation of the catecholic intermediate substrate responsible for the autoactivation kinetics of tyrosinase, *J. Biol. Chem.* 272 (1997) 26226–26235.
- [50] B. Kägedal, P. Konradsson, T. Shibata, Y. Mishima, High-performance liquid-chromatographic analysis of dopachrome and dihydroxyphenylalanine, *Anal. Biochem.* 225 (1995) 264–269.
- [51] J.L. Muñoz-Muñoz, F.J. García-Molina, R. Varón, P.A. García-Ruiz, J. Tudela, F.G. García-Cánovas, J.N. Rodríguez-Lopez, Suicide inactivation of the diphenolase and monophenolase activities of tyrosinase, *IUBMB Life* 62 (2010) 539–547.
- [52] J.L. Muñoz-Muñoz, F.J. García-Molina, P.A. García-Ruiz, M. Molina-Alarcón, J. Tudela, F.G. García-Cánovas, J.N. Rodríguez-Lopez, Phenolic substrates and suicide inactivation of tyrosinase: kinetics and mechanism, *Biochem. J.* 416 (2008) 431–440.
- [53] J.S. Chen, C.I. Wei, M.R. Marshall, Inhibition mechanism of kojic acid on polyphenol oxidase, *J. Agric. Food Chem.* 39 (1991) 1897–1901.
- [54] J. Cabanes, S. Chazarra, F. García Carmona, Kojic acid, a cosmetic skin whitening agent, is a slow-binding inhibitor of catecholase activity of tyrosinase, *J. Pharm. Pharmacol.* 46 (1994) 982–985.
- [55] J.C. Espín, H.J. Wichers, Slow-binding inhibition of mushroom (*Agaricus bisporus*) tyrosinase isoforms by tropolone, *J. Agric. Food Chem.* 47 (1999) 2638–2644.
- [56] M. Funayama, H. Arakawa, R. Yamamoto, T. Nishino, T. Shin, S. Muraio, Effects of alpha- and beta-arbutin on activity of tyrosinases from mushroom and mouse melanoma, *Biosci. Biotechnol. Biochem.* 59 (1995) 143–144.
- [57] I. Kubo, I. Kinoshita, Tyrosinase inhibitors from cumin, *J. Agric. Food Chem.* 46 (1998) 5338–5341.
- [58] J.S. Conrad, S.R. Dawso, E.R. Hubbard, T.E. Meyers, K.G. Strothkamp, Inhibitor binding to the binuclear active site of tyrosinase: temperature, pH, and solvent deuterium isotope effects, *Biochemistry* 33 (1994) 5739–5744.
- [59] D.E. Wilcox, A.G. Porras, Y.T. Hwang, K. Lerch, M.E. Winkler, E.I. Solomon, Substrate analogue binding to the coupled binuclear copper active site in tyrosinase, *J. Am. Chem. Soc.* 107 (1985) 4015–4027.
- [60] M. Sendovski, M. Kanteev, V.S. Ben-Yosef, N. Adir, A. Fishman, First structures of an active bacterial tyrosinase reveal copper plasticity, *J. Mol. Biol.* 405 (2011) 227–237.
- [61] K. Nihei, I. Kubo, Identification of oxidation product of arbutin in mushroom tyrosinase assay system, *Bioorg. Med. Chem. Lett.* 13 (2003) 2409–2412.
- [62] L.G. Fenoll, J.N. Rodríguez-Lopez, F. García-Sevilla, P.A. García-Ruiz, R. Varón, F.G. García-Cánovas, J. Tudela, Analysis and interpretation of the action mechanism of mushroom tyrosinase on monophenols and diphenols generating highly unstable *o*-quinones, *Biochim. Biophys. Acta* 1548 (2001) 1–22.
- [63] I. Kubo, I. Kinoshita, Tyrosinase inhibitory activity of the olive oil flavor compounds, *J. Agric. Food Chem.* 47 (1999) 4574–4578.
- [64] D.F. Healey, K.G. Strothkamp, Inhibition of the catecholase and cresolase activity of mushroom tyrosinase by azide, *Arch. Biochem. Biophys.* 211 (1981) 86–91.
- [65] M. Sugumaran, A caution about the azide inhibition of enzymes associated with electrophilic metabolites, *Biochem. Biophys. Res. Commun.* 212 (1995) 834–839.

Title	Biochemical and structural characterisation of the copper containing oxidoreductases catechol oxidase, tyrosinase, and laccase from ascomycete fungi
Author(s)	Chiara Gasparetti
Abstract	<p>Catechol oxidase (EC 1.10.3.1), tyrosinase (EC 1.14.18.1), and laccase (EC 1.10.3.2) are copper-containing metalloenzymes. They oxidise substituted phenols and use molecular oxygen as a terminal electron acceptor. Catechol oxidases and tyrosinases catalyse the oxidation of <i>p</i>-substituted <i>o</i>-diphenols to the corresponding <i>o</i>-quinones. Tyrosinases also catalyse the introduction of a hydroxyl group in the <i>ortho</i> position of <i>p</i>-substituted monophenols and the subsequent oxidation to the corresponding <i>o</i>-quinones. Laccases can oxidise a wide range of compounds by removing single electrons from the reducing group of the substrate and generate free radicals. The reaction products of these oxidases can react further non-enzymatically and lead to formation of polymers and cross-linking of proteins and carbohydrates, in certain conditions.</p> <p>The work focused on examination of the properties of catechol oxidases, tyrosinases and laccases. A novel catechol oxidase from the ascomycete fungus <i>Aspergillus oryzae</i> was characterised from biochemical and structural point of view. Tyrosinases from <i>Trichoderma reesei</i> and <i>Agaricus bisporus</i> were examined in terms of substrate specificity and inhibition. The oxidation capacity of laccases was elucidated by using a set of laccases with different redox potential and a set of substituted phenolic substrates with different redox potential. Finally, an evaluation of the protein cross-linking ability of catechol oxidase from <i>A. oryzae</i>, tyrosinases from <i>T. reesei</i> and <i>A. bisporus</i> and laccases from <i>Trametes hirsuta</i>, <i>Thielavia arenaria</i>, and <i>Melanocarpus albomyces</i> was performed.</p>
ISBN, ISSN	ISBN 978-951-38-7934-1 (soft back ed.) ISSN 2242-119X (soft back ed.) ISBN 978-951-38-7935-8 (URL: http://www.vtt.fi/publications/index.jsp) ISSN 2242-1203 (URL: http://www.vtt.fi/publications/index.jsp)
Date	October 2012
Language	English
Pages	124 p. + app 55 p.
Keywords	<i>Trichoderma reesei</i> , <i>Agaricus bisporus</i> , <i>Aspergillus oryzae</i> , <i>Thielavia arenaria</i> , tyrosinase, catechol oxidase, laccase, purification, characterisation, oxidation capacity, inhibition, three-dimensional structure, cross-linking
Publisher	VTT Technical Research Centre of Finland P.O. Box 1000, FI-02044 VTT, Finland, Tel. 020 722 111

VTT Technical Research Centre of Finland is a globally networked multitechnological contract research organization. VTT provides high-end technology solutions, research and innovation services. We enhance our customers' competitiveness, thereby creating prerequisites for society's sustainable development, employment, and wellbeing.

Turnover: EUR 300 million

Personnel: 3,200

VTT publications

VTT employees publish their research results in Finnish and foreign scientific journals, trade periodicals and publication series, in books, in conference papers, in patents and in VTT's own publication series. The VTT publication series are VTT Visions, VTT Science, VTT Technology and VTT Research Highlights. About 100 high-quality scientific and professional publications are released in these series each year. All the publications are released in electronic format and most of them also in print.

VTT Visions

This series contains future visions and foresights on technological, societal and business topics that VTT considers important. It is aimed primarily at decision-makers and experts in companies and in public administration.

VTT Science

This series showcases VTT's scientific expertise and features doctoral dissertations and other peer-reviewed publications. It is aimed primarily at researchers and the scientific community.

VTT Technology

This series features the outcomes of public research projects, technology and market reviews, literature reviews, manuals and papers from conferences organised by VTT. It is aimed at professionals, developers and practical users.

VTT Research Highlights

This series presents summaries of recent research results, solutions and impacts in selected VTT research areas. Its target group consists of customers, decision-makers and collaborators.

Biochemical and structural characterisation of the copper containing oxidoreductases catechol oxidase, tyrosinase, and laccase from ascomycete fungi

Catechol oxidase (EC 1.10.3.1), tyrosinase (EC 1.14.18.1), and laccase (EC 1.10.3.2) are copper-containing metalloenzymes. They oxidise substituted phenols and use molecular oxygen as a terminal electron acceptor. Catechol oxidases and tyrosinases catalyse the oxidation of *p*-substituted *o*-diphenols to the corresponding *o*-quinones. Tyrosinases also catalyse the introduction of a hydroxyl group in the *ortho* position of *p*-substituted monophenols and the subsequent oxidation to the corresponding *o*-quinones. Laccases can oxidise a wide range of compounds by removing single electrons from the reducing group of the substrate and generate free radicals. The reaction products of these oxidases can react further non-enzymatically and lead to formation of polymers and cross-linking of proteins and carbohydrates, in certain conditions.

The work focused on examination of the properties of catechol oxidases, tyrosinases and laccases. A novel catechol oxidase from the ascomycete fungus *Aspergillus oryzae* was characterised from biochemical and structural point of view. Tyrosinases from *Trichoderma reesei* and *Agaricus bisporus* were examined in terms of substrate specificity and inhibition. The oxidation capacity of laccases was elucidated by using a set of laccases with different redox potential and a set of substituted phenolic substrates with different redox potential. Finally, an evaluation of the protein cross-linking ability of catechol oxidase from *A. oryzae*, tyrosinases from *T. reesei* and *A. bisporus* and laccases from *Trametes hirsuta*, *Thielavia arenaria*, and *Melanocarpus albomyces* was performed.

ISBN 978-951-38-7934-1 (soft back ed.)

ISBN 978-951-38-7935-8 (URL: <http://www.vtt.fi/publications/index.jsp>)

ISSN 2242-119X (soft back ed.)

ISSN 2242-1203 (URL: <http://www.vtt.fi/publications/index.jsp>)

